PATHOBIOLOGY AND IMMUNE RESPONSES OF EGYPTIAN ROUSETTE BATS (ROUSETTUS AEGYPTIACUS): STUDIES OF ORTHOMARBURGVIRUS INFECTION AND TISSUE-BASED INSIGHTS INTO HEALTH AND DISEASE

by

JESSICA A. ELBERT, DVM, DIPL. ACVP

(Under the Direction of Elizabeth W. Howerth and Jonathan S. Towner)

ABSTRACT

Bats (Order Chiroptera) are a highly diverse and ecologically important group of mammals recognized for their unique biological traits and increasing relevance to infectious disease research. The Egyptian rousette bat (ERB; *Rousettus aegyptiacus*; common name Egyptian rousette) is the only confirmed natural reservoir host for orthomarburgviruses, Marburg virus and Ravn virus, and is a putative or confirmed reservoir for additional high-consequence zoonotic viruses. Despite its growing use in infectious disease modeling and immunologic research, fundamental gaps persist in our understanding of ERB biology, particularly regarding the species' lymphoid system, background pathology in free-ranging populations, and host immune responses to diverse viral exposures. This dissertation addresses these gaps through a series of studies designed to 1) characterize the histologic architecture of the ERB lymphoid system, 2) characterize histology of free-ranging ERBs, and 3) evaluate viral shedding dynamics and

long-term immunity in ERBs following inoculation with genetically diverse orthomarburgvirus isolates.

These studies lay the immunologic and pathologic foundations of this reservoir species, providing a novel lymphoid tissue atlas and baseline health prolife for free-ranging ERBs. Experimental infection studies demonstrated that Ravn virus, despite its ~20% genetic divergence from Marburg virus, follows similar shedding kinetics and infection dynamics with increased rectal shedding. Furthermore, animals previously co-infected with diverse viruses mounted rapid, sterilizing immune responses upon homotypic and heterotypic inoculation, suggesting robust cross-protective immunity despite prior coinfection. Taken together, these findings expand our understanding of ERB reservoir competence and virus-host interactions, while establishing critical anatomical and immunological resources for future research. This work contributes to the broader fields of comparative pathology, viral ecology, and bat immunobiology, with direct implications for spillover risk assessment and the development of preclinical bat model systems for emerging zoonotic diseases.

INDEX WORDS: Egyptian rousette bat, Chiroptera, immunology, lymphoid system, pathology, histology, immunohistochemistry, virology, Marburg virus, Ravn virus, filovirus, coinfection, reservoir

PATHOBIOLOGY AND IMMUNE RESPONSES OF EGYPTIAN ROUSETTE BATS (ROUSETTUS AEGYPTIACUS): STUDIES OF ORTHOMARBURGVIRUS INFECTION AND TISSUE-BASED INSIGHTS INTO HEALTH AND DISEASE

by

JESSICA A. ELBERT, DVM, DIPL. ACVP

BA, WASHINGTON UNIVERSITY IN ST. LOUIS, 2002

DVM, IOWA STATE UNIVERSITY COLLEGE OF VETERINARY MEDICINE, 2018

A Dissertation Submitted to the Graduate Faculty of The University of Georgia in Partial Fulfillment of the Requirements for the Degree

DOCTOR OF PHILOSOPHY

ATHENS, GEORGIA

2025

PATHOBIOLOGY AND IMMUNE RESPONSES OF EGYPTIAN ROUSETTE BATS (ROUSETTUS AEGYPTIACUS): STUDIES OF ORTHOMARBURGVIRUS INFECTION AND TISSUE-BASED INSIGHTS INTO HEALTH AND DISEASE

by

JESSICA A. ELBERT, DVM, DIPL. ACVP

Major Professor:	Elizabeth W. Howerth
	Jonathan S. Towner
Committee:	Nicole M. Nemeth
	Samantha Schlemmer
	S. Mark Tompkins

Electronic Version Approved:

Ron Walcott
Vice Provost for Graduate Education and Dean of the Graduate School
The University of Georgia
August 2025

DEDICATION

This work is dedicated to my family, without whom none of this would have been possible.

To my parents, Steve and Marilyn: Your unwavering support and belief in me, across all iterations of myself, has been immeasurable. I quite literally cannot thank you enough. I strive every day to make you proud, and I carry your encouragement with me in everything I do.

To my sister, Emily: You have been a constant source of strength and steadiness for me throughout my life, and I am eternally grateful you are my sister and my friend.

To my husband, Gary: Thank you for being my greatest supporter, my sounding board, and my partner in all things. Your patience and love have sustained me through every phase of this journey.

To my cats, Phoebe and Max: Thank you both for your tireless assistance with writing, your commitment to keyboard occupation, and your well-timed reminders to pause for snacks, naps, and perspective. You brought levity to even the most serious of days.

Finally, this work is dedicated in loving memory to my grandparents, Raymond and Madeleine Elbert, and Robert and Kathryn Lowe. Their wisdom, love, and influence have shaped the person and scholar I am today, and I carry their memory with deep gratitude and pride.

ACKNOWLEDGEMENTS

First and foremost, I would like to express my deepest gratitude to my family and their unwavering support throughout every phase of my life and academic journey. Your constant encouragement has given me the confidence to pursue my goals, and I am endlessly grateful for your belief in me.

I am especially thankful to Dr. Elizabeth Howerth for her steadfast mentorship throughout both my residency training and graduate research. Buffy, your guidance, wisdom, and encouragement over the past seven years has been an extraordinary gift. I am profoundly grateful to have been your student. I would also like to thank Deb Carter for her help and guidance in Buffy's lab, and for always being willing to talk about bats.

I extend my heartfelt appreciation to Dr. Jonathan Towner and the entire Virus-Host Ecology Team - Amy Schuh, Brian Amman, Jonathan Guito, Tara Sealy, and James Graziano – as well as all members of the Viral Special Pathogens Branch at the Centers for Disease Control and Prevention. Jon, thank you for your mentorship and support throughout my graduate research. I feel incredibly fortunate to have contributed to the world-class research carried out at CDC, and working alongside the Virus-Host Ecology team has been the highlight of my scientific career. I am especially grateful to Dr. Amy Schuh; your expertise, patience, and generous guidance made the high-containment studies possible. Thank you, Amy.

I am grateful to my dissertation committee members - Drs. Nicole Nemeth, Samantha Schlemmer, and S. Mark Tompkins – for their thoughtful feedback, direction,

and support throughout this process. The Department of Pathology at University of Georgia's College of Veterinary Medicine has been an exceptional academic home over the last seven years. I am thankful for the outstanding instruction and training I received from many faculty members, including Drs. Jesse Hostetter, James Stanton, Nicole Gottdenker, Daniel Rissi, Paige Carmichael, Betsy Uhl, Brittany McHale, Rita McManamon, Kaori Sakamoto, Corrie Brown, Uriel Blas-Machado, Doris Miller, Pauline Rakich, and Cathy Brown.

I have been fortunate to share this journey with a truly remarkable group of residentmates and graduate student colleagues, including Justin Stilwell, Chris Siepker, Martha Frances Dalton, Abby Armwood, Dani Lieske, Silvia Carnaccini, Chloe Chan Goodwin, Troy Mulder, Justin Farris, Alaa Bani Salman, and Caroline Piotrowski. Your camaraderie and support have meant the world to me, and I'm so honored to be your colleague. I am especially grateful to Shannon Kirejczyk for being both a mentor and a treasured friend throughout my time at UGA and CDC.

I would also like to thank my mentors at Iowa State University's College of Veterinary Medicine, who helped nurture my love of veterinary pathology. Special thanks to Drs. Amanda Fales-Williams, Jesse and Shannon Hostetter, Claire Andreasen, Mark Ackermann, Joseph Haynes, Michael Yaeger, Eric Burrough, Rachel Derscheid, and Heather Flaherty for their early guidance and inspiration. To Ariel Nenninger, Lisa Uhl, and Katy Martin – I am eternally thankful for your enduring friendship, both in vet school and beyond, and feel lucky to continue our careers together as colleagues. A special thank you to Katy for her assistance with parasite identification, even while managing her own graduate research.

I would like to acknowledge the exceptional administrative team in the UGA Pathology Department and Graduate School - Amanda Wages, Megan Troutman, Nicole Wingard, and Lisa Norris – for their vital support in helping me navigate both residency and graduate school. I am deeply grateful for all that you do.

Finally – and most humbly – I acknowledge the Egyptian rousette bats at the heart of this research. Their essential role in advancing our understanding of host-pathogen interactions and reservoir pathobiology cannot be overstated, and it is with deep respect and gratitude that I recognize their contribution. I hope that the insights gained from this work deepen our understanding of this remarkable species, advance translational outcomes for both wildlife and human health, and contribute meaningfully to scientific discovery and the ongoing stewardship of wildlife populations.

TABLE OF CONTENTS

Page

LIST OF TABLES

Page

LIST OF FIGURES

Page

CHAPTER 1

INTRODUCTION AND LITERATURE REVIEW

1. INTRODUCTION

Bats (Order Chiroptera, meaning “hand wing”) are incredibly diverse, with 1,487 known species inhabiting all continents except Antarctica, and having broad ecological, anatomical, and environmental diversity that is nearly unparalleled within the animal kingdom.[1,2] The Egyptian rousette bat (ERB; *Rousettus aegyptiacus*; common name Egyptian rousette) is medium-sized pteropid bat with a widespread and fragmented host geographic range, plays an important ecology role as a pollinator and seed disperser, and is a known reservoir for orthomarburgviruses (Marburg virus (MARV) and Ravn virus (RAVV), family *Filoviridae*), Sosuga virus (family *Paramyxoviridae*), and putative reservoir for Kasokero virus (family *Nairoviridae*).[3-10] ERBs are common inhabitants of managed care zoo facilities and are a popular animal research model for viral infectious diseases, immunology, and neurological research.[11-20] Despite their increasing use in infectious disease research and critical role as a natural reservoir for orthomarburgviruses, fundamental knowledge regarding this species is lacking. For example, a comprehensive histologic characterization of the ERB immune system has not been performed to date, nor has characterization of species-specific features and subclinical morbidities in free-ranging ERBs. Without this foundational knowledge, experimental conclusions may be limited, potentially overlooking key factors that influence these bats' immunity, health status, and overall population dynamics. Further,

viral shedding dynamics of RAVV, a genetically diverse viral "brother" to MARV, has never been characterized in ERBs and as such the extent to which this genomic diversity may alter receptor binding or cellular tropism or may alter the short- and long-term dynamics of the host immune response is unknown. Also unknown is the role of viral coinfections in ERBs in establishing long-term immunity, which is of increased importance in ERBs as they host numerous high-consequence zoonotic pathogens.

The goal of the studies presented herein was to characterize baseline pathologic features of the ERB lymphoid system and of free-ranging ERBs, to establish viral shedding characteristics for RAVV infection in ERBs, and to elucidate the influence of viral coinfections in long-term immunity upon inoculation with highly diverse orthomarburgviruses. This chapter will introduce this work by discussing the background, research problem, specific aims, objectives and research questions, the significance of the results and the limitations of the studies, followed by an in-depth literature review of the ERB, orthomarburgviruses, and viral coinfections.

Bats are the focus of diverse scientific research, including ecology and conversation, bioacoustics and sensory biology, evolutionary biology and genetics, immunology and disease resistance, biomechanics and flight physics, microbiome and gut health, neuroscience and sleep research, and infectious diseases and spillover.[21-35] The critical role of bats as viral reservoirs and potential sources of zoonotic spillover has garnered increasing scientific attention. This significance was underscored by the recent SARS-CoV-2 pandemic, which has led to nearly 7.1 million deaths worldwide as of February 2025 and is hypothesized to have originated in horseshoe bats (*Rhinolophus* spp.) in Asia.[36-39] The spillover of orthomarburgviruses and other *Filoviridae* members,

such as Ebola virus, remains a subject of significant scientific, social, economic, and political concern. This urgency is underscored by recent outbreaks of MARV in Tanzania and Sudan virus (species *Orthoebolavirus sudanense*) in Uganda, both occurring in January 2025.[40,41] A deeper understanding of these viruses and their reservoir hosts remains a critical and timely area of research.

An in-depth understanding of the baseline pathologic and histologic characteristics of an animal species is essential for accurate interpretation of experimental results and appropriate experimental design. For example, in early tuberculosis research, lack of understanding of the guinea pig's unique immune system led to erroneous conclusions and extrapolations to human infections.[42,43] Further, early researchers studying the common marmoset (*Callithrix jacchus)* made inappropriate conclusions about their health and pathology due to a lack of understanding of the species' unique biological and ecological characteristics.[44] This led to misleading conclusions regarding stress responses and age-related pathologies, which may not accurately reflect their health status in free-ranging settings.[44] A deeper understanding of the fundamental biology and pathology of an animal species enhances the formulation of our scientific inquiries and strengthens the robustness of our experimental findings. This knowledge base allows for more precise hypotheses and methodologies, ultimately leading to more reliable and applicable results in research. To date, a comprehensive histologic characterization of the ERB lymphoid system remains incomplete. Additionally, characterization of species-specific features and subclinical morbidities in free-ranging ERBs has not been conducted. Without this foundational knowledge, experimental conclusions may be

limited, potentially overlooking key factors that influence these bats' immunity, health status, and overall population dynamics.

Numerous ecological and experimental studies have confirmed the role of ERBs as a natural reservoir host for orthomarburgviruses.[4,5,45-50] The viral species *Orthomarburgvirus marburgense* contains two distinct viruses: Marburg virus (MARV) and Ravn virus (RAVV). The full genomic sequence of RAVV differs by up to 21% from MARV, and the amino acid sequence of the RAVV glycoprotein (GP) differs by ~22% from MARV GP.[49,51] This genomic diversity may alter receptor binding or cellular tropism, and may alter the short- and long-term dynamics of the host immune response.[51] Despite complete characterization of the pathogenesis, viral dynamics, transmission, and shedding of MARV in its ERB reservoir host, similar characterization of RAVV infection in ERBs has not been completed.

Finally, viral coinfections and their impact on long-term immunity represent a relatively understudied area in disease ecology and infectious disease research. Coinfections—instances where a host is infected simultaneously with two or more pathogens—can influence the host's susceptibility to future infections, alter host and pathogen population dynamics, modify infection and shedding patterns, impose evolutionary pressures, and affect the risk of zoonotic spillover. Viral coinfections have been documented in free-ranging bats, raising questions about how these interactions influence immune responses, viral shedding, and pathogen maintenance within the natural host population.[52-76] This is particularly critical for reservoir hosts like the ERB which harbor zoonotic pathogens of significant public health importance, given the genetic diversity among co-circulating viral species, e.g. MARV and RAVV, and the

potential implications for the development of protective immunity and subsequent viral inoculation outcomes. The role of previous coinfections in ERBs and subsequent effects on immunity have not been investigated.

The overarching goal of this dissertation work was to better elucidate the pathobiology of the ERB via characterization of baseline pathologic features of the ERB lymphoid system and of free-ranging ERBs, experimental characterization of viral shedding dynamics for RAVV infection in ERBs, and elucidation of the influence of viral coinfections in long-term immunity upon inoculation with highly diverse orthomarburgviruses. To this end, a research plan was formulated with the following objectives:

1. Research objective 1 – Compile a literature review and histology atlas to summarize and expand current knowledge in the field of ERB immunology
2. Research objective 2 – Characterize macro- and microscopic lesions in free-ranging ERBs to delineate baseline knowledge of free-ranging ERB health parameters and pathology
3. Research objective 3 – Complete a multifaceted experimental inoculation study to investigate factors that may affect orthomarburgvirus infection within an individual animal and viral maintenance within a larger population (e.g., a cave roost) via:
    a. Characterization of viral shedding dynamics of experimental infection with RAVV in ERBs.
    b. Evaluation of viral shedding dynamics and long-term immunity following homotypic (MARV) and heterotypic (RAVV) inoculation with highly

diverse orthomarburgvirus isolates in previously co-infected and singly infected ERBs.

These studies will contribute to our knowledge of this critically important reservoir host, ERB immunology and pathology in general and furthers the validation of the only established reservoir model for any filovirus. A comprehensive understanding of the immune system and pathology of reservoir hosts is essential for advancing infectious disease research, particularly for zoonotic viruses with significant global health implications. The development of a lymphoid histology atlas in a bat species that serves as both an important infectious disease model and a natural reservoir for orthomarburgviruses provides a critical foundation for comparative immunology and pathogenesis studies. This resource enables standardized assessment of immune architecture, facilitating accurate interpretation of experimental infections and vaccine responses. Additionally, characterizing pathologic findings in free-ranging, apparently healthy bats provides essential baseline data to distinguish normal physiologic variation from early or subclinical disease, a distinction that is often lacking in wildlife pathology. Further, the characterization of Ravn virus in its reservoir bat host offers novel insights into virus-host dynamics, shedding light on mechanisms of viral persistence, shedding, and potential spillover risks. Finally, investigating the role of prior coinfections in shaping short- and long-term immunity in bats, particularly in response to diverse viral challenges, is essential for understanding how reservoir hosts maintain tolerance to multiple pathogens while occasionally serving as sources for emergent spillover events. Together, these lines of research contribute to a more nuanced understanding of bat

immunology, viral ecology, and disease emergence, with direct applications to public health and pandemic preparedness.

These studies have several inherent limitations. The prolonged fixation of tissues from free-ranging ERBs resulted in the presence of an intractable contaminant in the samples following nucleic acid extraction, precluding the use of robust ancillary diagnostic techniques such as next-generation sequencing for unbiased pathogen discovery. Consequently, our analyses were restricted to histologic characterization, relying on standard hematoxylin and eosin staining without the ability to incorporate molecular methodologies. In the experimental studies, constraints in both available space within the high-containment laboratories at the CDC and the ERB breeding colony's animal numbers limited the feasibility of serial euthanasia at defined post-infection time points. This limitation prevented comprehensive histopathologic comparisons, assessment of clinical pathology parameters, and quantification of organ viral loads throughout the study. Furthermore, due to spatial constraints, concurrent cohorts of MARV-infected ERBs and control bats could not be included, thereby restricting direct comparisons of viral shedding dynamics between RAVV and MARV. However, prior studies have extensively characterized control ERBs and MARV-infected ERBs, providing well-established comparative data to contextualize our findings.

2. BATS

Second only to rodents in species diversity, bats inhabit all continents except Antarctica and have broad ecological, anatomical, and environmental diversity that is nearly unparalleled within the animal kingdom.[1,2] The only mammal capable of powered

flight, all bats are thought to have evolved from a common, flighted ancestor that displayed many features we still recognize in bats today, including the ability to echolocate and specializations for fruit and nectar feeding.[77] Bats are subdivided into two suborders: 1) Suborder Yangochiroptera (or Vespertilioniformes), which includes most of the microbat families except for Rhinopomatidae, Rhinolophidae, Hipposideridae, Craseonycteridae, and Megadermatidae, and 2) Yinpterochiroptera (or Pteropodiformes), which includes taxa formerly known as "megabats" and the aforementioned five microbat families. Yangochiroptera bats have a diverse diet ranging from small animals (mammals, reptiles, fish), fruit, nectar, and blood. They rely on echolocation for navigation and hunting due to poor eyesight. Pteropodiformes are known as "fruit bats", due to their predominantly frugivorous diet of fruit, nectar, and pollen. Pteropid bats are excellent climbers, aided by a claw on each wing, are generally larger, and have excellent eyesight.[1]

While most bat species live in tropical to subtropical climes, they can be found in a variety of habitats, from arid to tropical, with variably sized home ranges. Depending on the climate in which they live, bats may remain year round, may hibernate, or may migrate, in rare cases up to almost 2,500 km.[78] Bats are as diverse in size as they are in habitat, ranging from the insectivorous, ~2-gram Kitti's hog-nosed bat (*Craseonycteris thonglongyai*), inhabiting the limestone caves of Thailand to the frugivorous ~1.2 kilogram giant golden-crowned flying fox (*Acerodon jubatus*) of the Philippines, with a 1.7-meter (5.6 foot) wingspan. Approximately 70% of bats are insectivorous; the majority of the remaining 30% are frugivorous, although some species, like the greater bulldog bat (*Noctilio leporinus*) and common vampire bat (*Desmodus rotundus*) follow specialized

piscivorous or hematophagous diets, respectively.[1] Bats have been identified as natural reservoir hosts for many zoonotic pathogens, including members of the viral families *Coronaviridae*, *Filoviridae*, *Rhabdoviridae*, and *Paramyxoviridae.*[6,51,79-85] More than 200 viruses spanning 32 viral families have been associated with bats through serology, molecular detection, or virus isolation.[86-88]

a. Egyptian Rousette Bats

The ERB is a yinpterochiropteran pteropodid bat that inhabits parts of Africa, western Asia, the Mediterranean, and the Indian subcontinent. They are predominantly cave-dwelling, gregarious and social animals, living in densely packed roosts that can contain more than 100,000 bats.[9] While ERBs have been found in arid biomes, they thrive in tropical rain and deciduous forests with abundant forest cover, roosting opportunities, and fruiting trees.[9] They are frugivorous, preferring soft, pulpy fruits such as figs, mangoes, and dates, and play an important ecological role as pollinators and seed dispersers.[10] In tropical areas, ERBs have a biannual breeding season, with a gestation period of approximately 106 days.[9] Females typically give birth to a single pup which is carried by the dam for 6 weeks, until the pup can independently hang in the roost.[10] Pups become independent between 3 – 6 months of age and reach sexual maturity between 14 and 18 months.[10] ERBs are estimated to live up to 2 years in the wild[47]; in captivity, ERBs can live up to 22 years, with the oldest known ERB living to 25 years.[9] They are one of the few megabats to use echolocation, producing a series of short, repetitive clicks of the tongue against the side of the mouth to aid in navigation.[10,89-92] In the wild, ERBs are predated by many large raptors, including the Lanner falcon, Palm-nut vulture, and

African fish eagles, mammals such as genets, and cave-dwelling reptiles such as cobras, pythons, and Nile monitor lizards (J. Towner, personal communication).

i. Reported pathogens in free-ranging Egyptian rousette bats

The majority of research in free-ranging ERBs has focused on ecological and epidemiological investigation into their role as a natural reservoir for orthomarburgviruses.[3,48,49,93-96] However, numerous pathogens have been serologically or molecularly identified in free-ranging ERBs across viral, bacterial and fungal families, as well as numerous parasite species. Most reported ERB pathogens are viral, which may reflect research bias within the scientific community on efforts to investigate viral families with known zoonotic potential, or may reflect the putative enhanced ability of ERBs to more successfully tolerate viral infection and replication than other mammalian species.[20,97-102]

1. Reported viral pathogens in free-ranging Egyptian rousette bats

RNA viruses are of critical importance as high-consequence zoonotic pathogens that originate in wildlife. Representing approximately 94% of zoonotic viruses[34], numerous ecological and biological factors contribute to the success of RNA viruses as pandemic pathogens, including their high mutation rate and frequency of recombination.[103,104] In addition to MARV and RAVV[5,48,93,95,105-108], numerous RNA viruses have been identified using serology and molecular diagnostics such as polymerase chain reaction (PCR) in free-ranging ERBs. Identified RNA viruses include members of the families *Coronaviridae* (e.g. Coronavirus spp.)[109-112], *Flaviviridae* (e.g. West Nile virus, Yellow fever virus, Zika virus)[113,114], *Orthomyxoviridae* (e.g. Influenza A virus)[115], *Paramyxoviridae* (e.g. Hendra-like virus, Nipah virus, Sosuga virus)[6,61,85,116],

and *Rhabdoviridae* (e.g. Lagos bat virus).[81,82,117] There have been no reports of clinical illness in free-ranging ERBs with RNA viral disease. DNA viruses, including members of the family *Adenoviridae*[118], *Herpesviridae*[119-121], and *Poxviridae*[122,123], have been reported in free-ranging ERBs, the latter of which has been associated with morbidity and mortality in ERBs in Israel and is zoonotic.[124]

2. Reported bacterial and fungal pathogens in free-ranging Egyptian rousette bats

There are few reports of bacterial pathogens in free-ranging ERBs and even fewer reports of clinical illness associated with bacterial infection. ERBs exhibit low colonization rates of *Staphylococcus aureus* and *S. schweitzeri*, with phylogenetic analysis suggesting significant geographical dispersal of *S. schweitzeri* among wildlife hosts.[125] Hemotropic mycoplasmas have been identified in two ERBs in Nigeria[126], while *Leptospira* sp. were identified in ERBs in South Africa.[127] *Borrelia* sp. was detected in 59 ERBs from a cave linked to a human case of relapsing fever following a soft tick bite.[128] *Escherichia coli* was identified in 2 ERBs from Republic of Congo[129], and *Bartonella* sp. have also been identified in ERBs from Kenya,[130,131] Zambia,[132] and South Africa.[131,133] The only report of bacterial-associated clinical disease in free-ranging ERBs is in Israel, where primarily pups and young adults are seasonally afflicted with abscessation due to *S. aureus*.[134] To the author's knowledge, there are no reports of fungal identification or disease in free-ranging ERBs.

3. Reported parasitic pathogens in free-ranging Egyptian rousette bats

Current knowledge of ectoparasites in ERBs encompasses a wide range of arthropod parasites, including bat flies (Nycteribiidae), soft ticks (Argasidae), mites, and fleas, with more than 50 unique species reported throughout the ERB range. These

ectoparasites are known to play potential roles in the transmission of pathogens; e.g. *Eucampsipoda aegyptia,* a host-specific bat fly within the family Nycteribiidae, has been reported in at least 10 countries within the ERBs northern range[134-138], with 36.9%[137] to 43.9%[139] PCR positivity for *Bartonella* sp. in *E. aegyptia* collected from ERBs across 7 countries. Furthermore, the argasid *Ornithodoros (Reticulinasus) faini* serves as a tick vector in the enzootic transmission cycle with ERBs of Kasokero virus.[19,140] While there is no evidence for the involvement of *Ornithodoros faini* in the enzootic maintenance of orthomarburgvirus within ERBs[141], further research is needed to investigate other ERB ectoparasites and their possible contribution to the dynamics of zoonotic disease.

Current understanding of endoparasites in ERBs is sparse, with reports primarily focusing on protozoal species within the phylum Apicomplexa. *Eimeria rousetti*[142] and novel pathogen *Gregarina rousetti* n. sp.[143] have been reported in ERBs in Egypt, as well as numerous *Plasmodium* sp. identified in ERBs in Nigeria[144], Ghana[145], Congo[146], and Guinea, Liberia, and the Ivory Coast[147]. *Trypanosoma* sp. have been reported in ERBs in Gabon[148] and South Africa[149], and there is a single report of the filarial nematode *Diptalonema vitae* in ERBs in Egypt[150]. Pentastomids, crustaceous arthropods commonly known as “tongue worms”, have been reported on the liver and spleen of ERBs in Uganda[3]. Future research on endoparasites in ERBs represents a compelling and underexplored avenue of study, offering significant potential to enhance our understanding of parasite-host dynamics and their implications for both bat health and zoonotic disease transmission.

ii. Reported pathogens in managed care Egyptian rousette bats

Reports of clinical disease and pathogen detection in managed care ERBs are limited, with much of the published literature focusing on iron overload disease, which will be discussed further in this chapter and in Chapter 3C. Reports of viral, bacterial, and fungal infections in ERBs in managed care are few. Two ERBs died from European bat lyssavirus 1 after importation into Denmark from a Dutch zoo.[117,151] Subsequent depopulation of all bats imported into Denmark and all members of the original Dutch colony revealed clinically silent European bat lyssavirus 1 infection in 11.9% and 13% of the ERBs, respectively.[81,117,151] Two novel members of the *Betaherpesvirinae* and *Gammaherpesvirinae* subfamilies were detected via nested PCR in pooled liver, lung, and small intestine samples from two deceased ERBs in Hungary[120], and two additional novel *Betaherpesvirinae* members were identified in oropharyngeal samples from clinically healthy ERBs in Spain.[119] In Israel, a novel poxvirus (Israeli *Rousettus aegyptiacus* pox virus; IsrRAPXV) was isolated from managed care ERBS in 2014[122] and 2019.[123] One adult female developed clinical, but non-fatal, poxviral disease with multifocal vesicular and nodular lesions on the wing membranes[122]; five years later, five juvenile ERBs developed fatal IsrRAPXV infection with typical pox-like lesions on the ventral abdomen, wing membranes, and tongue.[123] IsrRAPXV has since proven to be zoonotic, causing skin lesions in a volunteer at a bat sanctuary in Israel.[124] A novel papillomavirus, subsequently named *Rousettus aegyptiacus* papillomavirus type 1, was isolated from an ERB from a United States-based bat conservation organization that presented with multiple cutaneous papillomas and basosquamous carcinoma in both the lateral canthus of the left eye and multifocally throughout the left wing membranes.[152,153] Fifteen *Bifidobacterium* sp. were identified in environmental fecal swabs from ERBs in a

zoological park in Verona, Italy.[154] *Kluyvera ascorbata* was isolated from the blood of a deceased ERB from Korea, which has previously been reported in variable human clinical infections as well as isolated from subclinically infected Madagascan lemurs.[155] Additionally, yersinosis due to *Yersinia pseudotuberculosis* has been reported in three closed ERB colonies in managed care, resulting in ~10% mortality[156], 19.7% mortality[157] or depopulation.[158] Reports of fungal pathogens are scarce, with a single study detecting *Pneumocystis* sp. in 35.3% (6/17) of ERBs from two managed care colonies in France via nested PCR analysis of lung tissue.[159] A single report documents a fatal case of microsporidiosis due to *Encephalitozoon hellem* in a managed care ERB, possibly caused by mechanical transfer of spores from a nearby aviary.[160]

A diverse array of neoplasms have been documented, including adenomas[161,162], carcinomas[161], sarcomas[161,163,164], and lymphomas[165], affecting organs such as lungs[161,162,166], pancreas[162], liver[161,167], kidneys[161], bladder[161], and haired skin[165]. Etiological factors have been proposed in a few instances, such as a microchip-associated leiomyosarcoma[168] and papillomavirus infection linked to a basosquamous carcinoma in the wing membrane.[152,153] Iron overload has been suggested in the pathogenesis of hepatocellular carcinomas; in a retrospective study, ERBs with hemochromatosis were significantly more likely to have hepatocellular carcinomas than bats with hemosiderosis.[161] Other reports of disease within managed care ERB populations include instances of pneumonia[161,169], membranous glomerulopathy[161], renal tubular necrosis[161], chronic interstitial nephritis[161], liver failure[161], myocardial degeneration and/or fibrosis[161], bacterial sepsis (undisclosed etiology)[161], gall bladder rupture[161], thymic lymphoid depletion[169], hepatocellular degeneration[169], multicentric hyperostosis linked to

fluorosis[170] and "skin disease" (results anonymized) in 22% of managed care ERBs from two zoos.[171] Iatrogenic mortality due to pulmonary embolism of gelatin hemostatic sponge has additionally been reported in two ERBs.[172]

iii. Egyptian rousette bats and iron

Due to their endearing physical characteristics and success in managed care environments, ERBs are commonly kept in zoo collections throughout the world. ERBs in managed care environments are commonly afflicted with iron overload (IO), also reported in the literature as iron storage disease or iron overload disorder.[161,173-175] Dysregulation of iron homeostasis and subsequent IO is a cause of hepatocellular damage and increased mortality, and has been described in humans as well as in numerous exotic species, including ERBs.[161,176-188] A histologic distinction is made between hemochromatosis, which is increased iron storage with concurrent cellular injury, such as necrosis and fibrosis, and hemosiderosis, or increased iron storage without pathologic change. In humans, hemochromatosis is caused by several genetic disorders, the majority of which result in loss-of-function mutations in regulatory components of hepcidin synthesis.[189,190] Hepcidin is an important liver-derived iron regulatory hormone and negative regulator of iron absorption from the gastrointestinal tract and iron release from bone marrow stores. In response to plasma iron levels, hepcidin binds its ligand, the cellular iron export protein ferroportin. This results in internalization and degradation of the protein and subsequent down-regulation of iron absorption and inhibition of iron release from bone marrow stores, macrophages, and hepatocytes.[189] Although ERBs may have a diminished ability to upregulate hepcidin expression during dietary iron excess, the pathophysiology of IO in bats has not been determined.[174,191] ERBs are frugivorous

bats, and dietary factors such as high levels of ascorbic acids and lower levels of tannins and phytates, which enhance and reduce iron bioavailability, respectively, are theorized to play a role in inappropriate iron accumulation.[9,192] Iron accumulation in ERBs is most prevalent in the liver and spleen, with iron additionally detected in the pancreas, kidney, skeletal muscle, and lung.[161] The role of iron as a risk factor and in the pathogenesis of hepatocellular carcinoma has been studied in human literature, but further research is needed to clarify whether iron accumulation is the primary driver of liver carcinogenesis.[193] A recent case series investigating a mortality event in managed care Leschenault's rousette bats (*Rousettus leschenaultii*) found that 86% (6/7) had concurrent IO and neoplasia.[194] ERBs with hemochromatosis are significantly more likely to develop hepatocellular carcinoma versus those with hemosiderosis.[161]

Iron metabolism and accumulation can play a role in infectious disease, as some viruses are able to alter iron homeostasis either via manipulating cellular processes (hepatitis C virus, HIV-1, human cytomegalovirus) or by using the host protein transferrin receptor 1 to gain entry into cells (New World hemorrhagic arenaviruses, canine and feline parvoviruses, mouse mammary tumor virus).[174,195] In vitro administration of iron chelators in cells infected with HIV-1, human cytomegalovirus, vaccinia virus, herpes simplex virus 1, or hepatitis B virus curbs viral growth.[195]

3. ORTHOMARBURGVIRUSES

a. Virus classification, structure, entry, and replication

Marburg virus (MARV) and Ravn virus (RAVV) are the only two known members of the species *Orthomarburgvirus marburgense* (family *Filoviridae;* genus *Orthomarburgvirus*), and are the causative agents of Marburg virus disease (MVD), a

severe, often fatal disease that typically emerges in sub-Saharan Africa characterized by human-to-human transmission and high case fatality ratios up to 90%.[196] Though MARV and RAVV are in the same viral species, they differ by >20% at the amino acid level in the surface glycoprotein.[48] *Orthomarburgvirus* members form 80 nm wide x 14,000 nm long, pleomorphic virions and are enveloped, with a non-segmented, single-stranded, negative-sense, ~19 kb RNA genome (GenBank accession NC_001608).[196]

MARV virions are pleomorphic particles, variably appearing as rod- or ring-like, filamentous, crook- or six-shaped, or round.[197] The mean particle length has been reported to be 790 to 892 nm, with a mean diameter of 91 nm; this variation may be reflective of differences between cryo-EM and conventional EM.[198,199] MARV particles are enclosed by a host-derived membrane, containing homotrimers of the MARV glycoprotein (GP), which surrounds a central core of the ribonucleoprotein complex (RNP complex) formed by the viral RNA genome encapsidated by tightly associated nucleocapsid proteins.[198,199]

The genome of MARV isolates range in size from 19,111 to 19,114 bases in length and contain 7 linear, monocistronic genes: NP, VP35, VP40, GP, VP30, VP24, and L.[196,198,199] These proteins and their functions are summarized in Table 1-1. Filovirus proteins can be generally subdivided into three categories: those that form the nucleocapsid (NP, VP30), the polymerase complex (L, VP35), and those that are associated with the envelope (GP, VP40, VP24).[196,198,199] Each gene consists of a highly conserved transcription start and stop signal, an extended 3' and 5' untranslated region (UTR), and an open reading frame (ORF).[196,198,199] Gene separation varies, occurring either through short intergenic regions or, in the case of all filoviruses and other members

of the order *Mononegavirales*, through an overlapping arrangement where the transcription stop signal of the upstream gene and the transcription start signal of the downstream gene share five highly conserved nucleotides.[196,198,199]

Table 1-1: Orthomarburgvirus proteins and their function

Protein	Amino Acids	Predicted Molecular Mass	Function
NP	695	94 kDa	Encapsidation of RNA genome, nucleocapsid formation, budding, essential for transcription and replication
VP35	329	32 kDa	Polymerase cofactor, nucleocapsid formation, IFN antagonist, Inhibits NP oligomerization and RNA binding
VP40	303	38 kDa	Budding, antagonist of IFN signaling, mediates viral egress, regulates viral transcription and replication, blocks signal transducer and activator of transcription (STAT)1 and STAT2 signaling
GP	681	170 – 200 kDa	Attachment, receptor binding, fusion, tetherin antagonist
VP30	281	28 kDa	Nucleocapsid formation
VP24	253	24 kDa	Maturation of nucleocapsids, budding
L	2331	~220 kDa	Catalytic domain of RNA-dependent RNA polymerase

Adapted from Hume, Olejnik, Brauberger[196,198,199]

The MARV virion has one membrane-bound surface protein, the glycoprotein (GP), which is a Type 1 transmembrane protein inserted into the viral envelope via homotrimeric spikes.[200] After translation within the host cell cytosol, the precursor GP (GP_0) undergoes numerous posttranslational modifications within the ESCRT secretory pathway from the endoplasmic reticulum, trans-Golgi network, to eventual placement in the plasma membrane, including glycosylation, acylation, and phosphorylation.[199] GP_0 is cleaved by host furin proteases in the trans Golgi, leading to the formation of a $GP_{1,2}$ heterodimer that is held together by a single disulfide bond.[201] Unlike orthoebolaviruses, MARV does not produce a secreted form of its GP.[202]

MARV initiates infection by attaching to target cells through MARV GP interactions with cell surface molecules, inducing receptor-mediated macropinocytosis.[196,203] Following endocytosis, endosomal proteases cleave GP_1, exposing its binding site for Niemann-Pick C1 (NPC1), the critical entry receptor.[204] Membrane fusion is then mediated by GP_2 in a pH-dependent manner, allowing the viral nucleocapsid to be released into the cytoplasm.[205-207] Once inside the host cell, transcription of the viral genome begins, producing mRNAs that are subsequently translated by host ribosomal machinery.[196] GP synthesis occurs in the endoplasmic reticulum, where it undergoes extensive post-translational modifications before progressing through the classical secretory pathway.[199] Concurrently, positive-sense antigenomes are synthesized from the incoming viral genomes, serving as templates for the replication of new negative-sense genomes.[196,199] After proteolytic processing in the Golgi, GP is transported to multivesicular bodies and subsequently to the plasma membrane, where viral budding occurs.[196,199] Viral nucleocapsids and VP24 are recruited to these budding sites, a process primarily orchestrated by VP40, which drives the formation and release of new viral particles.[208,209]

b. Emergence

MARV was first identified in 1967 after laboratory workers in Marburg and Frankfurt, Germany and Belgrade (former Yugoslavia) became ill after working with African green monkeys imported from Uganda.[210] To date, there have been 19 known orthomarburgvirus outbreaks, the most recent of which occurred in Tanzania in January 2025 (Table 1-2).[40] RAVV was first identified in 1987 following a fatal VHF case in a tourist who visited Kitum Cave in Mount Elgon National Park, Kenya.[211] Designated as a

distinct virus within the *Orthomarburgvirus marburgense* species in 1996, RAVV has since been identified in two subsequent outbreaks, with the most recent, non-fatal case reported in Uganda in 2007.[48,211,212] Although details about its natural distribution are limited, RAVV has thus far only been detected in regions of East and South Africa where ERBs are found.[213]

Table 1-2: History of orthomarburgvirus outbreaks

Year	Location	Origin	Cases, Deaths, and Case Fatality Rate (%)	Virus	Notes
1967	Germany and Yugoslavia	Uganda	31 cases, 7 deaths (23%)	MARV	Concurrent outbreaks occurred among laboratory workers who were handling African green monkeys imported from Uganda.[210]
1975	South Africa	Zimbabwe	3 cases, 1 death (33%)	MARV	Outbreak in a recent traveler to Zimbabwe, a travel companion, and a health care worker.[214]
1980	Kenya	Mount Elgon National Park, Kenya	2 cases, 1 death (50%)	MARV	Associated with travel history to Kitum Cave.[215]
1987	Kenya	Mount Elgon National Park, Kenya	1 case, 1 death (100%)	RAVV	Associated with travel history to Kitum Cave. RAVV isolate: Rav Ken or 810040.[211]
1990	Russia	Russia	1 case, 1 death (100%)	MARV	Infection due to laboratory contamination.[216]
1998-2000	Democratic Republic of Congo (DRC)	Durba and Watsa, DRC	154 cases, 128 deaths (83%)	MARV, RAVV	Associated with gold mining; multiple genetic lineages of MARV. One RAVV isolate: 09DRC.[212]

2004-2005	Angola	Uige Province, Angola	252 cases, 227 deaths (90%)	MARV	Outbreak spread from Uiga Province to multiple nearby provinces.[49]
2007	Uganda	Kamwenge and Ibanda District, Uganda	4 cases, 1 death (25%)	MARV, RAVV	Associated with lead and gold mining. One RAVV isolate: 02Uga.[217]
2008	USA	Queen Elizabeth National Park, Uganda	1 case, 0 death (0%)	MARV	Associated with travel history to Maramagambo Forest in Queen Elizabeth National Park, Uganda.[218]
2008	Netherlands	Queen Elizabeth National Park, Uganda	1 case, 1 death (100%)	MARV	Associated with travel history to Python Cave in Maramagambo Forest in Queen Elizabeth National Park, Uganda and contact with bats.[219]
2012	Uganda	Kabale, Ibanda, Mbarara, and Kampala Districts, Uganda	15 cases, 4 deaths (27%)	MARV	Associated with putative spillover from ERBs.[220]
2014	Uganda	Kampala District, Uganda	1 case, 1 death (100%)	RAVV	8 exposed contacts developed symptoms but tested negative.[221]
2017	Uganda	Kween District, Uganda	4 cases, 3 deaths (75%)	MARV	No transmission outside of original family cluster.[222]
2021	Guinea	Guéckédou, Guinea	1 case, 1 death (100%)	MARV	Post-mortem diagnosis.[223]
2022	Ghana	Ashanti Region, Ghana	3 cases, 2 deaths (67%)	MARV	No transmission outside of original family cluster.[224,225]
2023	Equatorial Guinea	Kie-Ntem, Littoral, and Centro Sur provinces, Equatorial Guinea	17 cases, 12 deaths (71%)	MARV	Additional 23 probable cases, all fatal, also reported.[226,227]

2023	Tanzania	Kagera region, Tanzania	9 cases, 6 deaths (67%)	MARV	No evidence of link between Eq. Guinea and Tanzania outbreaks.[40,226,228]
2024	Rwanda	Kigali, Rwanda	66 cases, 15 deaths (23%)	MARV	Most cases in healthcare workers.[229-231]
2025	Tanzania	Biharamulo and Muleba districts, Kagera region, Tanzania	10 cases, 10 deaths (100%)	MARV	Epidemiologic investigations are ongoing.[232]

c. Marburg virus Disease

Human cases of Marburg virus disease (MVD) begin 2 to 21 days after initial infection with flu-like symptoms such as fever, chills, headache, myalgia, and general malaise. After approximately 5 – 7 days, the disease progresses to nausea, vomiting +/- hematemesis, mucosal bleeding and petechiation, diarrhea, and a maculopapular rash. End-stage disease quickly progresses to disseminated intravascular coagulation (DIC), lymphopenia and thrombocytopenia, with liver, renal, and/or multi-organ failure and in ~50% of cases, massive hemorrhaging.[233] MARV rapidly replicates in and is disseminated by cells of the macrophage and dendritic cell lineage, causing host immunosuppression and immune dysregulation via failure of appropriate macrophage maturation and lack of T-cell co-stimulation, as well as bystander apoptosis within lymphoid tissues (spleen, lymph nodes) and specific inhibition of the Type 1 interferon system by a variety of viral proteins.[233-240] Vascular dysfunction in end stage disease occurs due to production of tissue factor by macrophages and decreased clotting factor synthesis, both of which occur due to widespread hepatocellular necrosis and the ensuing liver failure.[233]

In juxtaposition to the severe, frequently fatal disease seen in humans infected with MARV and RAVV, ERBs remain clinically healthy following experimental inoculation with MARV and RAVV, developing low-level viremia with widespread, multi-organ virus dissemination detectable by PCR.[4,50] Highest viral loads are detected in the liver, spleen, haired skin at the site of inoculation, and in lymph nodes.[4,50] The predominant histopathologic lesion is mild, transient hepatitis characterized by small, randomly-scattered aggregates of macrophages and lymphocytes, with occasional neutrophils, necrotic, apoptotic, or degenerating hepatocytes, karyorrhectic cellular debris, and scant hemorrhage.[50] Liver lesions peak at 7 days post infection, which correlates with a statistically significant increase in alanine aminotransferase (ALT) and viral load PCR data.[50]

d. Ecology, Experimental Studies and Animal Models

Numerous longitudinal ecological studies have identified the ERB as a natural reservoir host for both RAVV and MARV.[3,48,50,94-96] Epidemiological investigations into the protracted 1998-2000 MVD outbreak in DRC linked documented cases to gold mining activity.[212,241] Large cave-dwelling colonies of ERBs adjacent to these mines were found to harbor MARV-specific RNA and IgG antibodies, with short viral RNA sequences similar or identical to those detected in human cases.[94] Studies conducted at the 2007 and 2008 MVD outbreak sites of Kitaka Mine and Python Cave in Queen Elizabeth National Park in Uganda confirmed the presence of seropositive, RNA-positive ERBs capable of transmitting MARV and harboring genomic sequences closely resembling those in human cases.[3,48] These studies revealed that adult ERBs exhibited the highest IgG antibody levels, while juvenile bats (approximately 6 months old) showed

the highest levels of active infection, along with a temporal association between MARV disease spillover to humans and seasonal, biannual pulses of active MARV infection in juvenile ERBs.[3,46,48] Between 2007-2009, infectious MARV was isolated from a total of 21 ERBs sampled at Kitaka Mine and Python Cave in Queen Elizabeth National Park[3,48,93], including the first successful isolation of infectious RAVV.[48] To date, at least four ERB isolates ("44Bat," "188Bat," "982Bat," "1304 Bat") of RAVV have been obtained.[242]

Experimental studies have identified the ERB as a competent model for orthomarburgviruses[4,45,50,243,244], as well as documented successful horizontal transmission of MARV between experimentally inoculated and naïve, co-housed ERBs in an laboratory setting.[46] ERBs experimentally inoculated with MARV exhibit transient subclinical disease characterized by viremia (detected 1-16 days post infection (DPI), 12/12 bats (100%), mean duration = 6.0 days, mean day of mean peak load = 6.8 DPI)[46], oral shedding (detected 5-19 DPI, 11/12 bats (91.7%), mean duration = 4.6 days, mean day of mean peak load = 9.1 DPI) with successful isolation of infectious MARV from 9/51 (17.6%) of MARV RT-qPCR-positive oral swabs[46], and rectal shedding (detected 6-13 DPI, 4/12 bats (33.3%), mean duration = 1.5 days, mean day of mean peak load = 6.8 DPI). MARV shedding in the urine of experimentally infected ERBs has been documented (detected 10-16 DPI, 2/12 bats (16.7%))[46] but is limited by the challenging nature of specimen collection and likely not fully characterized.[4,46] In previous studies, MARV-inoculated ERBs exhibited robust seroconversion to MARV, with MARV IgG antibodies peaking between 12 DPI and 28 DPI[4,46,244], followed by a decline of antibody levels falling below the threshold of seropositivity by 3 months post-infection (MPI).[46]

Despite diminished IgG levels, robust longstanding immunity to reinfection upon experimental inoculation with MARV has been documented in ERBs up to two years after initial infection.[47]

MARV has been well-studied in numerous animal models and in vitro and in vivo experimental studies, including recent research utilizing transcriptomics to elucidate ERB immunology and responses to infection.[15,98,101,233,235,245-252] However, there has been limited experimental characterization of RAVV and of comparisons of virulence between RAVV and MARV in ERBs, both are which are of heightened importance due to the >20% genetic difference in the surface glycoprotein between MARV and RAVV.[48] To date, the limited studies utilizing RAVV include vaccine efficacy studies in cynomolgus macaques[253,254], mice[255] and guinea pigs[256], therapeutic treatment trials of MARV and RAVV infection in non-human primates (NHPs) with human monoclonal antibodies[257] and small interfering RNA (siRNA)[258], and characterization of the lack of observable clinical disease upon experimental inoculation with RAVV in ferrets.[259,260] Genetic variation between MARV and RAVV could influence transmission dynamics, pathogenicity, and potentially responses to treatments or vaccines. A recent study comparing experimental infection of different orthomarburgviruses in macaques found distinct pathogenicities between RAVV, MARV Angola, and variant isolates Musoke and Ozolin, and additionally found that, despite seroconversion in all animals, RAVV is lethal in cynomolgus macaques but not rhesus macaques.[261] Further, a comparison of the pathogenesis of RAVV, MARV variant isolates Musoke and Popp, and MARV Angola in a serially adapted outbred guinea pig model found delayed increases in circulating inflammatory and prothrombotic elements, lower viremia levels, less severe histologic

disease, and a delay in mean time to death in RAVV infection compared to MARV Angola.[247] To date, experimental characterization of RAVV infection in its ERB reservoir has not been completed.

4. IMMUNOLOGY

Prior to the early 2000's, research into bat immunology was scant at best, hampered by a lack of immunological reagents reactive to bat proteins, significant species diversity within Chiroptera[262], and a limited number of established captive colonies for experimental research.[86] Recently there has been renewed interest in the field, thanks in part to the detection or isolation of numerous viruses from bats that cause severe and economically important disease within both the human and animal populations, including Hendra virus, Nipah virus, orthoebolaviruses, and SARS-CoV.[41,263-271]

There are four ERB genomes listed in NCBI; the reference genome (mRouAeg1.p) is a near-complete (98.7%) genome submitted in August 2020 by The Bat1K project, and has proven to be a valuable resource for understanding the genomic basis of bat adaptions and cross-species comparisons.[272] The annotated ERB genome has revealed unique features that support the theory of disease tolerance for this species: 1) expansion of the type I interferon family, most notably interferon-ω genes, 2) expansion of natural killer (NK) cell receptors, many of which have inhibitory signaling capabilities, and 3) the presence of Major Histocompatibility Complex (MHC) class I genes outside of the typical chromosomal loci, which is suggestive of possible MHCI gene dispersion and expansion.[99] Recent immunological advances include characterization of the STAT1 protein[273], and in vivo and in vitro data which shows that, upon infection with Marburg

virus, ERBs demonstrate inducible cell- and tissue-specific interferon responses, and upregulate antiviral genes such as *ISG15*, *IFIT1* and *OAS3*, yet with minimal concurrent upregulation of proinflammatory genes including *CCL8*, *FAS*, and *IL6*.[97,101] Additionally, infection of dendritic cells derived from the bone marrow of ERBs showed low levels of transcription and significant downregulation in DC maturation and adaptive immune-stimulatory pathways, while simultaneously upregulating interferon-related pathogen sensing pathways.[100]

5. COINFECTIONS

The prevalence of coinfections in free-ranging bat populations is poorly understood, typically noted incidentally rather than through systematic study.[52] A recent retrospective analysis of ERB tissues from bats living in Kitaka Mine, Uganda showed that 19% of the juvenile bats actively infected with MARV were also infected with SOSV and identified an ERB simultaneously coinfected with MARV, SOSV, and Yogue virus (family *Orthonairoviridae*, genus Orthonairovirus).[274] Broader surveillance across various bat species and regions has revealed coinfections involving viruses from multiple families, highlighting the ecological complexity of viral maintenance in bats. A comprehensive surveillance effort in China revealed that 42% of sampled bats from six genera and 15 species were coinfected with at least two viruses spanning 12 viral families.[55] In Madagascar and Mozambique, 2.4% of samples tested from 28 bat species across 8 families tested positive for coinfections involving astroviruses, coronaviruses, and paramyxoviruses.[57] Coinfections with highly divergent astrovirus strains have been reported in free-ranging insectivorous bats in Poland[53], with numerous coronavirus strains in bats in China[56,58], Hong Kong[54], Viet Nam[63], Cambodia[59], Ghana[64], with

flaviviruses in *Molossus sp.* bats in Trinidad[65], with paramyxoviruses in Pteropid bats in Australia[62], with herpesviruses in Germany[66] and Indonesia[67], with endogenous retroviruses in *Myotis tricolor* bats in Kenya[68] and with rubulaviruses in ERBs in South Africa.[60] High rates of coronavirus and adenovirus coinfections were found in gastrointestinal samples of *Myotis ricketti* bats in Macau.[69] In Zimbabwe, up to 3.5% of insectivorous and frugivorous bats were coinfected with coronaviruses and astroviruses[71], with additional cases observed in a *Pipistrellus pipistrellus* bat in Hungary[72], and in 15 *Hipposideros cervinus* bats in Borneo.[73] In Denmark, two *Myotis* sp. bats were coinfected with coronavirus and astrovirus, while another *Myotis* sp. bat was coinfected with at least seven viruses: two astroviruses, two coronaviruses, two caliciviruses and a polyomavirus.[73] Coronavirus and paramyxovirus coinfections have been reported in one *Pipistrellus pipistrellus* bat in Italy[74] and in one *Rhinopoma hardwickii* and two *Chaerephon pumilus* bats in Ethiopia.[75] Lastly, surveillance in the Republic of Korea identified coinfections of a bat retrovirus and coronavirus in a *Rhinolophus ferrumequinum* bat, alongside the discovery of two distinct picornaviruses from a fecal sample.[76]

There are few reports of coinfections in bats with either divergent bacterial species within the same family, with bacterial and viral pathogens, or with fungal and viral pathogens. In Bangladesh, investigation into *Bartonella* spp. prevalence in bats revealed a coinfection producing distinct clade A and B sequences on a single blood spot.[275] Bartonella spp. surveillance in northern China found one *Myotis fimbriatus* bat coinfected with phylogroup II and VI, and one *Myotis pequinius* bat with phylogroup I and IX.[276] *Leptospira* spp. and paramyxovirus coinfections were frequently detected in

Mormopterus francoismoutoui bats, a molossid bat endemic to Réunion Island, Seychelles.[277] Finally, there is a single report of a rabies virus and fungal pathogen *Histoplasma capsulatum* coinfection in a *Molossus molossus* bat in Brazil.[278]

Mathematical models using susceptible (S), exposed (E), infectious (I), and recovered (R) compartments (SEIR models) have been employed to estimate orthomarburgvirus transmission patterns in ERB populations.[279] Using this model, a closed population of 40,000 ERBs with a biannual birth pulse and 21-day latent period predicted an active MARV infection prevalence of less than 2.0%, closely matching the 2.5% observed in previous ecological studies[3] and is corroborated by serological data from MARV experimental studies in managed care ERBs.[4,46,243,244] While the SEIR framework is useful for modeling filovirus ecology, additional ecological and biological factors likely shape reservoir host and infection trajectories, e.g. metapopulation dynamics, the duration of protective immunity, natural immune stressors, and the role of coinfection in shaping susceptibility patterns and immune responses.[98,280] Whether coinfection in ERBs alters the duration of immunity or hastens the return to susceptibility remains unknown but carries significant implications for viral persistence and transmission in free-ranging host populations.

Immunological memory is established by a system's specific, adapted response utilizing both cell-mediated immunity (development, selection, and maintenance of an antigen-specific memory T-cell pool) and humoral immunity (activation of B cells, differentiation into antibody-secreting plasma cells and memory B cells via affinity maturation (somatic hypermutation of antibody-variable-region (V-region) genes) and class switching).[281] Despite being within the same viral species, the full genomic

sequence of RAVV differs by up to 21% from MARV and the amino acid sequence of the RAVV glycoprotein (GP) differs by ~22% from MARV GP[48,49], and as such may generate antigenically distinct pathogen-associated molecular patterns (PAMPs). Therefore, the more sensitive and specific actions of effector T cells and class-switched, affinity-matured antibodies that would provide protective immunity for homotypic inoculation may not be able to block infection of a heterotypic isolate, and viral replication and shedding may be seen. The extent to which heterotypic inoculation will allow viral replication and shedding in a previously MARV-monoinfected ERB or in a previously KASV+MARV coinfected ERB is currently unknown.

A recent experimental study found that viral coinfection in ERBs can modulate viral shedding dynamics and subsequent antibody development, suggesting alterations to long-term immunity.[282] ERBs experimentally infected with SOSV+MARV had significant reduction in the duration of MARV shedding, whereas ERBs coinfected with KASV+MARV had significantly increased peak magnitude and duration of MARV viremia and oral shedding, resulting in significantly higher cumulative MARV shedding in KASV+MARV coinfected bats.[282] Prior to this study, experimental studies on coinfections in bats were limited to investigations into interactions between coronaviruses and non-viral pathogens. A 60-fold increase in coronavirus RNA was observed in the intestines of *Myotis lucifugus* bats coinfected with *Pseudogymnoascus destructans*, the fungal pathogen that causes white nose syndrome.[283] Considering the frequent occurrence of viral coinfections in free-ranging populations and the high contact rates in densely populated roosts that result in viral re-exposure, the effect of viral coinfections on subsequent viral inoculation needs to be better understood.

This chapter provides an overview of the relevant literature pertaining to the unique natural history traits of bats, with a focus on the ERB. A review of viral, bacterial, fungal, and parasitic pathogens previously reported in free-ranging and managed care ERBs, and iron overload are provided. Further, an introduction to the emergence, virology, pathogenesis and associated pathology, and experimental studies of orthomarburgviruses, as well as a discussion of coinfections in bats, is presented. These topics are presented as an introduction to the dissertation chapters presented herein, which will elucidate ERB pathobiology via characterization of baseline pathologic features of the ERB lymphoid system and of free-ranging ERBs, experimental characterization of viral shedding dynamics for RAVV infection in ERBs, and elucidation of the influence of viral coinfections in long-term immunity upon inoculation with highly diverse orthomarburgviruses.

CHAPTER 2

IMMUNOLOGIC REVIEW AND ATLAS OF NORMAL GROSS AND HISTOLOGIC LYMPHOID ANATOMY OF THE EGYPTIAN ROUSETTE BAT (*ROUSETTUS AEGYPTIACUS)*[1]

[1] Elbert JA, Amman BR, Sealy TK, Atimnedi P, Towner JS, and Howerth, EW. To be submitted to a peer-reviewed journal.

ABSTRACT

Bats possess highly specialized immune systems that enable them to serve as subclinical reservoir hosts for numerous zoonotic viruses of public health importance. The Egyptian rousette bat (ERB; *Rousettus aegyptiacus*) is a key reservoir host for multiple high-consequence zoonotic pathogens, yet fundamental aspects of its immune system remain underexplored. This study presents a comprehensive review of the innate and adaptive immune responses of ERBs, integrating current literature encompassing experimental infection data, comparative genomics, and in vitro organoid models. Distinctive features of bat antiviral immunity are described, including tightly regulated interferon response, restructure proinflammatory cytokine expression, expanded immunogenetic repertoires, and developmental variation in lymphoid cell populations. In addition, this work presents a novel histologic and immunohistologic atlas of the ERB lymphoid system, detailing the structure and cellular organization of primary and secondary lymphoid organs. The resulting resource provides critical anatomical and cellular context for researchers investigating ERB immunobiology, host-pathogen interactions, and comparative pathology. These findings contribute to a broader understanding of the unique immune adaptations that enable viral tolerance in bats and offer new insights to inform future research on reservoir competence, zoonotic spillover, and emerging infectious disease ecology.

KEYWORDS: Egyptian rousette bat, *Rousettus aegyptiacus,* histology, immunology, lymphoid system, reservoir

INTRODUCTION

Bats (Order Chiroptera, meaning "hand wing") are incredibly diverse, with more than 1,400 known species that account for more than 20% of the world's mammalian population.[2] Second only to rodents in species diversity, bats inhabit all continents except Antarctica and have broad ecological, anatomical, and environmental diversity that is nearly unparalleled within the animal kingdom.[1,2] Bats are divided into two major suborders: Yinpterochiroptera, which includes pteropid fruit bats and several microbat families, and Yangochiroptera, comprising the remaining microbat families; these groups differ markedly in echolocation strategies, diet, and immune gene evolution, reflecting deep phylogenetic divergence within Chiroptera.[284,285]

Bats are known to host an incredible diversity of viruses, with sequences of over 22,000 strains from more than 200 viruses across 32 viral families associated with bats through serology, molecular detection, or virus isolation; however, they likely host many more.[286,287] Evidence from experimental viral studies and natural viral infections in bats have largely demonstrated little to no clinical or pathological signs of disease.[4,16-18,46,48,288-291] Exceptions to this include rabies virus and the closely related Australian bat lyssavirus[83,292,293], Tacaribe virus in natural[294] and experimental[295] infections in *Artibeus jamaicensis* bats, and *Miniopterus schreibersii* bat die-offs in Europe associated with Lloviu virus infection.[296] Additionally, bats host parasitic, bacterial, and fungal pathogens that, unlike viral infections, have been shown to cause significant disease. Examples include mass mortality events in North American bat populations associated with *Pseudogymnoascus destructans*, the fungus that causes White-Nose Syndrome, bacterial abscesses in ERBs in Israel, and, to a lesser extent, pathology has been associated with

the tick-borne bacteria *Borrelia* spp., and some enteric bacteria.[297-300] It has been theorized that bats may have evolved mechanisms to eliminate viral pathogens at the expense of their ability to eliminate bacterial, fungal, and parasitic pathogens, with mitochondrial adaptations possibly playing a role in this evolution.[301]

The Egyptian rousette bat (ERB; *Rousettus aegyptiacus;* common name Egyptian rousette), a yinpterochiropteran pteropodid species, is a key natural reservoir host for the orthomarburgviruses Marburg virus and Ravn virus (MARV; RAVV; family *Filoviridae*; genus *Orthomarburgvirus*)[3,48,50], both of which are the causative agents of Marburg virus disease (MVD), a severe viral hemorrhagic fever that typically emerges in sub-Saharan Africa characterized by human-to-human transmission and high case fatality ratios up to 90%.[49,196] ERBs also serve as a vertebrate reservoir for Kasokero virus (KASV; family *Orthonairoviridae*, genus *Orthonairovirus*)[8], and are presumed to be a natural reservoir for Sosuga virus (SOSV; family *Paramyxoviridae*, genus *Pararubulavirus*).[6,7,116,282] The increasing emergence of zoonotic, frequently high-consequence pathogens such as MARV, Hendra virus, and SARS-CoV, have heightened research interest in bats as vectors of disease and natural reservoir hosts, with special focus on understanding the immunological and virological mechanisms by which bats serve as vectors for often severe, frequently zoonotic diseases with minimal to asymptomatic clinical disease in themselves.[36,56,263,302]

Given the central role of ERBs in filovirus ecology and zoonotic spillover events, a comprehensive understanding of ERB-specific immunology and lymphoid tissue architecture is essential to elucidate host-pathogen interactions and inform public health strategies. This review begins with an overview of the existing literature on ERB

immunity, followed by an in-depth review of its lymphoid system. In support of this effort, presented herein is a detailed, ERB-specific gross and histologic atlas of primary and secondary lymphoid tissues, designed to serve as a reference for pathologists, scientists, and researchers working with this important reservoir species.

MATERIALS AND METHODS

Two ERB fetuses from free-ranging dams, in addition to two juvenile and two adult captive-born[4] ERBs were used in this study. As previously described, all capturing, processing, and procedures were performed in accordance with an institutionally approved animal care and use protocol.[3,48] Bat collections were completed with the approval of the Uganda Wildlife Authority and following the American Veterinary Medical Association guidelines on euthanasia and the National Research Council recommendations for the care and use of laboratory animals.[3]

The two ERB fetuses were near-term (approximately stage 24 and 25 of embryonic development[303]) and collected in 2008-9 as part of investigative efforts conducted by the Centers for Disease Control and Prevention (CDC) into discovery of the orthomarburgvirus natural reservoir host. Sex was not determined. Fetal carcasses were fixed in 10% neutral buffered formalin as intact specimens at the time of capture. Necropsies were performed in 2023, and representative sections of primary and secondary lymphoid tissues were taken.

Two 6-month-old juvenile ERBs (one male, one female) were utilized as negative controls in an experimental study where ERBs were euthanized at study termination.[282] Cranial, abdominal +/- thoracic cavities were exposed to allow for 10% neutral buffered formalin fixation, and carcasses were fixed as intact specimens. Necropsies were

performed and representative sections of primary and secondary lymphoid tissues were collected.

Two adult ERBs (male, 10-year-old; female, 12-year-old) were selected from the managed care research colony at CDC. Blood samples (≤10 μL) were collected via venipuncture from the cephalic vein on the propatagium and immediately used to prepare four to five thin blood smears on glass slides per bat. Blood smears were inactivated via submersion in 10% neutral buffered formalin for 20 minutes and stained with Epredia Shandon Kwik-Diff Stains (Thermo Fisher Scientific, Waltham, MA, USA). Bats were euthanized as previously described.[282] Tissue samples from all bats were routinely processed and embedded in liquid paraffin. Sections were cut at 4 μm, mounted on glass slides, and stained with hematoxylin and eosin (HE).

Immunohistochemical stains for ionized calcium-binding adapter molecule 1 (Iba1), a pan-macrophage and dendritic cell marker; CD3, a T cell marker; CD79a, a B cell marker; and Granzyme B, a natural killer cell and cytotoxic T lymphocyte marker; were performed on formalin-fixed, paraffin-embedded (FFPE) sections of all primary and secondary lymphoid tissue using an automated stainer (Nemesis 3600, Biocare Medical, Concord, CA, USA) at the University of Georgia Histology Laboratory. For the Iba1 protocol, a rabbit polyclonal antibody directed against Iba1 (1:8000 final dilution; Wako, Richmond, VA, USA.; catalog #019-19741) was incubated on the tissue for 60 min. For the CD3 protocol, a rabbit polyclonal antibody targeting the CD3 epsilon subunit (1:1000 final dilution; Dako, Carpinteria, CA, USA.; catalog #A0452) was incubated on the tissue for 60 min. For the CD79a protocol, a mouse monoclonal antibody directed against CD79a (1:50 final dilution; Biocare Medical, Pacheco, CA, USA; catalog #CM067C)

was incubated on the tissue for 60 min. For the Granzyme B protocol, a rabbit polyclonal antibody directed against Granzyme B gene 3002 (1:200 final dilution; Spring BioScience/Roche, Pleasanton, CA, USA; catalog #E2582) was incubated on the tissue for 60 min. Antigen retrieval for all stains was performed using Antigen Retrieval Citra Solution 10X (Biogenex/Thermo Fisher Scientific, Waltham, Massachusetts, USA) at a 1:10 dilution for 15 min at 110 °C. A biotinylated rabbit or mouse secondary antibody (Vector Laboratories, Burlingame, CA, USA) was used to detect the antibody targets, and the immunoreactions were visualized using a 3,3-diaminobenzidine substrate (DAB; Dako, Santa Clara, CA, USA) for 12 min. The slides were counterstained with hematoxylin and cover slipped.

LITERATURE REVIEW

The mammalian host immune response can be broadly broken down into two components: innate immunity and adaptive (or acquired) immunity. While many aspects of Chiropteran immunity are still unknown, bats maintain many conserved features of mammalian immunity. This review provides an overview of these immune components with a focus on unique features of ERBs.

1. OVERVIEW OF BAT IMMUNITY

a. SUBORDERS AND IMMUNE STRATEGY DIFFERENCES

Numerous reviews in recent years have explored the chiropteran immune system and recent advancements in our understanding of chiropteran immunity.[26,86,262,304-309] Bats from the two major suborders, i.e., Yinpterochiroptera and Yangochiroptera, have distinct immune strategies shaped by their evolutionary divergence. Yinpterochiropteran bats, such as pteropodids (e.g., ERBs) often show constitutive expression of type I interferons

(IFNs) and interferon-stimulated genes (ISGs), suggesting an "always on" antiviral state that may contribute to viral tolerance without excessive inflammatory output.[99,272,310] In contrast, Yangochiropterans, including many insectivorous species such as *Myotis* sp., have more inducible IFN responses, with stronger transcriptional activation only upon viral challenge, possibly reflecting a more conventional mammalian immune strategy.[27,272,311] These differences likely underlie variation in disease tolerance and viral reservoir competence observed between bat species.

b. RESERVOIR COMPETENCE AND TOLERANCE HYPOTHESIS

To be considered a reservoir host of a pathogen, an animal must support replication and shedding of a pathogen, typically without developing severe disease, and contribute to maintenance of the pathogen indefinitely in the reservoir host population.[312,313] Key traits include the ability to harbor the pathogen persistently or intermittently, to shed the infectious agent into the environment or to other hosts, and to transmit the pathogen under natural conditions to one or more target species, including humans.[314] Reservoir hosts often exhibit tolerance mechanisms that limit immunopathology despite ongoing infection, allowing them to act as asymptomatic carriers.[315] Additional ecological traits such as high population density, broad geographic distribution, migratory behavior, and frequent human or domestic animal contact can further enhance their role in zoonotic spillover.[33,280,314]

Numerous longitudinal ecological studies have identified the ERB as a natural reservoir host for both RAVV and MARV.[3,48,50,94-96] These studies revealed that adult ERBs had the highest IgG antibody levels, while juvenile bats (approximately 6 months old) showed the highest levels of active infection, along with a temporal association

between MARV disease spillover to humans and seasonal, biannual pulses of active MARV infection in juvenile ERBs.[3,46,48] Additionally, numerous experimental studies have identified the ERB as a competent natural reservoir model for orthomarburgviruses[4,45,50,243,244,289], as well as have documented successful horizontal transmission of MARV between experimentally inoculated and naïve, co-housed ERBs.[46]

Early theories posited that bats possess unique resistance mechanisms that allow them to effectively clear viral infections, contributing to their role as reservoir hosts.[316] However, accumulating evidence now supports a more nuanced model of viral disease tolerance, wherein bats limit immunopathology rather than eliminating viral infection.[301,316,317] This tolerance is characterized by dampened proinflammatory responses, constitutive or tightly regulated IFN signaling, and an enhanced capacity to coexist with high viral loads without developing disease.[15,20,27,97,317-325] These features distinguish bats from other accidental hosts, which often experience severe pathology and mortality from infection with the same viruses.[317] Genomic, in vitro, and in vivo research that supports this theory of viral tolerance as it pertains to ERBs will be discussed throughout this review.

2. INNATE IMMUNITY

Innate immunity serves as the body's first line of defense, providing immediate and nonspecific protection against pathogens. Key features of the innate immune response include 1) physical and chemical defenses at epithelial barriers to block microbial entry 2) providing the initial responses to control or eliminate infection 3) elimination of damaged cells and early reparative mechanisms and 4) activation and

modulation of the adaptive immune response.[326] Anatomic and physiologic barriers – such as intact skin, mucociliary clearance mechanisms, low gastric pH, and bacteriolytic lysozyme in tears, saliva, and other secretions - provide the crucial first line of defense against pathogens.[327] Innate immunity augments the protection offered by anatomic and physiologic barriers, relying on a limited repertoire of receptors that target conserved microbial components to detect invading pathogens.

Intrinsic antiviral immunity constitutes a cell-autonomous branch of innate immunity that restricts viral replication and assembly.[328] When a virus enters a host cell, pathogen-associated molecular patterns (PAMPs) - such as single- and double-stranded viral RNA (ssRNA and dsRNA) – are recognized by pattern recognition receptors (PRRs).[326] These include toll-like receptors (TLRs) 3, 7, 8 and 9, as well as RNA helicases such as melanoma differentiation-associated protein 5 (MDA5) and retinoic-acid inducible gene I (RIG-I).[326] TLRs have been described in *Rousettus leschnaultii* bats and are highly conserved between bats and other mammals.[329] In vitro functional assays of TLR2 - which forms heterodimers with TLR1 or TLR6 on cell membranes that recognize PAMPS – have shown significantly reduced activity in bats, resulting in dampened inflammatory signaling.[330] Upon activation, PRRs trigger downstream signaling cascades that activate interferon regulatory factors (IRFs) 1, 3, and 7, leading to the production of a suite of proinflammatory and anti-viral cytokines.[326] These include IFNs, interleukin-6 (IL-6), tumor necrosis factor (TNF), pro-IL-1β, and IL-12.[326]

a. MOLECULAR AND GENOMIC FEATURES

i. COMPARATIVE GENOMICS AND TRANSCRIPTOMICS

In 2015, the first annotated transcriptome of the ERB was published, revealing that 2.75% of the *Rousettus* genome (roughly 407 genes) is immune-related.[331] This foundational work enabled further genomic investigation and supported in silico data mining for immune function in this species. Building on this resource, Pavlovich et al. developed and analyzed an updated annotated genome for ERBs. Their findings included expanded and diversified repertoires of natural killer (NK) cell receptors, major histocompatibility complex (MHC) class I genes, and type I IFNs, features that suggest novel modes of antiviral defense.[99] Subsequent analysis led to the discovery of a remarkable expansion of IFN-ω genes in ERBs, with 22 members identified in the INF-ω subfamily.[102]

Recent single-cell and spatial transcriptomic analyses of ERBs have provided key insights into the bat's immune architecture, particularly within barrier tissues.[318] Despite extensive genomic rearrangements in type I IFN gene families, the expression and inducibility of IFNs in ERBs were found to be highly conserved and comparable to those observed in mice and humans.[318] Notably, IFN induction was restricted to a discrete subset of monocytes following immune stimulation, suggesting tight regulatory control aimed at minimizing excessive inflammation.[318] In contrast, the complement system of ERBs exhibited remarkable transcriptional and evolutionary divergence. Core complement components—including genes encoding the membrane attack complex—were uniquely and highly expressed in epithelial cells of the bat lung and gut, especially within intestinal crypt regions.[318] This expression pattern was not observed in human or mouse tissues.[318] Proteomic analysis further confirmed the abundance of complement proteins in bat serum, and functional assays demonstrated strong hemolytic activity,

reflecting a robust and active complement system.[318] Additionally, a transcriptomics analysis comparing the in vitro antiviral response across bat species revealed species-specific strong upregulation of genes associated with disease tolerance in ERB cells.[332] Analyses of in vivo filovirus infection in ERBs showed reduced induction of proinflammatory genes during infection.[97,267] While not specifically tested in ERBs, significant dampening of the NLR family pyrin domain containing 3 (NLRP3) inflammasome has been reported in *Pteropus alecto* primary immune cells.[310] Importantly, ERBs share an identical amino acid sequence of the N-terminal NLRP3, suggesting that a similar dampened inflammasome may occur in this species as well.[310]

ii. GENOMIC ADAPTATIONS

ERBs possess a structurally conserved but highly diversified form of tetherin - a restriction factor that inhibits the release of certain viruses from host cells.[333] This form of tetherin is expressed across multiple tissue types and is upregulated in response to immune stimulation with TLR agonists.[333] Evidence of strong positive selection acting on ERB tetherin genes suggests that this antiviral factor has undergone adaptive evolution, likely in response to selective pressures from enveloped viruses.[333]

Genomic analysis of the IRF gene family in ERBs has revealed evidence of positive selection in several key IRF genes, including IRF-1, IRF-4, IRF-5, IRF-6, and IRF-9, suggesting adaptive optimization of antiviral and immunomodulatory pathways.[334] IRF-1 and IRF-9, which play central roles in type 1 IFN signaling and the induction of ISGs, exhibited strong signatures of positive selection that may enhance early and IFN-independent antiviral responses.[334] In contrast, IRF-4 and IRF-5, which regulate pro-inflammatory signaling through TLR pathways, also showed signs of positive selection,

potentially reflecting a refined ability to limit excessive inflammation and preventing immune-mediated tissue damage.[334] Interestingly, IRF-6, typically associated with epithelial development, also displayed positively selected sites that may relate to mucosal immune regulation, suggesting an additional layer of immune specialization at epithelial barriers.[334]

iii. INTERFERON SIGNALING PATHWAYS AND ANTIVIRAL EFFECTORS

A critical component of the ERB innate immune system is the role of IFN in mediating viral defense and tolerance.[100,335-337] Type I IFNs, primarily IFN- α and IFN- β, are cytokines produced by a wide range of cell types upon detection of viral nucleic acids through PRRs such as RIG-I and TLRs.[326] Type I IFNs signal through the IFNAR receptor complex to induce hundreds of ISGs that establish an antiviral state, enhance antigen presentation, and modulate both innate and adaptive immune responses.[338,339] These ISGs include protein kinase receptor (PKR), an inhibitor of viral transcription and translation; 2',5' oligoadenylate synthetase (OAS) and RNase L, which promote viral RNA degradation; and Mx GTPases, which inhibit viral gene expression and virion assembly.[326] IFN-γ is the only Type II IFN, primarily produced by activated T cells and NK cells, playing a central role in orchestrating cell-mediated immunity.[340,341] IFN-γ promotes antigen presentation by upregulating MHC class I and II molecules, activates macrophages, and enhances the antimicrobial and antiviral activity of immune cells.[340,341] IFN-λ, also known as type III IFN, is a recently classified IFN primarily produced by epithelial cells and plasmacytoid dendritic cells (pDCs) in response to viral infection.[342,343] IFN-λ signals through a distinct receptor complex (IFNLR1 and IL10R2), with expression largely restricted to epithelial tissues, where it plays a crucial

role in mucosal antiviral defense with reduced proinflammatory effects compared to type I IFNs.[342,343]

IFNs exert their antiviral effects by binding to specific cell surface receptors, which in turn activate the JAK-STAT signaling pathway.[326] Upon receptor engagement, Janus kinase (JAK) enzymes associated with the receptors become activated, leading to the phosphorylation of cytoplasmic signal transducer and activator of transcription (STAT) proteins.[273,281,326] Once phosphorylated, STAT1 and STAT2 form a dimer and interact with IRF9. This complex translocates into the nucleus, where it promotes the expression of ISGs that work collectively to establish an antiviral state within the cell.[273,281,326] In ERB cells, stimulation with human IFN-α resulted in phosphorylation and translocation of STAT1 into the nucleus, demonstrating that the JAK-STAT signaling cascade is conserved and function in ERBs, similar to what is observed in other mammals.[273]

In ERB RoNi/7 cells, investigation of the OAS-RNase L pathway revealed that treatment with IFN-α or viral infection induces expression of all three ERB OAS mRNAs, primarily OAS3, while RNase L mRNA is constitutively expressed.[344] This suggests that RNase L activation is primarily dependent on OAS3, that OAS proteins serve as PRRs, and that the OAS-RNase L pathway functions as a primary antiviral response rather than a secondary effect of IFN signaling.[344] Type I IFNs also play an important role in immune cell trafficking by promoting the sequestration of lymphocytes in lymph nodes. This is mediated through upregulation of CD69 and downregulation of the sphingosine 1-phosphate receptor (S1PR1) on lymphocytes, increasing the likelihood that lymphocytes will encounter viral antigens.[326] In addition, type I IFNs enhance

cytotoxic responses by boosting NK cell and CD8+ T cell cytotoxicity and upregulating MHC-I expression, thereby increasing the visibility of infected cells to cytotoxic lymphocytes.[326] Finally, type I IFNs induce the expression of TNF-related apoptosis-inducing ligand (TRAIL) on NK cells.[326,345] This provides an additional mechanism for eliminating infected target cells that is independent of traditional NK cell activating receptors. In ERB cells, the lone type II IFN, IFN-γ, is induced in response to Marburg virus infection, but not Ebola virus (EBOV), highlighting the disparate immune responses of ERBs to these two filoviruses.[346] In ERB-derived organoids, INF-ε, a non-canonical type 1 IFN, was constitutively expressed in pulmonary and small intestinal organoids, leading to elevated baseline expression of genes encoding innate immune effectors.[347]

Previous studies investigating IFN expression have shown idiosyncratic IFN expression, both within and between chiropteran species. *Pteropus alecto* bats and *Cynopterus brachyotis* bats had high baseline expression of IFN-α and other IFN signaling molecules, suggesting a primed immune state that enables rapid responses to microbial infections.[348,349] In contrast, ERBs had a lower constitutive IFN-α expression, indicating that a uniformly elevated baseline IFN response is not a universal trait among bat species.[346] Interestingly, more recent findings show significantly elevated constitutive IFN-α protein plasma levels in ERBs and *Pteropus rodricensis* bats, compared to *Eidolon helvum* bats and *Pteropus lylei* bats.[350] The constitutive *Ifna* gene expression appears to induce a profile of ISGs that are non-inflammatory, potentially explaining how elevated *Ifna* expression in some bat species does not lead to chronic inflammatory pathology.[305] When primary kidney cells from *R. leschnaultii* were stimulated with polyinosinic–polycytidylic acid (poly(I:C)), a synthetic TLR ligand, there was increased production

and mRNA expression of both IFN-α and IFN-β.[335] However, no expression was detected without poly(I:C) induction, and it is worth noting that kidney cells differ significantly from circulating immune cells in vivo.[335]

In ERB-derived organoids, INF-ε, a non-canonical type 1 IFN, was constitutively expressed in pulmonary and small intestinal organoids, leading to elevated baseline expression of genes encoding innate immune effectors.[347] Expression of this IFN subtype was not driven by viral PAMPs or PRR signaling, and the mechanisms behind INF-ε expression and production have yet to be elucidated.[351] In ERB organoids, genes encoding type III IFNs (specifically IFNL1-like and IFNL3-like) were the most strongly induced among all IFN-encoding genes, highlighting a central role for type III IFN signaling in bat antiviral immunity.[347,351]

b. CELLULAR COMPONENTS

i. INNATE IMMUNE CELL POPULATIONS

Immune cells that play key roles in innate antiviral defenses include macrophages, monocytes, dendritic cells (DCs) and NK cells.[326] DCs are professional antigen-presenting cells (APCs) that serve as key sentinels of the innate immune system, detecting invading pathogens through PRRs such as TLRs and RIG-I-like receptors.[326] Upon pathogen recognition, DCs produce cytokines and chemokines, upregulate costimulatory molecules (e.g., CD80, CD86), and migrate to lymphoid tissues to activate naïve T cells, thereby serving as a critical bridge between innate and adaptive immunity.[352,353] Certain subsets of DCs, such as pDCs, are also potent producers of type I IFNs, notably IFN-α, greatly enhancing systemic antiviral responses.[354]

NK cells utilize activating and inhibitory receptors to detect abnormal cells, particularly those with downregulated MHC class I molecules, which is a common viral evasion strategy. Key activating receptors include NKG2D and natural cytotoxicity receptors (NCRs), while inhibitory receptors such as KIRs (killer cell immunoglobulin-like receptors) and CD94/NKG2A recognize MHC-I and prevent inappropriate destruction.[355-357] Upon activation, NK cells induce apoptosis in target cells via two primary mechanisms: release of cytotoxic granules containing perforin and granzymes, and engagement of death receptors like Fas (also known as CD95 or APO-1 or TNFRSF6) with Fas ligand (FasL). NK cell activity is further modulated by cytokines such as IL-12, IL-15, and IL-18, which activate signaling cascades through JAK-STAT pathways, enhancing cytotoxicity.[355,357] They are additionally the primary producers of IFN-γ, which facilitates several crucial immune functions: it promotes the activation of phagocytic cells and APCs, supports the maturation of DCs from monocyte precursors, and guides downstream T cell responses.[358] NK cells also express FcγRIII, which enables them to recognize immunoglobulin molecules on the surfaces of target cells and to mediate antibody-dependent cellular cytotoxicity (ADCC).[358] Through these mechanisms, NK cells operate at the interface of innate and adaptive immunity, making them a vital component of both branches of the immune response.[359]

ii. REGULATORY VS. INFLAMMATORY CELL DISTRIBUTIONS

Using single-cell RNA sequencing, Friedrichs et al. recently characterized the immune cell landscape in juvenile, subadult, and adult ERBs, revealing 22 transcriptomically unique leukocyte subsets, along with conserved subsets and age-associated enrichments.[360] Juvenile bats showed higher proportions of CD79a+ B cells

and CD11b+ T cells, while neutrophils, CD206+ myeloid cells, and CD3+ T cells were more prominent in adults.[360] These findings provide additional support for the tolerance hypothesis by demonstrating that tolerance may be associated with immunological development in bats and reflected at a cellular level. This is evidenced by a greater abundance of putative regulatory CD206+ myeloid cells in adults, alongside elevated levels of putative activated CD11b+ T cells and PLAC8-expressing B cells in juveniles.[360]

3. ADAPTIVE IMMUNITY

The adaptive immune response generates a pathogen-specific response by presenting virus-derived antigens on class I and II MHCs. These antigens are displayed by antigen presenting cells, including DCs, Langerhans cells, macrophages and B cells, to T lymphocytes, which in turn guide the differentiation of the T cell subsets (i.e., Th1, Th2, Th17, etc.).[361] Adaptive immunity is composed of two primary branches: humoral and cell-mediated immunity. Humoral immunity is mediated by B lymphocytes, which produce antigen-specific antibodies that primarily target extracellular pathogens.[362] These antibodies support a variety of immune functions, including neutralization of pathogens, ADCC and antibody-dependent cellular phagocytosis (ADCP) and complement activation.[362]

Cell-mediated immunity (CMI) is a branch of the adaptive immune system that is primarily responsible for recognizing and eliminated intracellular pathogens, as well as targeting malignant or foreign (i.e., “non-self”) cells.[362] CMI is primarily mediated by T lymphocytes, predominantly CD8+ cytotoxic T cells, which directly kill infected or abnormal cells via the release of perforin and granzymes and through Fas-FasL

interactions, leading to target cell apoptosis.[363-365] Activated CD4+ helper T lymphocytes orchestrate immune responses by initiating intracellular signaling cascades involving lymphocyte-specific protein tyrosine kinase (Lck), zeta-associated protein of 70 kDa (ZAP-70), and downstream transcription factors like nuclear factor of activated T cells (NFAT), nuclear factor kappa-light-chain-enhancer of activated B cells (NF-κB), and activator protein-1 (AP-1), which drive proliferation, differentiation, and cytokine production.[365] CMI is essential for the elimination of virus-infected cells, the activation of antibody production, and the orchestration of cytokine signaling cascades essential for immune coordination.[304]

a. IMMUNOGLOBULIN DIVERSITY AND GENE ORGANIZATION

In 2021, Larson et al. annotated the immunoglobulin (Ig) heavy chain locus of ERBs and identified several distinctive features. These included an expanded set of immunoglobulin variable (V) genes, two functional and distinct Immunoglobulin epsilon (IgE) genes, four distinctive functional immunoglobulin gamma (IgG) genes, a detailed description of the Fc receptor repertoire, and a noted absence of short pentraxins, which are involved in the acute phase response in humans.[15] One particularly unique feature of ERB immunoglobulin gene organization is that D and J genes segments are interspersed, rather than sequentially arranged as seen in human and mouse Ig loci.[366] This unusual genomic feature may contribute to ERBs enhanced immune tolerance and attenuated inflammatory responses by expanding combinatorial possibilities for V(D)J recombination.

b. B CELL RESPONSES AND ISOTYPE USAGE

Bats appear to mount antibody responses to antigens in a sequence similar to other mammals, with an initial production of IgM followed by IgG.[306,307,367] IgA, IgG, IgM and IgE subtypes as well as both κ and λ light chains have been identified across both Yangochiropteran and Yinpterochiropteran bat species, however IgD appears to only be present in insectivorous bats.[306,307,368-372]

The heavy chain variable region genome (V_H or IGHV) of the immunoglobulin genome encodes the antibody-binding site that determines antibody specificity for antigens. In bats, this region appears to be highly diverse, suggesting that bats may rely more on combinatorial diversity – the reshuffling of gene segments - rather than on somatic hypermutation to generate antibody specificity.[307,308,373] Interestingly, body temperature fluctuations, which correspond to different physiological states (e.g., torpor or flight) may have a significant impact on bats' antibody repertoires.[374]

Despite mounting a strong IgG response after infection, ERB convalescent sera rarely neutralized virus, and never robustly.[375] Even when secondary exposures were tested, neutralizing antibodies were largely absent or ineffective, supporting the conclusion that antibody-mediated neutralization is not the primary mechanism by which ERBs clear MARV, EBOV, or SOSV.[375] Instead, it is likely that Fc-effector mechanisms and innate immune functions play a more significant role. Human monoclonal antibody studies support this, showing that Fc-dependent pathways, including innate immune pathways (e.g., IFN response), NK cell activation, or non-neutralizing antibody functions (e.g., antibody-dependent phagocytosis, ADCC, or opsonization), may be sufficient for viral clearance in the absence of strong neutralizing antibodies.[376] These mechanisms may similarly contribute to the ability of ERBs to clear infection without clinical disease,

supporting a model of immune control that does not rely on traditional neutralization.[375,376]

Maternal antibody transfer from dams to pups, and its subsequent postnatal decline, has been documented in *Pteropus alecto* bats, *Pteropus hypomelanus* bats, and *Eidolon helvum* bats.[377-379] While not yet studied in ERBs, seasonal pulses of MARV and coronavirus circulation in free-ranging ERB populations supports the presence of waning maternal antibodies in juvenile bats.[3,380]

c. T CELL RESPONSES AND CYTOKINE GENE CONSERVATION

The CD4 co-receptor has been characterized in ERBs, demonstrating greater sequence homology with cat and dog CD4 than with human and mouse homologs.[381] Additionally, several bat cytokine genes have been characterized. These include cDNAs corresponding to interleukin (IL) -2, IL-4, IL-6, IL-10, IL-12p40, and tumor necrosis factor (TNF) in *R. leschenaultii* bats, and appear to be highly conserved with those from other mammals.[329]

4. FUNCTIONAL IMMUNE RESPONSES IN EGYPTIAN ROUSETTE BATS

a. EXPERIMENTAL VIRAL INFECTIONS

i. MARBURG VIRUS AND RAVN VIRUS

ERBs experimentally infected with MARV have transient subclinical disease characterized by viremia, oral shedding, and rectal shedding.[46] Although MARV shedding in urine has also been documented, it remains incompletely characterized due to challenging nature of specimen collection.[4,46] In previous studies, MARV-inoculated ERBs robustly seroconverted to MARV, with MARV IgG antibodies peaking between 12 DPI and 28 DPI[4,46,244], followed by a decline of antibody levels falling below the

threshold of seropositivity by 3 months post-infection (MPI).[46] In contrast, another study found that 67% of bats experimentally infected with MARV retained detectable antibodies around 4 MPI, whereas 84% of naturally exposed bats still had MARV antibodies at least 11 months after capture.[382] Despite waning antibody levels, robust longstanding immunity to reinfection upon experimental challenge with MARV has been documented in ERBs up to two years after initial infection.[47]

Experimentally, MARV-infected ERBs have a rapid but transient induction of ISGs in peripheral blood mononuclear cells, peaking at 3 days post-infection and quickly returning to baseline, as well as no strong or sustained pro-inflammatory response, indicating an immune strategy that limits immune-mediated pathology.[20] Dexamethasone-induced immune suppression in ERBs bolstered MARV replication and shedding and hepatopathology, indicating that their ability to balance immunoprotective tolerance with MARV-resistant pro-inflammatory responses is compromised when immunosuppressed.[98]

ii. OTHER VIRUSES

ERBs experimentally infected with SOSV have subclinical disease characterized by viremia, viral loads detected in multiple tissues, detection of SOSV RNA with subsequent isolation of infectious SOSV from oral and rectal swabs, urine, and feces, and seroconversion by 21 DPI.[7] Interestingly, SOSV-infected ERBs had mild increases in mononuclear phagocytes and T cells despite the presence of SOSV NP antigen and villus ulcerations in the small intestines, a host response aligned with disease tolerance, in contrast to a statistically significant, robust and targeted mononuclear phagocyte cell response in the salivary glands at 21 DPI, where viral antigen was sparse.[17]

ERBs experimentally infected with KASV have high, prolonged viral loads in blood, oral, fecal, and urine specimens, followed by seroconversion by 21 DPI.[16] Serially sacrificed ERBs had high KASV loads indicative of virus replication in the liver, skin at the inoculation site, spleen, tongue, and inguinal lymph node tissue.[16,18] Significant gross and histological lesions were limited to the liver; KASV-infected ERBs developed mild to moderate, self-limiting, KASV-induced lymphohistiocytic hepatitis that was first detected at 3 DPI and resolved by 20 DPI.[16,18] The more significant hepatic pathology identified in this experimental infection may reflect that KASV is less host-adapted to the ERB compared to MARV or RAVV, as KASV is maintained in an enzootic transmission cycle with the soft tick *Ornithodoros faini*.[19,140]

ERBs immunized with a monovalent inactivated rabies vaccine produced rabies virus antibodies and mounted an amnestic response upon boosting at 30 days.[383] However, since the vaccinated bats were not challenged with a virulent rabies virus, the functional effectiveness of the antibody response remains unknown.[383] It is also important to note that this immune response likely does not represent a natural rabies virus or lyssavirus infection, as inactivated vaccines are unable to infect cells and influence the IFN response. Additionally, the presence of adjuvant is designed to stimulate a more robust antibody response than would naturally occur.[305]

In SARS-CoV-2 susceptibility studies, ERBs seroconverted by 8 days post-infection, with RT-qPCR detection of viral RNA in the respiratory tract persisting up to 21 days post infection. [271] Additionally, transmission to a contact bat – specifically, a gravid female – was observed, confirming the potential for horizontal transmission under experimental conditions.[271] The gravid female was in the early stages of pregnancy, a

condition that may have increased her susceptibility to infection. Increased viral detection rates in bats during the reproductive phase have been reported, possibly due to pregnancy-associated immunosuppression.[384] Finally, numerous studies have shown that ERBs do not support productive EBOV virus infection, despite seroconversion 10-16 days post infection.[45,385]

iii. IN VITRO AND IN VIVO IMMUNE RESPONSES

In vitro experimental infections of ERB cells with EBOV or MARV results in the induction of IFN-β but seemingly not IFN-α.[346,348] In vitro Marburg virus infection elicited a strong reaction in ERB cells, with earlier induction of IFN and ISGs than was seen in in vitro EBOV virus infection.[346] This disparity in immune response may reflect evolutionary adaptations that allow the ERB to serve as a natural reservoir for MARV, while being less permissive to EBOV.[304] Further in vitro investigations of ERB ISG15, a key ISG, revealed significant antiviral activity when transduced into various cell types.[27] These antiviral effects were observed against H1N1 Influenza A virus and HCoV-229E (a human coronavirus associated with the common cold). However, ISG15 expression did not reduce SARS-CoV-2 replication, highlighting virus-specific differences in susceptibility to this antiviral effector.[27]

As highlighted previously, ERB cells have previously shown idiosyncratic induced IFN responses upon viral challenge.[99,101,346,386,387] For example, infection of ERB DCs with a bat isolate of MARV induced transcription of IFN-related genes, but simultaneously inhibited cytokine and chemokine production, downregulated DC maturation and suppressed adaptive immune-stimulatory pathways, all while upregulating IFN-related pathogen-sensing pathways.[100] ERB cells and organoids

challenged with MARV rapidly induced type III IFNs and robust expression of ISGs, whereas the human innate immune response was stifled and inflammatory.[347,351] Recent in vivo investigation of the transcriptional host cell response in MARV-infected ERBs showed upregulation of canonical antiviral genes seen in other mammals, such as ISG15, IFIT1, and OAS3, but showed minimal induction of proinflammatory genes classically implicated in primate filoviral pathogenesis, including CCL8, FAS, and IL6.[97] It is possible that the induced immunity of ERBs may select for viruses with faster replication rates that remain nonpathogenic in bats but could become highly virulent in spillover hosts (like humans) that lack comparable antiviral control mechanisms.[387]

b. ORGANOIDS

Organoids are engineered, tissue-derived, three-dimensional models that recapitulate the physiological state of tissues and their in vivo multicellular composition.[351] Organoids offer a powerful in vitro model for investigating tissue-specific immunity and host-pathogen interactions, particularly at mucosal surfaces where zoonotic viruses frequently initiate infection. Compared to traditional monolayer cultures or immortalized cell lines, bat-derived organoids provide greater physiological relevance by preserving cellular diversity, polarization, and innate immune features found in vivo.[388] For example, bat organoids exhibit higher basal expression of ISGs and more rapid antiviral responses compared to human organoids, mirroring bats' unique immune tolerance and lack of inflammatory output.[347,389] As described earlier, in ERB organoids, both type I and III IFN responses are robustly induced upon viral stimulation, with IFN-λ playing a prominent role in mucosal immunity.[347] Beyond ERBs, intestinal organoids have been developed in Jamaican fruit bats[390] and Chinese horseshoe bats[389,391] and used

to investigate susceptibility to SARS-CoV-1 infection in bat intestinal epithelium and the subsequent cellular antiviral mechanisms. These platforms allow for controlled studies of IFN dynamics, epithelial antiviral signaling, and virus-specific host responses that are otherwise difficult to access in vivo.[347] However, organoids are not without limitations. Organoids lack systemic immune components such as peripheral blood mononuclear cells and vasculature; some cell types may require additional stimulation to differentiate in the absence of in vivo microbial cues; and immune responses may differ from those in an intact organism.[347] Nonetheless, these systems bridge the gap between in silico modeling, in vitro cell lines, and live animal studies, making them indispensable tools for dissecting the immune landscape in bats and understanding their role as reservoirs of high-consequence zoonotic pathogens.

5. ADDITIONAL IMMUNE RESPONSES

Perturbation of the ERB gut microbiome with lipopolysaccharide (LPS), an inflammatory endotoxin derived from gram-negative bacteria, altered the composition of the gut bacterial community. These changes were significantly correlated with circulating haptoglobin levels, an acute phase protein associated with inflammation.[392] Eleven bacterial taxa were associated with haptoglobin concentration, with nine of these taxa emerging as potential predictors of immune response magnitude and, by extension, infection severity. Among the most notable were members of the genera *Weissella* and *Escherichia*, suggesting a functional link between specific microbiome constituents and host immune modulation.[392]

Finally, in response to Marburg virus infection, ERBs exhibit upregulation of hepcidin in the liver, suggesting a potential protective mechanism that limits systemic

iron availability to restrict viral replication and modulate inflammation.[267] This response, accompanied by changes in other iron-regulatory genes such as ceruloplasmin and ferritin, reflects a coordinated hepatic adaptation that may contribute to viral tolerance and clearance.[267]

6. LITERATURE REVIEW SUMMARY

Current knowledge on the immune response of the ERB is defined by a highly specialized balance between effective antiviral control and minimal immunopathology, facilitating its role as a reservoir host for multiple zoonotic viruses. Innate immunity is characterized by tightly regulated type I INF responses, with rapid yet transient upregulation of ISGs, limited induction of proinflammatory cytokines, and species-specific adaptations including expanded and positively selected tetherin alleles, epithelial-restricted complement expression, and conserved yet inducible IFN signaling pathways. Transcriptomic and genomic analyses have revealed positive selection in key IRFs, diversification of NK cell receptors, and an expanded IFN-ω gene repertoire, indicating evolutionary pressure toward immunomodulatory efficiency. Adaptive immune responses include typical immunoglobulin class switching and T cell-mediated cytotoxicity; however, neutralizing antibody response to viral infection are typically absent or weak, with immune clearance likely mediated by FC-effector mechanisms such as ADCC, opsonization, and phagocytosis. Experimental MARV infections result in transient viremia and mucosal shedding, robust IgG seroconversion, durable protection against reinfection, and a lack of sustained inflammatory response, even under high viral replication. Together, these features reflect a unique tolerogenic and tightly controlled immunological strategy that permits persistent, subclinical viral infection while

minimizing host damage and supporting reservoir competence. Building on the current understanding of the ERBs immune responses at the molecular and functional levels, it is essential to next examine the structural organization of its immune system, beginning with a review of primary and secondary lymphoid organs and an accompanying gross and histologic atlas.

7. LYMPHOID ANATOMY OF THE EGYPTIAN ROUSETTE BAT

Previous gross and histological analysis have shown that bats have similar immune cells and primary and secondary lymphoid organs as are found in other mammals.[360,367,370,393,394] Primary lymphoid organs include bone marrow and thymus, and are where lymphocytes first express antigen receptors and attain phenotypic and functional maturity.[395] Secondary lymphoid organs include the lymph nodes, spleen, and components of the mucosa-associated lymphoid tissue (MALT), and are where lymphocyte responses to foreign antigens are initiated and develop.[395] Although mean weights of some ERB lymphoid organs have been previously reported, the sample sizes were limited, and additional data are required to establish robust and biologically meaningful reference values.[396] The subsequent sections will detail the structure and function of each primary and secondary lymphoid organ, highlighting relevant findings from ERB-specific studies.

a. BONE MARROW

Evaluation of blood and bone marrow can be challenging in smaller species, and in the ERB, its small blood volume precludes the ability to access serial blood chemistry values. While definitive characterization of bone marrow often requires cytological aspirates or smears, assessment of histological bone marrow sections provides

information regarding tissue architecture and hematopoietic status. Although the ERB is unlikely to become a standard model for hematologic disorders in toxicology studies, a comprehensive understanding of its bone marrow is critical for thorough post-mortem analysis and lymphoid system characterization. Used in conjunction with a complete blood cell count (CBC), the histological examination of bone marrow provides information regarding the hematopoietic systems that might otherwise be missed by examination of peripheral blood alone.

Bone marrow, a primary lymphoid organ, is housed within central cavities of axial and long bones and consists of hematopoietic tissue islands and adipocytes interspersed within a trabecular bone framework.[395,397] As the primary post-fetal hematopoietic organ, erythrocytes, granulocytes, monocytes, DCs, mast cells, platelets, B- and T- lymphocytes, and innate lymphoid cells all originate from a common hematopoietic stem cell in the bone marrow.[395] The endosteal lining is composed of reticular connective tissue, osteoblasts, and osteoclasts.[397] Long bones receive vascular supply through nutrient canals, through which a nutrient artery enters the marrow cavity and, after branching into arterioles and capillaries and anastomosing with venous sinuses, eventually drain via the nutrient veins.[397]

Hematopoiesis is a compartmentalized process, with erythropoiesis occurring in distinct erythroblastic islands, granulopoiesis occurring in less distinct adjacent foci, and megakaryopoiesis occurring adjacent to sinus endothelium.[397] Blood cell production is driven by pluripotent stem cells differentiating into myeloid or lymphoid lineages, with further maturation influenced by lineage-specific growth factors and cytokines.[395,397]

A comprehensive hematopoietic evaluation integrates peripheral blood analysis (CBC and differential blood count), bone marrow smears, and histopathology. Bone marrow histology is useful for assessing architecture, cellularity, estimation of the myeloid:erythroid ratio, cell lineages, iron stores, and other pathological changes such as neoplasia or inflammation.[397] In dogs, biopsies are typically obtained from the iliac crest, sternum, proximal humerus, or femur; in rodents, active hematopoietic sites include the sternum, ribs, humerus, and proximal femur.[397] Normal marrow composition varies by age and site, with fat and hematopoietic tissue proportions varying. In formalin-fixed, paraffin-embedded, and decalcified H&E-stained sections, mature erythroid and myeloid cells, adipocytes, mast cells, and megakaryocytes are identifiable, though stem cells and immature hematopoietic precursors are not consistently distinguishable (Fig. 2-1E, F). Erythroid cells exhibit dense, basophilic nuclei with increasing cytoplasmic eosinophilia during maturation, while granulocytes have large, bean-shaped, vesicular nuclei that are less basophilic than in erythropoietic cells.[397] Megakaryocytes are distinguished by their large size and multilobulated nuclei.[397] Discussion of fixation, decalcification techniques, and tissue processing and staining is available in Travlos 2006.[397]

Histopathologic changes reported in bone marrow of laboratory animal models include increased nucleated cells in response to increased cell demand, hematopoietic cell depletion, hypocellularity, hypoplasia, or atrophy, hematopoietic cell dysplasia, focal stromal cell hyperplasia, myelostromal proliferation, focal lipomatosis, fibrosis, fibro-osseous lesions and fibrous osteodystrophy, necrosis/degeneration, inflammatory changes involving erythrophagocytosis as well as lymphocytes and plasma cells, primary

neoplasia involving hematopoietic cells, stromal cells, or endothelial cells, or secondary neoplasia from distant metastases or a locally invasive tumor.[398]

b. THYMUS

The thymus, a primary lymphoid organ, is the site of T cell development and selection. It consists of two lobes connected by a connective tissue isthmus, located in the pericardial mediastinum, with species-specific variations in cervical extension (Fig. 2-2A).[399,400] A structurally distinct cortex and medulla, separated by the corticomedullary zone, house developing T cells, epithelial cells, DCs, macrophages, and variable B cells (Fig. 2-2B, C).[399,400]

Thymic arteries enter at the corticomedullary junction, forming cortical capillary arcades that, along with epithelial and macrophage components, create the blood-thymus barrier, restricting antigen exposure.[399,400] Medullary capillaries are fenestrated and permeable. The thymus lacks afferent lymphatics; efferent lymphatics drain into local nodes. [399,400]

The cortex contains densely packed immature T cells, sparse epithelial cells, and macrophages that phagocytose apoptotic lymphocytes.[399,400] Rapidly proliferating lymphoblasts are present subcapsularly. The corticomedullary junction harbors arterioles, perivascular B cells, plasma cells, and antigen-presenting DCs.[399,400] The less cellular medulla contains mature T cells, prominent epithelial cells, macrophages, DCs, and Hassall's corpuscles—keratinized epithelial aggregates involved in T cell regulation (Fig. 2-2E, F).[399,400]

Prothymocytes are immature T cell progenitors that are recruited from the bone marrow to the thymus, entering at the corticomedullary junction. Prothymocytes undergo

multiple stages of differentiation, expansion, selection, and maturation as they migrate from the cortex to the medulla before entering circulation as mature T cells to populate secondary lymphoid organs.[399,400] This process includes positive selection to ensure T cells recognize self-MHC, while negative selection eliminates self-reactive clones via apoptosis, shaping central tolerance.[399,400]

Age-related declines in thymic cellularity are classified as involution, whereas reductions due to malnutrition, stress, or toxic exposures are considered thymic atrophy.[401] Histologically, both processes appear similar, characterized by cortical lymphocyte depletion and lobular shrinkage. Furthermore, stress and toxic insults can exacerbate or overlay normal age-associated lymphocyte loss, making differentiation between atrophy and involution in older animals inherently challenging.[401] Thymic lesions reported in laboratory animal models include epithelial hyperplasia, neoplasia such as thymoma and thymic lymphoma, or decreased thymic cellularity due to inadequate nutrition, stress, steroid hormone levels, or immunotoxicity.[401]

c. LYMPH NODES

Lymph nodes are secondary lymphoid organs present along the course of lymphatic vessels.[402,403] The functional unit of the lymph node is the lymphoid lobule, structured into three main regions: 1) the B-cell rich follicle-containing cortex, 2) the T-cell rich paracortex or deep cortical unit, and 3) the medulla (Fig. 2-3B, C).[402] The lymph node is filled by a delicate, porous reticular meshwork composed of stellate, spindle-shaped, or elongated fibroblastic reticular cells (FRCs) and their associated reticular fibers.[403] This subdivides the lobule into numerous narrow channels and spaces, which

are occupied by lymphocytes, macrophages, and APCs, which typically obscure the underlying meshwork.[402,403]

Lymphocytes enter lymph nodes via high endothelial venules (HEVs), specialized blood vessels in the interfollicular cortex and paracortex, which regulate immune cell trafficking (Fig. 2-3D).[395,402,403] Following entry, B cells home to superficial primary cortical follicles to survey follicular dendritic cells (FDCs) presenting antigen-antibody complexes.[402,403] Upon antigen recognition, B cells undergo clonal expansion and proliferate, forming a distinctive central germinal center surrounded by a darker mantle of displaced resting B cells; the follicle is now a secondary follicle (Fig. 2-3B-F).[402,403] Following antigen exposure, germinal centers develop within 3–4 days, peak at 7–10 days, and decline in the absence of continued stimulation.[402,403] Activated B cells differentiate into memory B cells or plasma cell precursors, the latter of which matures into plasma cells during migration to the medullary cords where they secrete antibodies into the lymph.[402,403]

Following entry into the lymph node via the HEVs, T cells home to the paracortex, where they interact with DCs.[395] DCs are powerful APCs that originate from hematopoietic stem cells in the bone marrow and are distributed throughout most tissues, most notably at external barriers such as the skin and mucosal surfaces.[402,403] Upon encountering an antigen, DCs migrate to the lymph nodes via afferent lymph and localize to the paracortex to present antigen to T cells, promoting T-cell activation and expansion.[402,403] Stimulated and proliferating T lymphocytes enlarge the paracortex but do not create structures analogous to germinal centers.[402,403]

Gross anatomical characterization of lymph nodes in ERBs has previously been characterized, with the anatomical location and number of lymph nodes listed as follows: superficial cervical (1-2), facial (2-4), internal jugular (1-3), posterior cervical (1-4), brachial (1-3), axillary (1-4)(Fig. 3A), inguinal (2-6), popliteal (2-3), gluteal (2-5), iliac (1-4), renal (1-3), and cranial mesenteric (1-5).[404,405] Pregnant ERBs have more numerous and larger lymph nodes that non-pregnant females or males, and typically lymph nodes on the left of the body are larger.[404]

Normal histologic findings within lymph nodes may encompass a wide range of histologic presentations. For example, sinus histiocytosis has been reported as a normal finding in mesenteric lymph nodes and the macrophages may contain endogenous pigment (hemosiderin, lipofuscin) or exogenous pigments reflecting antigen uptake from the digestive tract.[402,406] The mandibular lymph nodes are continually exposed to antigens from the oropharyngeal region and will typically have well-development secondary follicles and considerable numbers of plasma cells within medullary cords, whereas lymph nodes lacking frequent antigen exposure will be comprised of primary follicles. Common findings reported in laboratory animal models include lymphoid necrosis, lymphatic sinus ectasia, vascular lesions such as sinus congestion, sinus erythrocytosis, nodal and perinodal angiectasia, hemorrhage, and vascular proliferation, intracellular pigment (hemosiderin or ceroid/lipofuscin), amyloidosis, lymphadenitis, lymphocyte hyperplasia, plasma cell hyperplasia, macrophage hyperplasia, lymphoma, and metastatic lesions.[406]

d. SPLEEN

The spleen, the largest secondary lymphoid organ, contains ~25% of the body's lymphocytes and is essential for blood-borne immune responses and filtration of foreign material and senescent erythrocytes.[407,408] It is composed of two distinct compartments: the white pulp, which is the lymphoid component involved in adaptive immunity, and the red pulp, which functions in filtration, iron storage, and hematopoiesis (in rodents and neonates).[407,408]

Enclosed by a fibroelastic capsule with smooth muscle trabeculae, the spleen lacks afferent lymphatics and is instead integrated into systemic circulation.[407,408] Blood enters via the splenic artery, branching into trabecular and central arterioles, eventually flowing into venous sinuses (~90%) or the reticular meshwork before drainage into the splenic vein.[407,408] Because of this unique vascular structure, spleens do not have high endothelial venules.[409]

The red pulp consists of splenic cords and venous sinuses, forming a macrophage-rich, reticular network that removes aged erythrocytes and particulate matter.[407,408] Erythrocytes, granulocytes, and circulating mononuclear cells are present between cords, as are lymphocytes, hematopoietic cells, plasma cells, and plasmablasts that migrate from the follicles and the outer periarteriolar lymphoid sheath (PALS) after antigen-specific differentiation.[407,408]

The white pulp, supported by a similar reticular framework, consists of the periarteriolar lymphoid sheath (PALS), follicles, and the marginal zone.[407,408] The PALS are divided into an inner T-cell-dominant area (CD4+ and CD8+ subsets with interdigitating DCs) and an outer region containing B and T lymphocytes, macrophages,

and plasma cells.[407,408] B-cell rich follicles are continuous with PALS and may develop germinal centers upon antigenic stimulation.[407,408]

The marginal zone, positioned at the red-white pulp interface, serves as a critical antigen-screening site.[407,408] It contains marginal zone B cells, macrophages, fibroblasts, and DCs, facilitating systemic antigen surveillance.[407,408] A band of metallophilic macrophages and the marginal sinus demarcate this zone from PALS and follicles.[407,408]

ERB splenic structure is similar to humans and rodents, in that they have a thin capsule and variably sized collagenous and smooth muscle trabeculae (Fig. 2-4B).[410] *Rousettus* sp. bats have been reported to have few erythroid and myeloid cells and no megakaryocytes in their red pulp, with prominent marginal zones in white pulp (Fig. 2-4C-F).[410] The spleen may become smaller in response to stress.[411] Reticular networks connecting the marginal zones and periarteriolar lymphoid sheaths have been reported in *R. leschnaultii* bats.[412] These structures, known as the marginal zone bridging channels, are thought to facilitate the migration of lymphocytes from marginal zones to periarticular lymphoid sheaths. Frequently present in clusters within the red pulp and marginal zone, arterial capillaries are surrounded by prominent, dense, circumferential clusters of macrophages known as ellipsoids, periarterial macrophage sheaths, or Schweigger-Seidel sheaths (Fig. 2-4E, F).[407] Ellipsoids play a role in filtration and capture of circulating particular material and can trap immune complexes.[413] Periellipsoid lymphoid sheaths have been reported in *R. leschnaultii* bats.[412] Previously reported in species without marginal zones (i.e., poultry and reptiles), these sheaths function as a blood-spleen barrier; their role in *Rousettus* spp. bats has not been elucidated.[414]

Common splenic lesions reported in laboratory animal models include non-proliferative lesions such as atrophy, pigment, parenchymal and capsular fibrosis, lipidosis/fatty infiltration/lipid metaplasia, vacuolization of splenic histiocytes, amyloidosis, splenic necrosis/infarcts, lymphoid necrosis/apoptosis, extramedullary hematopoiesis, focal red pulp hyperplasia, focal white pulp hyperplasia, and neoplastic lesions such as lymphocyte hyperplasia and lymphosarcoma, various leukemias, histiocytic sarcomas, mast cell tumors, hemangiomas and hemangiosarcomas, and mesotheliomas.[415]

e. MUCOSA-ASSOCIATED LYMPHOID TISSUE

Mucosa-associated lymphoid tissue (MALT) is a critical component of the immune system, initiating antigen-specific immune responses along mucosal surfaces.[395] It functions independently of the systemic immune system and comprises approximately half of the body's lymphocytes.[416]

MALT is distributed across various organs, including gut-associated lymphoid tissue (GALT), nasopharynx-associated lymphoid tissue (NALT), and bronchus-associated lymphoid tissue (BALT), with additional sites in the conjunctiva (CALT), lacrimal ducts (LDALT), larynx (LALT), salivary ducts (DALT), and many more.[416,417] Functionally, MALT can be categorized as inductive sites, where antigen-primed B and T cells are activated, and effector sites, where immune responses occur. However, this distinction is not absolute, as the roles of some lymphoid aggregates, like cryptopatches and lymphocyte-filled villi, remain unclear.[417] Inductive sites, such as Peyer’s patches in the GALT and NALT in rodents and non-human primates, contain organized lymphoid structures where IgA class switching and B-cell clonal expansion occur following T-cell

activation.[416] Activated lymphocytes then migrate to effector sites, where sIgA is secreted.[416,417] Effector sites, found throughout mucosal tissues, predominantly contain CD4+ T cells, IgA-secreting plasma cells, DCs, and macrophages.[416,417] Intraepithelial lymphocytes, mainly CD8+ T cells, are interspersed among epithelial cells and are crucial for mucosal immunity, thought to enter the epithelium after activation in the lymph nodes and spleen.[417]

MALT in most regions shares fundamental compartments: follicles, mantles, germinal centers, interfollicular areas, subepithelial domes, and follicle-associated epithelium (FAE) containing microfold (M) cells.[417] M cells are specialized epithelial cells that transport luminal antigens to underlying immune cells, facilitating antigen recognition.[416] MALT does not have afferent lymphatics or medullary regions, with high endothelial venules (HEVs) serving as primary entry points for lymphocytes.[416,417]

Species variability in GALT is significant. Rodents have uniformly distributed Peyer's patches, whereas dogs exhibit two distinct types: small, discrete patches in the jejunum and upper ileum, and a single, large ileal patch encircling the distal ileum.[416] In rhesus macaques, ileal Peyer's patches are prominent, while baboons have smaller patches with fewer IgA+ centroblasts.[416] Rabbits possess a unique sacculus rotundus and appendix, both rich in lymphoid follicles.[416] In the current study, GALT was identified in ERBs as both isolated lymphoid follicles and, more commonly, as Peyer's patches within the jejunum, ileum, and proximal and distal colon (Fig. 2-5). GALT was not able to be grossly appreciated.

NALT, present in rodents, rabbits, chickens, and non-human primates, consists of paired lymphoid aggregates within the nasal passages.[416,417] Compared to Peyer's

patches, NALT has fewer intraepithelial lymphocytes, a balanced B- and T-cell population, and fewer DCs in the subepithelial dome (Fig. 2-6).[416,417]

BALT is described in a variety of vertebrates, including mammals, birds and reptiles. Rabbits and rats typically have the most BALT, followed by mice and guinea pigs.[417] BALT is absent in germ-free pigs, reduced in germ-free rats, and present only upon postnatal antigenic stimulation in mice and humans.[416,417] Structurally, BALT resembles NALT but lacks FDCs and contains fewer intraepithelial lymphocytes and germinal centers (Fig. 2-7).[416]

Tonsils are absent in rodents but present in most species.[416] Dogs possess four types: lingual, palatine, pharyngeal, and tubal tonsils, with either crypts (follicular tonsils) or without.[416,417] Tonsillar crypts are blind invaginations of the surface epithelium into the submucosal lymphoid tissue for antigen capture.[416] In the current study, palatine tonsils were not identified in any section; however, they are presumed to be present in this species. Palatine tonsils have been referenced in Jamaican fruit bats[418], and while there is species diversity among bats, palatine tonsils are likely conserved and were simply missed in section in our study. Lingual and pharyngeal tonsils also were not identified. Future work is needed to better elucidate this component of MALT in ERBs. Paraepiglottic tonsils were easily identified at the lateral basis of the epiglottis (Fig. 2-8), and tubal tonsils adjacent to the Eustachian tube were additionally identified (Fig. 2-9). Reticular epithelium containing M cells, lymphocytes, macrophages, and DCs overlies the apices of lymphoid follicles; non-reticular epithelium overlies remaining tonsillar tissue (Fig. 2-8E).[416]

Reported histopathological changes in MALT of laboratory animal models include inflammation, macrophage aggregates, and granulomatous inflammation; degeneration, necrosis and mineralization; neoplasia (most commonly lymphoma); and neoplastic metastasis/tumor emboli.[419] Tertiary lymphoid structures identified in the pancreas of an adult male free-ranging ERB are included here for completeness (Fig. 2-10C-F). Tertiary lymphoid structures, less commonly referred to as ectopic lymphoid tissue, consist of lymphocyte-specific microdomains in nonlymphoid tissues under chronic inflammatory conditions.[420,421] These structures have been reported in various species, including mice, rats, pigs, buffalo, and dogs.[422-425]

f. IMMUNOHISTOCHEMISTRY

Immunohistochemistry (IHC) is a laboratory technique that uses antigen-antibody interactions to detect and visualize specific proteins or cellular markers within histologic tissue sections. By applying antibodies conjugated to enzymes or fluorophores, IHC allows for spatial localization of target molecules while preserving tissue architecture.[426] This technique is widely used for diagnostic pathology, tumor classification, and infectious disease identification, as well as investigating the distribution of immune cell populations, cytokines, and structural proteins.

There are few studies to date that have utilized IHC to investigate ERB diseases; most have focused on tumor classification, infectious disease, and immunomodulation in the context of viral infection.[17,45,50,153,157,162,163,166-168] Despite most commercially available IHCs being produced for use in human or companion animals, there has been success in cross-reactivity in ERB tissues. Table 2-1 provides information on primary antibodies that have been used in immunohistochemical evaluation of ERB tissues.

In the current study, B cell markers CD20, CD21, and Pax-5 were all unsuccessful in labeling the respective target cells on ERB tissues. Factor VIII related antigen and smooth muscle actin were previously completed as part of unpublished research and are included in Table 2-1. Fetal tissues frequently had absent to scant immunolabeling across all examined lymphoid organs. Fetal cells are often less differentiated and therefore may not express the target protein yet or express it at lower levels or as a different isoform or precursor not yet recognized by the antibody.[426] Epitopes may not have the correct conformation, glycosylation, or post-translational modifications to allow for antibody binding even if the protein is present.[426] Additionally, overall tissue quality may have degraded due to extended (~15 year) fixative exposure, rendering tissues less amenable to labeling. In image panels, efforts were made to include identical sections of tissues across stains, when possible. Histologic comparisons of Iba1, CD3, CD79a, and Granzyme B immunolabeling in fetal, juvenile, and adult ERB lymphoid tissues are show in Figures 2-11 through 2-16.

g. CLINICAL PATHOLOGY

Characterization of immune cells has been achieved in the Brazilian free-tailed bat (*Tadarida brasilensis*), Indian flying fox (*Pteropus giganteus*), black flying fox (*Pteropus alecto*), among many other species.[367,393,394,427,428] Reported hematological and clinical chemistry parameters for ERBs have been summarized in Rissmann et al.[429], with variation possibly due to differences in reference panels/profiles and analyzers used at each facility.[429-435] Despite this variation, there is agreement that no sex- or age-related differences have been found in ERBs.[429,432,436]

ERBs exhibit mild polychromasia, with fine eosinophilic granulation in the cytoplasm of neutrophils, similar lymphocytes and monocytes with occasional nuclear indentation, and eosinophils with homogenous, round, light lavender, small cytoplasmic granules.[432,437] ERBs have slightly lower hematocrit, hemoglobin, leukocyte, lymphocyte counts, and triglycerides compared to others bats, while creatine kinase was higher.[432] Serum protein electrophoresis showed five fractions: albumin, α-, β_1-, β_2-, and γ-globulins.[432] Average manual differential leukocyte count (200 leukocytes) of the two adult ERBs included in this study are presented in Table 2-2, and are slightly higher than those reflected in the current literature, which may be reflective of their advanced age.[432] Due to formalin-fixation-induced artifacts, leukocyte images are not provided herein but can be found in Moretti et al.[432]

DISCUSSION

This chapter provides the most comprehensive synthesis to date of the immunologic profile and lymphoid tissue architecture of the Egyptian rousette bat, a species of increasing important in virology, disease ecology, and comparative immunology. By integrating a detailed literature of ERB innate and adaptive immunity with a novel gross and histologic atlas of the lymphoid system, this work addresses longstanding gaps in our understanding of this key reservoir host. The findings presented herein highlight the unique immunologic adaptations of ERBs, adaptations that appear finely tuned for viral disease tolerance, while also offering functional anatomical and histologic data critical to experimental design, immunopathologic interpretation, and translational modeling.

The literature synthesis reinforces the growing evidence that ERBs do not rely on canonical mammalian strategies of pathogen clearance but instead maintain tolerance to viral disease through tightly regulated interferon responses, attenuated proinflammatory signaling, and robust antiviral gene repertoires. Comparative genomic studies have revealed positive selection in innate immune effectors, particular interferon regulatory factors and tetherin, alongside expanded IFN gene families and a highly active, epithelial-centric complement system. Meanwhile, adaptive immune responses appear effective in terms of seroconversion and Fc-mediated clearance but lack the strong neutralizing antibody response typically associated with viral immunity in other mammals. This combination of rapid ISG induction, immune compartmentalization, and regulatory bias offers mechanistic insight into the ERB's ability to coexist with high-consequence pathogens like Marburg virus and Ravn virus without clinical disease.

Complementing this immunogenomic framework, the histologic atlas developed herein provides an in-depth reference for ERB lymphoid tissues across developmental stages, with a focus on the juvenile as the established experimental model age. The structural organization and cellular composition of primary and secondary lymphoid tissues are described in detail, alongside validation of immunohistochemical markers for key immune cell populations. These data indicate that ERB lymphoid organs are architecturally conserved relative to other mammals, with nuanced variations that may reflect functional adaptations, for example, the presence of periarterial macrophage sheaths and marginal zone bridging channels in the spleen, or the pronounced GALT throughout the intestinal tract. Furthermore, the characterization of age- and tissue-specific immune cell distributions, including CD3+, CD79a+, Iba1+, and Granzyme B+

cells, supports the hypothesis that immune tolerance in bats in developmentally modulated and spatially compartmentalized.

This study had several limitations. The sample size was small, limiting statistical interpretation and generalizability. All fetal tissues were collected more than a decade prior to analysis and were subject to extended fixation times, which likely impacted antigenicity and immunohistochemical staining quality. Additionally, while immunohistochemistry enabled identification of major lymphoid lineages, cross-reactivity and marker sensitivity remain challenging in non-model species, and not all immune cell subtypes could be characterized. Lastly, this study did not incorporate functional assays, single-cell or spatial transcriptomics, or flow cytometry, which would further elucidate immune cell activation states, diversity, and ontogeny.

Looking forward, there are several promising avenues for future research. First, expanding histologic and immunophenotypic studies to larger cohorts and wild-caught animals would allow for investigation of natural variability, sex- and age-based differences, and environmental influences on immune architecture, as well as comparing findings in animals that may be coinfected with two or more agents. Second, leveraging single-cell and spatial transcriptomics tools would provide high-resolution insights into cell-cell interactions, tissue microenvironments, and age-related immunologic shifts. Third, functional characterization of mucosal immunity and MALT, particularly the tonsillar and intestinal systems, could improve our understanding of initial pathogen encounter and viral shedding mechanisms. Finally, comparative studies across bat species, or between bats and other reservoir hosts, will continue to elucidate which

immunologic traits are species-specific, pan-chiropteran, or convergent strategies for viral disease tolerance.

In conclusion, this chapter offers both a conceptual framework and practical resource for understanding the immunobiology of Egyptian rousette bats. These findings not only enhance our capacity to interpret infectious disease dynamics in ERBs but also hold translational relevance for zoonotic disease modeling, vaccine development, and public health preparedness in the context of emerging infectious threats.

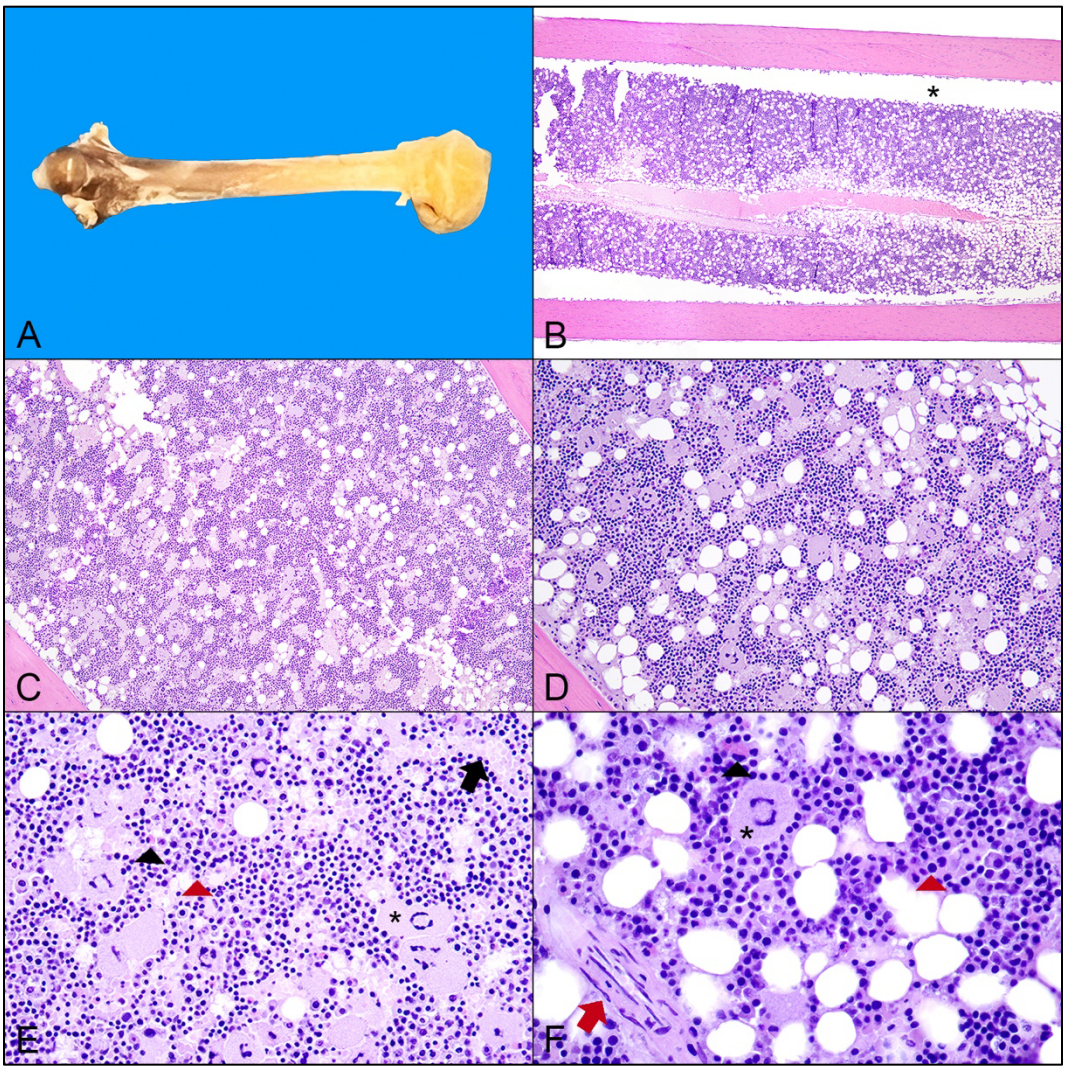

Figure 2-1: Gross and histologic features of hematopoietic bone marrow in a 6-month-old Egyptian rousette bat (*Rousettus aegyptiacus*). A) Gross image of a femur, with red-brown hematopoietic bone marrow extending from the femoral head (left) to mid-diaphysis. B) Longitudinal section of femoral bone marrow extending from the proximal (left) to mid-diaphysis, showing a large central artery and vein and increased presence of adipocytes toward the mid-diaphysis. Shrinkage artifact (black asterisk) of bone marrow away from cortical bone is an artifact associated with histologic processing of the bone. 2x, Hematoxylin and eosin (HE). C and D) Representative example of bone marrow cellularity in a juvenile ERB. Bone marrow contains clusters of hematopoietic cells admixed with adipocytes. C) 10x, HE. D) 20x, HE. E) The highly cellular bone marrow has areas of myeloid (black arrowhead) and erythroid (red arrowhead) hematopoiesis as well as megakaryocytes (black asterisk) and a venous sinus (black arrow). Degeneration of the megakaryocyte nuclei is reflective of artifactual change from fixation procedures (i.e., fixing the limb whole vs. opening the marrow cavity to be directly exposed to 10% neutral buffered formalin). 40x, HE. F) Higher magnification image showing myeloid (black arrowhead) and erythroid (red arrowhead) hematopoiesis with admixed adipocytes, as well as megakaryocytes (asterisk) and a nutrient artery (red arrow). 60x, HE.

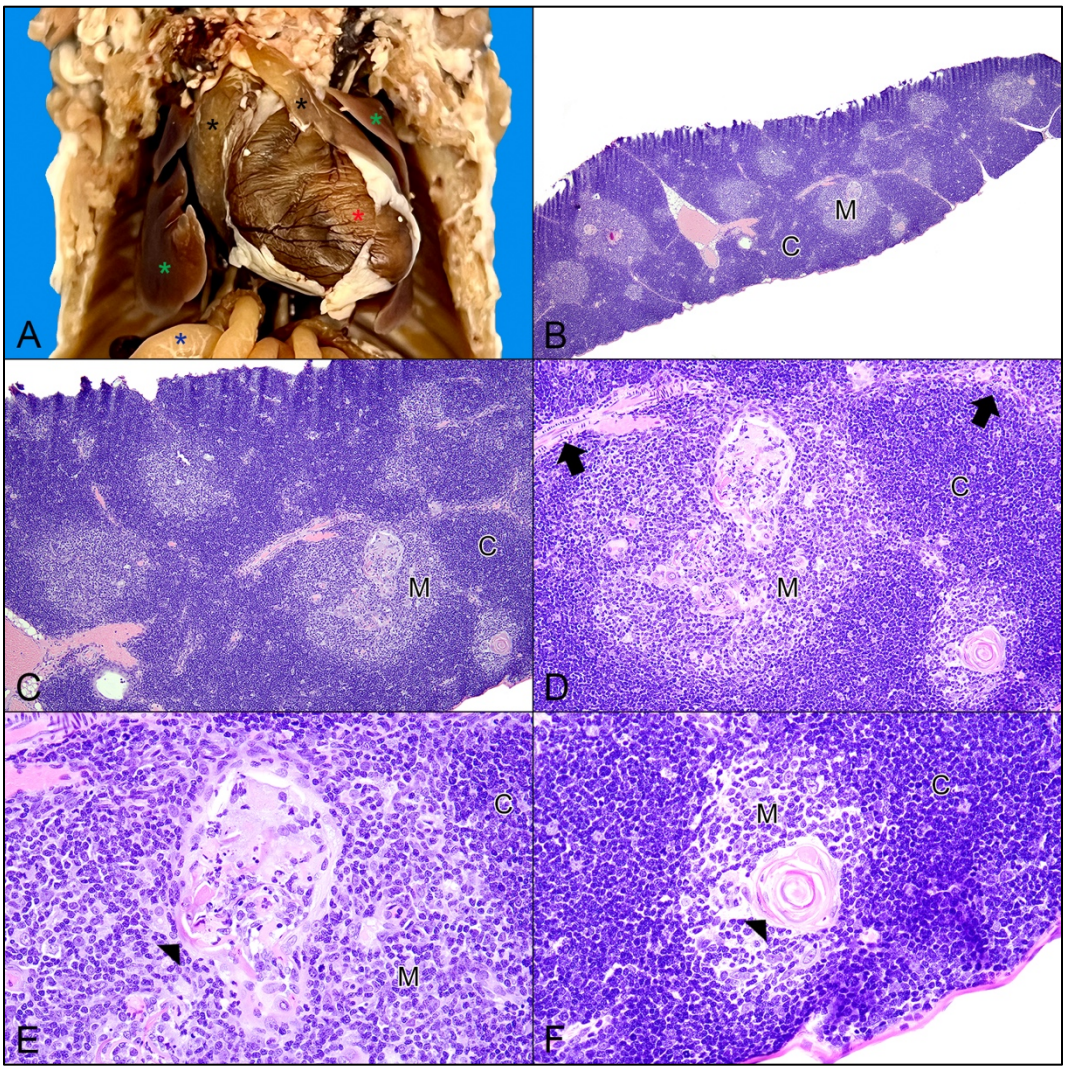

Figure 2-2: Gross and histologic features of the thymus in a 6-month-old Egyptian rousette bat (*Rousettus aegyptiacus*). A) Gross ventrodorsal view of the thoracic cavity showing the bilobed thymus (black asterisks) in the pericardial mediastinum. Additionally visible are the heart (red asterisk), lungs (green asterisks), and intestines (blue asterisk). Overlying ribs, sternum, and within the abdominal cavity, liver and diaphragm, have been removed. B and C) Single thymic lobe showing the relative amounts of cortex (C) and medulla (M). The ERB thymus is partially subdivided into indistinct lobules by thin bands of connective tissue that are continuous with the thin connective tissue capsule. Tissue chattering at the top of the organ is an artifact of processing. B) 4x, HE. C) 10x, HE. D) Corticomedullary junction containing arterioles with scant perivascular connective tissue. 20x, HE. E) A large Hassall's corpuscle (black arrowhead) in the thymic medulla containing numerous epithelial cells with large nuclei, degenerative, eosinophilic, granular cytoplasm and scant cytoplasmic keratinization admixed with cellular debris. Note the prominent cellularity difference between the epithelial cells within the medulla and the small lymphocytes that predominantly compose the cortex. 40x, HE. F) Another example of a Hassall's corpuscle containing whorls of keratin. 40x, HE.

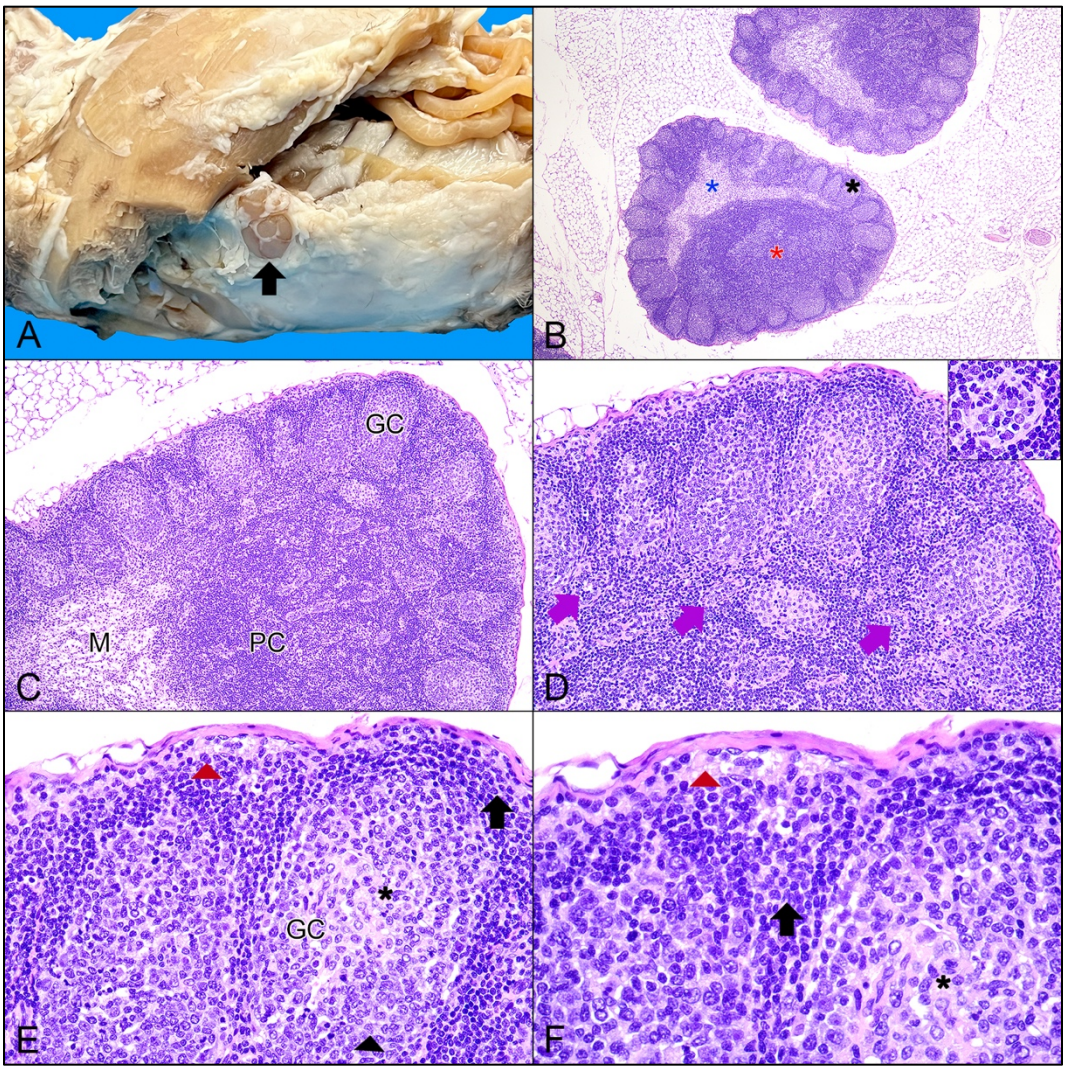

Figure 2-3: Gross and histologic features of the lymph node in a 6-month-old Egyptian rousette bat (*Rousettus aegyptiacus*). A) Right lateral view of an ERB in dorsal recumbency, showing the location of the axillary lymph node (black arrow). The right humerus has been removed. B and C) Cross section of an axillary lymph node, showing the cortex containing numerous secondary follicles with germinal centers (black asterisk; GC), robust paracortex (red asterisk; PC), and medulla (blue asterisk; M). B) 4x, HE. C) 10x, HE. D) Numerous arterioles lined by high endothelial venules are present within the corticomedullary junction (purple arrows) Inset: Higher magnification image of a high endothelial venule. 60x, HE. E) Proliferating B-cell precursors within germinal centers of secondary follicles displace mature B-cells to the periphery, where they form a basophilic mantle or corona (black arrow). Mature germinal centers may have a basal population of large, densely packed centroblasts (black arrowhead) and an apical population of smaller, less densely packed centrocytes (black asterisk). Apical to the secondary follicles is the subscapsular sinus (red arrowhead). 40x, HE. F) Higher magnification of E. 60x, HE.

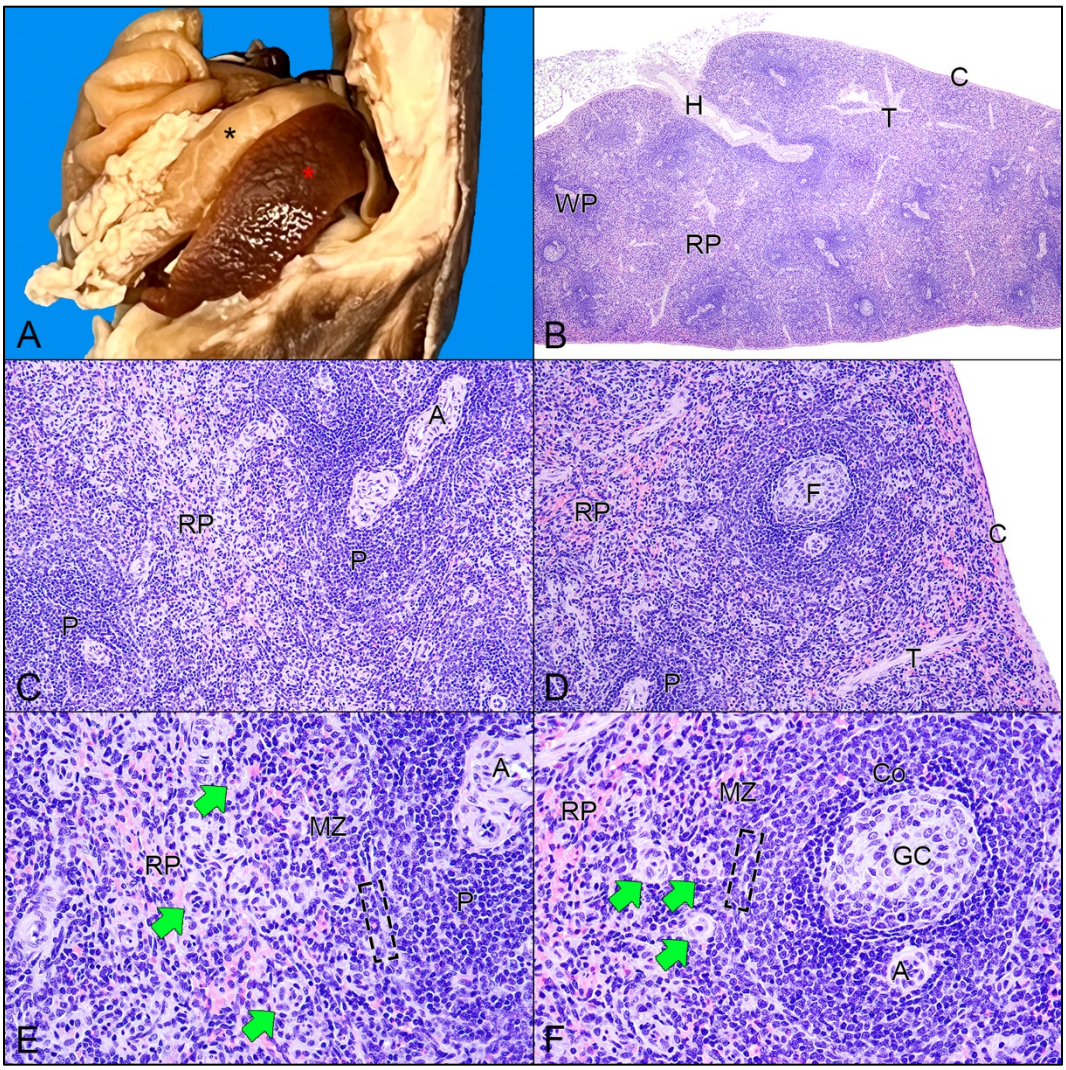

Figure 2-4: Gross and histologic features of the spleen in a 6-month-old Egyptian rousette bat (*Rousettus aegyptiacus*). A) Left lateral view of an ERB in dorsal recumbency, showing the location of the spleen (red asterisk) along the greater curvature of the stomach (black asterisk). The liver and left lateral flank have been removed. B-F) Cross sections of the spleen showing the splenic hilus (H), white pulp (WP), red pulp (RP), capsule (C), trabeculae (T), central arteries (A), periarteriolar lymphoid sheaths (P), white pulp follicles (F) with germinal centers (GC), surrounding mantle zone/corona (Co), marginal sinus (rectangular box with dashed lines), marginal zone (MZ), and clusters of ellipsoids (green arrows). B), 4x, HE. C and D) 20x, HE. E and F) 40x, HE.

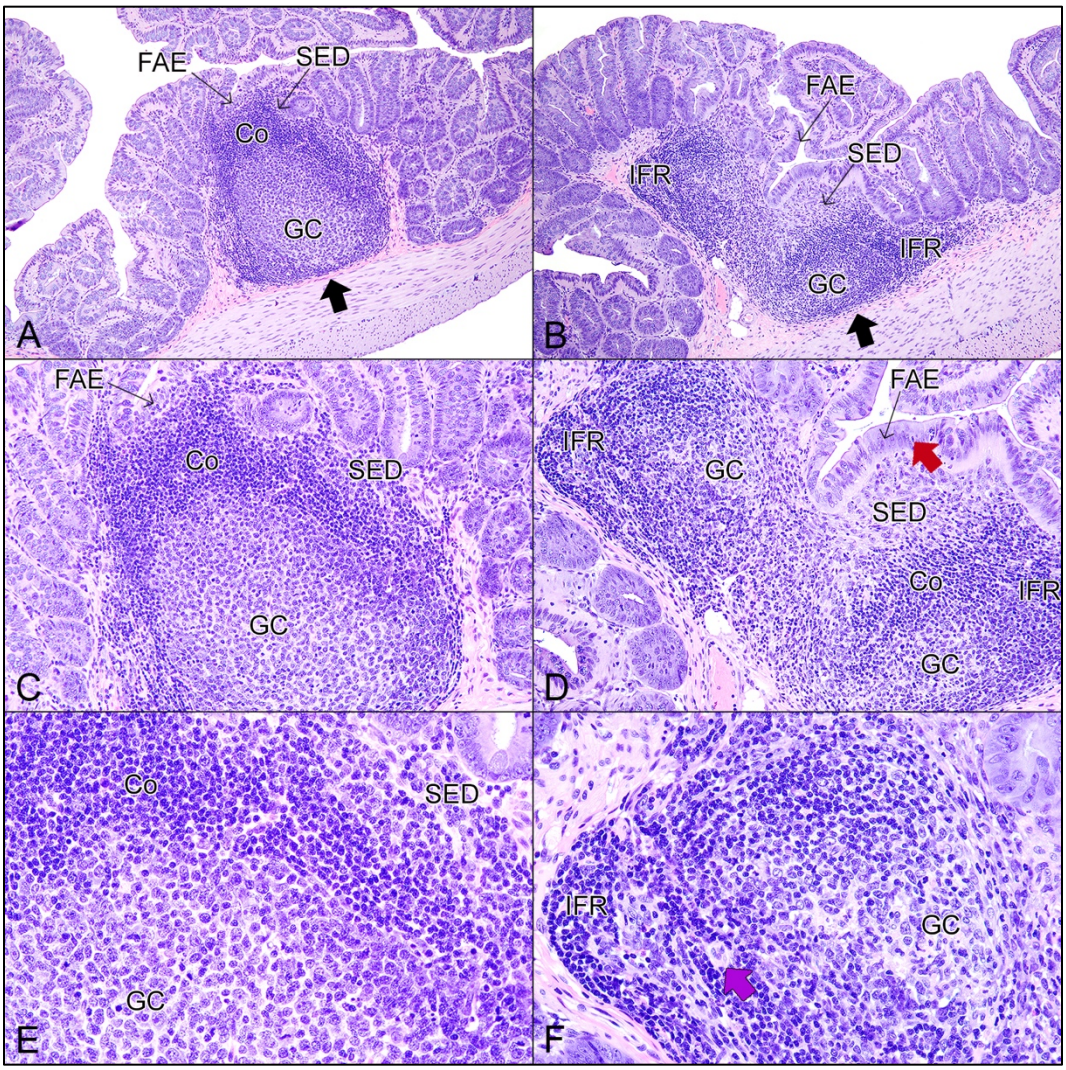

Figure 2-5: Histologic features of gastrointestinal-associated lymphoid tissue (GALT) in a 6-month-old Egyptian rousette bat (*Rousettus aegyptiacus*). A, C, E) A isolated lymphoid follicle (black arrow) with a germinal center (GC) and overlying mantle zone/corona (Co) expands the lamina propria of the proximal colon. The follicle-associated epithelium (FAE) is separated from the subepithelial dome region (SED). A) 10x, HE. C) 20x, HE. E) 40x, HE. B, D, F) A Peyer's patch expanding the laminal propria of the proximal colon. Low numbers of intraepithelial lymphocytes (red arrow) are present. Interfollicular regions (IFR) contain numerous high endothelial venules (purple arrow). B) 10x, HE. D) 20x, HE. F) 40x, HE.

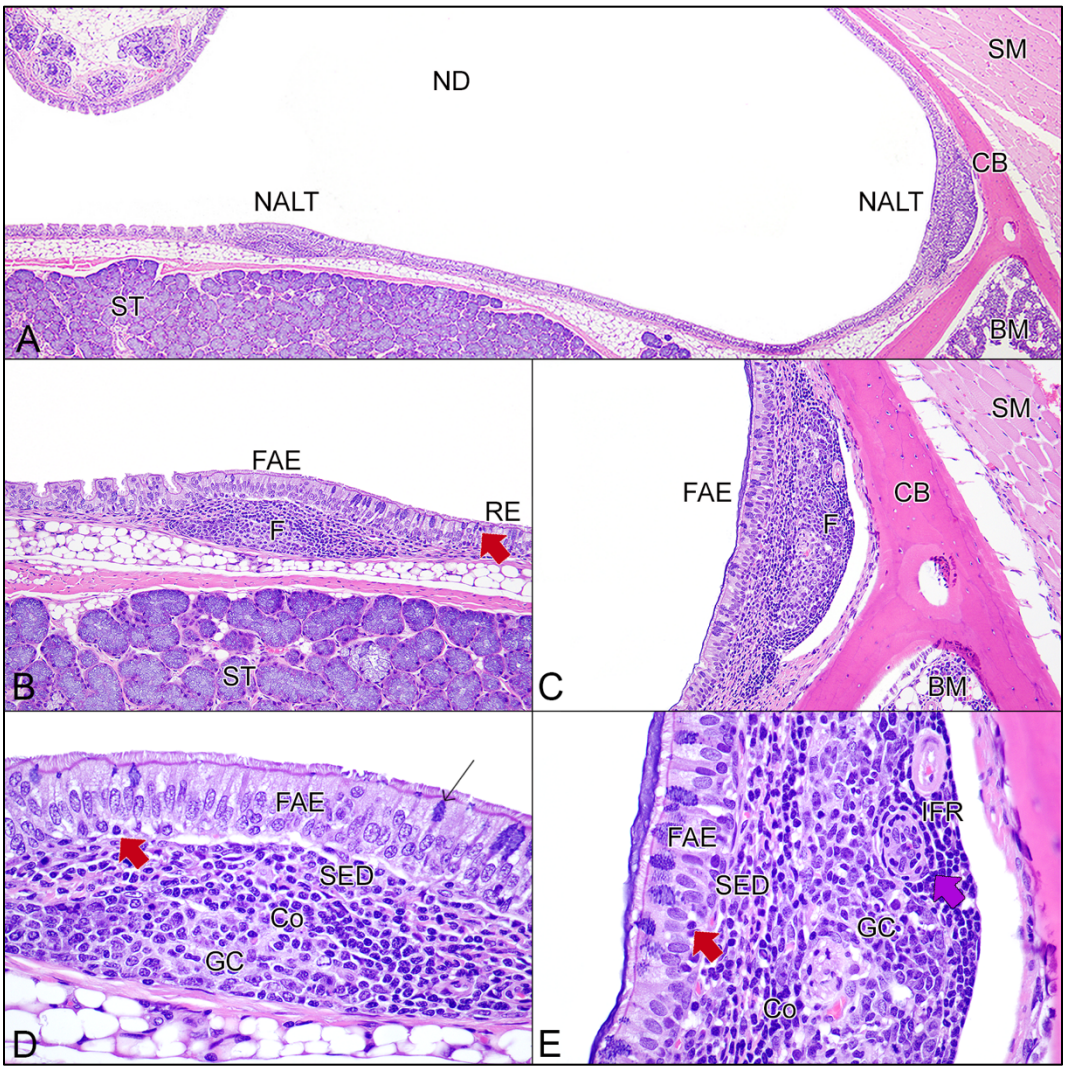

Figure 2-6: Histologic features of nasal-associated lymphoid tissue (NALT) in a 6-month-old Egyptian rousette bat (*Rousettus aegyptiacus*). A) Nasal-associated lymphoid tissue (NALT) on the lateroventral and ventral floor of the proximal nasophargyngeal duct (ND). Salivary tissue (ST) is present between the ND and hard palate (out of frame). BM = Bone marrow. SM = Skeletal muscle. CB = Cortical bone. 4x, HE. B and D) A well-defined NALT follicle (F). Goblet cells (thin black arrow) and intraepithelial lymphocytes (red arrow) are typically absent in the follicle-associated epithelium (FAE) immediately overlying the follicle, however, can be found on the peripheral FAE and throughout normal respiratory epithelium (RE). FAE remains densely ciliated. GC = Germinal center, Co = Corona/mantle zone, SED = Subepithelial dome. B) 20x, HE. D) 60x, HE. C and E) A less-well defined NALT follicle. The germinal center (GC), corona/mantle zone (Co), and subepithelial dome (SD) are more difficult to distinguish. Prominent high endothelial venules (purple arrow) are present within the interfollicular region (IFR). There are occasional intraepithelial lymphocytes (red arrow) within the follicle-associated epithelium (FAE).

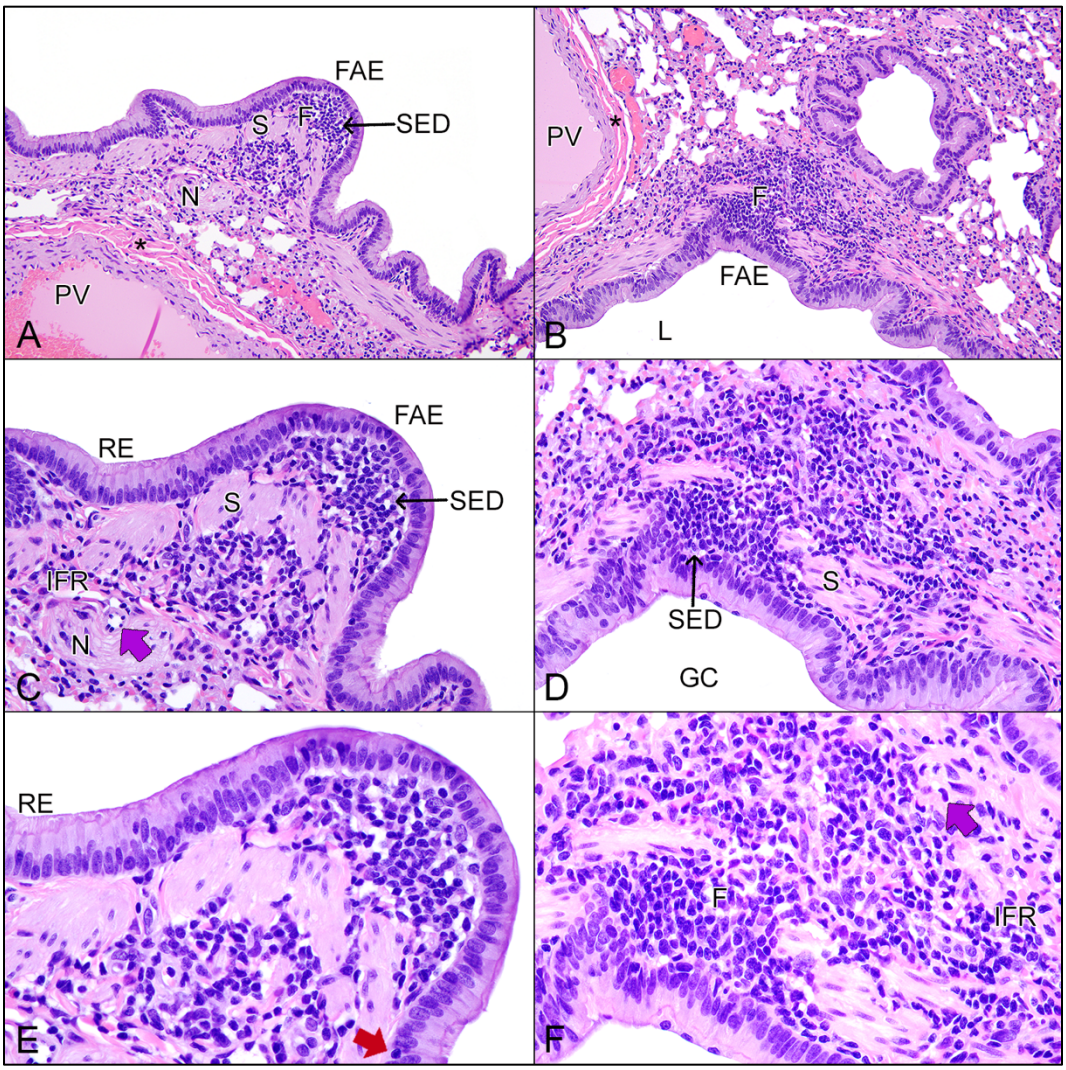

Figure 2-7: Histologic features of bronchus-associated lymphoid tissue (BALT) in a 6-month-old Egyptian rousette bat (*Rousettus aegyptiacus*). A-F) Two examples of BALT along a primary bronchiole. Germinal centers within follicles (F) are uncommon, and thin subepithelial domes (SED) and interfollicular regions (IFR) are difficult to distinguish. Overlying follicle-associated epithelium (FAE) generally lacks cilia and goblet cells. The presence of high endothelial venules (purple arrow) may be the only way to distinguish the IFR. N = Nerve, PV = Pulmonary vein, Black asterisk = cardiomyocytes surrounding pulmonary vein, S = Smooth muscle, red arrow = intraepithelial lymphocyte. A-B) 20x, HE. C-D) 40x, HE. E-F) 60x, HE.

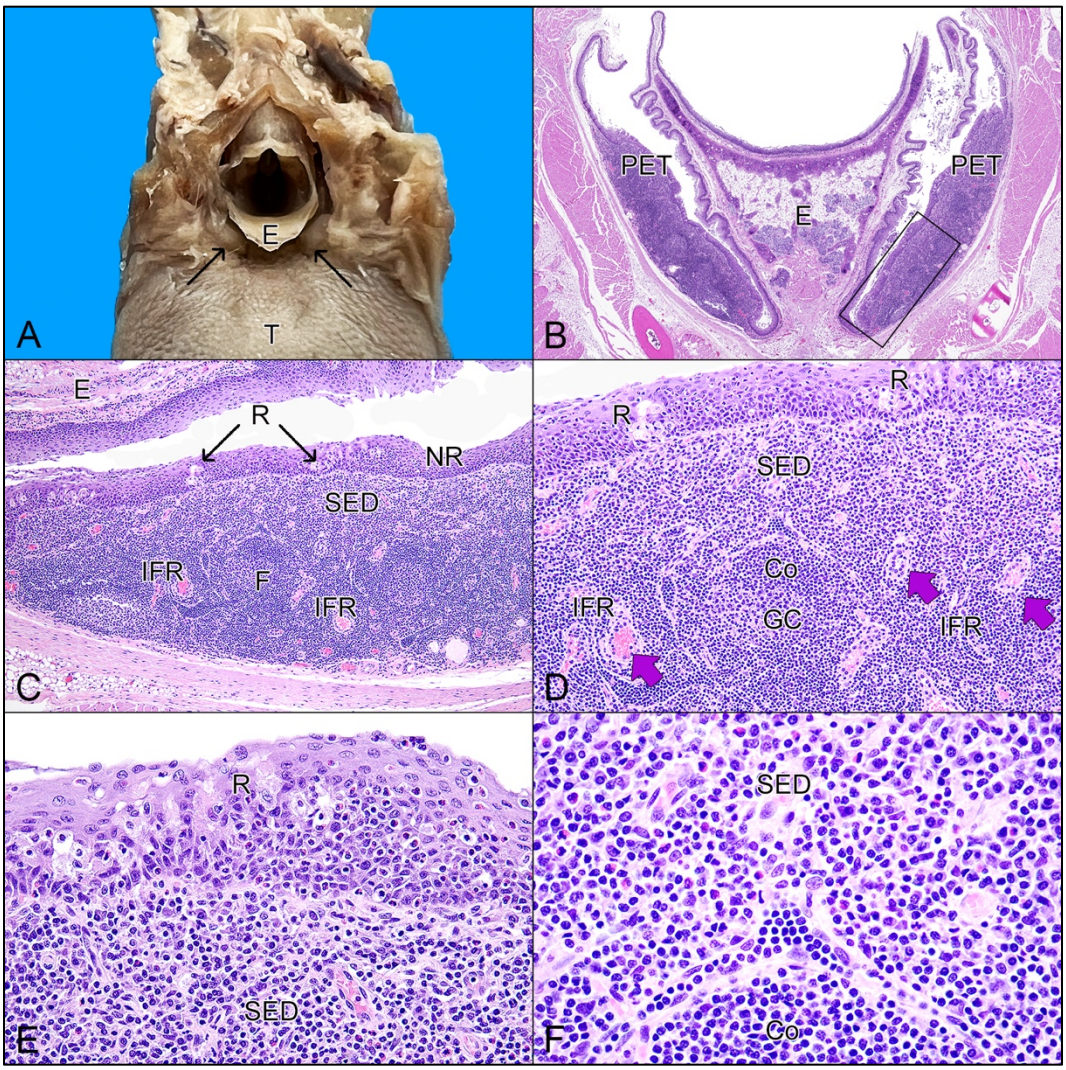

Figure 2-8: Gross and histologic features of the paraepiglottic tonsils in a 6-month-old Egyptian rousette bat (*Rousettus aegyptiacus*). A) Rostral view of the larynx, showing the epiglottis (E), paraepiglottic tonsils (thin black arrows), and tongue (T). The pharyngeal roof, soft palette, and adjacent soft tissue and skeletal muscle have been removed. B) Transverse section of epiglottis (E) and paraepiglottic tonsils (PET). The area in C-F is delineated with a black rectangle. 2x, HE. C-F) Reticular (R) and non-reticular (NR) epithelium overlies the paraepiglottic tonsil, which is otherwise structurally similar to a Peyer's patch. E = epiglottis, SED = subepithelial dome, F = follicle, IFR = interfollicular region, GC = germinal center, Co = corona/mantle zone, R = reticular epithelium, NR = non-reticular epithelium, purple arrows = high endothelial venules. C) 10x, HE. D) 20x, HE. E) 40x, HE. F) 60x, HE.

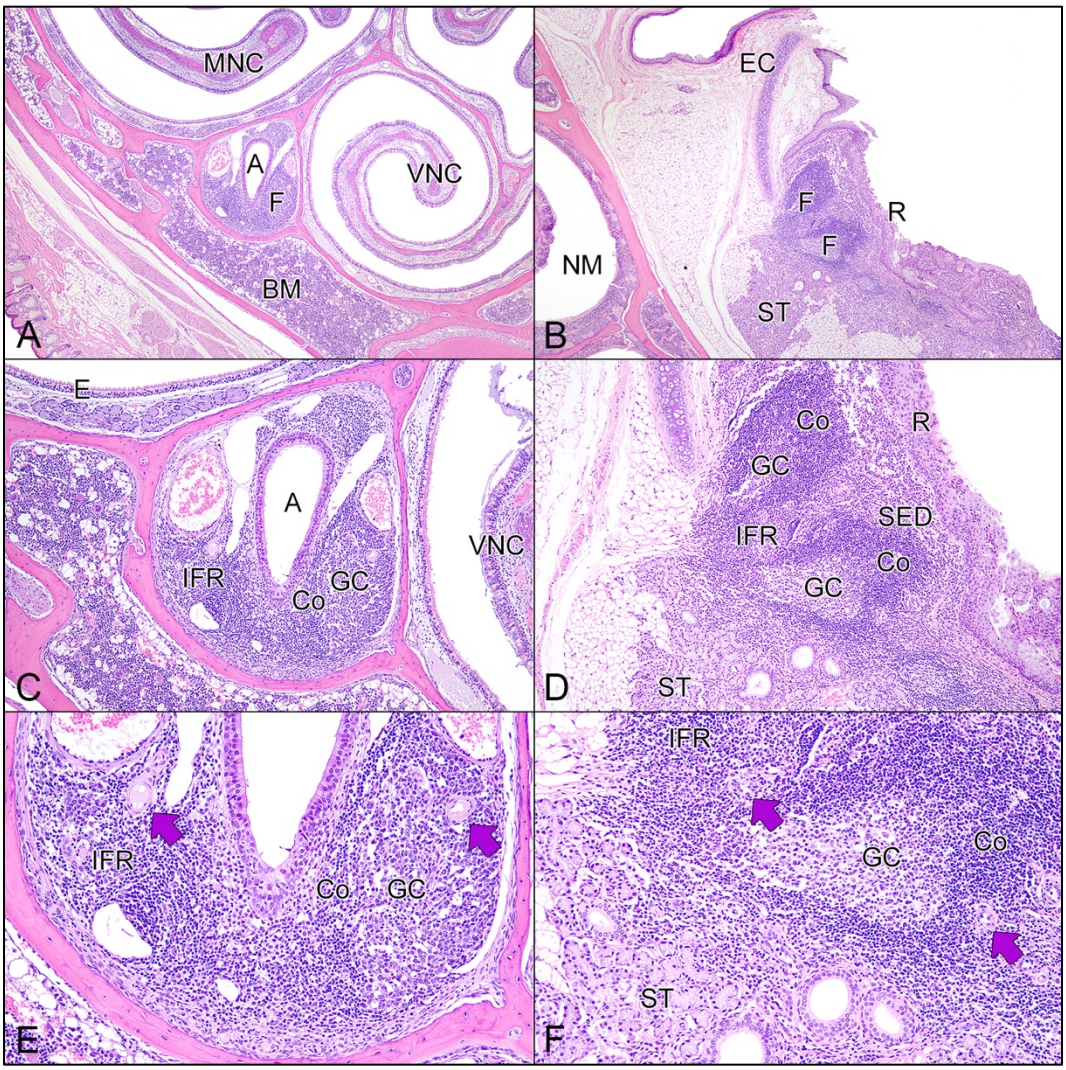

Figure 2-9: Histologic features of the tubal tonsil in a 6-month-old Egyptian rousette bat (*Rousettus aegyptiacus*). A, C, E) Tubal tonsil surrounding the auditory or Eustachian tube (A), with typically ventrolateral follicles (F). MNC = middle nasal concha, VNS = ventral nasal concha, BM = bone marrow, GC = germinal center, Co = corona/mantle zone, IFR = interfollicular region, purple arrow = high endothelial venules. A) 4x, HE. C) 10x, HE. E) 20x, HE. B, D, F) Tubal tonsil located at the opening of the auditory tube. EC = Elastic cartilage, F = follicle, NM = nasal meatus, ST = salivary tissue, R = reticular epithelium. B) 4x, HE. D) 10x, HE. F) 20x, HE.

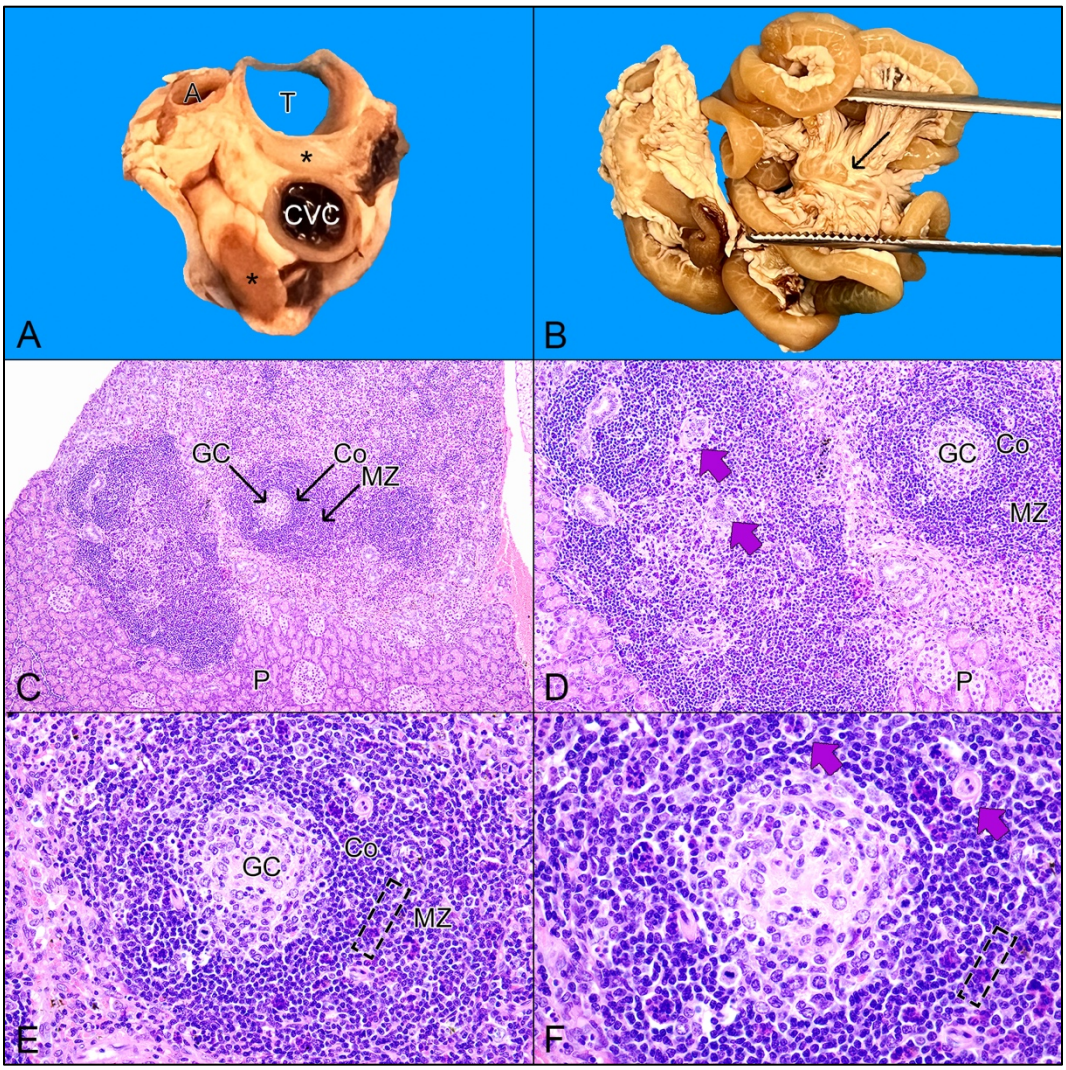

Figure 2-10: Additional gross and histologic features of lymphoid tissue in Egyptian rousette bat (*Rousettus aegyptiacus*). A) Transverse section through thoracic tissue immediately caudal to the aortic arch shows the location of tracheobronchial lymph nodes (black asterisks). T = trachea, A = aorta, CVC = cranial vena cava. B) Cranial mesenteric lymph node (black arrow) within the root of the mesentery. C-F) Tertiary lymphoid structures within a locally extensive focus of chronic inflammation in the pancreas of an adult male free-ranging ERB. GC = germinal center, Co = corona/mantle zone, MZ = marginal zone, P = pancreas, black dashed rectangle = marginal sinus, purple arrows = high endothelial venules. C) 10x, HE. D) 20x, HE. E) 40x, HE. F) 60x, HE.

Table 2-1: Compiled information on antibodies used on Egyptian rousette bat (*Rousettus aegyptiacus*) tissues. Information provided includes antibodies utilized in this study, published in the general literature, and used for unpublished diagnostic evaluations. NS = Not stated, R = Rabbit, M = Mouse, C = Canine, GP = Guinea Pig

Antibody	Host	Source, Catalog ID	Antigen Retrieval	Dilution	Chromogen	Autostainer	Positive Control	Successful	Ref.
Anti-cholineacetyl transferase	R	Chemicon, AB143	NS	1:1500	DAB	NS	NS	Yes	[438]
Anti-serotonin	R	Chemicon, AB938	NS	1:7500	DAB	NS	NS	Yes	[438]
Anti-tyrosine hydroxylase (TH)	R	Chemicon, AB151	NS	1:6000	DAB	NS	NS	Yes	[438]
Caspase 3	R	Biocare Medical, CP229B	High pH antigen retrieval 15min @110C	1:8000	DAB	Biocare Intellipath	R lymph node	Yes	[17]
CD3	R	Dako, A0452	Citrate 15min @115C; NS	1:1000 or NS	DAB or NS	Biocare Intellipath or NS	C lymph node	Yes, No[165]	[17,165] Current study
CD20	R	Biocare Medical, ACR3004B	Citrate 15min @115C	1:500	DAB	Biocare Intellipath	C lymph node	No	Current study
CD21	M	Cell Marque, 12R-16	Citrate 15min @115C	1:75	DAB	Biocare Intellipath	C lymph node	No	Current study

CD79a	M	Dako, M7051; Biocare Medical, CM067C	Reveal Decloaker 15min @115C; NS	1:50 or NS	DAB	Biocare Intellipath or NS	C lymph node	Yes, No[165]	[165] Current study
CD117 (c-kit)	R	Dako, A4502	Citrate buffer	1:200	DAB	NS	C	Yes	[163]
Cytokeratin (Pan)	M, NS	Dako; NS	Citrate buffer; NS	1:100 or NS	NovaRed or NS	NS	C haired skin; C; sebaceous epithelial cells; NS	Yes, No[168]	[162,165,166,168]
Cytokeratin 19	M	Dako, IR615	NS	Ready to use	DAB	NS	C, ERB liver	Yes	[167]
Desmin	R, M	Dako, M0760; Dako, Clone D33; NS	Citrate buffer; no treatment; NS	1:200 or NS	DAB, NovaRed, or NS	NS	Equine cardiomyocytes; vascular and intestinal smooth muscle; C	Yes	[163,165,166,168]
E-cadherin	M	BD Biosciences, 610181	Citrate 15min @115C	1:500	DAB	Biocare Intellipath	M skin	Yes	Unpublished data
Ebola virus	R	Viral Special Pathogens Branch, CDC	Proteinase K 15 min @ RT, followed by Ultra	1:250	Fast Red	NS	NS	Yes	[45]

			V Block 10 min @ RT						
Factor VIIIRA	R	Cell Marque, 250A-18	Citrate 15min @110C	Ready to use	DAB	Biocare Intellipath	R lymph node	Yes	Unpublished data
Glypican-3	M	Santa Cruz Biotechnology, SC-65443	NS	1:50	DAB	NS	C, ERB liver	Yes	[167]
Granzyme B	R	Spring BioScience, E2582	Citrate 15min @115C	1:200	DAB	Biocare Intellipath	Feline intestinal T-cell lymphoma	Yes	Current study
HepPar-1	M	Dako, IR624	NS	Ready to use	DAB	NS	C, ERB liver	Yes	[167]
HPV (1, 6, 11, 16, 18, 31)	M	Chemicon	NS	NS	NS	NS	NS	Yes	[153]
Iba1	R	WAKO, 019-19741	Citrate 15min @115C; NS	1:1000, 1:8000	DAB	Biocare Intellipath or NS	C brain; NS	Yes	[17,167] Current study
Ki-67	M	Dako, IR626	NS	Ready to use	DAB	NS	C, ERB liver	Yes	[167]
Laminin	R	Dako, Z0097	Proteinase K	1:100	DAB	NS	C	Yes	[163]
Marburg virus	R	Viral Special Pathogens Branch, CDC	Proteinase K 15 min @ RT,	1:250	Fast Red	NS	NS	Yes	[45,50]

			followed by Ultra V Block 10 min @ RT						
Neuronal Nuclear Antigen (NeuN)	GP	MilliporeSigma, ABN90P	NS	1:2000	DAB or Strepdavidin	NS	NS	Yes	[439]
Pax-5	M	Santa Cruz Biotechnology, SC-13146	Citrate 15min @115C	1:1500	DAB	Biocare Intellipath	C spleen	No	Current study
S100	R	Dako, Z0311	Citrate buffer	1:100 or 1:800	DAB or NovaRed	NS	C	Yes	[163,166]
Smooth Muscle Actin (SMA)	M	Dako, M0851	Citrate 15min @115C, or no treatment, or NS	1:100, 1:200, or 1:1500	DAB, NovaRed, or NS	Biocare Intellipath or NS	M intestine; equine cardiomyocytes; C; NS	Yes	[163,166,168] Unpublished data
Sosuga virus	R	Genscript	Reveal Decloaker 15min @115C	1:2000	Fast Red	NS	SOSV-infected Vero cell pellet	Yes	[17]
Vimentin	M	Dako, M0720; Dako Clone V9; Dako, Clone 3B4; NS	Proteinase K, or Citrate buffer, or NS	1:100, 1:200	DAB, NovaRed, or NS	NS	C haired skin; Canine; Vascular and intestinal smooth muscle	Yes, No[166]	[163,165,166,168]

Yersinia pseudotuberculosis serotypes O1, O2, O3, O4, O5 and O6	R	Denka-Seiken Co.	NS	NS	NS	NS	NS	Yes	157
Yersinia enterocolitica serotypes O1–2, O3, O5, O8 and O9	R	Denka-Seiken Co.	NS	NS	NS	NS	NS	Yes	157

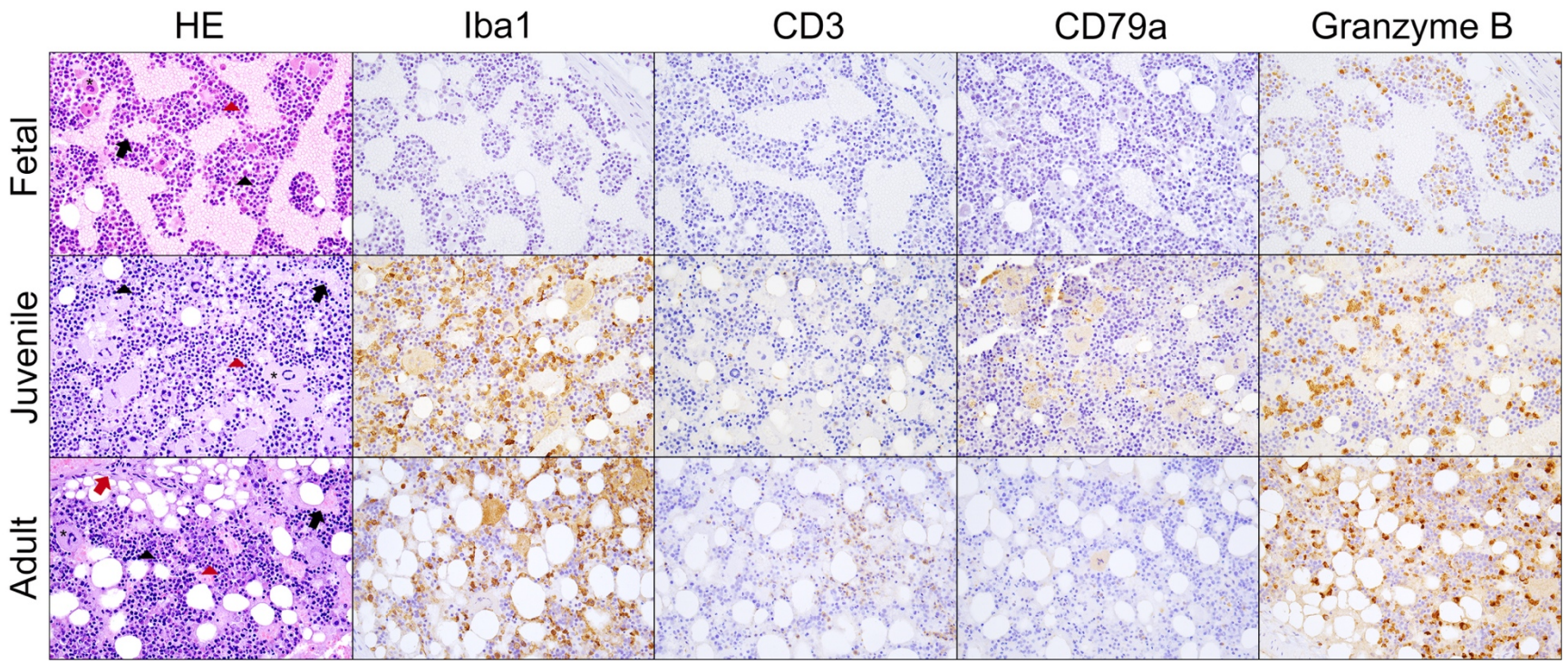

Figure 2-11: Comparison of bone marrow immunolabeling across fetal, juvenile, and adult Egyptian rousette bat (*Rousettus aegyptiacus)* tissues. Sections are reflective of bone marrow sections within or immediately adjacent to the femoral head. 40x magnification. HE: Hematoxylin and eosin. Iba1: Ionized calcium-binding adapter molecule 1. Monocyte/macrophage lineage; cytoplasmic reactivity. CD3: Cluster of differentiation 3. T cell receptor complex; membranous or cytoplasmic reactivity. CD79a: Cluster of differentiation 79a. B cell receptor complex; primarily cytoplasmic reactivity, membranous reactivity additionally occurs. Granzyme B: Neutral serine proteases in specialized lytic granules in CTLs and NK cells; cytoplasmic reactivity. Fetal bone marrow has positive immunoreactivity with Granzyme B. Juvenile and adult bone marrow has low positive immunoreactivity with CD3 and CD79a, with additional cytoplasmic labeling of megakaryocytes, and robust positive immunoreactivity with Iba1 and Granzyme B. Black arrowhead = myeloid hematopoiesis, red arrowhead = erythroid hematopoiesis, black asterisk = megakaryocyte, red arrow = nutrient artery, black arrow = venous sinus.

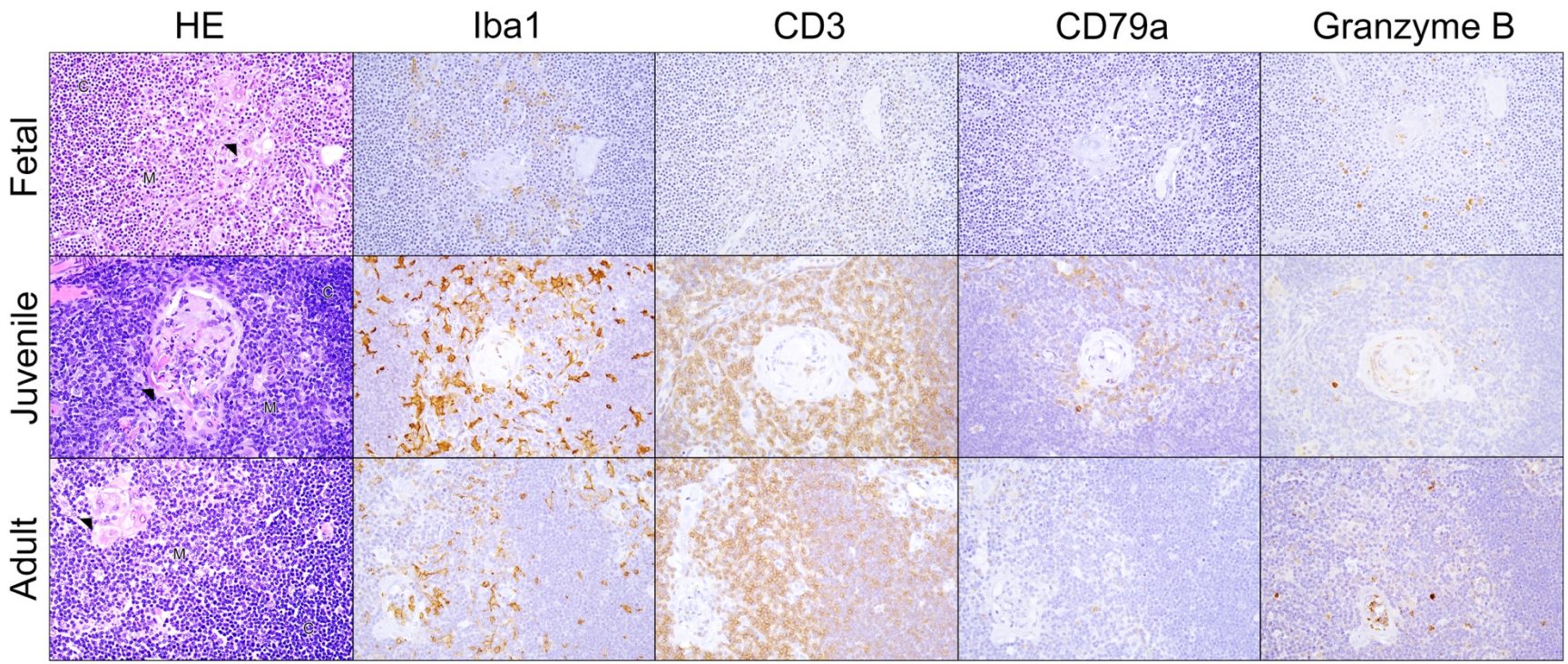

Figure 2-12: Comparison of thymic immunolabeling across fetal, juvenile, and adult Egyptian rousette bat (*Rousettus aegyptiacus)* tissues. Sections are reflective of the corticomedullary junction, with Hassall's corpuscles and blood vessels included where possible. 40x magnification. 40x magnification. Fetal thymus has scant positive immunoreactivity with CD3 and low positive immunoreactivity with Iba1 and Granzyme B. Juvenile and adult bone marrow has low positive immunoreactivity with CD79a and Granzyme B, with additional cytoplasmic labeling of megakaryocytes, and moderate to robust positive immunoreactivity with Iba1 and CD3. CD3 immunolabeling highlights the concentration of CD3+ T cells within the thymic medulla. Black arrowhead = Hassall's corpuscle, C = cortex, M = medulla.

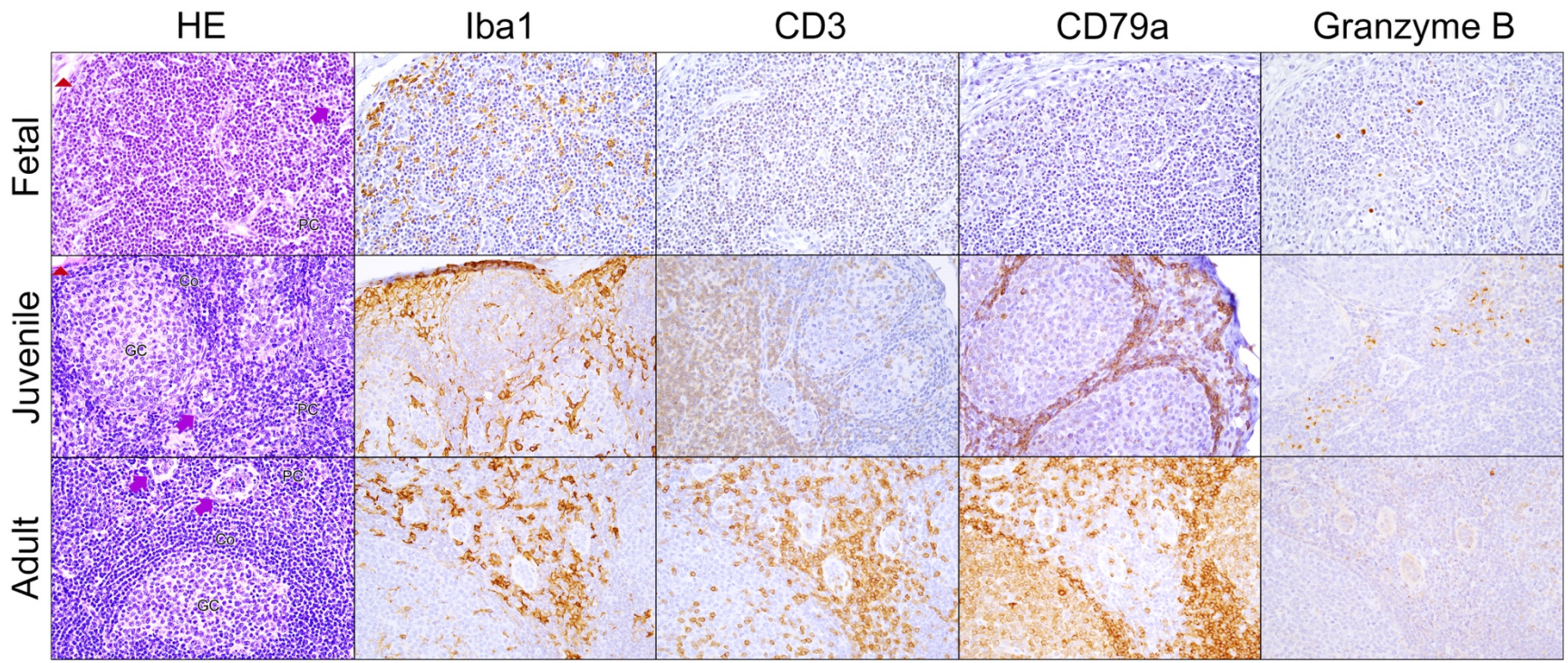

Figure 2-13: Comparison of lymph node immunolabeling across fetal, juvenile, and adult Egyptian rousette bat (*Rousettus aegyptiacus*) tissues. Sections are reflective of the subcapsular sinus, cortex containing secondary follicles (juvenile and adult), and subjacent paracortex. 40x magnification. Fetal lymph node has faint positive immunoreactivity with CD3 and strong positive immunoreactivity with Iba1 and Granzyme B. and moderate Iba1 and Granzyme B. Juvenile and adult lymph node has strong positive immunoreactivity with all stains, highlighting the concentrations of Iba1+ and CD3+ cells within the paracortex, CD79a+ cells within the germinal center and corona/mantle zone, and rare Granzyme B+ cells within the paracortex. Red arrowhead = subcapsular sinus, GC = germinal center, Co = corona/mantle zone, PC = paracortex, purple arrow = high endothelial venules.

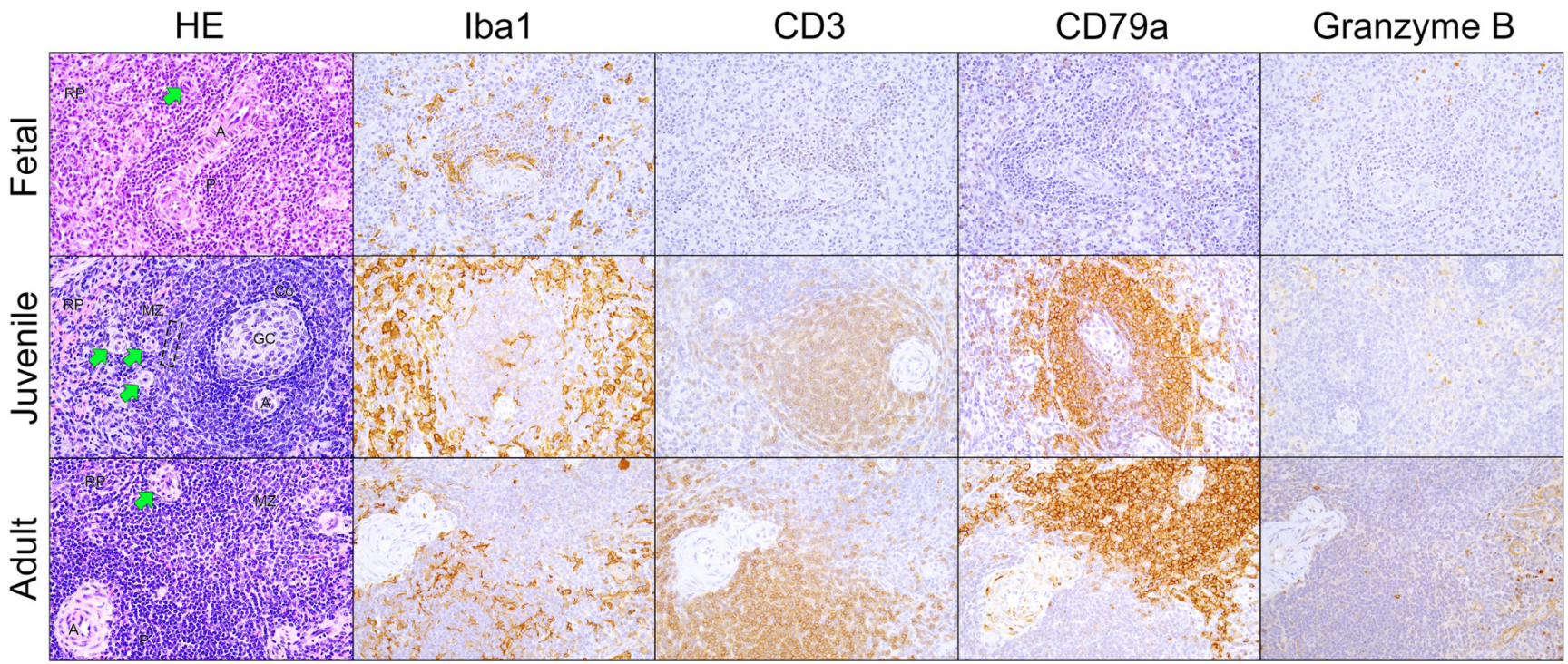

Figure 2-14: Comparison of splenic immunolabeling across fetal, juvenile, and adult Egyptian rousette bat (*Rousettus aegyptiacus*) tissues. Sections are reflective of white pulp, red pulp, and associated structures. 40x magnification. Fetal spleen has faint positive immunoreactivity with CD3 and CD79a and strong positive immunoreactivity with Iba1 and Granzyme B. Juvenile and adult spleen has strong positive immunoreactivity across all stains, highlighting the concentration of Iba1+, CD79a+, and Granzyme B+ cells within the marginal zone and CD3+ cells within periarteriolar lymphoid sheaths. RP = red pulp, A = central arteries, P = periarteriolar lymphoid sheaths, GC = germinal center, Co = corona/mantle zone, rectangular box with dashed lines = marginal sinus, MZ = marginal zone, green arrow = ellipsoid.

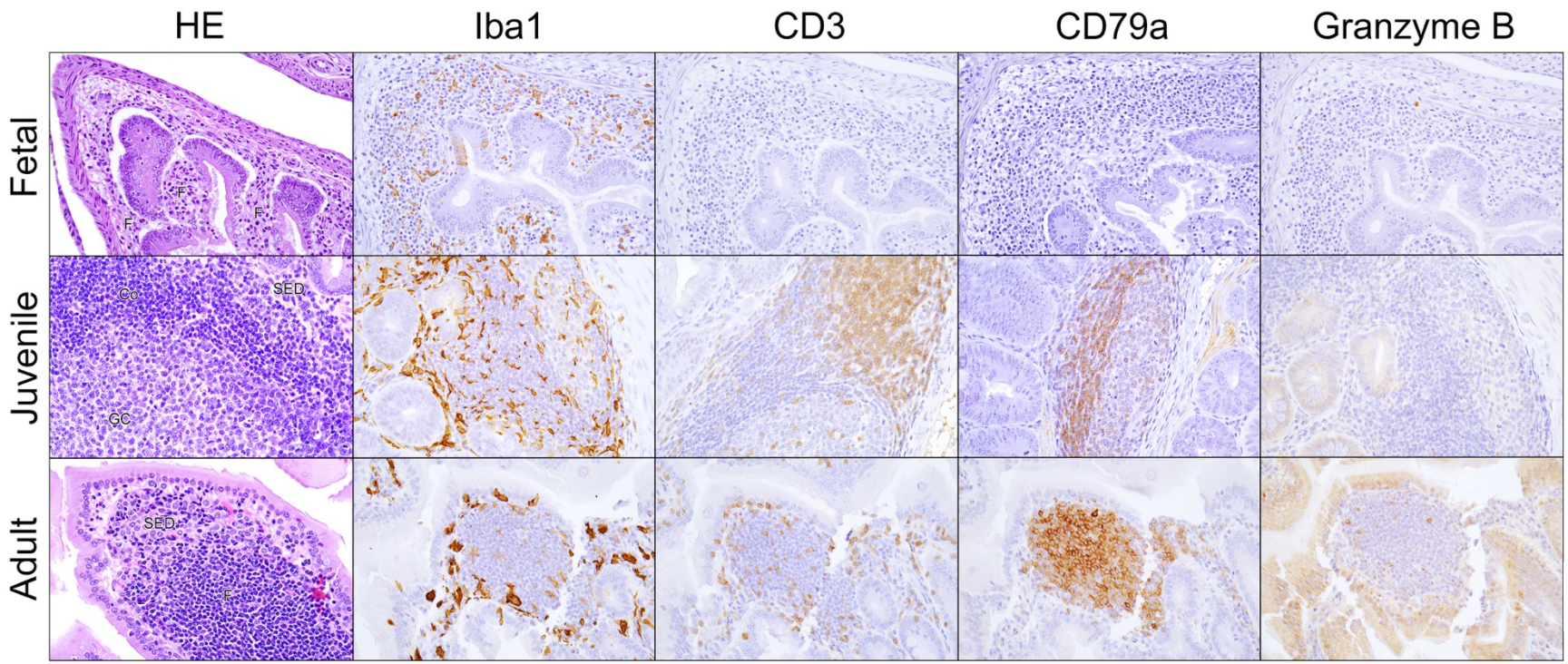

Figure 2-15: Comparison of gastrointestinal-associated lymphoid tissue (GALT) immunolabeling across fetal, juvenile, and adult Egyptian rousette bat (*Rousettus aegyptiacus*) tissues. Sections are reflective of Peyer's patches within the proximal colon. 40x magnification. Consistent with other lymphoid organs, Fetal GALT has faint positive immunoreactivity with CD3 and CD79a and strong positive immunoreactivity with Iba1 and Granzyme B. Juvenile and adult GALT have strong positive immunoreactivity with all stains except for faint positive immunoreactivity in juvenile tissue with Granzyme B. Adult GALT did not have well-defined germinal centers, likely from its relatively antigen-free managed care environment. F = follicle, GC = germinal center, Co = corona/mantle zone, SED = subepithelial dome.

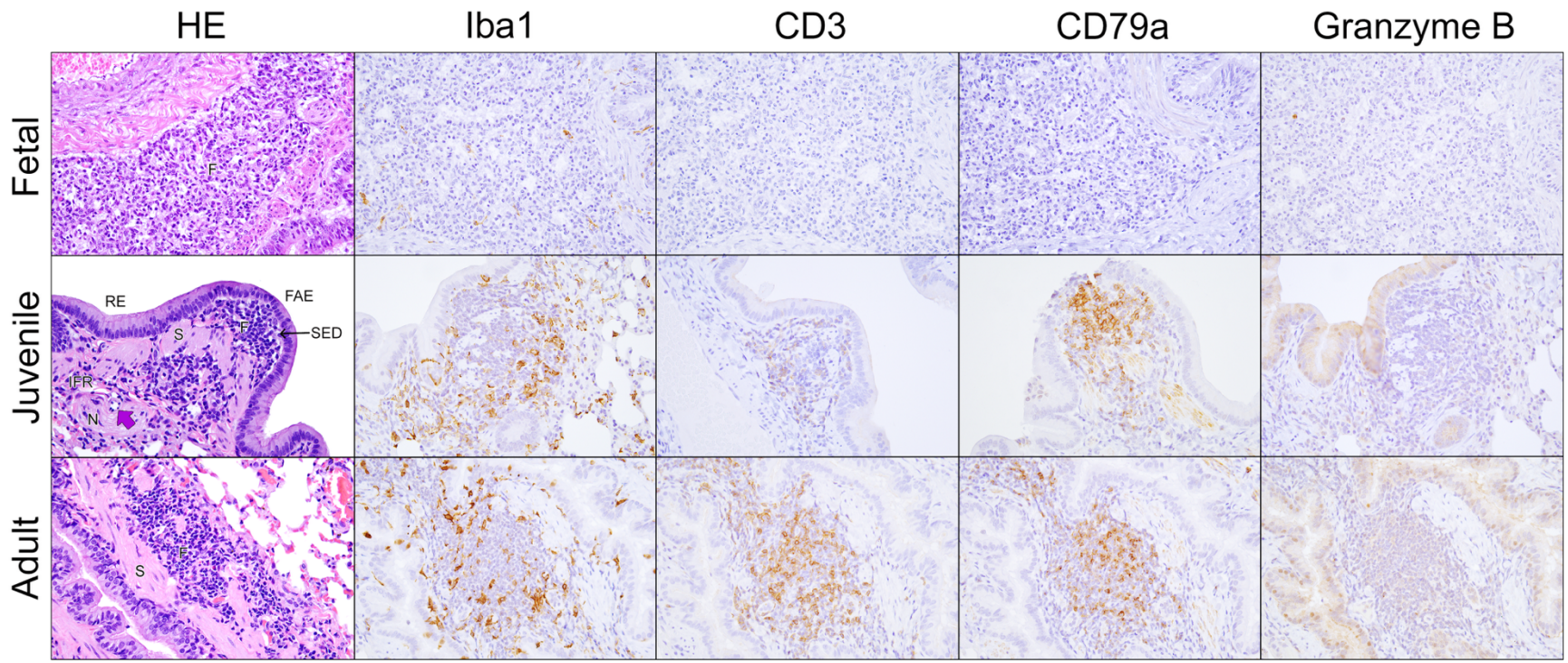

Figure 2-16: Comparison of bronchus-associated lymphoid tissue (BALT) immunolabeling across fetal, juvenile, and adult Egyptian rousette bat (*Rousettus aegyptiacus*) tissues. Sections are adjacent to major bronchioles. 40x magnification. Presumptive fetal BALT (areas of hypercellularity between large bronchioles and pulmonary vessels) has no immunoreactivity with CD3 and CD79a, and strong, rare positive immunoreactivity with Iba1 and Granzyme B. Juvenile and adult BALT have no to scant positive immunoreactivity with Granzyme B, but strong positive immunoreactivity with Iba1, CD3, and CD79a. Juvenile BALT displays the concentration of CD79a+ cells at the apical border of the BALT follicle. Adult BALT did not have well-defined BALT follicles, likely from its relatively antigen-free managed care environment. FAE = follicle-associated endothelium, RE = respiratory epithelium, F = follicle, SED = subepithelial dome, IFR = interfollicular region, S = smooth muscle, N = nerve, purple arrow = high endothelial venule.

Table 2-2: Manual differential leukocyte counts of adult Egyptian rousette bats (*Rousettus aegyptiacus*). Results per bat as presented as average count/200 cells (1st line) and as the percentage of each cell type identified (2nd line). The average of 4 (male) or 5 (female) blood smear slides are presented herein. yo = years old.

	Neutrophils	**Lymphocytes**	**Monocytes**	**Eosinophils**	**Basophils**
Female (12 yo)	22.4	155.4	12.4	8.2	1.6
	11.2%	77.7%	6.2%	4.1%	0.8%
Male (10 yo)	18.5	160.75	11.25	6.75	2.75
	9.25%	80.375%	5.625%	3.375%	1.375%

CHAPTER 3A

AN ATLAS OF EGYPTIAN ROUSETTE BAT (ROUSETTUS AEGYPTIACUS) HISTOLOGY AND LITERATURE REVIEW[2]

[2] Elbert JA, Amman BR, Sealy TK, Atimnedi P, Towner JS, and Howerth, EW. To be submitted to a peer-reviewed journal.

ABSTRACT

The Egyptian rousette bat (*Rousettus aegyptiacus*) has gained increasing scientific attention due to its unique physiological adaptations, its role as a natural reservoir for emerging zoonotic pathogens, and its potential as a model organism for comparative mammalian biology. Despite this interest, histological characterizations of this species remain limited and fragmented. In this manuscript, we synthesize the current published literature on the anatomy and histology of Egyptian rousette bats, providing a critical overview of existing knowledge while identifying gaps that require further investigation. Additionally, we present a novel and comprehensive histological atlas of wild-caught Egyptian rousette bats, encompassing key organ systems and tissue structures. This atlas, created using standardized histological techniques, serves as a foundational tool and vital resource for researchers studying Egyptian rousette bat physiology, immunology, and pathology. By offering a centralized reference for Egyptian rousette bat histology, this work enhances comparative studies with other mammalian species, facilitates biomedical research, supports future investigations into bat-host interactions with infectious agents, and advances our understanding of bat biology and its implications for public health and conservation.

KEYWORDS: Egyptian rousette bat, *Rousettus aegyptiacus*, histology, pathology, natural reservoir

INTRODUCTION

Bats, belonging to the order Chiroptera (derived from the Greek words "cheir" for hand and "pteron" for wing), are incredibly diverse. With over 1,400 recognized species, bats constitute approximately 20% of all mammalian species, second only to rodents in terms of diversity.[2] As the only mammals capable of sustained, self-powered flight, bats occupy a vast array of ecological niches across every continent except Antarctica and have broad ecological, anatomical, and environmental diversity that is nearly unparalleled within the animal kingdom.[1,2] Fossil evidence suggests that bats have existed for at least 52 million years, with early specimens displaying fully developed wings, indicating that flight evolved early in their lineage.[440] All bats are thought to have evolved from a common, flighted ancestor that displayed many features we still recognize in bats today, including the ability to echolocate and specializations for fruit and nectar feeding.[77] Bats are divided into two major suborders: Yinpterochiroptera, which includes pteropid fruit bats and several microbat families, and Yangochiroptera, comprising the remaining microbat families. These groups differ markedly in echolocation strategies, diet, and immune gene evolution, reflecting deep phylogenetic divergence within Chiroptera.[284,285]

The Egyptian rousette bat (ERB; *Rousettus aegyptiacus*; common name Egyptian rousette) is a yinpterochiropteran species of pteropodid bat that inhabits parts of Africa, western Asia, the Mediterranean, and the Indian subcontinent. They are predominantly cave-dwelling, gregarious and social animals, living in densely-packed roosts that can contain more than 100,000 bats.[9] While ERBs have been found in arid biomes, they prefer tropical rain and deciduous forests with abundant forest cover, roosting opportunities, and fruiting trees.[9] They are frugivorous, preferring soft, pulpy fruits such

as figs, mangoes, and dates, and play an important ecological role as pollinators and seed dispersers.[10] In tropical areas, ERBs have a biannual breeding season, with a gestation period of approximately 106 days.[9] Females typically give birth to a single pup which is carried by the dam for 6 - 8 weeks, until the pup can independently hang in the roost.[10] Pups become independent between 3 – 6 months of age and reach sexual maturity between 14 and 18 months.[10] ERBs are estimated to live on average up to 2 years in the wild[47]; in captivity, ERBs can live up to 22 years, with the oldest known ERB living to 25 years.[9] They are one of the few megabats to use echolocation, producing a series of short, repetitive clicks of the tongue against the side of the mouth to aid in navigation.[10,89-92] In the wild, ERBs are predated by many large raptors, including the Lanner falcon, Palm-nut vulture, and African fish eagles, mammals such as genets, and cave-dwelling reptiles such as cobras, pythons and Nile monitor lizards (J. Towner, personal communication).

ERBs are of critical public health importance as a natural reservoir host for both Marburg virus (MARV) and Ravn virus (RAVV), and have been the focus of investigation in numerous longitudinal ecological studies.[3,48,50,94-96] MARV and RAVV, close viral relatives to Ebola virus, are the only two known members of the species *Orthomarburgvirus marburgense (*family *Filoviridae*, genus *Orthomarburgvirus*) and are the causative agents of Marburg virus disease (MVD), a severe viral hemorrhagic fever that typically emerges in sub-Saharan Africa characterized by human-to-human transmission and high case fatality ratios up to 90%.[49,196]

The ERB has gained increasing scientific attention due to its unique physiological adaptations, its role as a natural reservoir for emerging zoonotic pathogens, and its

potential as a model organism for comparative mammalian biology. Despite this interest, histological characterizations of this species remain limited and fragmented. Given their role in filovirus ecology and zoonotic spillover, a comprehensive understanding of ERB histology is essential for elucidating host-pathogen interactions and advancing public health preparedness. In this manuscript, we synthesize the current published literature on the anatomy and histology of Egyptian rousette bats, providing a critical overview of existing knowledge while identifying gaps that require further investigation.

Additionally, we present a novel and comprehensive histological atlas of wild-caught Egyptian rousette bats, encompassing key organ systems and tissue structures. This atlas, created using standardized histological techniques, serves as a foundational tool and vital resource for researchers studying Egyptian rousette bat physiology, immunology, and pathology. Due to the breadth of anatomical structures present in ERBs and the necessity of maintaining a focused and representative histological survey, this atlas does not encompass every tissue and organ. Instead, emphasis is placed on larger, functionally significant organs that provide a comprehensive overview of the species' histology while serving as a valuable reference for future research in virology, ecology, and comparative anatomy. By offering a centralized resource for Egyptian rousette bat histology, this work enhances comparative studies with other mammalian species, facilitates biomedical research, supports future investigations into bat-host interactions with infectious agents, and advances our understanding of bat biology and its implications for public health and conservation.

MATERIALS AND METHODS

Sixty-nine free-ranging ERBs (juvenile = 49; adult = 20 (forearm length > 89 cm[3,441]); male = 35; female = 34), were collected in 2008-9 as part of investigative efforts conducted by the Centers for Disease Control and Prevention (CDC) into discovery of the orthomarburgvirus natural reservoir host. As previously described, all capturing, processing, and procedures were performed in accordance with an institutionally approved animal care and use protocol.[3,48] Bat collections were completed with the approval of the Uganda Wildlife Authority and following the American Veterinary Medical Association guidelines on euthanasia and the National Research Council recommendations for the care and use of laboratory animals.[3] Whole blood and spleens were removed at the time of capture for Marburg virus quantitative reverse transcription polymerase chain reaction (RT-qPCR) (negative = 41; positive = 27; unknown = 1). RT-qPCR was completed as previously described.[48] Abdominal +/- thoracic cavities were exposed to allow for 10% neutral buffered formalin fixation, and carcasses were fixed as intact specimens. The specimens were transferred to 70% ethanol after fixation; a definitive timepoint for this transfer is unknown.

In 2023, full necropsies were performed on each bat. Representative sections from a full set of tissues (including but not limited to heart, trachea, lungs, lymph nodes, liver, kidney, adrenal gland, tongue, gingiva, esophagus, stomach, pancreas, small and large intestines, haired skin, plagiopatagium, salivary gland, adipose, thymus, thyroid, bone marrow, ear canal, eyes, nasal turbinates, peripheral nerves, skeletal muscle, male and female reproductive organs, and brain) were processed and embedded in liquid paraffin. Sections were cut at 4 μm, mounted on glass slides, and stained with hematoxylin and eosin (HE). As splenic tissue from the wild-caught bats was prioritized for Marburg virus

RT-qPCR at the time of capture, splenic tissue images provided here were taken from 5–7-month-old, managed care ERBs from the research colony at CDC.

LITERATURE REVIEW AND HISTOLOGIC ATLAS

OVERVIEW

ERBs are medium sized pteropid bats; adults range from 80 to 180 grams (average 130 grams), with an average wingspan of 60 cm and average body length of 15 cm.[9] Males are typically slightly larger than females; both sexes have a dorsal pelage ranging from dark brown to medium gray and paler ventral pelage, frequently with a pericervical collar of pale yellow or orange fur, and two glandular areas of specialized stiffer hairs at the sides of neck.[9,10,442] The skin underlying the paler colored collar around the neck is characterized by a thin, one to two cell layers thick, epidermis with the subjacent dermis containing nests of hair follicle-associated alveolar sebaceous glands that are similar, but larger, to those in other regions of the body.[443] These glands are twice as large in males as in females, and are thought to play a role in individual recognition and communication by chemical means.[443] They have a short, externally distinct tail, and a broad, dog-like muzzle.[10,442]

SKELETAL

The ERB skeletal structure has been thoroughly described.[9,10,442,444-446] They have seven cervical, 13 thoracic, five lumbar, six sacral (fused), and five caudal vertebrae, a sternum with three keels to allow for an enlarged attachment area of the pectoralis muscle, thirteen ribs (seven sternal, six vertebral), long and narrow scapula, and have many skeletal adaptations for flight, including greater digit diameters in planes with the greatest bending forces and relatively short metacarpals to allow for a high camber

(curvature) of the wing during downstroke and to reduce drag during upstroke.[445,447] The powerful musculus palmaris longus additionally contributes to the high camber of the wing. Regarding their skeletal musculature, ERBs have a highly specialized pectoralis (pars posterior) optimized to generate power in flight.[448] The elbow flexion/extension muscles (biceps brachii and triceps brachii) have comparable physiological cross-sectional areas but shorter fiber lengths to the pectoralis, which indicates optimization for generation of large forces.[448] ERBs have enlarged pectoralis muscles and elbow flexion and extension muscles (bicep brachii and triceps brachii) to aid powered flight, which is more similar to flying birds than non-flying mammals (Fig. 3-1A).[448] Type IIa and Type IIa/x muscle fibers make up the highest proportion of total muscle mass, with infrequent detection of Type I and Type IIx fibers.[449] Interestingly, ERB capillary density in skeletal muscle, representing efficiency of oxygen and nutrient delivery, was lower than in insectivorous bats *Myotis myotis* and *Molossus ater*, potentially reflecting variations in flight patterns.[450]

WING

Rousettus sp. bats become volant at approximately 6 weeks.[451] The wing membranes of ERBs are consistent with most bats in that they have a uropatagium or tail membrane, a plagiopatagium extending from the dorsum to the fifth digit of the hand, the dactylopatagium (also known as the chiropatagium) extending between the phalanges and subdivided into major, medius, minus, and brevis, and the propatagium extending from the shoulder to the thumb, forming the leading edge of the wing.[437,452] Tissue composition varies between the plagiopatagium, dactylopatagium, and uropatagium, with a general structure of a stratified squamous epithelial bilayer (ventral and dorsal) separated by

connective tissue containing sweat and apocrine glands, skeletal muscle, pilosebaceous units, blood and lymphatic vessels, collagen, and linearly arranged elastin fibers (Fig. 3-1B).[437,452] Strongly tapered, tactile hairs on both dorsal and ventral surfaces of the wing are involved in sensing air flow for improved flight maneuverability.[453] ERBs have claws on the terminal phalanx of the first and second thoracic limb digits; the first digit is opposable.[9,437] Compared to birds, ERBs have less variation in wing span during flight due to the need to prevent folding back the manus during flight, as would cause the collapse of the plagiopatagium.[454] ERBs lack a calcar, a bony or cartilaginous structure associated with the first row of tarsal bones in many bat species, which functions to spread and support the uropatagium.[455]

BRAIN

The ERB brain is pear shaped, wider at the back than in the front, similar in shape to the guinea pig brain, and weighs approximately 2.0 g to 2.4 g (average: 2.15 g) (Fig. 3-1D-F).[456] While there is embryonic development of primordial vomeronasal organ in early gestation (up to 14 mm crown to rump length), later gestational ages, neonates, and adult *R. leschenaultii* bats, a closely related species to ERBs, lack a vomeronasal system.[457] ERBs additionally lack an accessory olfactory bulb, which is the functional relay center for the vomeronasal organ in the central nervous system.[457-460] Research into the distribution and morphology of cholinergic, putative catecholaminergic and serotonergic neurons in ERB brains identified discrete nuclei absent in *Miniopterus schribersii* bats, potentially suggesting that Yinpterochiroptera may phylogenetically align most closely with primates.[438,461] Further, investigations into hippocampal formation and entorhinal cortex, neural components that are crucially involved in

learning, memory, and spatial navigation, show that ERBs have entorhinal-dentate gyrus projections that are more similar to primates than rodents.[439] Vitamin B_{12} deficiency has been experimentally induced in managed care ERBs with subsequent demyelination of the lateral and ventrolateral white matter of the caudal cervical and cranial thoracic regions of the spinal cord, but this has not been reported in free-ranging ERBs.[462] The lipid composition and sphingolipid fatty acids of the ERB spinal cord and brain are similar to other mammals with differences, most notably in the spinal cord, theorized to result from variations in the ratio of gray to white matter.[463,464]

EYE

The ERB eye exhibits many features typical of a nocturnal animal, with a markedly curved cornea that occupies approximately one-third of the globe, large anterior and posterior chambers relative to the vitreous, and lack of a fovea.[465] Numerous studies have been conducted to better elucidate and characterize the ERB retina in comparison to other chiroptera and to other mammalian species such as non-human primates.[466-471] ERB retinas share the same pattern of retinal decussation, or the crossing of nerve fibers or tracts from one side of the central nervous system to the other, as other pteropid bats and primates.[472] Like most pteropodid bats, ERBs have an avascular retina with thick retinal layering up to or beyond 250 μm.[473] Conical or spike-like choroidal papillae project into the retina and are thought to provide nourishment to sections of the retina greater than 140 μm from the vascular choroid (Fig. 3-1G, H).[437,467,473] This undulation causes an increase in retinal surface area and number of photoreceptors, aiding in nocturnal visual acuity and light-gathering capabilities.[465,467] Dried eye lens weight has been investigated as an indicator of age and may be a more accurate measurement than traditional means of

age determinations in bats, i.e., forearm length.[474] Harderian glands, lacrimal glands, and well-developed nasolacrimal ducts have been reported in *R. leschenaultii* bats.[475]

ECHOLOCATION

ERBs have both excellent vision and the ability to echolocate, allowing them to use variable sensory modalities to navigate in a wide range of light conditions and environments.[90-92,476,477] Echolocation in ERBs is produced by clicks of the tongue emitted in pairs, 0.6 – 1 ms duration, with a frequency range of 12-70 kHz and peak frequency at 20-40 kHz.[90] The pinnae are highly mobile, powered by five individual muscles; high numbers of motor neurons within the facial motor nucleus allow for sophisticated pinnae movements.[478] Investigations into the timing of echolocation signals and pinnae movement have found that echolocation in free flights corresponds with the downward wingstroke and forward movement of the pinnae, and that the ears have the greatest sensitivity to click stimuli when forward-facing.[89]

SALIVARY GLAND

Salivary glands have been previously described in *R. amplexicaudatus* bats, and include the principal parotid gland (Fig. 3-2A, B), accessory parotid gland, accessory submandibular gland, parotid gland, principal submandibular gland (Fig. 3-2C).[479] ERBs have lingual salivary glands that contain von Ebner's glands (serous secreting glands that express acidic mucopolysaccharides in ERBs) and Weber's glands (mucous secreting glands that secret neutral mucopolysaccharides) that intercalate between striated muscles (Fig. 3-2E, F)[480], although one publication only reports the presence of Weber’s glands in the median and posterior lingual region.[481] In frugivorous bats, the parotid secretory granules are generally seromucous instead of serous.[482] In the current study, hard palette,

(Fig. 3-2F), soft palette (Fig. 3-3B), buccal (Fig. 3-2F), and sublingual mucoid salivary glands were confirmed, the latter of which is located between the rostral mandible and the tongue.

TONGUE

The ERB tongue has a concave midline with prominent, abundant mechanical papillae. There are seven subtypes of filiform papillae varying in shape, size, density, direction; the degree of fringing indicates high adaptation for a frugivorous diet.[481] Additionally present are scattered gustatory (fungiform), conical papillae and circumvallate papillae.[480,483-487] The dorsal epithelium is composed of keratinized stratified squamous epithelium characterized by basal, spinous, and outermost highly keratinized layers (Fig. 3-2D).[480] ERBs have an entoglossal plate associated with the lingual root which supports the tongue and is characterized by a core of thin compact bone with central hematopoietic tissue, associated with elastic cartilage.[480]

GASTROINTESTINAL TRACT

ERBs have evolved a specialized gastrointestinal tract that allows them to digest carbohydrate-rich diets efficiently and rapidly, with high rates of carbohydrate paracellular absorption thought to compensate for their relatively short intestinal tract.[488] This allows ERBs to store large amounts of glycogen in hepatocytes, which appears histologically as feathery vacuolation of the hepatocellular cytoplasm, typically diffusely spread throughout the tissue.[437,488] Additionally involved in glucose absorption is the pancreas, of which 9.1% is endocrine, more than in typical domestic mammals (Fig. 3-3D).[489] Endocrine cells are distributed in pancreatic islets throughout the gland and also as discrete cells in the exocrine ducts.[489] Michelmore et al. demonstrated four endocrine

cell types: insulin (β) cells (51.4%) were located throughout the islet and extended between the glucagon (α) cells (30.6%), with somatostatin (δ) cells (8.8%) and pancreatic polypeptide cells (17.1%) irregularly scattered throughout the islets.[489]

The ERB stomach is an elongated C-shape, with a long, convex greater curvature and shorter, almost straight lesser curvature (Fig. 3-4A, B).[490] It is divided into three regions: the fundus, which contains a blunt-ended diverticulum sometimes referred to as the "fundic cecal region" (Fig. 3-4C), the cardia, and the pylorus (Fig. 3-4D).[490] The pyloric sphincter is externally appreciable by a slight diameter constriction and narrow circumferential muscular band.[490] As in many mammalian species, the stomach is organized in four layers: mucosa, submucosa, tunica muscularis, and serosa.[481,490,491] Mucosal villi-like folds (rugae) are long and curved with lesser numbers of gastric glands that contain abundant parietal cells, as well as surface and neck mucous cells and chief cells (Fig. 3-4C, D).[481,491]

The small intestinal mucosa contains elongated, anastomosing, and apically sharp villi, packed in a zigzag shape containing absorptive enterocytes and goblet cells, with long, slender microvilli.[481,492] Collagenous fibers in the submucosa are thin and irregular.[491] Occasional Brunner's glands are present within the duodenum (Fig. 3-3E).[493] Intestinal transit time is 18-100 minutes, with greater than 90% absorption of ingested sugars.[494] Maximum assimilation of fructose occurs within 5 minutes, whereas maximum uptake of glucose occurs in 30 minutes.[495] Interestingly, in addition to sodium-coupled, mediated sugar transport, ERBs appear to rely on passive, paracellular absorption for the majority of their glucose intestinal absorption to a significantly greater extent than non-volant mammals.[496] Unlike many mammals, the ERB small intestine is freely permeable

to calcium with no active transport mechanism.[9,497] ERBs lack a cecum, appendix, and ascending and transverse colons.[493]

HEART

Rousettus sp. bats have been reported to have a larger heart size relative to other bat species and have a higher vertebral heart score than mammals in general (Fig. 3-5C).[498,499] Gross anatomy of the great cardiac vessels has previously been described, with noted venous drainage variations such as a single left pulmonary vein and two groups of right pulmonary veins draining into the left atrium.[500] Additional variations include retention of both cranial vena cava as part of the overall upper limb requirements for flight.[500]

LUNG

Historical studies have been completed in numerous bat species to investigate pulmonary morphometric properties and structural adaptations to elucidate how bats meet the immense oxygen demands required by flight.[501-503] In general, bats have the same overall lung morphology as most mammals, with bats exhibiting a high lung volume relative to birds or terrestrial mammals, small subdivision of air spaces, and a very thin blood-gas barrier (Fig. 3-5H).[501-503] Bronchus-adjacent hyaline cartilage is limited to the primary bronchi and occasionally shows rudimentary ossification.[504] Mucous membrane sections overlying hyaline cartilage are flat (i.e., not rugated/folded) and are connected to the subjacent cartilage by connective tissue; bronchial glands and smooth muscle in these sections are absent.[504] Secondary bronchi and beyond are surrounded by well-developed, circumferential smooth muscular layers, with prominent folding of the bronchial epithelium.[504] Bronchiolar epithelium transitions from ciliated pseudostratified

epithelium with rare goblet cells in the primary bronchi to simple columnar in secondary bronchi to simple cuboidal epithelium in terminal/respiratory bronchi, before transitioning into the thin alveolar epithelium that lines alveolar ducts and subsequent alveoli (Fig. 3-5G, H). As in rodents, pulmonary veins in ERBs have a layer of 1-5+ cardiomyocytes, which have a larger sarcoplasm than adjacent smooth muscle cells and are more easily appreciable in large caliber vessels.[505]

ADRENAL GLAND

Adrenal glands follow the common mammalian structure of a cortex divided into the zona glomerulosa, zona fasciculata, and zona reticularis and a central medulla (Fig. 3-6A, B).[506] ERB adrenal glands are small proportionally to body weight and increase in weight during pregnancy.[411,507,508] A 27% incidence of macroscopic and numerous microscopic accessory adrenocortical bodies have been reported, however they were not appreciated in the current study.[507]

KIDNEY

The thick renal cortex in ERBs contains few Bowman's capsules in the outermost region, increasing in number with inward progression toward the corticomedullary region, as has been described in *R. leschenaultii* bats.[509] Large and numerous medullary rays invade the cortical tissue, obscuring a defined corticomedullary junction and conferring a streaming hypercellularity to the tissue (Fig. 3-6C). ERBs have a very short, conical papilla, consistent with the lesser urine concentrating ability required in frugivorous bats.[509] However, measurement of urine specific gravities of free-ranging ERBs in Israel indicate that ERBs are able to highly concentrate their urine.[510]

THYROID

Histologic features of the ERB thyroid is similar to that of other mammals, composed of numerous, small follicles lined with follicular and parafollicular epithelial cells (Fig. 3-6F).[511] Parathyroid glands composed of ribbons of chief cells, oxyphils, and transitional cells were identified in numerous ERBs. While the role of the parathyroid gland has been investigated in hibernating bat species, to the author's knowledge this organ has not been investigated in the ERB.[512,513] ERBs do not undergo hibernation or torpor.[514]

LYMPHOID

Previous gross and histological analysis have shown that bats have similar primary and secondary lymphoid organs as are found in other mammals, including thymus (Fig. 3-7A, B), spleen (Fig. 3-7C, D), bone marrow (Fig. 3-7E, F), and lymph nodes (Fig. 3-6G, 3-7G, H), as well as widely dispersed immune cells.[360,367,370,393,394] Gross anatomical characterization of lymph nodes in ERBs has previously been characterized, with the anatomical location and number of lymph nodes listed as follows: superficial cervical (1-2), facial (2-4), internal jugular (1-3), posterior cervical (1-4), brachial (1-3), axillary (1-4), inguinal (2-6), popliteal (2-3), gluteal (2-5), iliac (1-4), renal (1-3), and cranial mesenteric (1-5).[404,405] Pregnant ERBs have more numerous and larger lymph nodes that non-pregnant females or males, and typically lymph nodes on the left of the body are larger.[404] Splenic structure is similar to humans and rodents, in that they have a thin capsule and variably sized collagenous and smooth muscle trabeculae.[410] *Rousettus* sp. bats have been reported to have few erythroid and myeloid cells and no megakaryocytes in their red pulp, with prominent marginal zones in white pulp.[410] The spleen may become smaller in response to stress.[411]

REPRODUCTIVE

Testes are abdominal in juvenile males and scrotal in adults (Fig. 3-8A, B). A prostate gland that incompletely surrounds the urethra (Fig. 3-8C), Cowper's glands/bulbourethral glands (Fig. 3-8D), seminal vesicles (Fig. 3-8E) and ampullary glands have been described.[515,516] The penis is composed of corpus spongiosum, prominent corpora cavernosa, a relatively large and well developed glans penis compared to other chiroptera, and a small os penis that resides fully within the glans, covered by a thin and retractile prepuce that slightly extends beyond the tip of the glans when flaccid (Fig. 3-8F).[515] An accessory corpora cavernosa is lacking.[517]

Females have concentric mammary tissue bilaterally on the lateral aspects of the thorax with a central teat (Fig. 3-9A-C). *R. leschenaultii* bats have been reported to have a human-like menstrual cycle.[518] The female uterus (Fig. 3-9D) is duplex and symmetrical; the two uterine horns are externally caudally united, but their lumina open at the vagina by separate cervical canals.[519-521] Reproductive asymmetry is common in Pteropodidae.[520,522]. During pregnancy, a single corpus luteum is on the same side of the reproductive tract as the developing embryo and persists until the next ovulation; the contralateral ovary contains primary and secondary follicles (Fig. 3-9E).[520,522] Delayed embryonic implantation has been reported in at least three chiropteran families[523] and has been anecdotally observed in ERB managed care colonies (J. Towner, personal communication). Rousettus spp. bats have discoid, labyrinthine, and hemochorial placentation with an intrasyncytial lamina and a solid glandular yolk sac at term. (Fig. 3-9F).[524,525] A broad, flattened clitoris is present within the genital tubercle (Fig. 3-9G).[521]

DISCUSSION

This study presents the most comprehensive histologic atlas to date of the Egyptian rousette bat, integrating a thorough review of the existing literature with original histologic characterization of a wide range of organ systems from wild-caught individuals. In doing so, it establishes a centralized, standardized reference for future comparative, pathological, and experimental investigations involving this species. As a natural reservoir host for orthomarburgviruses and an increasingly important model in infectious disease research, the ERB represents a key species at the interface of wildlife biology, public health, and translational science. Yet, prior to this work, a systematic histologic baseline from healthy, free-ranging individuals was lacking. This atlas fills that critical gap, offering detailed histologic descriptions that can now serve as a foundational comparator for studies in viral pathogenesis, vaccine efficacy, immunologic development, and age- or disease-related pathology.

The findings in this study have broad implications across multiple disciplines. Immunologically, detailed characterization of primary and secondary lymphoid tissues (included here and more in-depth in Chapter 2) enhances our understanding of baseline immune architecture in ERBs and provides a platform for evaluating tissue-specific responses in experimentally challenged or immunologically perturbed animals. Biologically, the data offer insights into the adaptations that support flight, frugivory, echolocation, and thermoregulation, while also highlighting the structural diversity of epithelial, vascular, endocrine, and neural tissues. From a comparative standpoint, this atlas facilitates cross-species analyses in mammalian anatomy and pathology and enables integration with ongoing research in immunology, virology, and bat-specific host-pathogen interactions.

This work lays the groundwork for multiple future research directions. Immunophenotypic and molecular profiling of tissues, especially lymphoid and mucosal tissues, via immunohistochemistry, in situ hybridization, or spatial transcriptomics, would extend the descriptive histology into functional domains. Similarly, evaluating histologic variation across life stages, reproductive states, and environmental exposures (e.g., captivity, diet, stress) will help disentangle normal physiologic variability from disease-associated changes. Serial histologic sampling in the context of longitudinal studies or experimental infections would further clarify temporal dynamics of tissues remodeling, immune activation, or pathogen tropism. Finally, coupling this atlas with emerging digital pathology platforms and 3D tissue imaging could yield interactive tools for education, diagnosis, and research, both within and beyond the bat research community.

Despite its contributions, this study has several important limitations. First, the prolonged fixation and unknown duration of formalin vs. ethanol storage in the wild-caught specimens may have led to a degree or artifact or tissue degradation, particularly in delicate structures such as neurologic or gastrointestinal tissues. Second, the absence of immunohistochemical validation precludes definitive identification of specific cell populations. Third, due to logistical constraints and retrospective sample availability, the cohort was skewed toward juvenile individuals and lacked neonates or aged bats, limiting the ability to assess age-related histologic variation. Additionally, tissues were collected during a single season, and environmental or temporal effects, such as seasonal breeding or pathogen exposure, could not be accounted for. Finally, although the sample size is relatively large for a wildlife histology study, it may not fully capture the natural

histologic variability present across the large, fragmented, and geographically diverse species' range. These limitations highlight the need for complementary studies that use prospectively collected specimens under more controlled conditions, integrate molecular techniques, and expand demographic representation.

Taken together, this work offers a critical and long-overdue resource to support the continued use of the Egyptian rousette bat in comparative and translational research. As a reservoir host for high-consequence zoonoses and a model of viral tolerance, the ERB presents a unique opportunity to investigate the fundamental biology of viral disease resistance, immune regulation, and host-pathogen co-evolution. This histologic atlas enhances the scientific infrastructure for such investigations, enabling more informed and nuanced experimental disease, more accurate histologic interpretation, and robust cross-species comparison. In doing so, it advances our broader understanding of mammalian biology and contributes to the foundational knowledge necessary for pandemic preparedness, wildlife health, and mitigation of zoonotic disease spillover.

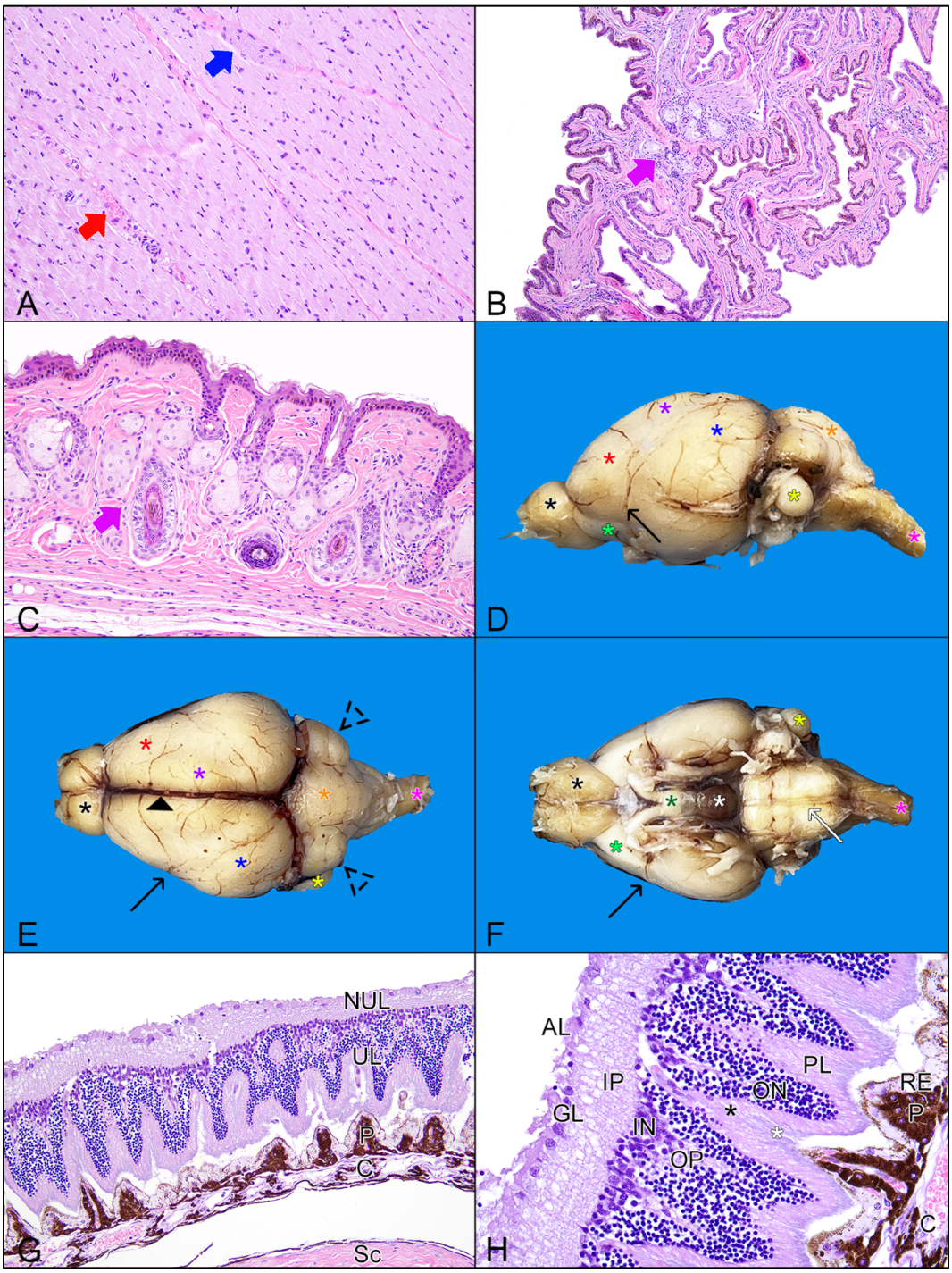

Figure 3-1: Gross and histologic features of skeletal muscle, wing membrane, haired skin, brain, and eye in Egyptian rousette bats (*Rousettus aegyptiacus*). A) Longitudinal section of pectoral skeletal muscle with small caliber vessel (red arrow) and nerve (blue arrow) in a juvenile female. 20x, Hematoxylin and eosin (HE). B) Wing membrane (plagiopatagium) with sebaceous units (purple arrow) in a juvenile male. 10x, HE. C) Haired skin from the dorsal head with multiple pilosebaceous units (purple arrow). 20x, HE. D) Left lateral view of the brain of an adult female. Asterisk legend: Black = olfactory bulb; Lime green = olfactory tubercle; Red = frontal lobe; Purple = parietal lobe; Blue = occipital lobe; Orange = cerebellar vermis; Yellow = dorsal paraflocculus (ventral paraflocculus lost upon removal from calvarium); Pink = spinal cord. Thin

black arrow = medial cerebral artery. E) Dorsal view of the brain of an adult female. Asterisk legend: Black = olfactory bulb; Red = frontal lobe; Purple = parietal lobe; Blue = occipital lobe; Orange = cerebellar vermis; Yellow = dorsal paraflocculus; Pink = spinal cord. Thin black arrow = medial cerebral artery. Black arrowhead = medial longitudinal fissure (interhemispheric fissure). Dashed black arrowheads = cerebellar hemispheres. F) Ventral view of the brain of an adult female. Asterisk legend: Black = olfactory bulb; Lime green = olfactory tubercle; Forest green = optic chiasm; White = Pituitary gland (hypophysis); Yellow = dorsal paraflocculus; Pink = spinal cord. Thin black arrow = medial cerebral artery. Thin white arrow = basilar artery. G) Retina in an adult female. Sclera (S), choroid (C) with its conical or spike-like choroidal papillae (P), retina (R) with undulating (UL) and non-undulating (NUL) layers. 20x, HE. H) Retina in an adult female. Choroid (C) with its conical or spike-like choroidal papillae (P), retinal epithelium (RE) with granular melanin pigment, photoreceptor layer (PL) comprising the inner segment (white asterisk) and outer segment (black asterisk), outer nuclear layer (ON), outer plexiform layer (OP), inner nuclear layer (IN), inner plexiform layer (IP), ganglion cell layer (GL), axon layer (AL). 40x, HE.

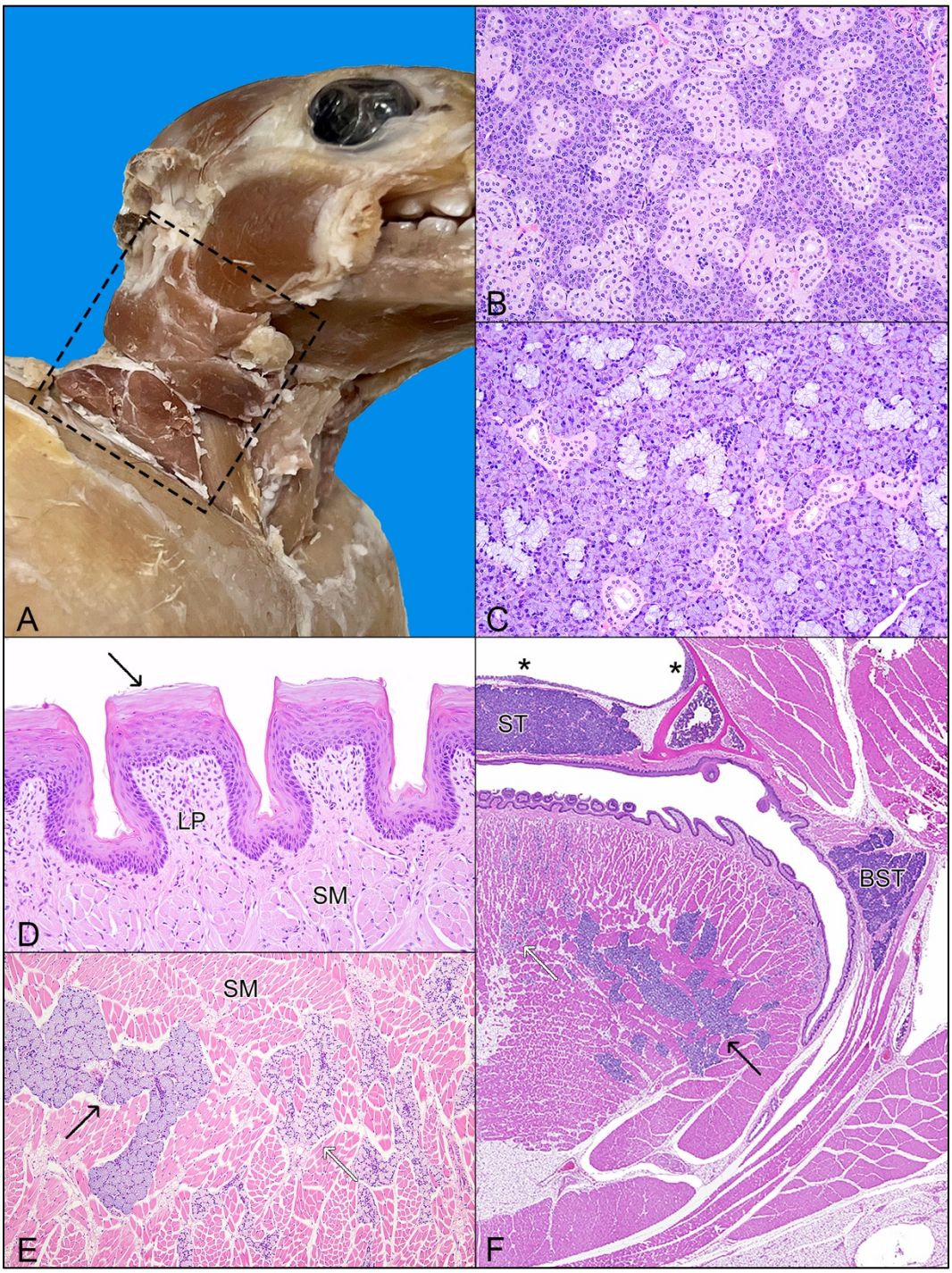

Figure 3-2: Gross and histologic features of salivary tissue, tongue, and oral cavity in Egyptian rousette bats (*Rousettus aegyptiacus*). A) Right lateral view of cervical region showing multi-lobed parotid salivary tissue and submandibular lymph node (black dashed square). B) Parotid salivary gland in an adult female. 20x, HE. C) Submandibular salivary gland in an adult female. 20x, HE. D) Tongue in a juvenile male with filiform papillae containing keratinizing stratified squamous epithelium (thin black arrow) overlying the lamina propria (LP) and subjacent skeletal muscle (SM). 20x, HE. E) Serous secreting von Ebner's glands (thin white arrow) and mucous secreting Weber's glands (thin black arrow) intercalating between lingual skeletal muscle (SM) in a juvenile male. 10x, HE. F) Cross section of oral cavity showing tongue

with lingual salivary tissue (thin black and white arrows), buccal salivary tissue (BST), hard palette salivary tissue (ST), and nasal-associated lymphoid tissue (black asterisks) in an adult female. 0.8x, HE.

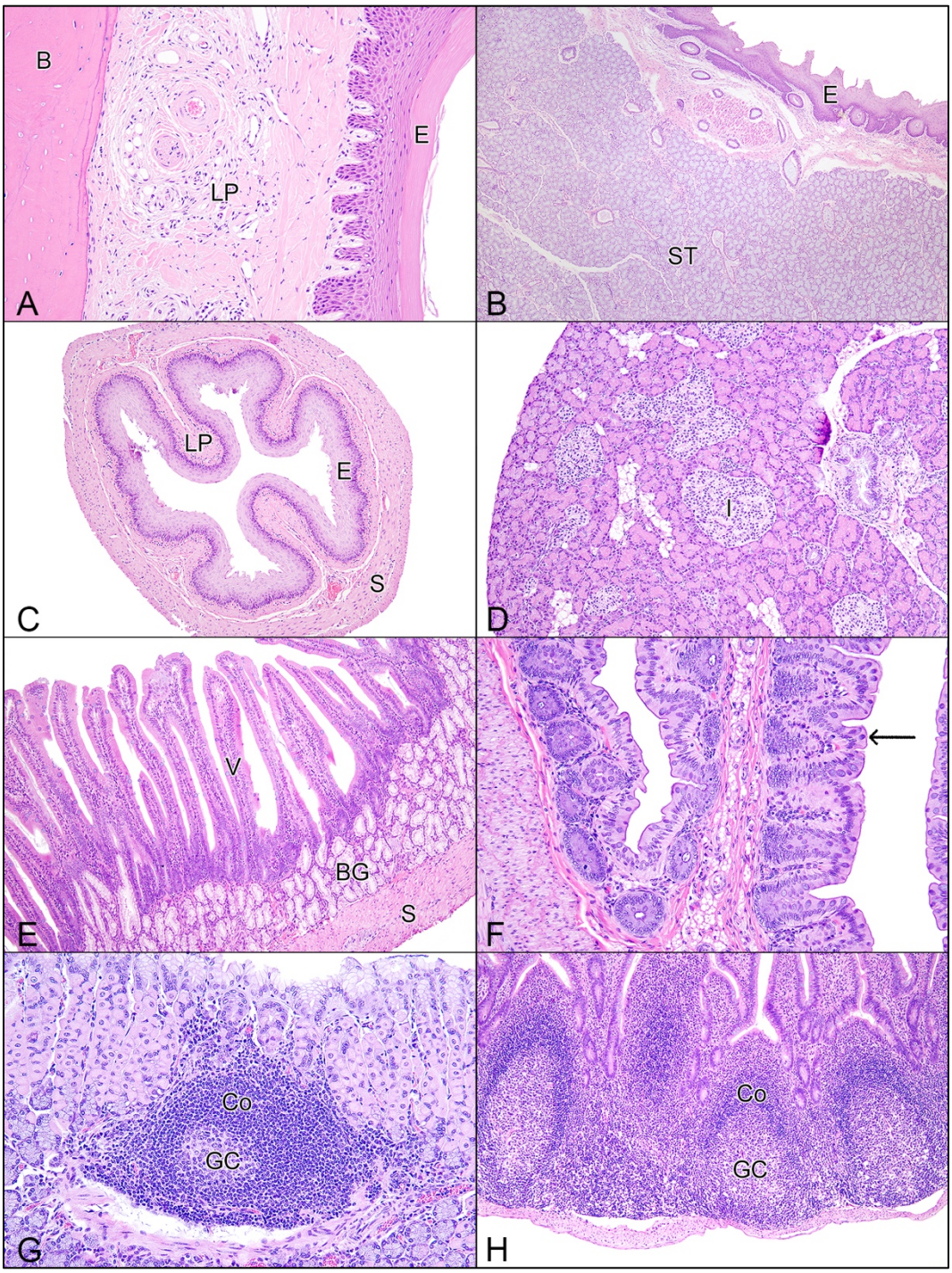

Figure 3-3: Histologic features of gingiva, salivary tissue, tongue, esophagus, pancreas, small and large intestine, and gastrointestinal-associated lymphoid tissue in Egyptian rousette bats (*Rousettus aegyptiacus).* A) Gingiva in an adult male with keratinizing stratified squamous epithelium (E) overlying the lamina propria (LP) and bone (B). 20x, HE. B) Serous salivary tissue (ST) in the soft palette of an adult male with keratinizing stratified squamous epithelium (E). 4x, HE. C) Cross section of esophagus in an adult male with keratinizing stratified squamous epithelium (E) overlying the lamina propria (LP) and smooth muscle (S). 10x, HE. D) Pancreas showing large endocrine islets (I) in a juvenile male ERB.10x, HE. E) Duodenum with long villi (V) and Brunner's glands (BG) within the lamina propria in an adult female ERB. 10x,

HE. F) Colon in an adult female ERB. The mucosal epithelium contains numerous goblet cells (thin black arrow). 20x, HE. G) Gastric lymphoid follicle with a germinal center (GC) and corona/mantle zone (Co) expanding the fundic mucosa of a juvenile female. 20x, HE. H) Peyer's patch with numerous germinal centers (GC) and corona/mantle zones (Co) in the ileum of a juvenile male. 10x, HE. Liver with portal triad and scant extramedullary hematopoiesis in a juvenile male. 10x, HE. H) Liver, higher magnification of the portal triad in a juvenile male. 40x, HE.

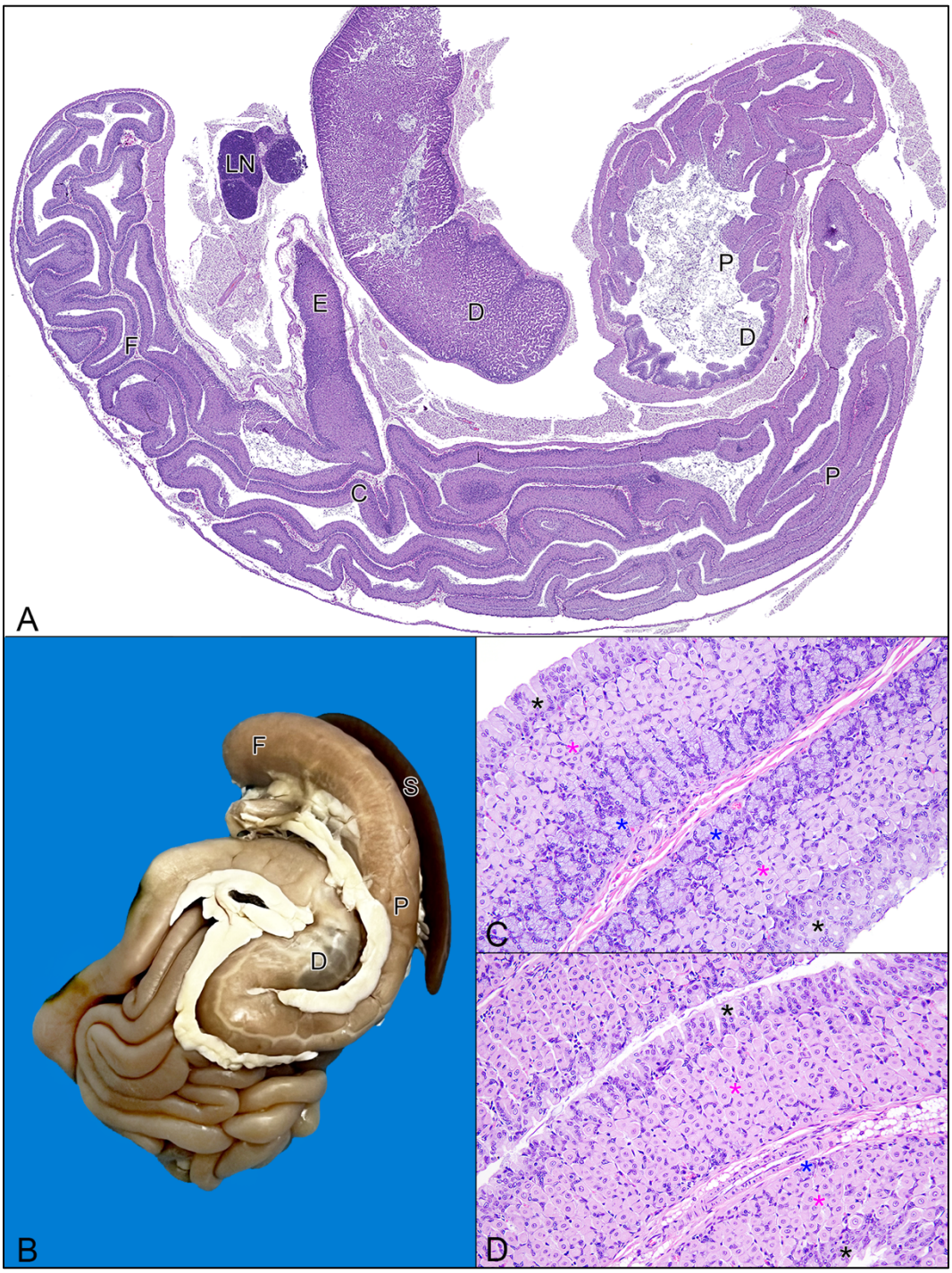

Figure 3-4: Gross and histologic features of the stomach in Egyptian rousette bats (*Rousettus aegyptiacus*). A) Subgross image of the stomach, showing the esophagus (E), fundus (F), cardia (C), pylorus (P), and duodenum (D) in an adult female. 2x, HE. B) Gross image of the gastrointestinal tract as it appears in vivo, showing the fundus (F), pylorus (P), and duodenum (D) in an adult female. The spleen (S) is present along the greater curvature of the stomach. C) Gastric fundus with surface mucous cells (black asterisk), parietal cells (pink asterisk), and chief cells (blue asterisk) in an adult female. 20x, HE. D) Gastric pylorus with surface mucous cells (black asterisk), parietal cells (pink asterisk), and rare chief cells (blue asterisk) in an adult female. 20x, HE.

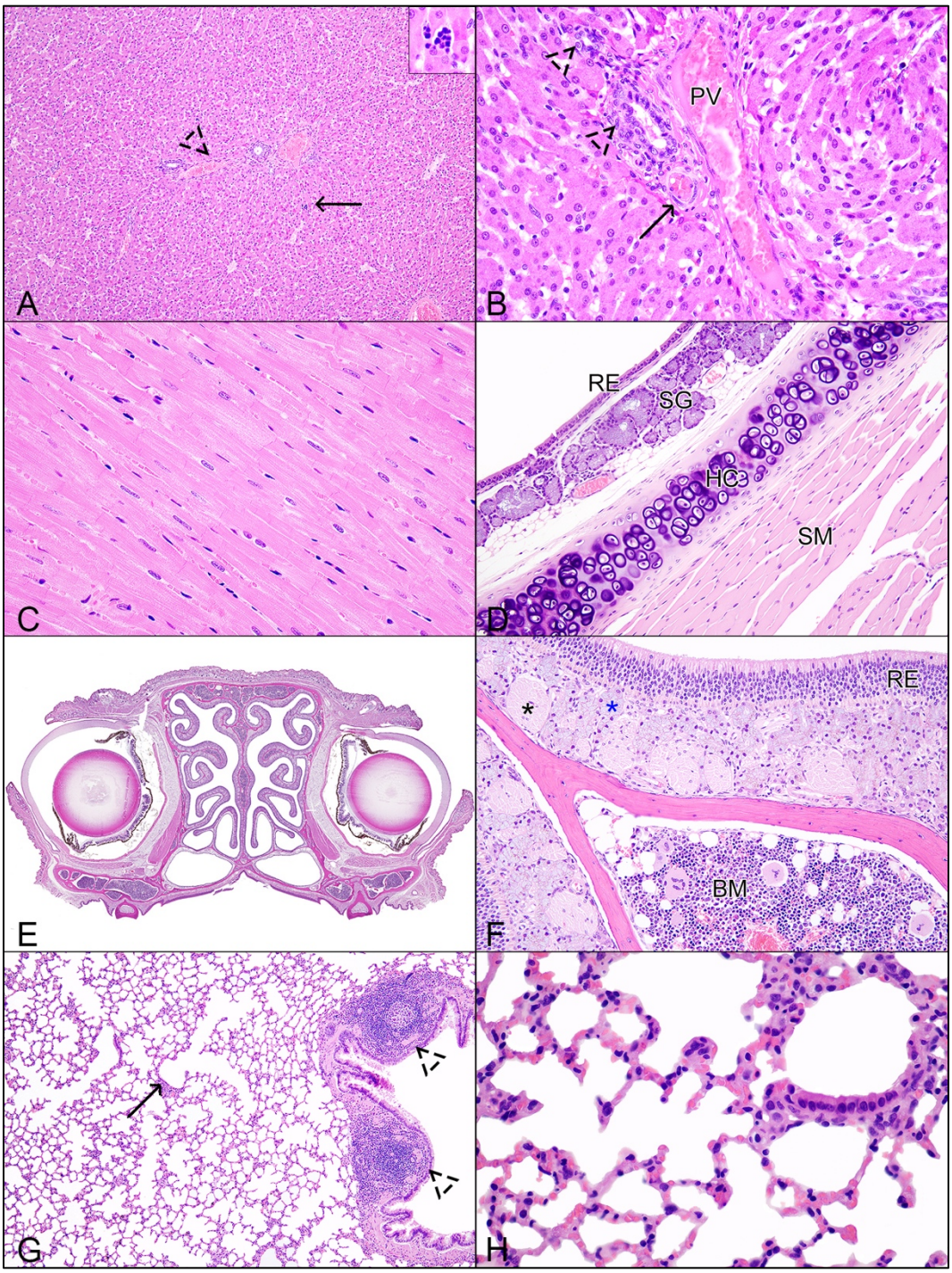

Figure 3-5: Histologic features of liver, heart, trachea, nasal turbinates, and lung in Egyptian rousette bats (*Rousettus aegyptiacus*). A) Liver with portal triad (dashed black triangle) and scant extramedullary hematopoiesis (thin black arrow) in a juvenile male.10x, HE. Inset: High magnification of extramedullary hematopoiesis. 60x, HE. B) Higher magnification of a portal triad with a portal vein (PV), bile duct (dashed black triangle) and hepatic artery (thin black arrow). 40x, HE. C) Cardiomyocytes in the right ventricle of an adult female. 40x, HE. D) Trachea with respiratory epithelium (RE), submucosal glands (SG), hyaline cartilage (HC), and smooth muscle (SM) in a juvenile male. 20x, HE. E) Coronal cross-section through the nasal turbinates at the level of the eyes. The mandible is not in frame. 0.9x, HE. F) Nasal turbinates

with overlying respiratory epithelium (RE), olfactory nerves (black asterisk), mucous glands (blue asterisk), and bone marrow (BM) within nasal turbinate bone in an adult female. 20x, HE. G) Section of lung with a large primary bronchus with bronchus-associated lymphoid tissue (BALT) (dashed black triangles), terminal/respiratory bronchioles transitioning to alveolar ducts (thin black arrow), and numerous alveoli. 10x, HE. F) Terminal/respiratory bronchus transitioning to an alveolar duct. 60x, HE.

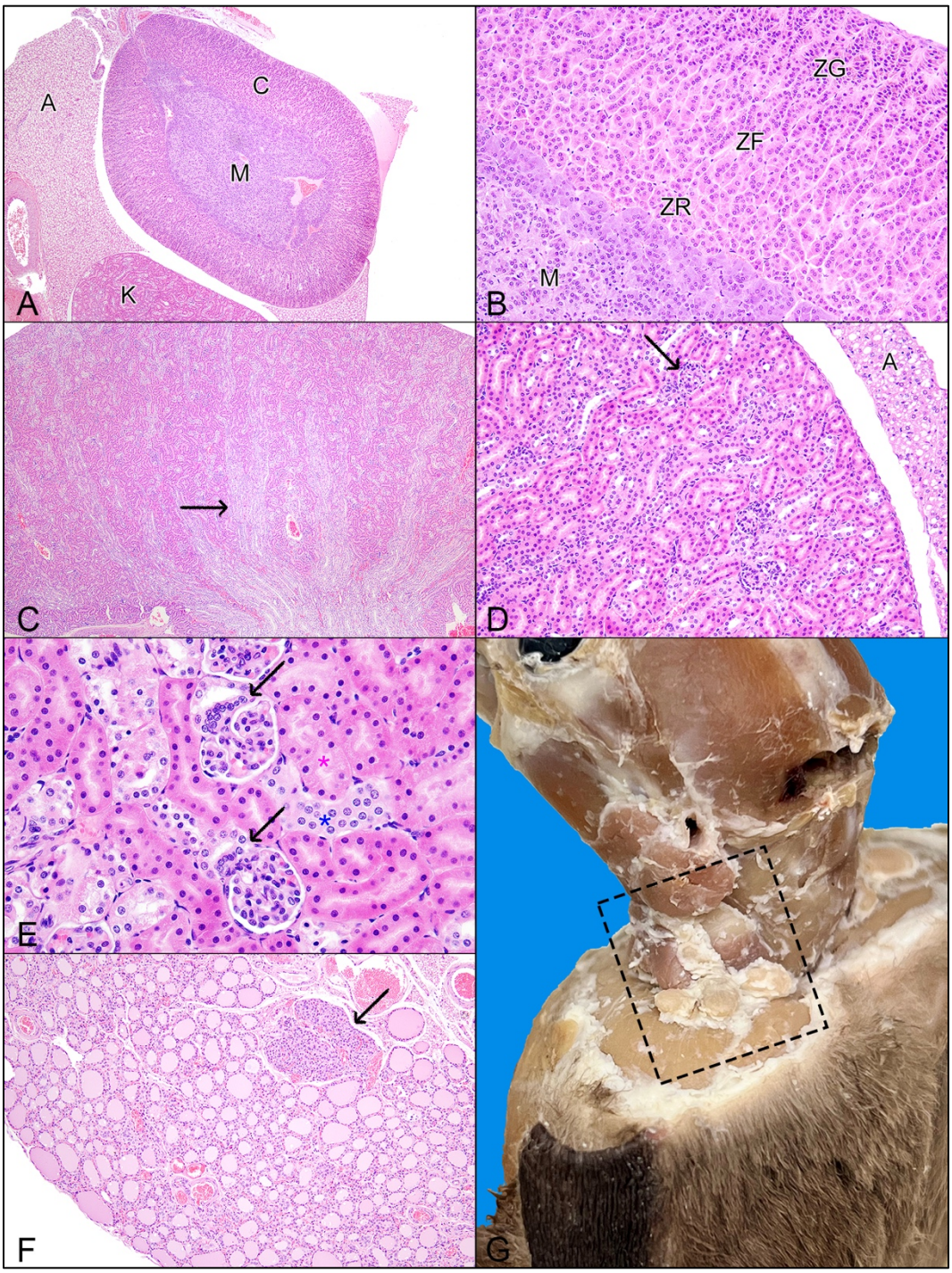

Figure 3-6: Gross and histologic features of adrenal gland, kidney, thyroid gland, parathyroid gland and lymph nodes in Egyptian rousette bats (*Rousettus aegyptiacus*). A) Adrenal gland with outer cortex (C) and inner medulla (M), surrounded by adipose (A) and a small section of kidney (K) in an adult female. 4x, HE. B) Adrenal cortex with zona glomerulosa (note scant brown intracellular pigment) (ZG), zona fasciculata (ZF), and zona reticularis (ZR) adjacent to the inner, basophilic medulla (M) composed primarily of chromaffin cells in an adult female. 20x, HE. C) Prominent medullary rays (thin black arrow) in the kidney of a juvenile male. 4x, HE. D) Renal cortex with fetal glomeruli (thin black arrow) and supracortical brown adipose (A) in a juvenile female. 20x, HE. E) Two glomeruli with juxtaglomerular apparatus

(thin black arrows), proximal convoluted tubules (pink asterisk), and distant convoluted tubules (blue asterisk) in the renal cortex of a juvenile female. 40x, HE. F) Thyroid gland with numerous small, colloid-filled follicles with internal parathyroid gland (thin black arrow) in an adult female. 10x, HE. G) Left caudolateral view of the cervical region showing a lymph node chain extending caudally beyond salivary tissue (black dashed rectangle).

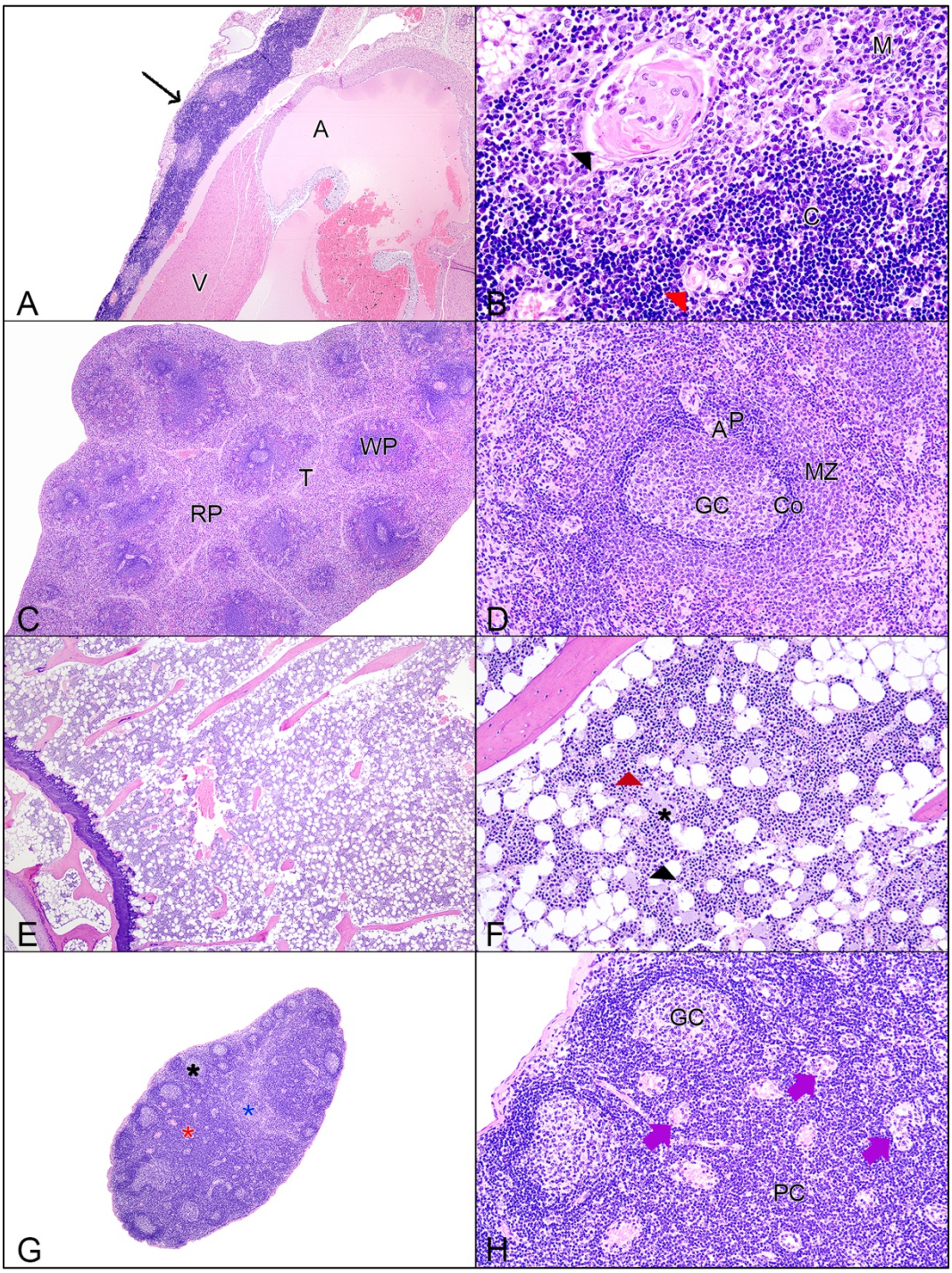

Figure 3-7: Histologic features of thymus, spleen, bone marrow, and lymph node in Egyptian rousette bats (*Rousettus aegyptiacus*). A) Left lobe of the thymus (thin black arrow) wrapping around the left atrium (A) and left ventricle (V) in a juvenile male. 4x, HE. B) Hassall's corpuscle (black arrowhead) in the thymic medulla (M) of a juvenile male. C = cortex, red arrowhead = capillaries. 40x, HE. C) Spleen with white pulp containing numerous lymphoid follicles (WP), red pulp (RP) and smooth muscle trabeculae (T) in a juvenile male. 4x, HE. D) Adjacent to numerous central arteries (A) surrounded by periarticular lymphoid sheaths (P) is a splenic lymphoid follicle with a central pale germinal center (GC) and an outer deeply basophilic corona/mantle zone (Co), further surrounded by a marginal zone (MZ) which delineates the

boundary between white pulp and red pulp. Juvenile male, 20x, HE. E) Bone marrow at the medullary cavity of the femoral head of a juvenile female. 2x, HE. F) Erythroid (red arrowhead) and lymphoid (black arrowhead) precursors admixed with megakaryocytes (black asterisk) and adipose at the femoral head of a juvenile female. 20x, HE. G) Lymph node with numerous cortical secondary follicles (black asterisk) overlying paracortical regions (red asterisk) and medullary sinus (blue asterisk) in an adult female. 4x, HE. H) B-cell rich secondary follicles with germinal centers (GC) in the cortex overly an indistinct T-cell rich paracortex (PC), with numerous high endothelial venules (purple arrows) in an adult female. 20x, HE.

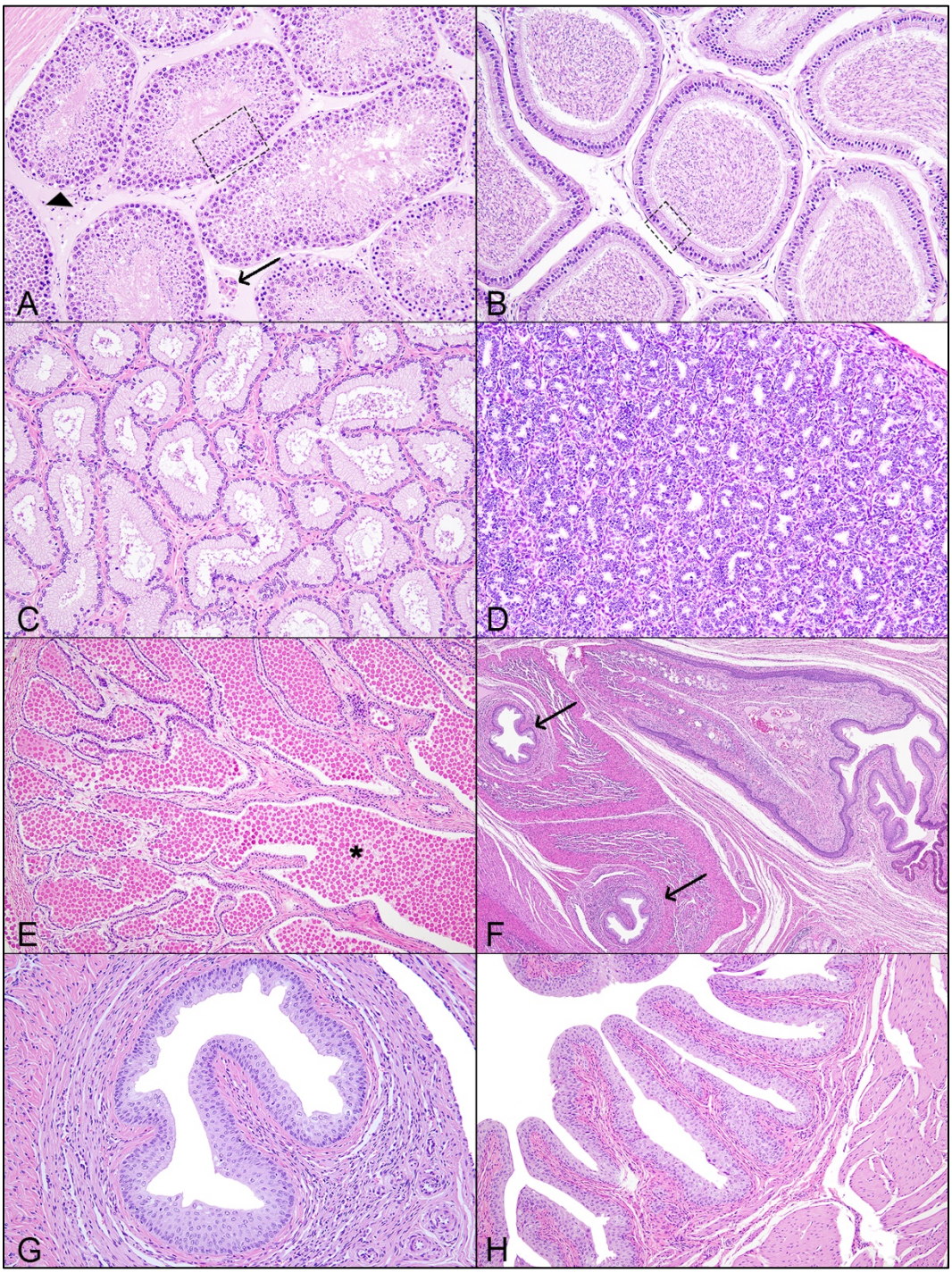

Figure 3-8: Histologic features of the male reproductive tract and urinary system in Egyptian rousette bats (*Rousettus aegyptiacus).* A) Seminiferous tubules in the teste of an adult male. The germinal epithelium (black dashed square) contains Sertoli cells and developing spermatocytes; testosterone-producing Leydig cells (thin black arrow) are present within the interstitial space, and myoid cells (black arrowhead) surround the tubules. 20x, HE. B. B) Tubules in the epididymis of an adult male. Tubules are lined by tall pseudostratified columnar epithelium with apical stereocilia (black dashed square) and contain spermatozoa within the tubular lumens. 20x, HE. C) Prostate gland in an adult male. Tubules composed of tall columnar epithelium is supported by a fibromuscular stroma.. 10x, HE. D) Bulbourethral/Cowper's gland in

an adult male, composed of numerous tubules lined by simple columnar epithelium. 20x, HE. E) Seminal vesicle with highly proteinaceous intraluminal seminal material (black asterisk) in an adult male. 10x, HE. F) Longitudinal section of retracted penis with cross sections of penile urethra (thin black arrows) in a juvenile male. 4x, HE. G) Cross section of urethra lined by stratified columnar epithelium in a juvenile male. 20x, HE. H) Urinary bladder with villous-like projections of the lamina propria lined by transitional epithelium and subjacent smooth muscle in a juvenile male. 10x, HE.

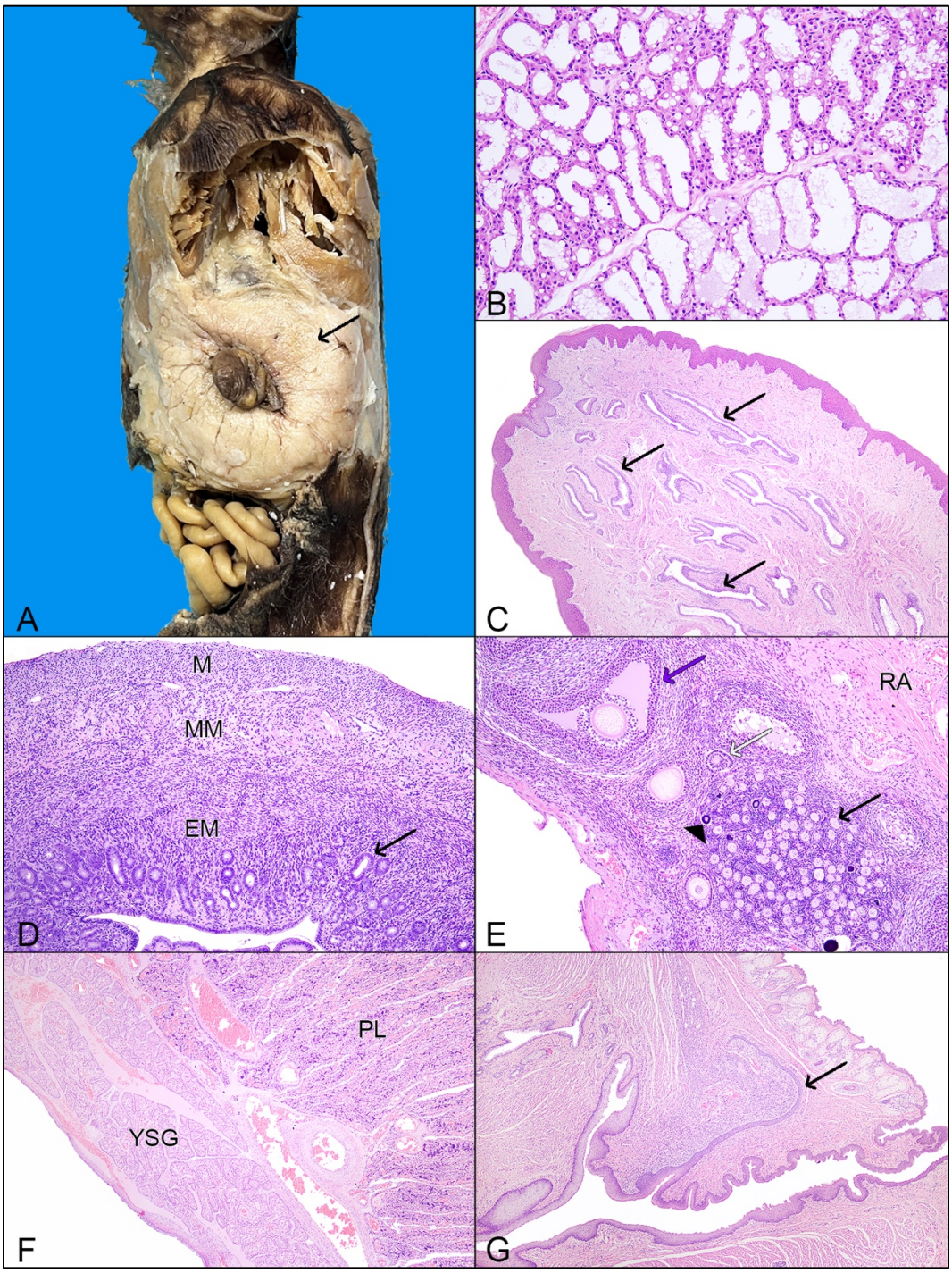

Figure 3-9: Gross and histologic features of the female reproductive tract in Egyptian rousette bats (*Rousettus aegyptiacus).* A) Left lateral view of mammary tissue (thin black arrow) with central teat in an adult female. B) Mammary tissue composed of numerous tubuloacinar secretory units in an adult female. 20x, HE. C) Longitudinal section of mammary teat with numerous teat sinuses (thin black arrows) in an adult female. 4x, HE. D) Uterine cross-section from a non-gravid adult female with endometrial glands (thin black arrow) within the endometrium (EM), vascular mesometrium (MM), and myometrium (M). 10x, HE. E) Ovarian cortex with numerous primordial follicles (thin black arrow), fewer primary follicles (thin white arrow), and one secondary follicle (thin purple arrow), with adjacent rete arteriosum (RA) in an

adult female. Follicular mineralization (black arrowhead) can be seen as part of normal atresia [526]. 10x, HE. F) Near-term placenta with placental labyrinth (PL) and yolk-sac gland (YSG) in an adult female. 4x, HE. G) Longitudinal section of vaginal vestibule and clitoris (thin black arrow) in an adult female. 4x, HE.

CHAPTER 3B

CHARACTERIZATION OF SPONTANEOUS GROSS AND HISTOLOGIC FINDINGS IN FREE-RANGING EGYPTIAN ROUSETTE BATS (ROUSETTUS AEGYPTIACUS) FROM UGANDA AND REVIEW OF REPORTED PATHOGENS[3]

[3] Elbert JA, Amman BR, Sealy TK, Atimnedi P, Towner JS, and Howerth, EW. To be submitted to a peer-reviewed journal.

ABSTRACT

The emergence of significant viral diseases and their potential threats to human and animal health have heightened interest in bats as vectors of disease and natural reservoir hosts. The Egyptian rousette bat (*Rousettus aegyptiacus*) is particularly important as a natural reservoir for orthomarburgviruses, whose two known members are Marburg virus and Ravn virus. While most studies focus on the presence of specific zoonotic agents in these bats, little is known about their basic pathology or the broader impacts of disease on their morbidity. Pathological investigations in free-ranging bats are limited, often constrained by small sample sizes or biased populations (e.g., animals found dead). In this study, 69 free-ranging Egyptian rousette bats from Uganda underwent post-mortem examination and histologic evaluation. These bats were captured as part of efforts to identify filoviral reservoir hosts, providing a unique opportunity to investigate spontaneous disease processes in an ostensibly healthy population. Gross lesions were seen in 85.5% (59/69) of bats, including scarring and fibrosis of the plagiopatagium and dactylopatagium (85.5%; 59/69), focal fibrotic nodules (17.4%; 12/69), and lacerations (17.4%; 12/69) within the wing membranes. All bats (100%; 69/69) had histopathologic changes, with a total of 794 lesions observed across 28 organs. The liver was the most frequently affected organ (81.2%; 56/69), followed by multi-organ perivascular cellular aggregates (79.7%; 55/69). This study represents the first comprehensive characterization of naturally occurring pathology in free-ranging Egyptian rousette bats from Uganda. Understanding the factors that influence the health of reservoir species is critical for elucidating the dynamics of zoonotic disease spillover and mitigating future outbreaks in humans and other susceptible hosts.

KEYWORDS: Egyptian rousette bat, *Rousettus aegyptiacus*, histology, pathology, natural reservoir

INTRODUCTION

Bats (Order Chiroptera, meaning "hand wing") are incredibly diverse, with more than 1,400 known species that account for more than 20% of the world's known mammalian diversity.[2] Second only to rodents in species diversity, bats inhabit all continents except Antarctica and have broad ecological, anatomical, and environmental diversity that is nearly unparalleled within the animal kingdom.[1,2] All bats are thought to have evolved from a common, flighted ancestor that displayed many features we still recognize in many bats today, including the ability to echolocate and specializations for fruit, nectar, insect and blood feeding.[77]

The Egyptian rousette bat (ERB; *Rousettus aegyptiacus*; common name: Egyptian rousette) is a species of pteropodid bat that inhabits parts of Africa, western Asia, the Mediterranean, and the Indian subcontinent.[9] They are predominantly cave-dwelling, gregarious and social animals, living in densely-packed roosts that can contain more than 100,000 bats.[9] ERBs are of critical importance as a natural reservoir host for both Marburg virus (MARV) and Ravn virus (RAVV), as investigated in numerous longitudinal ecological studies.[3,48,50,94-96] MARV and RAVV, close viral relatives to Ebola virus, are the only two known members of the species *Orthomarburgvirus marburgense (*family *Filoviridae*, genus *Orthomarburgvirus*) and are the causative agents of Marburg virus disease (MVD), a severe viral hemorrhagic fever that typically emerges in sub-Saharan Africa characterized by human-to-human transmission and high case

fatality ratios up to 90%.[196] In juxtaposition to the severe, frequently fatal disease seen in humans infected with MARV and RAVV, ERBs remain clinically healthy following experimental inoculation with MARV and RAVV, developing low-level viremia with widespread, multi-organ virus dissemination detectable by PCR.[4,50]

The majority of research in free-ranging ERBs has focused on ecological and epidemiological investigation into their role as a natural reservoir for orthomarburgviruses.[3,48,49,93-96] ERBs are additionally a putative reservoir for Sosuga virus (SOSV; family *Paramyxoviridae*), and a vertebrate reservoir for Kasokero virus (KASV; family *Orthonairoviridae*).[6,7,17,19,116] Recently, an experimental study investigating the role of viral coinfections in ERBs showed that SOSV+MARV and KASV+MARV coinfections differentially modulate MARV shedding and anti-MARV IgG responses, implicating coinfection dynamics as playing a critical role in bat-to-bat transmission dynamics and spillover potential.[282] Numerous pathogens have been serologically or molecularly identified in free-ranging ERBs across viral, bacterial and fungal families, as well as numerous parasite species. Most reported ERB pathogens are viral, which may reflect research bias within the scientific community on efforts to investigate viral families with known zoonotic potential, or may reflect the putative enhanced ability of ERBs to more successfully tolerate viral infection and replication than other mammalian species.[20,97-102] Previously reported pathogens and parasitic species found in both free-ranging and managed care ERBs will be discussed below and are included in Table 3-1.

Etiologies previously reported in free-ranging Egyptian rousette bats

Viral pathogens

RNA viruses are of critical importance as high-consequence zoonotic pathogens that originate in wildlife. Representing approximately 94% of zoonotic viruses[34], numerous ecological and biological factors contribute to the success of RNA viruses as pandemic pathogens, including their high mutation rate and frequency of recombination.[103,104] In addition to Marburg virus (MARV) and Ravn virus (RAVV)[5,48,93,95,105-108], numerous RNA viruses have been identified using serology and molecular diagnostics such as PCR in free-ranging Egyptian rousette bats (ERBs; *Rousettus aegyptiacus*; common name: Egyptian rousettes). These viruses include members of the families *Coronaviridae* (e.g. Coronavirus sp.)[109-112], *Flaviviridae* (e.g. West Nile virus, Yellow fever virus, Zika virus)[113,114], *Orthomyxoviridae* (e.g. Influenza A virus)[115], *Paramyxoviridae* (e.g. Henipavirus, Rubulavirus, Sosuga virus)[6,85,116,527], and *Rhabdoviridae* (e.g. Lagos bat virus)[81,82,117]. DNA viruses, including members of the family *Adenoviridae*[118], *Herpesviridae*[119-121], and *Poxviridae*[122,123], have additionally been reported in free-ranging ERBs, the latter of which has been associated with morbidity and mortality in ERBs in Israel and is zoonotic.[124]

Bacterial and fungal pathogens

There are few reports of bacterial pathogens in free-ranging ERBs and even fewer reports of clinical illness associated with bacterial infection. ERBs exhibit low colonization rates of *Staphylococcus aureus* and *S. schweitzeri*, with phylogenetic analysis suggesting significant geographical dispersal of *S. schweitzeri* among wildlife hosts.[125] Hemotropic mycoplasmas have been identified in two ERBs in Nigeria[126], while *Leptospira* sp. were identified in ERBs in South Africa.[127] *Borrelia* sp. were detected in 59 ERBs from a cave linked to human case of relapsing fever following a soft tick bite.[128]

E. coli was identified in 2 ERBs from the Republic of Congo[129], and *Bartonella* sp. have also been identified in ERBS from Kenya[130,131], Zambia[132], and South Africa.[131,133] The only report of bacterial-associated clinical disease in free-ranging ERBs is in Israel, where primarily pups and young adults are seasonally afflicted with abscessation due to *S. aureus*.[134] To the author's knowledge, there are no reports of fungal identification or disease in free-ranging Egyptian rousette bats.

Parasites

Current knowledge of ectoparasites in ERBs encompasses a wide range of arthropod parasites, including bat flies (Nycteribiidae), soft ticks (Argasidae), mites, and fleas, with more than 50 unique species reported throughout the ERB range (Table 3-1). These ectoparasites are known to play potential roles in the transmission of pathogens; e.g. *Eucampsipoda aegyptia,* a host-specific bat fly within the family Nycteribiidae, has been reported in at least 10 countries within the ERBs northern range[134-138], with 36.9%[137] to 43.9%[139] PCR positivity for *Bartonella* sp. in *E. aegyptia* collected from ERBs across 7 countries. Furthermore, the argasid *Ornithodoros (Reticulinasus) faini* serves as a tick vector in the enzootic transmission cycle with ERBs of Kasokero virus.[19,140] While there is no evidence for the involvement of *Ornithodoros faini* in the enzootic maintenance of orthomarburgvirus within ERBs[141], further research is needed to investigate other ERB ectoparasites and their possible contribution to the dynamics of zoonotic disease. Experimentally infected *Thaumapsylla breviceps breviceps* fleas inoculated intracelomically with MARV lacked vectorial capacity to transmit MARV biologically to ERBs[528], however the role of ectoparasites in mechanical transmission of MARV or other pathogens has yet to be investigated.

Current understanding of endoparasites in ERBs is sparse, with reports primarily focusing on protozoal species within the phylum Apicomplexa. *Eimeria rousetti*[142] and novel pathogen *Gregarina rousetti* n. sp.[143] have been reported in ERBs in Egypt, as well as numerous Plasmodium sp. identified in ERBs in Nigeria[144], Ghana[145], Congo[146], and Guinea, Liberia, and the Ivory Coast.[147] Trypanosoma sp. have been reported in ERBs in Gabon[148] and South Africa[149], and there is a single report of the filarial nematode *Diptalonema vitae* in ERBs in Egypt.[150] Pentastomids, crustaceous arthropods commonly known as "tongue worms", have been reported on the liver and spleen of ERBs in Uganda.[3] Future research on endoparasites in ERBs represents a compelling and underexplored avenue of study, offering significant potential to enhance our understanding of parasite-host dynamics and their implications for both bat health and zoonotic disease transmission.

Infectious and non-infectious diseases in managed care Egyptian rousette bats

Iron overload

Reports of clinical disease and pathogen detection in managed care ERBs are limited, with much of the published literature focusing on iron overload disease. Iron overload disease is the leading cause of morbidity and mortality in managed care ERBs and in other pteropid bats, possibly due to increased dietary iron or environmental exposure in managed care settings.[161,173-175,529-533] ERBs with iron overload disease accumulate iron most prominently in the liver, with iron accumulation additionally reported in the pancreas, lung, kidney, skeletal muscle, spleen, small intestine, adrenal cortex, urinary bladder, brain, dermis, and reproductive tissues.[161] A recent histopathologic comparison of hepatic iron overload between two managed care ERB

populations (zoo and research colony) and free-ranging ERBs identified a negative association between MARV infection status in the free-ranging ERB population and hemosiderosis, suggesting a possible hepatoprotective mechanism of hepcidin upregulation during MARV infection.[532] ERBs have been shown to have a limited ability to upregulate hepcidin expression, which may predispose to iron overload when faced with dietary iron excess[174]; MARV-infection-associated hepcidin upregulation may counteract this, however further research is needed to investigate this speculation.

Infectious pathogens

Reports of viral, bacterial, and fungal infections in ERBs in managed care are few. Two ERBs died from European bat lyssavirus 1 after importation into Denmark from a Dutch zoo.[117,151] Subsequent depopulation of all bats imported into Denmark and all members of the original Dutch colony found clinically silent European bat lyssavirus 1 infection in 11.9% and 13% of the ERBs, respectively.[81,117,151] Two novel members of the *Betaherpesvirinae* and *Gammaherpesvirinae* subfamilies were detected via nested PCR in pooled liver, lung, and small intestine samples from two deceased ERBs in Hungary[120], and two additional novel *Betaherpesvirinae* members were identified in oropharyngeal samples from clinically healthy ERBs in Spain.[119] In Israel, a novel poxvirus (Israeli *Rousettus aegyptiacus* pox virus; IsrRAPXV) was isolated from managed care ERBS in 2014[122] and 2019.[123] One adult female developed clinical, but non-fatal, poxviral disease with multifocal vesicular and nodular lesions on the wing membranes[122]; five years later, five juvenile ERBs developed fatal IsrRAPXV infection with typical pox-like lesions on the ventral abdomen, wing membranes, and tongue.[123] A novel papillomavirus, subsequently named *Rousettus aegyptiacus* papillomavirus type 1,

was isolated from an ERB from a United States-based bat conservation organization that presented with multiple cutaneous papillomas and basosquamous carcinoma in both the lateral canthus of the left eye and multifocally throughout the left wing membranes.[152,153] 15 *Bifidobacterium* sp. were identified in environmental fecal swabs from ERBs in a zoological park in Verona, Italy.[154] *Kluyvera ascorbata* was isolated from the blood of a deceased ERB from Korea, which has previously been reported in variable human clinical infections as well as isolated from subclinically infected Madagascan lemurs.[155] Additionally, Yersinosis due to *Yersinia pseudotuberculosis* has been reported in three closed ERB colonies in managed care, resulting in ~10% mortality[156], 19.7% mortality[157] or depopulation.[158] Reports of fungal pathogens are scarce, with a single study detecting *Pneumocystis* sp. in 35.3% (6/17) of ERBs from two managed care colonies in France via nested PCR analysis of lung tissue.[159] A single report documents a fatal case of microsporidiosis due to *Encephalitozoon hellem* in a managed care ERB, possibly caused by mechanical transfer of spores from a nearby aviary.[160]

Neoplasia

A diverse array of neoplasms have been documented, including adenomas[161,162], carcinomas[161], sarcomas[161,163,164], and lymphomas[165], affecting organs like the lungs [161,162,166], pancreas[162], liver[161,167], kidneys[161], bladder[161], and haired skin.[165] Etiological factors have been proposed in a few instances, such as a microchip-associated leiomyosarcoma[168] and papillomavirus infection linked to a basosquamous carcinoma in the wing membrane.[152,153] Iron overload has been suggested in the pathogenesis of hepatocellular carcinomas; in a retrospective study, ERBs with hemochromatosis were significantly more likely to have hepatocellular carcinomas than bats with

hemosiderosis.[161] Other reports of disease within managed care ERB populations include instances of pneumonia[161,169], membranous glomerulopathy[161], renal tubular necrosis[161], chronic interstitial nephritis[161], liver failure[161], myocardial degeneration and/or fibrosis[161], bacterial sepsis (undisclosed etiology)[161], gall bladder rupture[161], thymic lymphoid depletion[169], hepatocellular degeneration[169], multicentric hyperostosis linked to fluorosis[170] and "skin disease" (results anonymized) in 22% of managed care ERBs from two zoos.[171] Iatrogenic mortality due to pulmonary embolism of gelatin hemostatic sponge has additionally been reported in two ERBs.[172]

While the diversity of pathogens identified in ERBs provides valuable insight into the infectious pressures faced by this species, these data alone do not fully characterize the broader spectrum of tissue-level health and disease in free-ranging individuals. To date, no systematic histologic evaluation of free-ranging ERBs has been undertaken, and our understanding of their background pathology remains limited. The following section presents the first comprehensive description of spontaneous histologic lesions in free-ranging ERBs, establishing a foundational reference for future investigation into host health, disease ecology, and comparative pathology in this important reservoir species.

MATERIALS AND METHODS

Sixty-nine free-ranging ERBs (juvenile = 49; adult = 20 (forearm length > 89 cm[3,441]); male = 35; female = 34), were collected in 2008-9 as part of investigative efforts conducted by the Centers for Disease Control and Prevention (CDC) into discovery of the orthomarburgvirus natural reservoir host. As previously described, all capturing, processing, and procedures were performed in accordance with an institutionally approved animal care and use protocol.[3,48] Bat collections were completed with the

approval of the Uganda Wildlife Authority and following the American Veterinary Medical Association guidelines on euthanasia and the National Research Council recommendations for the care and use of laboratory animals.[3] Whole blood and spleens were removed at the time of capture for Marburg virus quantitative reverse transcription polymerase chain reaction (RT-qPCR) (negative = 41; positive = 27; unknown = 1). RT-qPCR was completed as previously described.[48] Abdominal +/- thoracic cavities were exposed to allow for 10% neutral buffered formalin fixation, and carcasses were fixed as intact specimens. The specimens were transferred to 70% ethanol after fixation; a definitive timepoint for this transfer is unknown.

In 2023, full necropsies were performed on each bat and all macroscopic findings recorded. Representative sections from a full set of tissues (including but not limited to heart, trachea, lungs, lymph nodes, liver, kidney, adrenal gland, tongue, gingiva, esophagus, stomach, pancreas, small and large intestines, haired skin, plagiopatagium, salivary gland, adipose, thymus, thyroid, bone marrow, ear canal, eyes, nasal turbinates, peripheral nerves, skeletal muscle, male and female reproductive organs, and brain) were processed and embedded in liquid paraffin. Sections were cut at 4 μm, mounted on glass slides, and stained with hematoxylin and eosin (HE). Additional staining methods were used depending on microscopic findings, i.e. for the detection of bacteria (Gram staining), fungi (Grocott's Gomori methenamine silver nitrate staining), iron (Perls' Prussian blue stain), and connective and collagen tissue (trichrome staining).

RESULTS

Overall statistics

Sixty-nine Egyptian rousette bat carcasses were examined. The examined population contained 49 juveniles (71%) and 20 adults (29%), with 35 males (50.7%) and 34 females (49.3%). Age was determined using a previously established metric of forearm length (juvenile = ≤ 89 cm; adult = > 89 cm).[3,441]

Post-mortem findings

Of the examined ERBs, 85.5% (59/69) had mild to moderate gross lesions, predominantly scarring and fibrosis of the plagiopatagium and dactylopatagium (85.5%; 59/69) (Fig. 3-10A), variably sized lacerations within the plagiopatagium and dactylopatagium (17.4%; 12/69) (Fig. 3-10A, B), focal fibrotic nodules within the plagiopatagium and dactylopatagium (17.4%; 12/69) (Fig. 3-10B, C), periosteal hemorrhage (4.3%; 3/69), osseous proliferation (4.3%; 3/69), focal dermal erosion (2.9%; 2/69), healed/callused mid-diaphyseal phalangeal fracture (fifth digit, first phalanx) (1.4%; 1/69) (Fig. 3-10D), subcutaneous hemorrhage (1.4%; 1/69), and multifocal ulcerative dermatitis (1.4%; 1/69) (Fig. 3-10E). One bat was missing its right eye at the time of capture (1.4%; 1/69), and two were gravid (2.9%; 2/69). Numerous Nycteribiidae "bat flies" were observed both freely floating in fixative and on carcasses (Fig. 3-10F). Due to the unknown number of fixative transfers and carcass manipulations since capture in ~2008, exact numbers were not counted as they were likely not representative of an in vivo ectoparasite burden.

Histologic findings

Histologic changes were observed in 69/69 (100%) bats, with 794 changes found in 28 organs; a summary of all changes can be found in Table 3-2. The most frequently affected organs were liver and multi-organ perivascular cellular aggregates (both 81.2%,

56/69), the latter of which will be considered a "vascular" lesion for this review. No changes were significant enough to have caused mortality had the animal not been captured for filoviral surveillance sampling.

Liver

The liver was the most affected organ with 194 histopathological changes across 56 ERBs (81.2%, 56/69). Glycogen accumulation progressing to vacuolar hepatopathy, glycogen type, was observed in 81.2% (56/69) of ERBs and has been previously reported as a common incidental finding in captive ERBs (Fig. 3-11A).[18,50,437] Mild to moderate, multifocal, lymphoplasmacytic and occasionally histiocytic hepatitis was identified in 74% of ERBs (51/69) (Fig. 3-11B-C), with frequent, predominantly mild necrosis (60.9%; 42/69) and hemorrhage (47.8%; 33/69). Of the ERBs with hepatitis, 51% were RT-qPCR-positive in splenic tissue for MARV and 49% (25/51) were negative. Evaluation of hepatic iron accumulation in this population using Perls' Prussian blue histochemical staining was previously reported; 40.6% (28/69) of ERBs had either mild (21.7%; 15/69) or moderate (18.8%; 13/69) hemosiderosis.[532] Additional findings include nodular hyperplasia (4.3%; 3/69), extramedullary hematopoiesis (2.9%; 2/69), sinusoidal inflammatory cell infiltrates (2.9%; 2/69), biliary ectasia (1.4%; 1/69), biliary hyperplasia (1.4%; 1/69), centrilobular degeneration (1.4%; 1/69), bridging fibrosis (1.4%; 1/69), and telangiectasia (1.4%; 1/69).

Multi-organ perivascular cellular aggregates

The most common histopathologic change was that of variably sized perivascular aggregates composed predominantly of lymphocytes, plasma cells, and occasional histiocytes, with 232 changes in one (15.9%; 11/69) or more (65.2%; 45/69) organs in 56

(81.2%, 56/69) ERBs. Cellular aggregates were most commonly found in adipose tissue (154/232 (66.4%), 47/69 (68.1%) ERBs) (Fig. 3-12C, F-H), followed by nerves (41/232 (17.7%), 26/69 (37.7%) ERBs) (Fig. 3-12A-B, D) and the tongue (10/232 (4.3%), 10/69 (14.5%) ERBs) (Fig. 3-12C). A summary of organ locations and severity can be found in Table 3-3.

Dermal (haired skin)

Thirty-nine ERBs (56.5%; 39/69) had 67 lesions of perivascular to interstitial, mild to severe dermatitis, variably characterized by lymphoplasmacytic infiltrates (59.7%, 40/67 lesions) (Fig. 3-11D), epidermal erosion with serocellular crusting (17.9%; 12/67), neutrophilic infiltrates (7.5%; 5/67), granuloma or abscess formation (4.5%; 3/67), pyogranulomatous inflammation (4.5%; 3/67), epidermal hyperplasia/acanthosis (3.0%; 2/67), or epidermal ulceration (3.0%; 2/67). The majority of the lesions were identified in whole body, head or pelvic cross sections; however, this may reflect a sampling bias more than is reflective of geographic localization of lesions.

Pulmonary

In this study, the majority of respiratory lesions (35 lesions in 26 ERBs (37.7%; 26/69)) were mild pulmonary hemorrhages (45.7%; 16/35 lesions), likely as a result of heightened cardiopulmonary stress upon capture or as a result of laceration during intracardiac exsanguination. Mild, chronic interstitial pneumonia was the most common inflammatory lesion (22.9%; 8/35) (Fig. 3-11E), with three cases of pneumonia with mixed inflammation (8.6%; 3/35), two cases of embolic pneumonia (5.7%; 2/35), and one focal lesion of endogenous lipid pneumonia (2.9%; 1/35) (Fig. 3-11F). Additional

findings include mild interstitial fibrosis (5.7%; 2/35) and mild-moderate, subacute to chronic, pleuritis (5.7%; 2/35).

Salivary gland

Twenty-four bats with salivary gland lesions (34.8%; 24/69) had mild to moderate, multifocal, lymphoplasmacytic sialadenitis (100%; 24/24) (Fig. 3-13A), with mild, multifocal, periductal fibrosis in two bats (8.3%; 2/24) and one bat (4.2%; 1/24) with low numbers of macrophages admixed within the lymphoplasmacytic population.

Lymph nodes

For the purposes of this study, lymph nodes will be grouped as "axillary" or "other". Of the 21 bats (30.4%; 21/69) with axillary lymph nodes changes; 11 had mild to moderate sinus erythrocytosis (40.7%; 11/27 total axillary lymph node changes) (Fig. 3-13C). Other changes include mild, multifocal mineralization of follicular germinal centers (37.0%; 10/27), erythrophagocytosis (7.4%; 2/27), follicular hyperplasia (7.4%; 2/27), and moderate to severe lymphadenitis, either with a prominent subcapsular histiocytosis (3.7%; 1/27) or a subacute, necrotizing, neutrophilic adenitis with granuloma formation, severe pyogranulomatous and mononuclear cellulitis and reactive endothelium (3.7%; 1/27) (Fig. 3-13B). Changes in all other examined lymph nodes (15.9%; 11/69) include moderate to severe, necrotizing, neutrophilic and/or mononuclear cellulitis and lymphadenitis (36.8%; 7/19 total lesions), mild to moderate phagocytosis (21.0%; 4/19), mild sinus erythrocytosis (15.8%; 3/19), mild to moderate fibrosis (10.5%; 2/19), mineralization of germinal centers (5.3%; 1/19), subcapsular foamy histiocytosis (5.3%; 1/19) (Fig. 4D), and edema (5.3%; 1/19).

Kidneys

Sixteen ERBs (23.2%; 16/69) had renal changes, with mild to moderate, lymphoplasmacytic, interstitial nephritis as the most common lesion (48.1%; 13/27 total lesions). Additionally present was mild tubular ectasia with proteinosis or granular casts (18.5%; 5/27), intracellular pigment most commonly within proximal tubular epithelium (11.1%; 3/27), mild, focally extensive chronic infarction (11.1%; 3/27), mild interstitial fibrosis (11.1%; 3/27), and mild tubular mineralization (3.7%; 1/27).

Wing Membrane

Fourteen ERBs (20.3%, 14/69) had predominantly inflammatory changes within their wing membranes, most commonly within the plagiopatagium and/or dactylopatagium. Neutrophilic and eosinophilic dermatitis, fibrosis, hyperkeratosis and acanthosis (each 85.7%; 12/14 total lesions) was the most common finding and was frequently associated with the presence of arthropod parasites, either within presumptive hair follicles or within the stratum corneum. Additional findings within wing membranes include mild perivascular to interstitial lymphoplasmacytic dermatitis (28.6%; 4/14), epidermal ulceration (28.6%; 4/14), and mild histiocytic dermatitis (7.1%; 1/14).

Gingiva

Eleven ERBs (15.9%; 11/69) had gingival changes, most commonly lymphoplasmacytic (50%; 5/10 total lesions), neutrophilic (10%; 1/10), or ulcerative (10%; 1/10) gingivitis (Fig. 3-13E), occasionally with intraepithelial pustules (30%; 3/10).

Skeletal muscle

Eleven ERBs (15.9%; 11/69) had 19 skeletal muscle changes, including mild to moderate, focally extensive to multifocal fibrosis (31.6%; 6/19), degenerative (26.3%;

5/19) and/or regenerative (21%; 4/19) myopathies (Fig. 3-13F), and mild to moderate myositis that ranged from lymphoplasmacytic (10.5%; 2/19), eosinophilic (5.3%; 1/19) or histiocytic (5.3%; 1/19).

Adrenal gland

Of the 9 ERBs with adrenal gland changes, 4 had mild cortical hyperplasia (44.4%; 4/9 total lesions) (Fig. 3-14A), and two had mild extramedullary hematopoiesis in the adrenal medulla and/or adrenal cortex (22.2%; 2/9). Brown, finely granular intracellular pigment was observed in the distal zona reticularis cells or in the proximal zona glomerulosa cells in 3 ERBs (33.3%; 3/9).

Additional organs

Additional changes in less than 10 ERBs per organ are listed in Table 3-2, including mammary gland (11.6%; 8/69) (Fig. 3-14B), nasal turbinates (10.1%; 7/69) external ear (8.7%; 6/69), small intestine (8.7%; 6/69) (Fig. 3-14C), colon (5.8%; 4/69), pancreas (5.8%; 4/69) (Fig. 3-14D), pharynx (2.9%; 2/69), prostate (2.9%; 2/69), adipose (1.5%; 1/69), brain (1.5%; 1/69) (Fig. 3-14E), cervix (1.5%; 1/69), eye (1.5%; 1/69), heart (1.5%; 1/69) (Fig. 3-14F), thymus (1.5%; 1/69), tongue (1.5%; 1/69), trachea (1.5%; 1/69), and uterus (1.5%; 1/69).

Parasites

Seventy-two parasites were identified in 39 ERBs (56.5%; 39/69), most commonly in sections of haired skin (30.8%; 20/65) and deep external ear canal (26.2%; 17/65) as well as wing membrane (13.8%; 9/65), small intestine (12.3%; 8/65), stomach (7.7%; 5/65), nasal turbinates (6.2%; 4/65), gingiva (4.6%; 3/65) and colon, esophagus, pancreas, extra-gastric, adipose, and urinary bladder (each 1.5%; 1/65). In many

instances, parasite degeneration hindered confident identification to even a family level, and no histologic descriptions of parasites associated with Egyptian rousette bats currently exist for comparison.

Numerous, variably sized organisms were identified within the subepithelial connective tissue or stratum corneum of the wing membrane, most frequently within the plagiopatagium (Fig. 3-15A-D) as well as deep within the external ear canal, often positioned immediately adjacent to the tympanic membrane (Fig. 3-15E-F). These organisms were characterized by a thin, ridged cuticle and striated musculature, consistent with a mite species, possibly *Psorergatoides* spp.[534-537] Organisms within haired skin sections were frequently located in the stratum corneum and were characterized by jointed appendages and cuticular spines (Fig. 3-16B-E), diagnostic features of Sarcoptidae mites, a family previously reported in ERBs.[145,538,539] Additional parasitic organisms were identified in various tissues, including larval ascarids with lateral alae and prominent lateral chords in an extra-gastric granuloma (Fig. 3-17A), a craspedote cestode with lateral vellum within the small intestinal lumen (Fig. 3-17B), trematode eggs within pancreatic tissue (Fig. 3-17C-D), and aphasmid nematodes expanding small intestinal villi (Fig. 3-17E-H).

DISCUSSION

This study represents the first comprehensive characterization of spontaneous pathology in free-ranging Egyptian rousette bats from Uganda, providing unprecedented insight into the spectrum of naturally occurring pathology in this important reservoir species. These bats were originally captured as part of efforts to identify filoviral reservoir hosts, providing a unique opportunity to investigate spontaneous disease

processes in an ostensibly healthy population. Through the detailed evaluation of 69 bats, 794 histologic lesions were identified across 28 organs, and gross abnormalities were documented in over 85% of animals.

In the liver, glycogen-type vacuolar hepatopathy and multifocal lymphoplasmacytic hepatitis likely represent physiologic adaptation and MARV or other infection-related hepatopathology. These findings were anticipated, given the well-documented propensity of ERBs for physiologic glycogen accumulation in the liver and the fact that 51% of the bats were RT-qPCR-positive in splenic tissue for MARV at the time of capture. 1,622 ERBs captured in Uganda in 2008 and 2009 were part of a MARV ecological study[3]; the MARV-positive bats included in this histologic analysis represent a targeted subset of that cohort, retained specifically because of their MARV positivity. This subset is therefore not representative of natural infection rates in free-ranging juvenile ERBs, which are approximately 2.5%.[3]

The most numerous histologic finding was the presence of perivascular inflammatory aggregates, which were seen in 17 different organs, most prominently in adipose tissue or adjacent to nerves. No overarching pattern in their geographic distribution was discerned, and their overrepresentation in specific sites—such as the heart base, mesentery, or pelvic cross-sections—likely reflects sampling bias. This finding has not been reported in ERBs evaluated from research colony or zoo managed care settings.[161,532] Perivascular inflammation is a common, non-specific histologic finding associated with a wide range of infectious and non-infectious processes. These include viral diseases (e.g., rabies virus[540], canine distemper virus[541], feline infectious peritonitis[542], West Nile virus[543]); bacterial infections (e.g., listeriosis[544], rickettsiosis[545]);

parasitic infections (e.g., toxoplasmosis[546], equine protozoal myeloencephalitis[547]); fungal infections (e.g., cryptococcosis[548]); immune-mediated diseases (e.g., granulomatous meningoencephalitis[549]); environmental toxicities (e.g., lead toxicosis[550], hairy vetch toxicosis[551]); and vascular or autoimmune disorders (e.g., atherosclerosis[552], pulmonary hypertension[552], systemic lupus erythematous and rheumatoid arthritis[553]). The mechanism underlying the formation of these aggregates remain unclear, and possibly reflects chronic antigenic stimulation, subclinical exposures to viral or parasitic agents, systemic immune surveillance, or environmental stressors. Future investigation into the possible roles that infectious pathogens, metabolic or aerobic stress, or ectoparasite burden may have in the development of systemic perivascular aggregates is warranted.

Additional lesions, including dermatitis, interstitial pneumonia, sialadenitis, and mild nephritis, further underscore the complexity of host-pathogen-environment interactions in free-ranging bats. Many of these lesions are unlikely to be clinically significant in isolation but may have cumulative effects on host health, particularly in juvenile or immunocompromised individuals.

This study provides the first macroscopic and microscopic images of wing membrane and deep external ear canal mites, suggestive of *Psorergatoides* sp. which have been reported in *Myotis macropus* in Australia[536], as well as additional ectoparasites and endoparasites affecting numerous body systems. Enhanced characterization of ERB endoparasites and ectoparasites is warranted, as parasitic infections may modulate host immunity and alter the dynamics of concomitant infections.[554,555] Uncharacterized ectoparasites could play an important role in the transmission or maintenance of endemic pathogens, as they are well-established vectors of numerous diseases.[556,557] This has

already been demonstrated in ERBs, where *Ornithodoros (Reticulinasus) faini* ticks maintain Kasokero virus through an enzootic transmission cycle with ERBs.[8,18,19,140] Future studies should prioritize robust field necropsy technique to ensure appropriate collection of parasites for macroscopic and microscopic evaluation, including deep dissection of the external ear canal and collection of intact specimens retained in 70-90% ethanol.[558]

Notably, no fungal pathogens were identified in this cohort of bats. However, due to the unknown number of fixative transfers and carcass manipulations since capture in ~2008, it is possible that grossly appreciable fungus was no longer evident and therefore not selected for histologic evaluation. All previously reported fungal pathogens in ERBs have been in managed care populations (Table 3-1).

Additionally, no neoplastic processes were identified in this cohort. This is consistent with the low rates of neoplasia in managed care ERBs. In general, bats are a long-lived and tumorigenesis-resistant species, with recent research suggesting that evolutionary adaptations and genomic characteristics that support this ability include negative selection to accumulation of non-long terminal repeat (non-LTR) retrotransposons in the genome[559], differential expression of telomerase maintenance genes[558,560], positive selection for multiple tumor suppressor and DNA-repair genes[561], and possibly even efficient prevention of oxidative stress-induced damage.[311]

This work is not without limitations. The samples analyzed were collected over a decade before analysis, and preservation artifacts may have impacted tissue quality and parasite morphology. The study was constrained to histologic techniques, without incorporation of parallel molecular diagnostics which would have enhanced etiologic

investigation. Molecular investigations to identify potential pathogens in affected tissues were not feasible due to nucleic acid degradation and unknown, intractable contaminants that could not be eliminated during nucleic acid extraction sample cleanup. As such, the extent to which viral pathogens contributed to identified inflammatory lesions in this study is unknown. Immunohistochemical staining was not attempted due to the contaminants identified during extraction efforts and prolonged sample exposure to fixatives. Application of special stains (Gram stain, Giemsa stain) did not elucidate the presence of bacterial pathogens in lesions with marked neutrophilic and/or histiocytic infiltrates. In addition, the population sample was skewed toward juveniles, and temporal or seasonal effects on disease prevalence could not be assessed. An additional limitation of this study was the unavailability of splenic tissue for histologic evaluation, as it was prioritized for Marburg virus RT-qPCR at the time of capture. Future studies should prioritize retaining fresh tissue samples for unbiased pathogen discovery using platforms such as Virocap[562] as well as reserving splenic tissue for diagnostic and histopathologic assessment.

In addition to the topics already mentioned, this study opens several promising avenues for future research. First, systematic molecular characterization of lesions, particularly those involving lymphoid organs, liver, and skin, could help identify underlying pathogens and clarify disease etiology. Second, deeper investigations into the immunologic consequences of systemic and chronic low-level inflammation, such as the perivascular infiltrated observed here, may shed light on how ERBs balance viral disease tolerance with immune control. Third, a more robust understanding of parasitic diversity, life cycles, and vector competence within ERBs is needed, especially given the role of

ectoparasites in pathogen transmission. Finally, longitudinal studies incorporating health status, reproductive condition, and seasonal variation could help delineate the interplay between disease burden, host fitness, and spillover potential.

This study provides the first tissue-based landscape of naturally occurring pathology in free-ranging ERBs, a key natural reservoir host for orthomarburgviruses[3,4,48,50], indicating that even outwardly healthy individuals harbor a wide range of histologic lesions, many with probable infectious or inflammatory origins. These findings underscore the importance of characterizing reservoir host health beyond the presence or absence of a particular pathogen and highlight the need for integrated approaches that combine pathology, molecular biology, and ecology to better understand the dynamics of zoonotic disease spillover and mitigating future outbreaks in humans or other susceptible hosts.

Table 3-1: Pathogens and parasites reported in Egyptian rousette bats (*Rousettus aegyptiacus).* S = Serology, M = Molecular biology, [#] = Antibodies in serum, * = found in feces under roosting *ERB* colonies, [@] = described in *Rousettus aegyptiacus occidentalis,* [$] = possibly accidental, [&] = described in *Rousettus aegyptiacus leachi*

Group	Family	Pathogen	Detection Method	Location	Ref
Virus (RNA)	*Astroviridae*	Astrovirus sp.	M	Gabon, Kenya	563,564
	Caliciviridae	Calicivirus sp.	M	Kenya	564
	Coronaviridae	Betacoronavirus sp.	M	Kenya	109
		Coronavirus sp.	M	Guinea, Kenya, South Africa	110-112,380,564
	Filoviridae	Zaire ebolavirus	S	Gabon	106
		Orthomarburgvirus marburgense (Ravn virus)	S, M	South Africa, Uganda	3,48,96
		Orthomarburgvirus marburgense (Marburg virus)	S	Gabon	3,5,48,93,96,105-108,565

	Flaviviridae	Uganda S virus	S	Uganda	[113]
		Entebbe bat virus	S	Kenya	[566]
		Israel turkey meningoencephalitis virus	S	Israel	[567]
		Ntaya virus	S	Kenya	[566]
		Usutu virus	S	Kenya	[566]
		Pegivirus	M	Kenya, Nigeria	[568]
		West Nile virus	S	Kenya, Israel	[566,567]
		Yellow fever virus	S	Uganda	[569]
		Zika virus	S	Uganda	[114,569]
	Nairoviridae	Kasokero virus	S	Uganda	[570]
		Yogue virus	S, M	Senegal	[571]
		Crimean-Congo hemorrhagic fever orthonairovirus	S	Gabon	[572]
	Orthomyxoviridae	Influenza A virus	M	Egypt	[115]
	Orthoreoviridae	Orthoreovirus	M	Zambia	[573,574]
	Paramyxoviridae	Hendra(-like) henipavirus	S	Ghana	[575]
		Nipah henipavirus	S	Ghana	[575]
		Cedar henipavirus	S	Ghana	[575]
		Sosuga pararubulavirus	S, M	Uganda, Sierra Leone	[6,116]
		Rubulavirus spp.	M	South Africa, Congo	[60,85]
		Sosuga pararubula(-like) virus	M	South Africa	[60]
		Henipavirus sp.	M	Gabon	[85]
	Peribunyaviridae	Bunyamwera orthobunyavirus	S	Uganda	[569]
	Phenuiviridae	Rift Valley Fever phlebovirus	S	Uganda[#]	[576]
	Rhabdoviridae	Lagos bat virus	M, S	Kenya, Nigeria[#], and Togo, Egypt, France via "Africa"	[82,577-579]
		European bat lyssavirus 1	M	Denmark and Netherlands (managed care)	[81,88,117,151]

		Shimoni bat virus	S	Kenya, Nigeria[#]	82,579
		Mokola virus	S	Nigeria[#]	82
		Ikoma lyssavirus	S	Nigeria[#]	82
	Sedoreoviridae	Rotavirus A	M	Kenya, Zambia	564,580
		Bukakata orbivirus	M	Uganda	581
	Togoviridae	Chikungunya virus	M	Senegal	88
		Semliki Forest virus	S	Uganda	569
		Alphavirus sp.	S	Uganda	576
		O'nyong'nyong virus	S	No information	582
Virus (DNA)	*Adenoviridae*	Bat mastadenovirus	M	South Africa	118
	Herpesviridae	Unclassified *Herpesviridae*	M	South Africa, Hungary (managed care)	120,583
		Betaherpesvirus sp. Gammaherpesvirus sp.	M	Southern Spain (managed care), Zambia	119,121
	Papillomaviridae	Rousettus aegyptiacus papillomavirus type 1	M	MI, USA (managed care)	152,153
	Polyomaviridae	Betapolyomavirus sp.	M	Zambia	584
		Unclassified *Polyomaviridae*	M	Kenya	585
	Poxviridae	Unclassified *Poxviridae*	M	Israel	122,123
Bacteria	*Bartonellaceae*	*Bartonella rousetti*	M, S	SW Nigeria, Zambia	132,586
		Bartonella spp.	M	Kenya, South Africa	130,131,133
	Bifidobacteriaceae	*Bifidobacterium* spp.	M	Italy (managed care)	154
	Borreliaceae	*Borrelia* sp.	M	Zambia	128
	Enterobacteriaceae	*Escherichia* sp.	M	Republic of Congo	129
		Kluyvera ascorbata	S	South Korea	155

				(managed care)	
	Leptospiraceae	*Leptospira interrogans*	M	South Africa	[127]
		Leptospira borgpetersenii (or -like)	M	South Africa	[127]
	Mycoplasmataceae	*Mycoplasma* sp.	M	Northern Nigeria	[126]
	Staphylococcaceae	*Staphylococcus aureus*	M	Gabon, Israel	[125,134]
		Staphylococcus schweitzeri	M	Gabon	[125]
	Yersiniaceae	*Yersinia pseudotuberculosis*	S, M	New York and Japan (managed care)	[157,158]
Fungal	*Ajellomycetaceae*	*Histoplasma sp.*	M	United States (managed care)	[437,587]
	Cryptococcaceae	*Cryptococcus sp.*	Unk	Unknown (managed care)	[437]
	Pneumocystidaceae	*Pneumocystosis sp.*	M	France (managed care)	[159]
	Unikaryonidae	*Encephalitozoon hellem*	M	United States (managed care)	[160]
Protozoa	*Eimeriidae*	*Eimeria rousetti*	Microscopy	Egypt	[142]
	Gregarinidae	*"Gregarina rousetti n. sp."*	Microscopy	Egypt	[143]
	Plasmodiidae	*Hepatocystis* sp.	M	North-Central Nigeria	[144]
		Plasmodium rousetti	S	Ghana, Congo	[145,146]
		Plasmodium voltaicum	S	Guinea, Liberia, Ivory Coast	[147]
	Trypanosomatidae	*Trypanosoma* spp.	M	Gabon, South Africa	[148,149]
Nematode	Filariidae	*Diptalonema vitae*		Egypt	[150]

Arthropod ("bed bugs")	Cimicidae	*Afrocimex leleupi*		Congo	[145]
	Cimicidae	*Afrocimex constrictus*		Kenya	[588]
Arthropod (Crustacean)	Phylum Pentastomida			Uganda	[3]
Arthropod (fleas)	Pulicidae	*Archaeopsylla metallescens*		Egypt	[134]
	Ischnopsyllidae	*Thaumapsylla breviceps*		South Africa	[134,589]
	Ischnopsyllidae	*Thaumapsylla breviceps orientalis*		Congo	[134,145]
Arthropod (flies)	Hippoboscidae	*Basila nana*		Lebanon	[135]
	Nycteribiidae	*Cyclopodia greefi greefi*		Ghana	[590]
	Nycteribiidae	*Eucampsipoda aegyptia*		Egypt, UAE, Yemen, Oman, Iran, Jordan, Turkey, Lebanon, Palestine, Saudi Arabia	[134-138]
	Nycteribiidae	*Eucampsipoda africana*		Gabon, South Africa, Republic of the Congo, Liberia, Zambia[&]	[137,589,591-593]
	Nycteribiidae	*Eucampsipoda africanum*		Congo, Ghana	[145,590]
	Nycteribiidae	*Eucampsipoda hyrtlii*		Iran, Turkey	[594,595]
	Nycteribiidae	*Eucampsipoda hyrtlii diversa*		Egypt, Israel, Lebanon	[134]
	Nycteribiidae	*Nycteribia alternata*		Ghana	[590]
	Nycteribiidae	*Nycteribia pedicularia*		Palestine, Israel, Lebanon	[134-136]

	Nycteribiidae	*Nycteribia schmidlii*		Palestine	[136]
	Nycteribiidae	*Nycteribia schmidlii scotti*		Gabon	[592]
	Streblidae	*Brachytarsina* sp.		Egypt	[134]
	Streblidae	*Brachytarsina (Nycteribosca) africana*		Congo	[145]
	Streblidae	*Brachytarsina (Nycteribosca) allaudi*		Congo, Gabon	[145,592]
	Streblidae	*Brachytarsina bequaerti*		Tanzania	[596]
	Streblidae	*Megastrebla (Aoroura) bequaerti*		Tanzania	[596]
	Streblidae	*Nycteribosca bequaerti*		Tanzania	[596]
Arthropod (mites)	Acarinae	*Acarus* sp.		Ghana	[590]
	Carpoglyphidae	*Carpoglyphus* sp.		Ghana	[590]
	Macronyssidae	*Chiroptonyssus robustipes*		Ghana	[590]
	Macronyssidae	*Liponyssus glutinosus*		Egypt	[134]
	Macronyssidae	*Liponyssus longimanus*		Egypt	[134]
	Macronyssidae	*Steatonyssus longipes*		Ghana	[590]
	Pyemotidae	*Pyemotes* sp.		Ghana	[590]
	Sarcoptidae	*Nycteridocoptes pteropodi*		Zaire[$]	[539]
	Sarcoptidae	*Nycteridocoptes rousetti*		Congo	[145,538]
	Sarcoptidae	*Teinocoptes eonycteri*		Egypt	[539]
	Sarcoptidae	*Teinocoptes pahangensis*		Angola, Cyprus, Egypt	[539]
	Sarcoptidae	*Teinocoptes rousetti*		Zaire	[539]
	Spinturnicidae	*Ancystropus aethiopicus Hirst*			[597]
	Spinturnicidae	*Ancystropus aequatorialis*		Equatorial Guinea	[598]
	Spinturnicidae	*Ancystropus leleupi*		Congo	[145]
	Spinturnicidae	*Ancystropus taprobanius*		Equatorial Guinea	[598]

	Spinturnicidae	*Ancystropus zelebori*		Equatorial Guinea, South Africa, Egypt, Congo	134,145,589,598
	Spinturnicidae	*Ancystropus zeleborii Kolenati*		Egypt	599
	Spinturnicidae	*Meristaspis kenyaensis*		Ghana, Egypt	590,599
	Spinturnicidae	*Meristaspis lateralis*		Iran, Egypt	594,599
	Spinturnicidae	*Periglischrus ojastii*		Ghana	590
	Spinturnicidae	*Periglischrus paracutisternus*		Ghana	590
	Spinturnicidae	*Spinturnix* sp.		Ghana	590
	Spinturnicidae	*Spinturnix americana*		Ghana	590
	Spinturnicidae	*Spinturnix delacruzi*		Equatorial Guinea	598
	Spinturnicidae	*Spinturnix lateralis*		Republic of the Congo, Egypt, Palestine, Cyprus	134,145
Arthropod (ticks)	Argasidae	*Alectorobius (Reticulinasus) camicasi*		Senegal[@]	134,600
	Argasidae	*Argas boueti*		Egypt, Israel	134
	Argasidae	*Argas vespertilionis*		Jordan, Israel, Sudan, Ghana	134,136,590
	Argasidae	*Carios vespertilionis*		Western Palearctic	601
	Argasidae	*Chiropterargas boueti*		Western Palearctic	601
	Argasidae	*Ornithodoros (Reticulinasus) salahi*		Jordan*, Egypt, Israel, Palestine, Cyprus, Iran*, Oman "Western Palearctic"	136

	Argasidae	*Ornithodoros faini*		South Africa	[589]
	Ixodidae	*Ixodes* sp.		Ghana	[590]

Table 3-2: Details on histologic changes in free-ranging Egyptian rousette bats (*Rousettus aegyptiacus*) from Uganda. Histologic changes were observed in 69/69 (100%) bats, with 794 changes in 28 organs.

Organ (# of affected ERBs)	Pathology	Localization	Character/Agent	Severity (Mild/Mod/ Severe)	n
Liver (56)	Glycogen accumulation / Vacuolar hepatopathy	Multifocal	Glycogen type	15/21/20	56
	Hepatitis	Multifocal	Lymphoplasmacytic, histiocytic	49/2/0	51
	Necrosis	Multifocal		41/1/0	42
	Hemorrhage	Multifocal		32/1/0	33
	Iron Accumulation (Hemosiderosis)	Zonal to Diffuse		15/13/0	28
	Hyperplasia	Multifocal	Nodular	2/1/0	3
	Extramedullary hematopoiesis	Multifocal		2/0/0	2
	Inflammatory cell infiltrates	Multifocal	Sinusoidal	2/0/0	2
	Biliary ectasia	Multifocal		0/1/0	1
	Biliary hyperplasia	Multifocal		1/0/0	1
	Centrilobular Degeneration	Focally extensive		1/0/0	1
	Fibrosis	Focally extensive	Bridging	1/0/0	1
	Telangiectasia	Focal		1/0/0	1
Vessels (56)	Perivascular cellular infiltrates	Multifocal	Lymphoplasmacytic, occasional histiocytes	134/71/27	232
Haired Skin (39)	Dermatitis	Multifocal	Lymphoplasmacytic	25/12/3	40
			Erosive (serocellular crusting)	10/1/1	12
			Neutrophilic	4/0/1	5
			Granuloma/abscess-forming	2/0/1	3
			Pyogranulomatous	2/0/1	3

			Epidermal hyperplasia	2/0/0	2
			Ulcerative	2/0/0	2
Lung (26)	Hemorrhage	Multifocal	Chronic	16/0/0	16
	Pneumonia	Multifocal	Interstitial	8/0/0	8
		Focal to multifocal	Mixed*	3/0/0	3
		Multifocal	Embolic	1/1/0	2
		Focal	Endogenous lipid	1/0/0	1
	Fibrosis	Multifocal	Interstitial	2/0/0	2
	Pleuritis	Focal, multifocal		1/1/0	2
	Granuloma	Focal	Foreign body	1/0/0	1
Salivary gland (24)	Sialadenitis	Multifocal	Lymphoplasmacytic	23/1/0	24
			Histiocytic	1/0/0	1
	Fibrosis	Periductular, multifocal		2/0/0	2
Axillary Lymph Node (21)	Draining hemorrhage	Multifocal		7/4/0	11
	Mineralization (Germinal centers)	Multifocal		10/0/0	10
	Erythrophagocytosis	Multifocal		2/0/0	2
	Follicular hyperplasia	Focally extensive		2/0/0	2
	Adenitis	Multifocal	Draining foamy histiocytosis	0/1/0	1
		Multifocal	Necrotizing, granuloma-forming, mixed*	0/0/1	1
Kidney (16)	Interstitial nephritis	Multifocal	Lymphoplasmacytic	10/3/0	13
	Tubular ectasia with proteinosis or granular casts	Multifocal		5/0/0	5
	Intracellular pigment (tubules)	Multifocal		2/1/0	3
	Infarction	Focally extensive		2/0/0	2
	Interstitial fibrosis	Multifocal		2/0/0	2
	Mineralization (tubules)	Multifocal		2/0/0	2

Wing (14)	Dermatitis	Perifollicular and follicular	Neutrophilic, eosinophilic	0/4/8	12
		Perivascular to interstitial	Lymphoplasmacytic	4/0/0	4
			Ulcerative	1/2/1	4
			Histiocytic	1/0/0	1
	Acanthosis, Hyperkeratosis			3/5/4	12
	Fibrosis			0/5/7	12
Gingiva (11)	Gingivitis	Multifocal	Lymphoplasmacytic	4/1/0	5
			Neutrophilic	1/0/0	1
		Focal	Ulcerative	1/0/0	1
	Pustule, intraepithelial	Focally extensive	Neutrophilic	2/0/0	2
			Ruptured	1/0/0	1
	Fibrosis	Multifocal, focally extensive		4/2/0	6
Skeletal muscle (11)	Degenerative myopathy	Multifocal		5/0/0	5
	Regenerative myopathy	Multifocal		4/0/0	4
	Myositis	Multifocal	Lymphoplasmacytic	1/1/0	2
		Focal	Eosinophilic	1/0/0	1
		Multifocal	Histiocytic	0/1/0	1
Lymph node (other) (11)	Cellulitis	Focally extensive	Neutrophilic, mononuclear	0/2/2	4
	Increased phagocytosis	Multifocal		2/2/0	4
	Adenitis	Focally extensive	Neutrophilic, necrotizing	0/1/2	3
			Subcapsular foamy histiocytosis	1/0/0	1
	Draining hemorrhage	Focally extensive		3/0/0	3
	Fibrosis	Multifocal		1/1/0	2
	Mineralization (Germinal centers)	Multifocal		1/0/0	1
	Edema			0/0/1	1

Adrenal gland (9)	Cortical hyperplasia	Multifocal		4/0/0	4
	Intracellular pigment	Multifocal	Brown, finely granular	3/0/0	3
	Extramedullary hematopoiesis	Multifocal		2/0/0	2
Mammary gland (8)	Mastitis	Multifocal	Lymphoplasmacytic	7/0/0	7
			Necrotizing	0/0/1	1
	Fibrosis	Multifocal		1/0/0	1
	Hemorrhage			0/0/1	1
Nasal Turbinates (7)	Sinusitis	Focal to multifocal	Lymphoplasmacytic	7/0/0	7
Ear (6)	Dermatitis	Multifocal, external ear canal	Erosive (serocellular crusting)	5/1/0	6
Small Intestine (6)	Edema	Locally extensive		2/1/0	3
	Enteritis	Multifocal	Lymphoplasmacytic	2/0/0	2
		Multifocal	Mixed*	1/0/0	1
		Segmental	Eosinophilic	1/0/0	1
Colon (4)	Inflammatory cell infiltrates	Multifocal, Intestinal mucosa and lamina propria	Lymphoplasmacytic	3/0/0	3
	Edema	Multifocal, lamina propria		2/0/0	2
Pancreas (4)	Pancreatitis	Multifocal	Lymphoplasmacytic, mixed*	1/0/2	3
	Fibrosis	Multifocal		0/2/0	2
	Lymphoid hyperplasia	Focal		0/1/0	1
Pharynx (2)	Pharyngitis	Focal	Lymphoplasmacytic	1/0/1	2
			Histiocytic, necrotizing	0/0/1	1
Prostate (2)	Prostatitis	Multifocal	Cystic	0/1/0	1
			Lymphoplasmacytic	1/0/0	1
Adipose (1)	Steatitis	Focally extensive	Eosinophilic	0/1/0	1
Brain (1)	Perivascular cuffing	Multifocal	Lymphoplasmacytic	1/0/0	1
Cervix (1)	Cervicitis	Multifocal	Lymphoplasmacytic	1/0/0	1

Eye (1)	Inflammatory cell infiltrates	Multifocal	Lymphocytic	1/0/0	1
Heart (1)	Myocardial degeneration	Focally extensive		1/0/0	1
Thymus (1)	Mineralization	Multifocal		1/0/0	1
Tongue (1)	Glossitis	Focal	Foreign body	1/0/0	1
Trachea (1)	Tracheitis	Focally extensive	Lymphoplasmacytic	1/0/0	1
Uterus (1)	Endometritis, myometritis	Multifocal	Lymphoplasmacytic	0/1/0	1

Figure 3-10: Selection of macroscopic findings in free-ranging Egyptian rousette bats (*Rousettus aegyptiacus*) from Uganda. A) Laceration with circumferential fibrosis in the plagiopatagium of a juvenile male. B) Small laceration (thin black arrow) and fibrotic parasitic nodule (thin white arrow) in the dactylopatagium of a juvenile female. C) Fibrotic parasitic nodule (thin white arrow) and multifocal dermal fibrosis (black arrowhead) in the dactylopatagium of a juvenile male. D) Callused mid-diaphyseal fracture (thin black arrow) of the first phalanx of the fifth digit in an adult male. E) Multifocal ulcerative dermatitis (black arrowheads) in the pericervical region of an adult male. F) Four Nycteribiidae "bat flies" in the axillary region of an adult female. The upper limb and humerus are dorsally reflected.

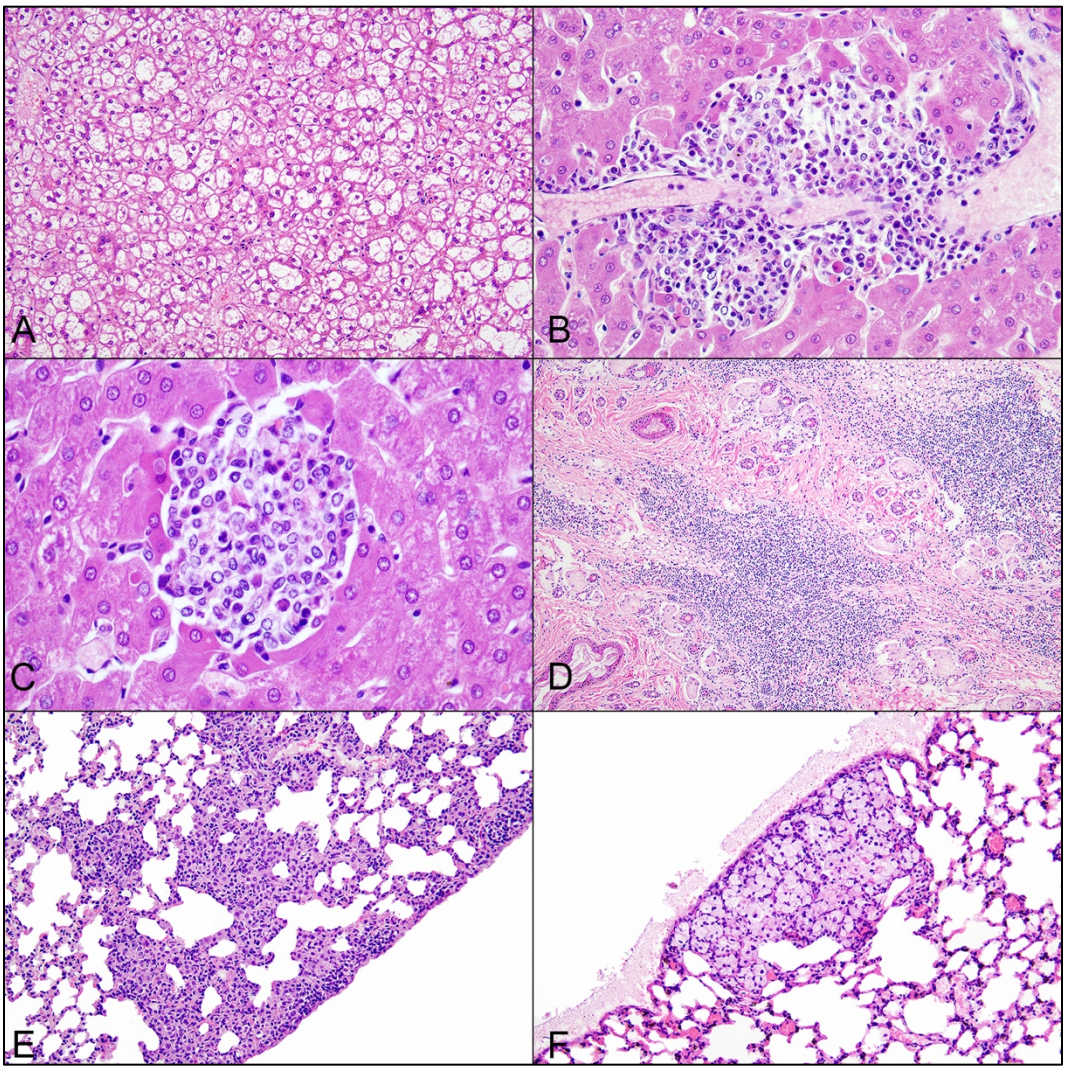

Figure 3-11: Pathologic histologic findings in the liver, dermis, and lung in Egyptian rousette bats (*Rousettus aegyptiacus).* A) Vacuolar degeneration, glycogen type, in the liver of an adult female. 20x, HE. B) Perivascular inflammatory focus composed of lymphocytes, plasma cells, macrophages, and few neutrophils, with hepatocellular necrosis, fibrin, and scant hemorrhage in the liver of a juvenile female. This ERB was MARV-RT-qPCR positive (spleen) at capture. 40x, HE. C) Inflammatory focus composed of lymphocytes, plasma cells, and macrophages in the liver of a juvenile female. This ERB was MARV-RT-qPCR positive (spleen) at capture. 60x, HE. D) High numbers of lymphocytes, plasma cells, macrophages, and fewer neutrophils dissect through superficial and deep dermal layers of the pelvis in a juvenile female. 10x, HE. E) Interstitial pneumonia in the lung of a juvenile male. Pulmonary septa are expanded by lymphocytes, plasma cells, macrophages, and rare neutrophils. 20x, HE. F) Subpleural focus of predominantly homogenous alveolar aggregates of foamy macrophages (endogenous lipid pneumonia) in the lung of an adult male. 20x, HE.

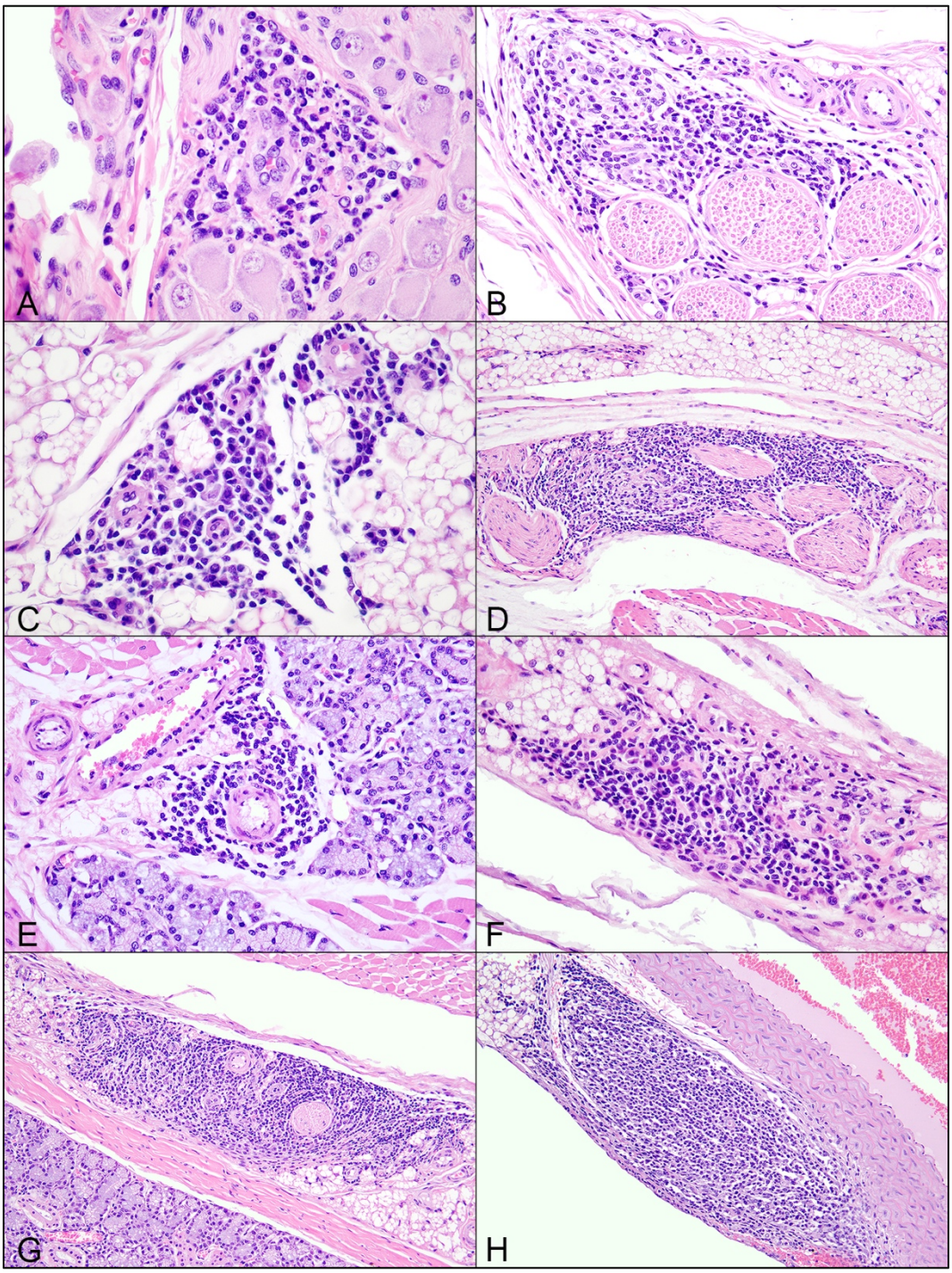

Figure 3-12: Systemic perivascular inflammatory aggregates in Egyptian rousette bats (*Rousettus aegyptiacus*). Perivascular aggregates of predominantly lymphocytes, plasma cells, and fewer macrophages in A) ganglia adjacent to the submandibular salivary gland, juvenile female, 60x, HE. B) ganglia in buccal subcutaneous adipose, juvenile male, 40x, HE. C) lingual adipose, juvenile male, 60x, HE. D) ganglia in caudal pelvic subcutaneous adipose, adult female, 20x, HE. E) perianal gland, adult female, 40x, HE. F) pelvic subcutaneous adipose, adult female, 40x, HE. G) adipose between orbicularis oculi muscle and parotid salivary gland, juvenile female, 20x, HE. H) adipose adjacent to aorta at heart base, juvenile male, 20x, HE.

Table 3-3: Organ locations and severity of perivascular cellular aggregates in free-ranging Egyptian rousette bats (*Rousettus aegyptiacus*) from Uganda. Variably sized perivascular aggregates composed predominantly of lymphocytes, plasma cells, and occasional histiocytes were present in one (15.9%; 11/69) or more (65.2%; 45/69) organs in 56 (81.2%, 56/69) ERBs.

Organ (# of bats)	Severity (Mild/Moderate/Severe)	Total Number
Adipose (48)	86/48/20	154
Nerves (26)	21/14/6	41
Tongue (10)	6/4/0	10
Heart (8)	6/2/0	8
Salivary tissue (3)	3/0/0	3
Kidney (2)	2/0/0	2
Liver (2)	2/0/0	2
Lung (2)	2/0/0	2
Wing (2)	2/0/0	2
Adrenal gland (1)	0/1/0	1
External Ear; ceruminous gland (1)	0/0/1	1
Great vessels (1)	1/0/0	1
Mammary gland (1)	1/0/0	1
Pancreas (1)	0/1/0	1
Teat (1)	1/0/0	1
Trachea (1)	0/1/0	1
Urinary bladder (1)	1/0/0	1

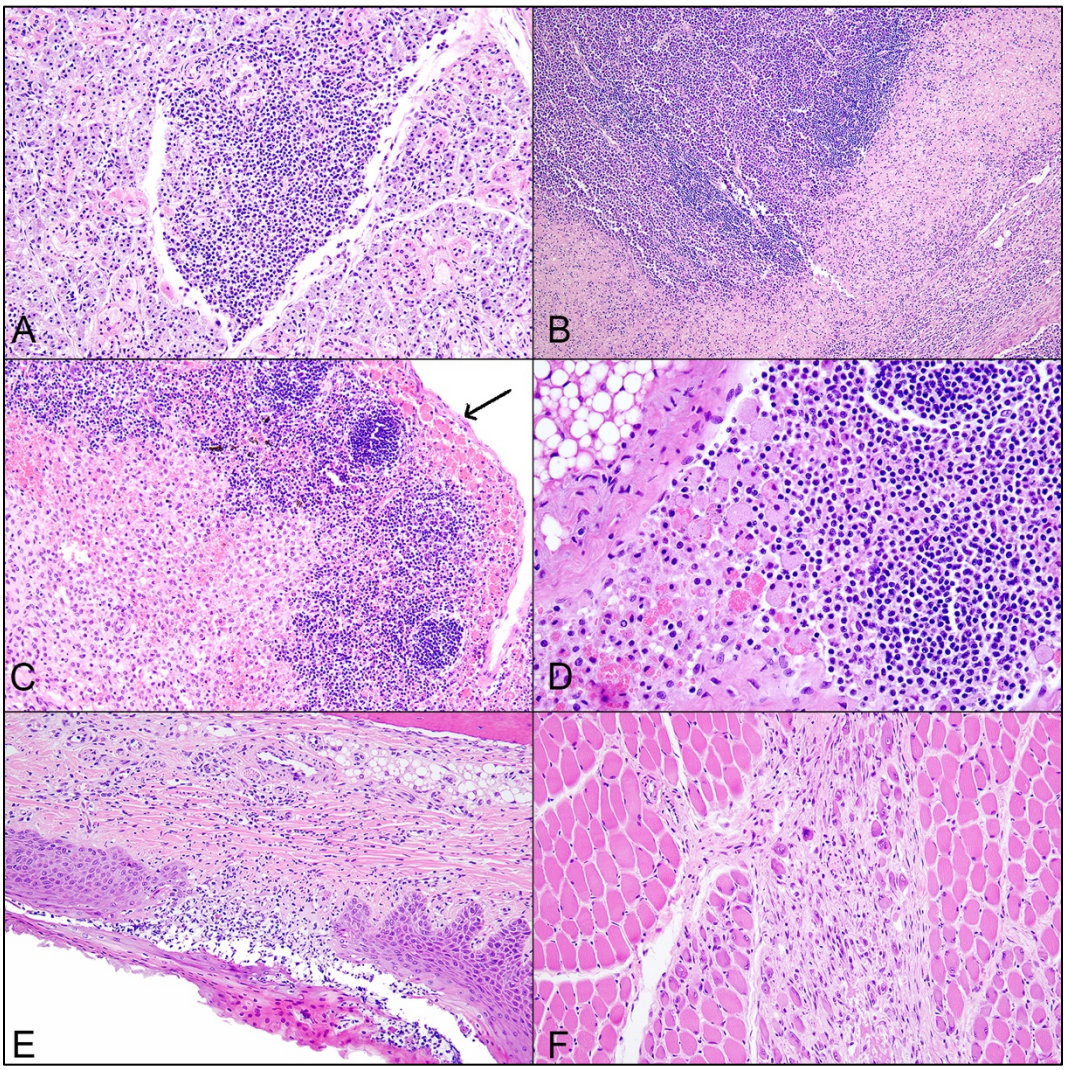

Figure 3-13: Pathologic histologic findings in the salivary gland, lymph nodes, gingiva, and skeletal muscle in Egyptian rousette bats (*Rousettus aegyptiacus).* A) Lymphoplasmacytic sialadenitis of the parotid salivary gland in a juvenile female. 20x, HE. B) Severe neutrophilic and histiocytic lymphadenitis and cellulitis with necrosis, obliterating lymph node and adjacent connective tissue parenchyma in a juvenile female. 10x, HE. C) Erythrocyte-laden macrophages expand the subcapsular sinus (thin black arrow), and numerous erythrocytes expand the cortex and paracortex in a juvenile male. 20x, HE. D) Subcapsular foamy histiocytosis in a lymph node of an adult female. 40x, HE. E) Focal ulceration and mucosal loss of the hard palette gingiva, with neutrophilic and histiocytic gingivitis and parakeratotic hyperkeratosis in a juvenile female. 20x, HE. F) Skeletal myocyte degeneration with regeneration, replacement fibrosis and infiltrating neutrophils and macrophages in a juvenile female. 20x, HE.

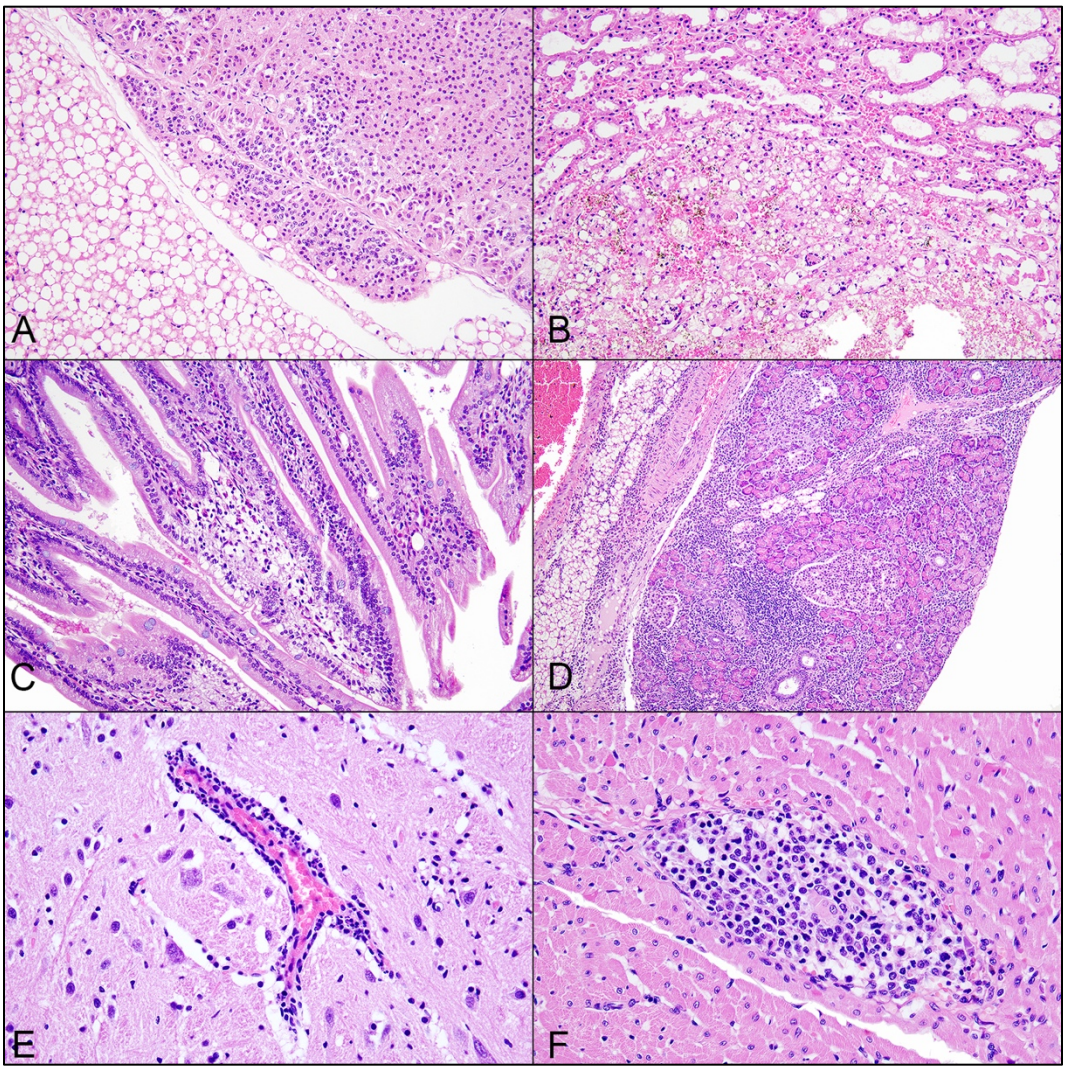

Figure 3-14: Pathologic histologic findings in the adrenal gland, mammary gland, small intestine, pancreas, brain, and heart in Egyptian rousette bats (*Rousettus aegyptiacus).* A) Adrenal cortical hyperplasia in an adult male. 20x, HE. B) Necrotizing mastitis with neutrophils, macrophages, multinucleated giant cells, and hemorrhage in an adult female. 20x, HE. C) Lymphoplasmacytic enteritis with villous edema and occasional neutrophils in a juvenile female. 20x, HE. D) Lymphoplasmacytic, histiocytic, and neutrophilic pancreatitis with necrosis in a juvenile male. 10x, HE. E) Lymphoplasmacytic perivascular cuffing in the brainstem of a juvenile female. 40x, HE. F) Lymphoplasmacytic and histiocytic cardiomyositis with scant hemorrhage in the left ventricle of a juvenile male. 40x, HE.

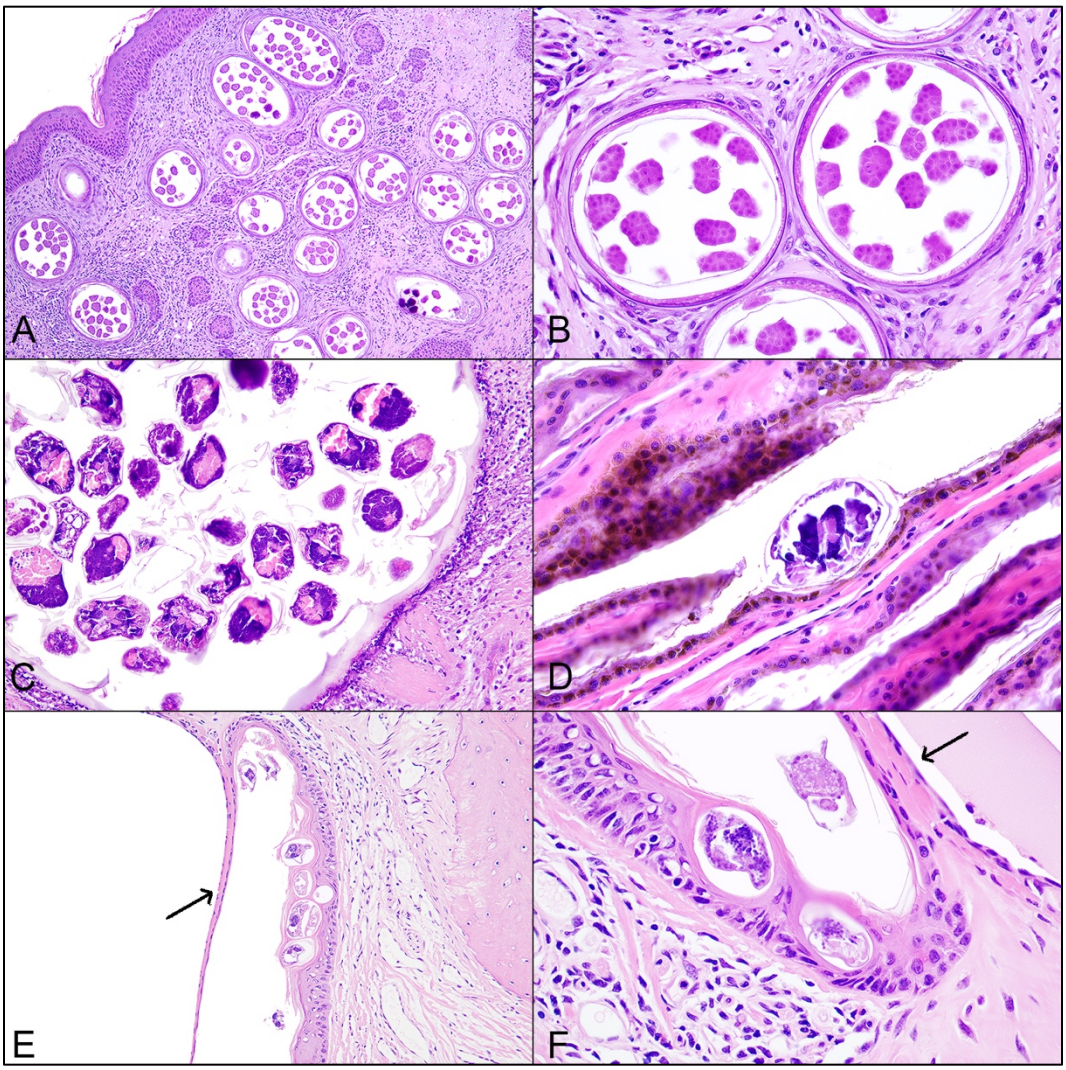

Figure 3-15: Ectoparasites in Egyptian rousette bats (*Rousettus aegyptiacus)* from Uganda. A) and B) Numerous multifocal, 150 – 300 µm parasitic cysts containing ~ 20 µm arthropod eggs expanding the subepithelial connective tissue of the wing membrane of a juvenile male. A) 10x, HE B) 40x, HE. C) 700 µm diameter parasitic cyst containing multiple, 60 - 90 µm arthropods (mites) expanding the subepithelial connective tissue of the wing membrane of a juvenile male. 20x, HE. D) Ovoid, 60 x 100 µm, arthropod (mite) within the stratum corneum of the wing membrane epithelium of a juvenile male. 40x, HE. E, F) Multiple, 25 – 45 µm arthropods (mites) with thin, ridged cuticles and striated musculature expanding the stratum corneum of the deep external ear canal. Mites are adjacent to the tympanic membrane (thin black arrow), within the deep external ear canal lumen of an adult female. E) 20x, HE. F) 60x, HE.

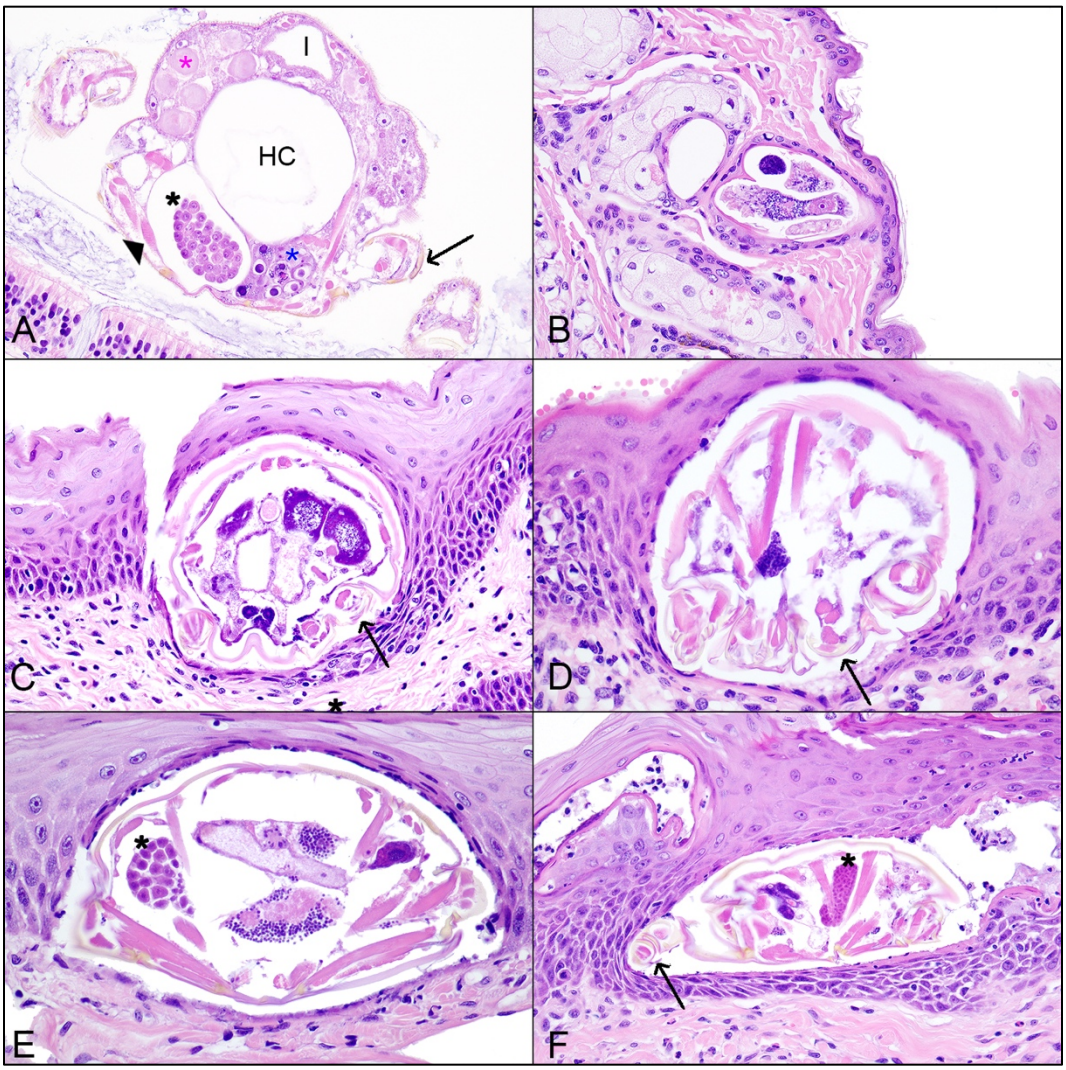

Figure 3-16: Selection of ectoparasites in Egyptian rousette bats (*Rousettus aegyptiacus)* from Uganda. A) 180 x 250 µm arthropod with chitinized appendages and cuticular spines in the nasal turbinate lumen of a juvenile female. Note the chitinous exoskeleton, dorsal spines, jointed appendages (thin black arrow), striated muscle (black arrowhead), body cavity (hemocoel, HC), and intestinal and reproductive structures. Single intestinal tube lined by flattened epithelium with an apical brush border (I), sperm (black asterisk), ovaries (pink asterisk) and developing eggs (blue asterisk). 40x, HE. B) 60 x 100 µm arthropod expanding the subepithelial adnexa of a juvenile male. 40x, HE. C – F) Arthropods with jointed appendages, striated muscle, and cuticular spines expanding the stratum corneum of C) cranial dermis of a juvenile female. 150 µm diameter. 40x, HE. D) perirectal dermis of a juvenile female. 130 µm diameter. 60x, HE. E) cranial dermis of a juvenile female. 105 x 185 µm. 40x, HE F) buccal mucosa of a juvenile female. 75 x 190 µm. 20x, HE.

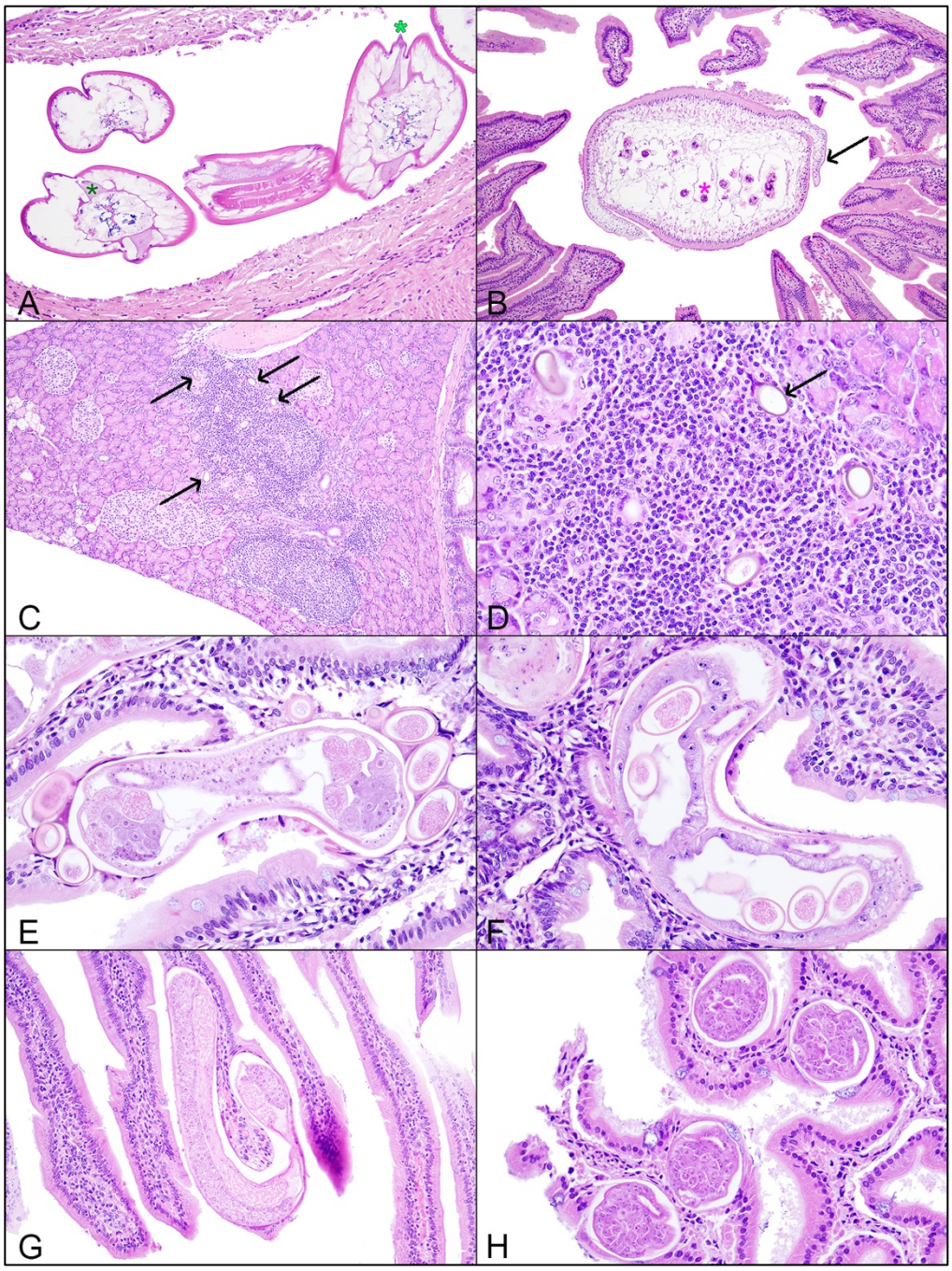

Figure 3-17: Selection of endoparasites in Egyptian rousette bats (*Rousettus aegyptiacus)* from Uganda. A) 175 x 200 µm larval ascarids with lateral alae (lime green asterisk), prominent lateral chords (forest green asterisk), and coelomyarian musculature within an 0.5 x 1.2 mm extragastric granuloma of an adult male. 20x, HE. B) Craspedote cestode with lateral vellum (thin black arrow) and central uterus with degenerate eggs (pink asterisk) in the small intestinal lumen of a juvenile male. 10x, HE. C) and D) Focally extensive section of lymphoplasmacytic and histiocytic pancreatitis with multiple trematode eggs (thin black arrows) with thick, yellow-brown shells in a juvenile male. C) 4x, HE. D) 20x, HE. G) Aphasmid nematode expanding a small intestinal villus of a juvenile male. 20x, HE. E) and F) Aphasmid nematode with multiple eggs with rare bipolar plugs expanding small intestinal villi in a juvenile female. 40x, HE. H) Cross sections of aphasmid nematodes expanding small intestinal villi of a juvenile female. 40x, HE.

CHAPTER 3C

HISTOLOGIC COMPARISON OF HEPATIC IRON OVERLOAD IN MANAGED CARE AND FREE-RANGING EGYPTIAN ROUSETTE BATS (ROUSETTUS AEYPGTIACUS)[4]

[4] Elbert JA, McHale B, Gottdenker NL, Burrell CE, McManamon R, Kirejczyk SG, Amman BR, Sealy TK, Atimnedi P, Towner JS, Howerth EW. Histologic comparison of hepatic iron overload in managed care and free-ranging Egyptian rousette bats (Rousettus aegyptiacus). Veterinary Pathology. 2025:03009858251352580.

ABSTRACT

Iron overload is a leading cause of morbidity and mortality in Egyptian rousette bats (ERBs; *Rousettus aegyptiacus*) within managed care settings. We compared hepatic iron accumulation and tissue damage in samples collected from managed care bats in a zoo setting, a research colony, and a free-ranging population with the goal of determining if iron overload was a potential cause of morbidity for free-ranging ERBs. Livers from 20 zoo bats, 8 research colony bats, and 69 free-ranging bats were histologically evaluated for fibrosis, necrosis, and iron accumulation in hepatocytes and Kupffer cells. Hemochromatosis was identified only in the zoo population, with hemosiderosis identified in all research colony bats and many free-ranging bats. There were statistically significant associations between age classification, population, and diagnosis and between Marburg virus infection status and histologic liver iron scores. Additionally, there were positive associations with statistical significance between age class (juvenile, adult) and histologic iron scores and between population type (zoo bats > research colony bats > free-ranging bats) and histologic iron scores. Excessive hepatic iron storage does not appear to be a source of morbidity within free-ranging Egyptian rousette bat populations.

KEYWORDS: Egyptian rousette bat, *Rousettus aegyptiacus*, iron, iron overload, liver, hemochromatosis, hemosiderosis

INTRODUCTION

The Egyptian rousette bat (*Rousettus aegyptiacus*; ERB) is a species of pteropodid bat (order Chiroptera, family Pteropodidae) that inhabits parts of Africa, the

Middle East, the Mediterranean, and the Indian subcontinent. One of the few pteropodid bats capable of echolocation, they are predominantly cave-dwelling, gregarious, and social animals that live in densely-packed roosts.[9] Due to their endearing physical characteristics and success in managed care environments, ERBs are commonly found in zoo collections throughout the world. ERBs in managed care environments are commonly afflicted with iron overload (IO), which is also reported in the literature as iron storage disease or iron overload disorder.[161,174,175]

Dysregulation of iron homeostasis and subsequent IO is a cause of hepatocellular damage and increased mortality, and has been described in humans as well as in numerous exotic species in managed care settings, including ERBs.[161,176] In animal species, a histologic distinction is made between hemochromatosis, which is increased iron storage with concurrent cellular injury, such as necrosis and fibrosis, and hemosiderosis, or increased iron storage without pathologic change. In humans, hemochromatosis is caused by several genetic disorders, the majority of which result in loss-of-function mutations in regulatory components of hepcidin synthesis.[189,190] Hepcidin is an important liver-derived iron regulatory hormone and negative regulator of iron absorption from the gastrointestinal tract and iron release from bone marrow stores. In response to plasma iron levels, hepcidin binds its ligand, the cellular iron export protein ferroportin. This results in internalization and degradation of the protein and subsequent down-regulation of iron absorption and inhibition of iron release from bone marrow stores, macrophages, and hepatocytes.[189] Although ERBs may have a diminished ability to upregulate hepcidin expression during dietary iron excess, the pathophysiology of IO in bats has not been determined.[174,191] ERBs are frugivorous bats that feed on soft

pulpy fruits such as figs, mangoes, and dates. Dietary factors such as high levels of ascorbic acids and lower levels of tannins and phytates, which enhance and reduce iron bioavailability, respectively, are theorized to play a role in inappropriate iron accumulation.[9,192] Iron accumulation in ERBs is most prevalent in the liver and spleen, with iron additionally detected in the pancreas, kidney, skeletal muscle, and lung.[161] Iron's role as a risk factor and its involvement in the pathogenesis of hepatocellular carcinoma have been explored in human studies.[193] However, further research is necessary to determine whether iron accumulation serves as the primary driver of liver carcinogenesis. A recent case series investigating a mortality event in managed Leschenault's rousette bats (*Rousettus leschenaultii*) found that 86% (6/7) had concurrent IO and neoplasia.[194] ERBs with hemochromatosis are significantly more likely to develop hepatocellular carcinoma versus those with hemosiderosis.[161]

Iron metabolism and accumulation can play a role in infectious disease, with some viruses being able to alter iron homeostasis either via manipulating cellular processes (hepatitis C virus, human immunodeficiency virus-1, human cytomegalovirus) or by using the host protein transferrin receptor 1 to gain entry into cells (New World hemorrhagic arenaviruses, canine and feline parvoviruses, mouse mammary tumor virus).[174,195] In vitro administration of iron chelators in infected cells with human immunodeficiency virus-1, human cytomegalovirus, vaccinia virus, herpes simplex virus 1, or hepatitis B virus curbs viral growth.[195]

ERBs are well-known for their role as a natural reservoir for Marburg virus (MARV), an RNA virus in the family *Filoviridae*. MARV is closely related to Ebola virus and causes severe hemorrhagic fever in humans and non-human primates. Infection

is characterized by person-to-person transmission and case fatality rates as high as 90%.[3,46,267] As of 2024, 85% of human MARV spillover events occurred during seasonal pulses of older juvenile (5-7 months) ERBs emerging from caves, which may elucidate a "perfect storm" of ERB infection permissiveness in which weaned juveniles lack maternal antibodies, are susceptible to horizontal transmission of infectious disease within the densely packed roost, and lack immunologic maturity to temper viral reproduction and subsequent shedding.[3,46] In order to determine if iron overload was a potential cause of morbidity in free-ranging ERBs, we compared hepatic iron accumulation and tissue damage in samples collected from managed care bats in a zoo setting, a research colony, and a free-ranging population.

MATERIALS AND METHODS

The electronic pathology records for all bats (order Chiroptera) submitted to the Zoo and Exotic Animal Pathology Service (ZEAPS) at the University of Georgia College of Veterinary Medicine from January 1, 2008, to July 7, 2023, were retrieved for analysis and then limited to case submissions representing Egyptian rousette bats (ERB; *Rousettus aegyptiacus*) (n = 20). Routine histology slides stained with hematoxylin and eosin (HE) and Perls' Prussian blue (PB) for iron were retrieved from the ZEAPS archives for evaluation. The age range of this population was 1-year to 14-years-old (adults = 20), with 13 males and 7 females. All zoo bats originated from the same zoo in the Upper Midwest, USA, with the population established in 2009 following a transfer from a zoo in the Southeastern USA. Information regarding the origin of the bats or any pathogen testing conducted at the time of population establishment at either location was not disclosed. Marburg virus testing on zoo ERB tissues was not completed at the time of

submission to ZEAPS, as these bats are presumed free of Marburg virus due to stringent import regulations and comprehensive screenings upon establishing a managed-care population. Comorbidities included (n=1 unless otherwise specified): Acute renal tubular degeneration, bronchioalveolar adenoma, cholangiocarcinoma, coalescing abscesses with mixed bacterial population, fibrinonecrotizing and pyogranulomatous bronchopneumonia, hepatocellular carcinoma, interstitial pneumonia (n=2), lenticular degeneration (n=2), lipoma, lymphocytic myocarditis, lymphoma, lymphoplasmacytic pneumonitis, myocardial necrosis, degeneration, and regeneration (n=2), myocyte atrophy, degeneration, regeneration (n=2), myofiber necrosis (n=2), neuroparenchymal hemorrhage, neutrophilic gastritis, neutrophilic and lymphoplasmacytic interstitial dermatitis, pulmonary edema (n=2), pulmonary fibrin thrombus, pulmonary fibrosis, purulent pyelitis with myriad gram-negative bacilli, pyogranulomatous lymphadenitis, splenic hematoma, and tracheal and pulmonary hemorrhage.

69 ERBs (juvenile = 49; adult = 20 [forearm length > 89 cm[3,441]]; male = 35; female = 34), were captured in Queen Elizabeth National Park in Uganda between August 2008 and November 2009 as part of Centers for Disease Control and Prevention filoviral surveillance efforts (CDC; Atlanta, Georgia 30329, USA). As previously described, all capturing, processing, and procedures were performed in accordance with an institutionally approved animal care and use protocol (animal use protocol 1731AMMULX approved by CDC Institutional Animal Care and Use Committee).[3,48] Bat collections were completed with the approval of the Uganda Wildlife Authority and following the American Veterinary Medical Association guidelines on euthanasia and the National Research Council recommendations for the care and use of laboratory

animals.[3,602,603] Whole blood and spleens were removed at the time of capture for Marburg virus quantitative reverse transcription polymerase chain reaction (RT-qPCR) (negative = 41; positive = 27; unknown = 1 (Unknown not included in statistical analysis)). RT-qPCR was completed as previously described.[48] Free-ranging ERBs were fixed whole and stored in 10% neutral-buffered formalin for up to 15 years. Post-mortem examinations were completed in 2023. Tissues (heart, trachea, lungs, lymph nodes, liver, kidney, adrenal gland, tongue, gingiva, esophagus, stomach, pancreas, small and large intestines, haired skin, plagiopatagium, salivary gland, adipose, thymus, thyroid, bone marrow, ear canal, eyes, nasal turbinates, peripheral nerves, skeletal muscle, male and female reproductive organs, and brain) were processed, paraffin-embedded, and stained with HE for histologic examination. Histologic findings included endo- and ectoparasitism (n=39), mild adrenal cortical hyperplasia (n=4), mild lymphoplasmacytic gingivitis (n=5), sialadenitis (n=24), colitis (n=3), interstitial nephritis (n=13), mastitis (n=7), and dermatitis (n=40), and mild to moderate, multifocal lymphohistiocytic hepatitis (n=51). PB staining was performed on liver sections. As all spleens had been previously removed for RT-qPCR testing at the time of capture, they were not available for histologic examination.

HE and PB staining was completed on previously formalin-fixed paraffin-embedded tissues from eight ERBs from the research colony at CDC. These bats (5-7 months old; juvenile = 6; adult = 2; male = 5; female = 3) had been negative control animals in previous CDC studies and came from a closed orthomarburgvirus-free breeding colony founded from free-ranging ERBs imported from Uganda in 2011.[4] To maintain consistency with the aging parameters used for the free-ranging Uganda ERB

population, two research colony ERBs (5-7 months old) were classified as adults due to having >89 cm forearm length.[3,441] These ERBs had no concurrent comorbidities.

Sections of liver were examined for necrosis, fibrosis, and iron accumulation in hepatocytes and Kupffer cells using a grading scheme adapted from Farina et al.[175] (Tables 3-4 and 3-5). Iron was identified in hepatocytes and/or Kupffer cells and characterized as fine to coarse intracellular granules that appear brown to gray in HE and blue in PB sections. Liver was classified as having no demonstrable iron, hemosiderosis (accumulation of iron without evidence of tissue damage), or hemochromatosis (severe iron accumulation with concurrent tissue damage), with further classification of mild, moderate, or severe.

Descriptive statistics were performed on all ERBs. A contingency table using Fisher's exact test compared categories (age, population, diagnosis) to determine if relationships existed between age class and diagnosis. A Wilcoxon rank sum test was used to evaluate associations between age and histologic iron scores and MARV infection status and histologic iron scores. A Kruskal-Wallis test was used to determine statistically significant associations between population type (free-ranging, research colony, zoo) vs histologic iron scores, and to calculate significant differences between the medians of each group. These group-histologic iron score relationships were further evaluated using Wilcoxon signed-rank test with Bonferroni correction for pairwise comparisons between each population and histologic iron scores. As many of the free-ranging ERBs had no demonstrable iron (functionally a value of zero), a hurdle model using both the truncated Poisson model and the binomial model were used to explore the overall relationship between histologic iron scores and MARV infection status. Statistical

analyses were conducted in R (R version 4.3.2, (R Core Team (2023). R: A Language and Environment for Statistical Computing. R Foundation for Statistical Computing, Vienna, Austria. https://www.R-project.org).

RESULTS

Livers from 20 zoo bats, 8 research colony bats, and 69 free-ranging bats were histologically evaluated for fibrosis, necrosis, and iron accumulation in hepatocytes and Kupffer cells. Mild to moderate hemosiderosis was present in 28 (40%) of the free-ranging ERBs (Fig. 3-18a, b), which suggests that iron accumulation in this species is not limited to managed care populations. Moderate hemosiderosis was present in 8 (100%) of the research colony ERBs (Fig. 3-18c, d), which was a surprising finding given their age classification (5-7 months). Hemochromatosis was identified only within the zoo population and represented 65% (13/20) of the evaluated population (Fig. 3-18e-h, Table 3-6). Of the 13 zoo ERBs diagnosed with hemochromatosis, one had a concurrent hepatocellular carcinoma, and another had a concurrent cholangiocarcinoma. For all populations, iron accumulation was frequently zonal, accumulating most frequently in periportal hepatocytes, but random speckling of iron accumulation in midzonal or centrilobular hepatocytes without periportal presence was occasionally seen.

There was a statistically significant association between age classifications (Fisher's exact test, $p<0.001$) as well as a significant association between population (free-ranging, zoo, research colony) and diagnosis (no demonstrable iron, hemosiderosis, and hemochromatosis) (Fisher's exact test, $p<0.0001$) (Fig. 3-19). There was a statistically significant positive association between age classification and histologic iron score (Wilcoxon rank sum test, $W=1828.5$, $p<0.0001$) (Fig. 3-19), and population and

histologic iron (Kruskal-Wallis test, chi-squared=55.27, df=2, $p<0.001$) (Fig. 3-20). A post-hoc pairwise Wilcoxon test between groups with Bonferroni corrections showed significant differences between the histologic iron scores between all three groups: zoo bats vs. research colony bats ($p<0.01$), zoo bats vs. free-ranging bats ($p<0.0001$), and research colony bats vs. free-ranging bats, ($p<0.001$) with median iron score ranks as follows: zoo bats > research colony bats > free-ranging bats. Within the free-ranging population, there was a statistically significant association between MARV infection status and histologic iron scores (Wilcoxon rank sum test, W=795.5, p=0.002), with MARV-negative bats having a significantly higher median iron score than positive bats (Fig. 3-20). Using a hurdle model to interpret the overall relationship between histologic iron and MARV infection status, the coefficients for MARV-positive ERBs in both the truncated Poisson model (β=-0.6073, SE 0.4958, z=-1.225, p=0.221) and the binomial model were negative (β=-1.2480, SE=0.6784, z=-1.840, p=0.066). The negative association between MARV infection status and the likelihood of observing a zero count of histologic iron scores in free-ranging bats implies that MARV-positive bats may be less likely to have higher iron scores compared to MARV-negative bats, but our sample size is limiting. Further investigation with larger sample sizes or additional data sources, or additional experimental studies may clarify the relationship between MARV infection status and iron scores in bats. Among older juvenile bats (5-7 months), the research colony had statistically significant higher histologic iron scores compared to the free-ranging bats (Wilcoxon Rank sum test, W=43, $p<0.0001$). There was no statistically significant association between sex and histologic iron scores (data not shown). It is important to note that all zoo bats were adults, which skews the data to the left.

ERBs are thought to live up to 2 years in the wild vs. up to 25 years in managed care settings.[9,46] Due to the lack of predation, abundant nutrition and excellent veterinary care provided in managed care settings, it is assumed that on average, the ERBs in managed care settings are older than free-ranging bats. A longer lifespan and subsequent progressive alimentary exposure to iron sources over time may contribute to the development of hemochromatosis, as hemochromatosis was only identified in the zoo population (Fig. 3-19).

While lifespan may play a role, the young age of the research colony ERBs and amount of iron accumulation suggests that age is not the lone factor. Dietary levels of iron are recommended to be <100 ppm dry matter basis to prevent IO.[529] This is difficult to achieve, in part due to iron contribution from other minerals such as dicalcium phosphate.[529] Research colony bats are fed chopped bananas, cantaloupe, seedless grapes, apples, and pears dusted with Lubee Fruit Bat Supplement (HMS Zoo Diets Inc, Bluffton, IN 46714, USA). The most recent trace mineral analysis of Lubee Fruit Bat Supplement contained 170 ppm dry matter basis of iron, which is thought to be from the supplement's calcium source (B. Pope, Lubee Bat Conservancy, personal communication). Both research colony and zoo bats are provided water ad libitum, and research colony bats are additionally provided fruit nectar. For both groups, liquids are provided in steel bowls. Numerous studies have shown that iron leaches from stainless steel into water and juices, and as such chronic exposure to leached iron via water and fruit juice is another possible source of iron exposure.[604,605] Other sources might include metal skewers used to hang fruit in zoo enclosures to encourage natural feeding behaviors and environmental enrichment.

Iron may also be present in municipal water used in maintenance of husbandry enclosures for all managed-care bats. The National Secondary Drinking Water Regulations established by the U.S. Environmental Protection Agency limits iron contaminant levels as 0.3 mg/L. However, National Secondary Drinking Water Regulations are non-mandatory and are provided only as a guideline for public water systems because the contaminants included in these secondary regulations are not considered a risk to human health.[606] Iron levels are not reported in the DeKalb County Department of Watershed Management Drinking Water Quality Report, which is the municipal water source for the research colony at the Centers for Disease Control and Prevention.[607]

The discovery of hepatic iron accumulation in the free-ranging ERB population may indicate a genetically determined affinity for increased iron absorption, possibly driven by evolutionary pressures to conserve micronutrients due to limited dietary iron or fluctuating environmental availability. An interesting finding in the current study was the negative association between MARV infection status and hemosiderosis within the free-ranging population. This could be due to a possible hepatoprotective mechanism of hepcidin upregulation during MARV infection. For example, a recent ERB experimental study found a >8 fold increase in hepcidin expression following MARV infection, as well as alterations in other genes that regulate iron homeostasis, such as ceruloplasmin and ferritin.[267] Hepcidin regulates iron homeostasis by binding ferroportin, a transmembrane protein that exports iron from enterocytes, macrophages, and hepatocytes into the bloodstream.[191,267] This binding causes the internalization and degradation of ferroportin, thereby reducing iron efflux and lowering serum iron levels.[191,267]

While hepatic iron accumulation was present in free-ranging ERB populations, IO does not appear to be a cause of morbidity for free-ranging ERBs, which is seen in ERBs in managed care. Future research is needed to elucidate mechanisms by which ERBs so successfully accumulate iron, and if hepatic iron accumulation confers a protective effect against MARV infection.

Table 3-4. Histologic iron grading scheme adapted from Farina et al.[175] Grading based on the distribution of intracytoplasmic iron and number of necrotic cells within 10 high-powered fields (HPF; 2.37 mm^2) and fibrosis. HE, hematoxylin and eosin; PB, Perls' Prussian blue.

	Iron Accumulation Hepatocytes (HE, PB)	**Iron Accumulation Kupffer Cells (HE, PB)**	**Hepatocellular Necrosis (HE)**	**Fibrosis (HE)**
Grade 0	No stainable iron in hepatocytes	No stainable iron in Kupffer cells	No necrotic hepatocytes in 10 HPFs	No identifiable increase in collagen within portal regions
Grade 1	Few fine periportal to diffuse iron granules within hepatocytes (<10 cells per 10 HPF)	Occasional or low numbers of Kupffer cells containing fine and/or coarse iron granules (<10 cells per 10 HPF)	Few necrotic hepatocytes (<10 cells per 10 HPFs)	Increased collagen expanded portal regions
Grade 2	Moderate to numerous fine iron granules in most cells and rare coarse iron granules (11-20 cells per 10 HPF)	Moderate numbers of Kupffer cells containing fine and/or coarse iron granules (11-20 cells per 10 HPF)	Moderate numbers of necrotic hepatocytes (11-20 cells per 10 HPF)	Increased collagen deposition extended to midzonal regions
Grade 3	Numerous fine iron granules in most cells and coarse iron granules in periportal cells and/or scattered within lobules (>20 cells per 10 HPF)	Coarse iron granules in most Kupffer cells +/- enlargement of the Kupffer cells (>20 cells per 10 HPF or cell	Large numbers of necrotic hepatocytes (>20 cells per 10 HPF) or coalescing foci of necrosis	Bridging fibrosis (connecting portal regions)

		aggregation/Kupffer cell aggregates)		

Table 3-5: Histologic iron scoring system. Histologic iron scored as the cumulative sum of all values: Iron accumulation in hepatocytes and Kupffer cells, hepatocellular necrosis, and fibrosis.

	Hemosiderosis Iron accumulation without necrosis or fibrosis	**Hemochromatosis Iron accumulation with necrosis and/or fibrosis**
Mild	1 or 2	8 or less
Moderate	3 or 4	9 or 10
Severe	5 or 6	11 or higher

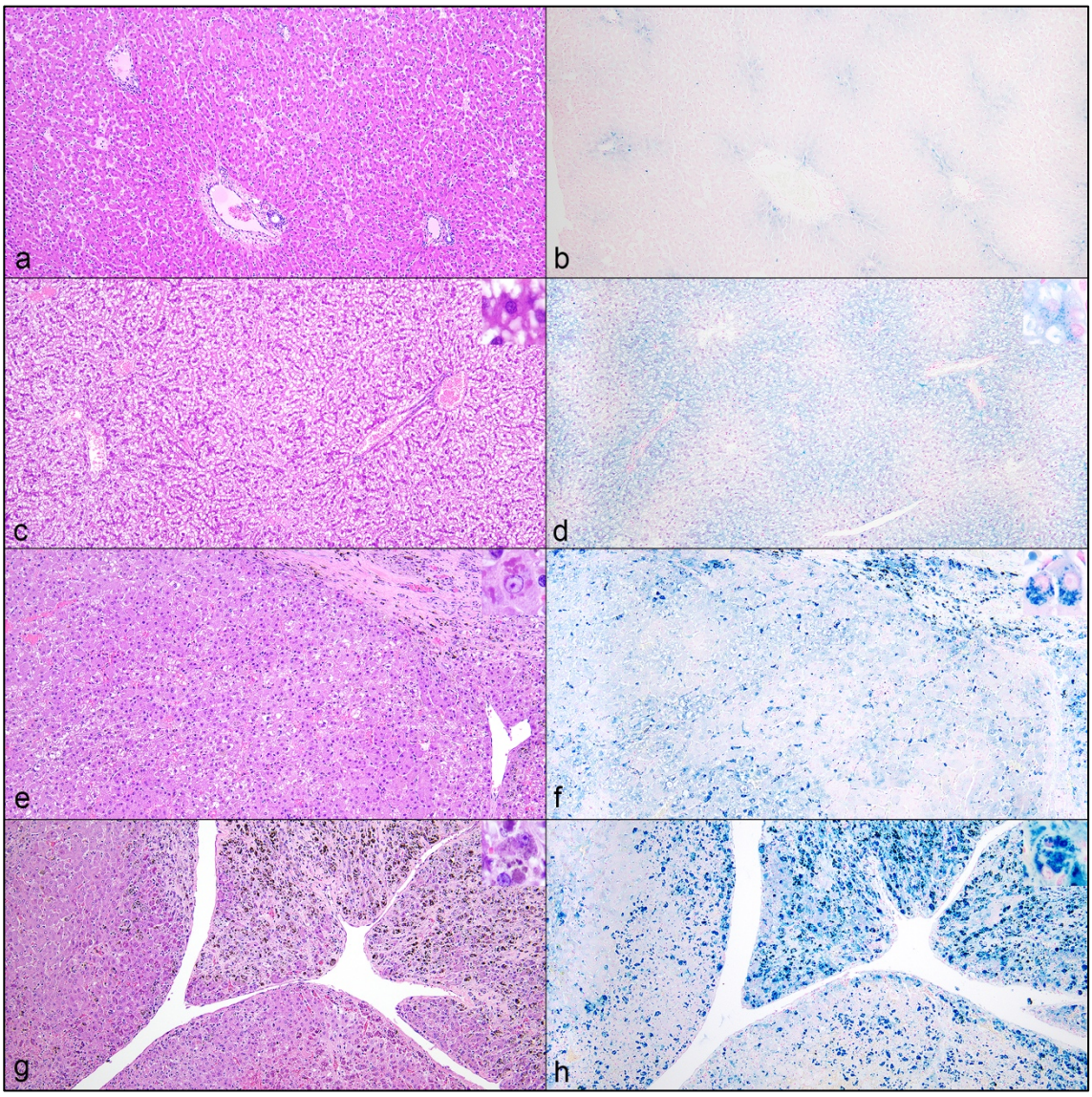

Figure 3-18: Histologic features of hepatic iron overload in four Egyptian rousette bats (ERB). (a, b) Liver from a free-ranging ERB with mild hemosiderosis. **a)** Finely granular, light brown staining consistent with iron accumulation. Hematoxylin and eosin (HE). **b)** Iron accumulation highlights the frequent periportal pattern. Perls' Prussian blue (PB). **(c, d)** Liver from a research colony ERB with moderate hemosiderosis. **c)** Hepatocytes contain prominent glycogenosis, which is a common incidental finding in ERBs. Inset: Indistinct, globular staining variations consistent with iron accumulation. HE. **d)** Iron accumulation is present in periportal and midzonal hepatocytes. Inset: Fine, teal blue iron granules. PB. **(e, f)** Liver from a zoo ERB with moderate hemochromatosis. **e)** Iron is finely granular and light brown with routine HE. The section contains bridging fibrosis, granular intracellular iron, and mild glycogenosis. Inset: Prominent iron granules. HE. **f)** Numerous fine iron granules are present in most cells along with rare coarse iron granules. Inset: Dense accumulation of fine and coarse iron granules. PB. **(g, h)** Liver from a zoo ERB with severe hemochromatosis. **g)** There is severe parenchymal damage with marked bridging fibrosis and finely granular and coarse intracellular iron. Inset: Fine and coarse, pink to gray/brown, iron granules. HE. **h)** There is marked iron accumulation with numerous fine and coarse iron granules in most cells within lobules. Inset: Marked fine and coarse iron granules. PB.

	No demonstrable iron		Hemosiderosis						Hemochromatosis					
			Mild		Moderate		Severe		Mild		Moderate		Severe	
Age	**J**	**A**	**J**	**A**	**J**	**A**	**J**	**A**	**J**	**A**	**J**	**A**	**J**	**A**
Zoo (n = 20)	0 (0%)	0 (0%)	0 (0%)	1 (5%)	0 (0%)	1 (5%)	0 (0%)	5 (25%)	0 (0%)	3 (15%)	0 (0%)	5 (25%)	0 (0%)	5 (25%)
Research Colony (n=8)	0 (0%)	0 (0%)	0 (0%)	0 (0%)	6 (75%)	2 (25%)	0 (0%)	0 (0%)	0 (0%)	0 (0%)	0 (0%)	0 (0%)	0 (0%)	0 (0%)
Free-ranging (n = 69)	34 (49%)	7 (10%)	7 (10%)	7 (10%)	8 (12%)	6 (9%)	0 (0%)	0 (0%)	0 (0%)	0 (0%)	0 (0%)	0 (0%)	0 (0%)	0 (0%)

Table 3-6: Histologic iron scores in zoo, research colony, and free-ranging Egyptian rousette bats. J = Juvenile, A = Adult.

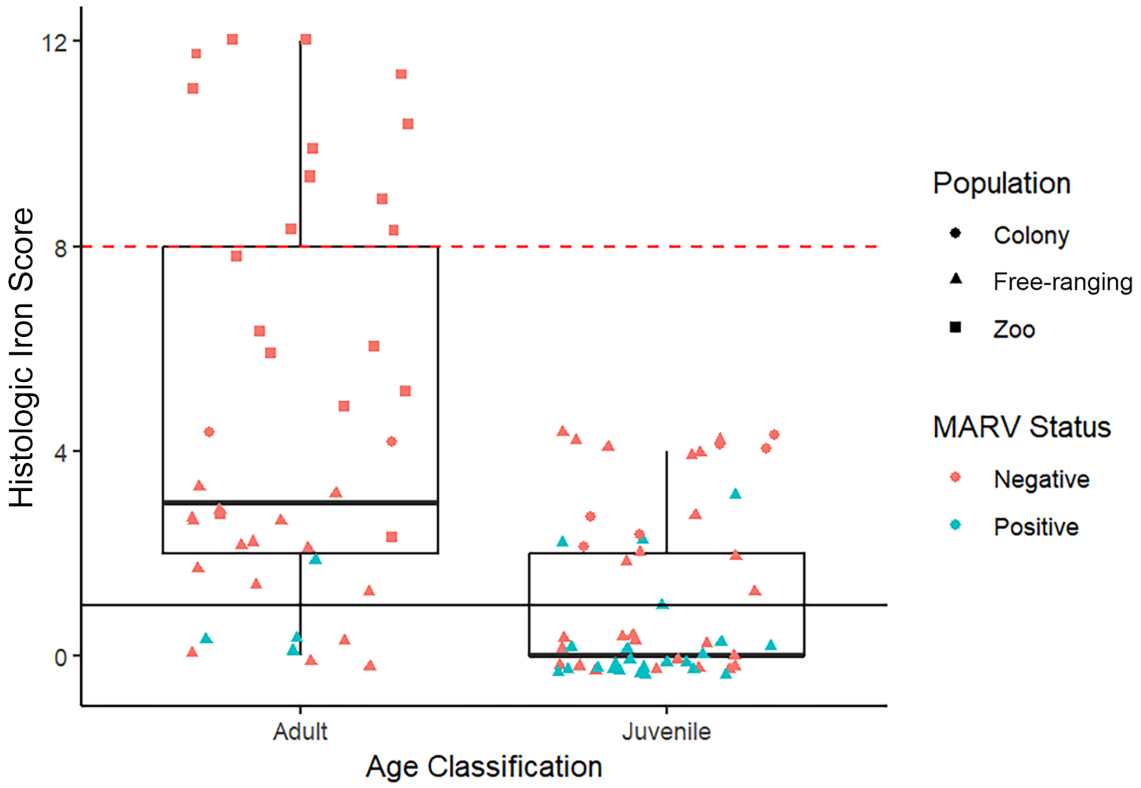

Figure 3-19: Comparison of histologic iron scores, age classifications, populations, and Marburg virus (MARV) infection status in Egyptian rousette bats. There was a significant association between age classification and population. Within the free-ranging population, there was a significant association between MARV infection status and to histologic iron, with MARV-negative bats having a significantly higher median iron score than positive bats. There was additionally a significant positive association between age classification and histologic iron score and between population and histologic iron score. The dashed line represents the distinction between hemochromatosis (above the dashed line) and hemosiderosis (below the dashed line and above the solid line). Statistical analyses were conducted in R.

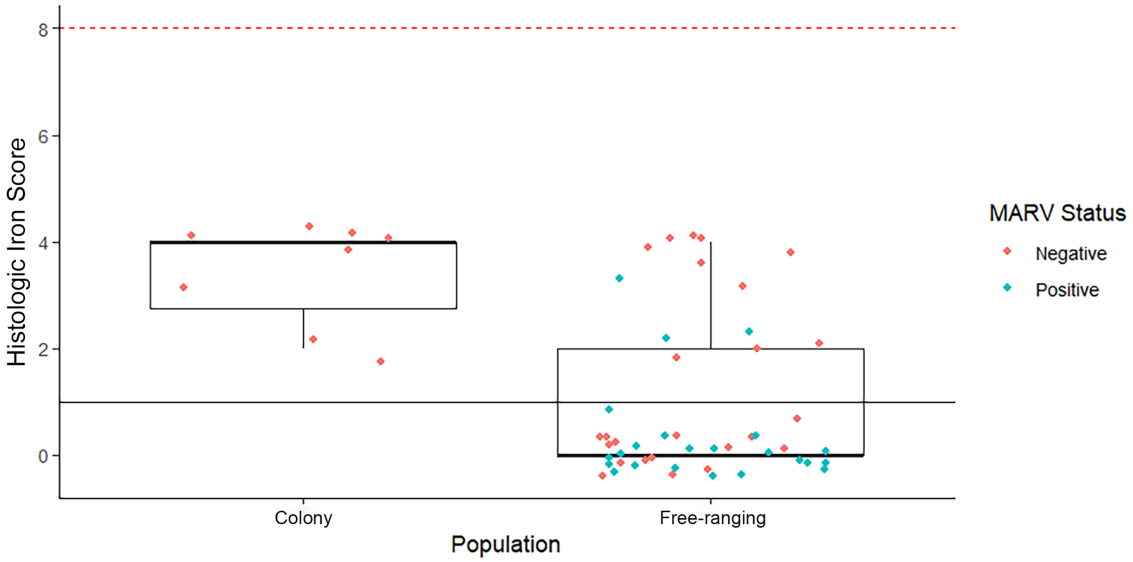

Figure 3-20: Comparison of histologic iron and population in juvenile Egyptian rousette bats. There was a positive association between population and histologic iron and, among juvenile bats (5-7 months), the research colony had higher histologic iron scores compared to the free-ranging bats. The red dashed line represents the distinction between hemochromatosis (above the dashed line) and hemosiderosis (below the red dashed line and above the solid black line). Statistical analyses were conducted in R. MARV, Marburg virus infection status.

CHAPTER 4A

CHARACTERIZATION OF RAVN VIRUS VIRAL SHEDDING DYNAMICS IN EXPERIMENTALLY INFECTED EGYPTIAN ROUSETTE BATS (ROUSETTUS AEGYPTIACUS)[5]

[5] Elbert JA, Schuh AJ, Amman BR, Guito JC, Graziano JC, Sealy TK, Howerth EW, Towner JS. Characterization of Ravn virus viral shedding dynamics in experimentally infected Egyptian rousette bats (Rousettus aegyptiacus). Journal of Virology. 2025 May 20;99(5):e00045-25

ABSTRACT

Marburg virus (MARV) and Ravn virus (RAVV), the only two known members of the species *Orthomarburgvirus marburgense (*family *Filoviridae*), are causative agents of Marburg virus disease, a severe viral disease that typically emerges in sub-Saharan Africa and is characterized by human-to-human transmission and high case fatalities. Despite robust characterization of MARV experimental infection in Egyptian rousette bats (ERBs; *Rousettus aegyptiacus*; common name Egyptian rousettes), a natural MARV reservoir, experimental infection with RAVV in ERBs has not been completed. Here, we experimentally infect 12 ERBs with RAVV and quantify viral loads in blood, oral swabs, and rectal swabs over a 21-day timeline, with serological and cumulative shedding data and baseline clinical parameters. Compared to previously described experimental MARV infection in ERBs, these bats experimentally inoculated with RAVV had significantly higher and prolonged rectal viral shedding loads, as well as significantly prolonged oral shedding and higher peak viremia. All ERBs seroconverted by 21 days post-infection. Additionally, all ERBs demonstrated marked heterogeneity in RAVV viral shedding loads consistent with the Pareto Principle and viral "supershedders". Our results introduce the possibility of variation in transmission dynamics and subsequent spillover differences between RAVV and MARV.

KEYWORDS: Egyptian rousette bat, *Rousettus aegyptiacus*, Marburg virus, Ravn virus, filovirus, virology, immunology

INTRODUCTION

Marburg virus (MARV) and Ravn virus (RAVV), viral relatives to Ebola virus, are the only two known members of the species *Orthomarburgvirus marburgense (*family

Filoviridae, genus *Orthomarburgvirus*) and are the causative agents of Marburg virus disease (MVD), a severe, often fatal disease that typically emerges in sub-Saharan Africa characterized by human-to-human transmission and high case fatality ratios up to 90%.[196] MARV was first identified in 1967 after laboratory workers in Marburg and Frankfurt, Germany and Belgrade (former Yugoslavia) became ill after working with African green monkeys imported from Uganda.[210] To date, there have been 18 known MARV outbreaks, the most recent of which occurred in Tanzania in January 2025.[608] RAVV was first identified in 1987 following a fatal VHF case in a tourist who visited Kitum Cave in Mount Elgon National Park, Kenya.[211] Designated as a distinct virus within the *Orthomarburgvirus marburgense* species in 1996, RAVV has since been identified in two subsequent outbreaks, with the most recent case reported in Uganda in 2007.[48,211,212] Although details about its natural distribution are limited, RAVV has only been detected in regions of Africa where Egyptian rousette bats (*Rousettus aegyptiacus,* common name Egyptian rousettes) are found.[96,213]

The Egyptian rousette bat (ERB) is a pteropodid bat (order Chiroptera, family Pteropodidae) that inhabits parts of Africa, western Asia, the Mediterranean, and the Indian subcontinent.[9] One of the few pteropodid bats capable of echolocation, they are predominantly cave-dwelling, gregarious and social animals, living in densely-packed roosts.[9] Numerous longitudinal ecological studies have identified the ERB as a natural reservoir host for both RAVV and MARV.[3,48,50,94-96] Adult ERBs had the highest IgG antibody levels, while juvenile bats (approximately 6 months old) showed the highest levels of active infection, along with a temporal association between MARV disease spillover to humans and seasonal, biannual pulses of active MARV infection in juvenile

ERBs.[3,46,48] MARV and RAVV have been isolated multiple times from ERBs sampled in Uganda.[3,48,93]

Despite being within the same viral species, the full genomic sequence of RAVV differs by up to 21% from MARV and the amino acid sequence of the RAVV glycoprotein (GP) differs by ~22% from MARV GP.[48,49] Bayesian coalescent analysis has estimated the most recent common ancestor (MRCA) between MARV and RAVV was approximately 700 years ago, with the known human and bat RAVV isolates sharing a MRCA approximately 50 years ago.[609] A phylogenetic tree highlighting a subset of complete MARV and RAVV genomes is provided in Fig. 4-1.

Experimental studies have identified the ERB as a competent natural reservoir model for MARV[4,45,50,243,244] and have also documented successful horizontal transmission of MARV between experimentally inoculated and naïve, co-housed ERBs.[46] ERBs experimentally inoculated with MARV have transient subclinical disease characterized by viremia (mean duration = 6.0 days, mean day of mean peak load = 6.8 DPI)[46], oral shedding (mean duration = 4.6 days, mean day of mean peak load = 9.1 DPI) with successful isolation of infectious MARV from 9/51 (17.6%) of MARV RT-qPCR-positive oral swabs[46], and rectal shedding (mean duration = 1.5 days, mean day of mean peak load = 6.8 DPI).[46] MARV shedding in the urine of experimentally infected ERBs has been documented but is limited by the challenging nature of non-invasive specimen collection and is not fully characterized.[4,46] In previous studies, MARV-inoculated ERBs robustly seroconverted to MARV, with MARV IgG antibodies peaking between 12 DPI and 28 DPI[4,46,244], followed by a decline of antibody levels falling below the threshold of seropositivity by 3 months post-infection.[46] Despite diminished IgG levels, robust

longstanding immunity to reinfection upon experimental inoculation with MARV has been documented in ERBs up to 2 years after initial infection.[47]

MARV has been well studied in numerous animal models and in vitro and in vivo experimental studies, including recent research utilizing transcriptomics to elucidate ERB immunology and responses to infection.[15,98,101,233,235,245-252] However, there has been limited experimental characterization of RAVV and of comparisons of virulence between RAVV and MARV. To date, the few studies utilizing RAVV include vaccine efficacy studies in cynomolgus macaques[253,254], mice[255] and guinea pigs[256], therapeutic treatment trials of MARV and RAVV infection in non-human primates with human monoclonal antibodies[257] and small interfering RNA[258], and characterization of the lack of observable clinical disease upon experimental inoculation with RAVV in ferrets[259,260]. Genetic variation between MARV and RAVV could influence transmission dynamics, pathogenicity, and potentially responses to treatments or vaccines. A recent study comparing experimental infection of different orthomarburgviruses in macaques found distinct pathogenicities between RAVV, MARV Angola, and variant isolates Musoke and Ozolin, and additionally found that, despite seroconversion in all animals, RAVV is lethal in cynomolgus macaques but not rhesus macaques.[261] Further, a comparison of the pathogenesis of RAVV, MARV variant isolates Musoke and Popp, and MARV Angola in a serially adapted outbred guinea pig model found delayed increases in circulating inflammatory and prothrombotic elements, lower viremia levels, less severe histologic disease, and a delay in mean time to death in RAVV infection compared to MARV Angola.[247] To date, experimental characterization of RAVV infection in its ERB reservoir has not been completed.

Here, we present an initial characterization of viral infection and shedding dynamics in ERBs experimentally infected with RAVV, with an aim to elucidate differences between RAVV and MARV and establish parameters for RAVV experimental infection in ERBs. We performed a 22-day experiment using 12 captive-bred, age- and sex-matched ERBs, subcutaneously inoculated with a low-passage (P2) wild-type RAVV (188Bat2007) isolated from a naturally infected bat in Uganda.[48]This work provides an important baseline for hypothesis-driven research, allowing successful extrapolation of research findings in controlled laboratory settings to wild ERB populations and enabling experimental comparisons between MARV and RAVV infections. Additionally, this work furthers the continued validation of the only established reservoir model for any filovirus.

MATERIALS AND METHODS

Animals and Biosafety

All experimental procedures were conducted with approval from the Centers for Disease Control and Prevention (CDC, Atlanta, Georgia, USA) Institutional Animal Care and Use Committee, and in strict accordance with the Guide for the Care and Use of Laboratory Animals (Committee for the Update of the Guide for the Care and Use of Laboratory Animals 2011). The CDC is a fully accredited research facility by the Association for Assessment and Accreditation of Laboratory Animal Care International. No recombinant or human patient-derived clinical materials were used in these studies.

Procedures conducted with infectious RAVV or infected bats were performed at the CDC under biosafety level 4 (BSL-4) laboratory conditions in accordance with Select Agent regulations (Animal and Plant Health Inspection Service and Centers for Disease

Control and Prevention 2014). All investigators and animal handlers followed strict BSL-4 safety and infection control practices.[610]

A total of 12 adult captive-born[4] ERBs (12-14 months old; six males and six females) were used in this study. The bats were housed in groups of six separated by sex in designated experimental and control caging (interior dimensions 61x71x76 cm long, wide, and high, respectively) in a climate-controlled BSL-4 laboratory animal room with a 12 h day/night cycle. The cages were housed within an isolation unit (Duo-Flow Mobile Units, Lab Products Inc., Seaford, Delaware, USA) with high efficiency particulate air-filtered inlet and exhaust air supply. The bats' daily food consisted of chopped bananas, watermelon, cantaloupe, seedless grapes, apples, and pears, dusted with a protein vitamin supplement (Lubee Bat Conservancy, Gainesville, Florida, USA).

Virus

Following the experimental design of a previous MARV study[46], 4 $\log_{10}$ 50% tissue culture infective dose ($TCID_{50}$) of a RAVV isolate (188bat2007 virus; second passage on Vero E6 cells), obtained from a naturally infected ERB (188bat) collected during a 2007 orthomarburgvirus outbreak ecological investigation at Kitaka Mine in southwestern Uganda, was prepared in 0.25 mL of sterile Dulbecco's modified Eagle's medium.[48]

Experimental Design

ERBs were acclimated in the BSL-4 laboratory for 7 days before the beginning of the study (acclimation phase). Baseline blood samples, body weights, and temperatures were recorded prior to inoculation. At 0 DPI, all 12 bats were inoculated subcutaneously under isoflurane anesthesia with the above-described RAVV inoculum in the caudal

abdominal region. As data from historical MARV control ERBs from previous studies was available, control ERBs were not utilized in this study. Blood samples, oral swabs, rectal samples, and temperatures were recorded daily; body weight was measured on 0 DPI, 7 DPI, 14 DPI and 21 DPI.

Specimen Collection

Specimen collection has previously been described in detail.[4,45,46] Blood (whole, nonheparinized; 10 and 21 mL for RT-qPCR and serology, respectively) was taken on -1 DPI and daily from 1-21 DPI from the cephalic wing vein using a sterile lancet (C&A Scientific, Manassas, VA, USA). Blood was tested for the presence of RAVV RNA by RT-qPCR through 15 DPI and RAVV IgG antibody responses were monitored weekly through 21 DPI. The oral mucosa was sampled daily through 21 DPI by swabbing the inside of the bat's mouth and cheeks using two polyester-tipped applicators (Fisher Scientific, Grand Island, NY, USA). After sampling, one oral swab was immediately placed in either a deep-well plate with 500 ml of MagMAX lysis buffer solution (Life Technologies, Grand Island, New York, USA) for RT-qPCR analysis and one oral swab was placed in sterile viral transport medium for attempted virus isolation of any RAVV RNA positive swabs. A temperature probe covered with a plastic sheath (MABIS Healthcare, Waukegan, Illinois, USA) was used to measure the daily rectal temperature of each bat. The plastic sheath was then cut and placed into a deep-well plate with 500 ml of MagMAX lysis buffer solution (Life Technologies) for fecal RT-qPCR analysis.

Euthanasia

At 22 DPI, all bats were euthanized under anesthesia via an overdose of isoflurane followed by cardiac exsanguination. Cardiac blood was collected and retained.

Nucleic Acid Extraction

Nucleic acid was extracted from blood, oral swab, and rectal probe covers using the MagMAX Pathogen RNA/DNA Kit (Thermo Fisher Scientific, Waltham, MA, USA) on the MaxMAX Express-96 Deep well Magnetic Particle Processor (Thermo Fisher Scientific, Waltham, MA, USA).

RT-qPCR

RT-qPCR procedures have been previously described in detail.[4,45,46] Reverse-transcribed RAVV and ERB beta-2-microglobulin (B2M) RNA were detected on the CFX Opus 96 Real-Time PCR System (Bio-Rad, Hercules, CA, USA) using the Luna Probe One-Step RT-qPCR 4x Mix with UDG (New England Biolabs Inc, Ipswich, MA, USA). The amplification utilized primers and reporter probes targeting the orthomarburgvirus viral protein 40 (VP40) gene (forward primer: GGACCACTGCTGGCCATATC, reverse primer: GAGAACATITCGGCAGGAAG, probe 1: 56-*FAM*-ATC CTA AAC-*ZEN*-AGG CTT GTC TTC TCT GGG ACT T-*3IABkFQ*, probe 2: 56-*FAM*-ATC CTG AAT-*ZEN*-AAG CTC GTC TTC TCT GGG ACT T-*3IABkFQ*) and the ERB B2M gene (forward primer: CAGCAAGGACTGGTCTTTCTAT, reverse primer: CCTCCATGATGCTGGTTAGTT, probe: *FAM*-TTC ACA CGG-*ZEN*-CAG CTG TAC TCA TCC-3*IABkFQ*), respectively. This assay was designed to detect a conserved sequence of VP40 present in all known species of orthomarburgvirus, including RAVV.[49] Relative RAVV $TCID_{50}$eq/mL (blood and oral specimens) were interpolated from standard curves generated from serial dilutions of the titrated 188bat RAVV spiked into appropriate biological specimens. Based on testing triplicate 10-fold serial dilutions of RAVV ranging from 5.8×10^6

$TCID_{50}$eq/mL to -1.12 x 10^6 $TCID_{50}$eq/mL, the lowest concentration of RAVV detected in all three replicates was 1.8 x 10^6 $TCID_{50}$eq/mL.

Virus Isolation and Immunofluorescence assay

Virus isolation and immunofluorescence assays have been previously described in detail.[4,45,46] Virus isolation was attempted on RT-qPCR-positive oral swab samples for orthomarburgvirus with CT values ≤ 32. Initially, monolayers of 85% confluent Vero E6 cells (American Type Culture Collection, CRL-1586) in 25 cm^2 tissue culture flasks were inoculated with 100 µL viral transport medium from wells containing the positive oral swabs, supplemented with 500 µL maintenance media (Dulbecco's Modified Eagle Medium containing 2%, heat-inactivated fetal bovine serum, 100 units/mL penicillin, 100 µg/mL streptomycin, and 2.50 µg/mL amphotericin B) and incubated for 1 h at 37 °C/5% CO_2. Subsequently, 7 mL of maintenance media was added, and cultures were further incubated under the same conditions. At 7 and 14 DPI, tissue culture monolayers were scraped to release virus-infected cells. Next, 1.5 mL of each cellular medium was suspended in 8 mL borate saline. After centrifugation to pellet the cellular suspensions, borate saline was decanted, and the cells were resuspended in 500 µL borate saline. Then, 25 µL of the cellular resuspensions was spotted onto 12-well spot slides, which were fixed in acetone and then exposed to 2 megarads of γ-irradiation.

All 7 and 14 DPI cultures were tested by immunofluorescence assay for orthomarburgvirus antigen. Spot slides were incubated with a 1:100 dilution of rabbit anti-MARV polyclonal (in-house) or normal rabbit serum (negative control; in-house) for 30 min at 37 °C. Slides were then rinsed twice with 1x PBS for 10 min, followed by incubation with 1:40 dilution of goat anti-rabbit fluorescein isothiocyanate (Capel-ICN

Pharmaceuticals, Aurora, OH, USA) for 30 min at 37 °C. After a 7 min rinse with 1x PBS, the slides were stained with Eriochrome Black T (in-house) for 7 min, followed by another 7 min rinse with 1x PBS. The slides were then observed under a fluorescence microscope.

Serology

As previously described[4,46,47], ELISA plates were coated with 50 ng per well of purified recombinant Marburg Angola NP or Reston NP expressed in *Escherichia coli* (GenScript, Piscataway, NJ, USA) diluted in PBS containing 1% thimerosal. Following an overnight incubation at 4 °C, the plates were washed with PBS containing 0.1% Tween-20 (PBS-T). A 1:100 dilution of gamma-irradiated bat whole blood in masterplate diluent (PBS containing 5% skim milk powder, 0.5% tween-20 and 1% thimerosal) was added to the first well, with subsequent fourfold serial dilutions in serum diluent (PBS containing 5% skim milk and 0.1% tween-20) performed through 1:6,400. After incubating for 1 h at 37 °C, the plates were washed with PBS-T and bound antibodies were detected using a 1:11,000 dilution of anti-goat bat IgG (Bethyl Laboratories, Montgomery, TX, USA) in serum diluent. Following a 1 h incubation with the secondary antibody at 37 °C, the plates were washed twice with PBS-T and the 2-Component ABTS Peroxidase System (KPL, Gaithersburg, MD, USA) was added. The substrate was allowed to incubate for 30 min at 37 °C before the plates were read on a microplate spectrophotometer at 410 nm.

To negate non-specific background reactivity, adjusted optical density (OD) values were calculated by subtracting the ODs at each fourfold dilution of wells coated with Reston NP from ODs at corresponding wells coated with MARV NP. The adjusted

sum OD value was then linearly transformed using the min-max normalization method. The seropositivity threshold was set at 0.07 after in-house assay optimization.

Data and Statistical Analyses

Statistical analyses were completed as previously reported.[46] Each comparator group comprised 12 bats. The number of bats per group was based on the reproductive capacity of the ERB breeding colony, the number of bats that could be safely handled daily, and the available space in the BSL-4 lab. Investigators were not blinded during the study, and no bats or individual data points were excluded from the analyses.

Excel (Microsoft 365, Redmond, WA) was used to manage data, and GraphPad Prism 10 (GraphPad, La Jolla, CA) was used to perform statistical analyses and generate figures. RAVV peak viral loads and the duration of viral shedding were determined for each bat according to sample type (blood, oral swab, and rectal swab). To assess RAVV infectiousness, cumulative viral shedding loads were calculated for each bat by summing viral loads detected in blood, oral swabs, and rectal swabs through the duration of the study. Using the approach of Jankowski et al.[611], bats were classified as supershedders if they shed RAVV at loads ≥ the 80th percentile. Raw data from Schuh et al.[46] were generously provided by the author for MARV statistical comparison.

The Shapiro-Wilk test was used to determine if peak viral load, duration of viral shedding, and cumulative viral shedding load datasets followed a normal or lognormal distribution. If datasets were normally distributed, then unpaired t-tests were used to determine if parameter means differed significantly between RAVV and MARV bat groups. If datasets were lognormally distributed, they were log-transformed before using unpaired *t*-tests to determine if parameter geometric means differed significantly between

RAVV and MARV bat groups. If datasets did not follow a normal or lognormal distribution, then non-parametric Mann-Whitney *U* tests were used to determine if parameter mean ranks differed significantly between RAVV and MARV bat groups. All *P* values are two-tailed and $P < 0.05$ is considered statistically significant. Each bat represents an individual biological replicate.

Results

RAVV replication and shedding dynamics

Prior to inoculation, none of the bats had detectable viremias (Fig. 4-2a) or anti-RAVV IgG (Fig. 4-3), indicating no prior exposure to RAVV. Viral RNA levels in blood (Fig. 4-2a), quantified through RT-qPCR analysis of viral RNA, and presented as mean $TCID_{50}$ equivalents per milliliter of fluid, were consistent with previous studies that characterized MARV infection and shedding dynamics.[4,46] RAVV viremia was detected in all 12 ERBs, with mean viral load values peaking on Day 5 (mean: $1.03x10^3$ $TCID_{50}$/mL; highest individual value: $3.65x10^3$ $TCID_{50}$/mL) and cleared by Day 13. The highest number of viremic ERBs was on 3-6 DPI (n=12 bats each day), with 79 positive viremic data points overall. The average length of detectable viremia was 6.6 days, ranging from 5 – 8 days. Blood samples for RT-qPCR were no longer collected after 15 DPI, following 3 consecutive days of negative RT-qPCR results from all bats.

RAVV RT-qPCR positive oral swabs were detected in all 12 ERBs, with mean viral load values peaking on 7 DPI (mean: $3.76x10^3$ $TCID_{50}$/mL; highest individual value: $3.33x10^4$ $TCID_{50}$/mL), and with sporadic RT-qPCR positivity through study completion at 21 DPI. The highest number of positive oral swab specimens was 7 DPI (n = 12), with 106 positive oral swab specimens overall. The average length of oral shedding was 8.8

days, ranging from 4 – 12 days. RT-qPCR-positive oral swab specimens with CT values ≤ 32 were selected for virus isolation; this represented 26 out of the 106 (24.5%) RAVV RNA positive oral swab samples, from 8 infected ERBs (451565, n=3 samples; 451575, n=6; 452033, n=2; 452049, n=5; 452065, n=1; 452121, n=4; 452235, n=3; 452455, n=2). Infectious RAVV was isolated from 20/26 (77%) samples.

RAVV RT-qPCR positive rectal swabs were detected in 11/12 (92%) ERBs, with mean viral load values peaking on 6 DPI (mean: $2.87x10^2$ $TCID_{50}$/mL; highest individual value: $2.46x10^3$ $TCID_{50}$/mL), and with sporadic RT-qPCR positivity through study completion at 21 DPI. Bat 451431 never had a RAVV-RT-qPCR-positive rectal swab, despite having positive oral swab and blood samples. The highest number of positive rectal swab specimens was at 6 DPI (n = 7), with 36 positive rectal swab specimens overall. The average length of rectal shedding was 3 days, ranging from 1 – 10 days. To avoid mucosal irritation or injury, duplicate rectal swab samples were not collected for isolation; therefore, isolation attempts on rectal swab samples were not performed.

Complete seroconversion in all bats

Consistent with previous studies[4,46,243,244,382], all ERBs demonstrated a robust primary immune response, with all inoculated bats (12/12) testing RAVV seronegative at 0 DPI and subsequently seroconverting to RAVV (mean peak adjusted sum optical density (OD)=0.28, s.d.=0.11; Fig. 4-3) by 21 DPI.

Heterogeneities in oral and rectal RAVV shedding

Heterogeneity in host shedding of pathogens plays an important role in infectious disease transmission dynamics and can be measured by assessing cumulative pathogen loads shed in excretory products of naturally or experimentally infected individuals[611-622].

Viral shedding was calculated for each inoculated bat by summing RAVV RNA loads detected 0-21 DPI in oral and rectal swabs. Total oral and rectal shedding varied considerably between individual bats, with sum $log_{10}TCID_{50}$ equivalents/mL ranging from 1.21 to 4.68 (mean=3.29, s.d.=0.91) and undetectable to 3.54 (mean=1.56, s.d.=1.03), respectively. As previously demonstrated[46], the Lorenz curve and associated Gini coefficient are effective at illustrating and quantifying inequality in a distribution, and herein are used to highlight heterogeneity in individual RAVV oral (Fig. 4-4a) and rectal (Fig. 4-4b) shedding. For example, Figure 4-4a demonstrates that 25.0% of the inoculated bats were responsible for 83.5% of RAVV oral shedding, 50.0% of the bats were responsible for 92.6% of oral shedding, and 75.0% of the bats were responsible for 99.2% of oral shedding. Figure 4-4b demonstrates that 25.0% of the inoculated bat population was responsible for 94.1% of RAVV rectal shedding, 50.0% of the bats were responsible for 98.9% of rectal shedding, and 75.0% of the bats were responsible for 99.8% of rectal shedding. Using a previously established approach[46,611], two inoculated bats (452121 and 452049) were classified as supershedders for both oral and rectal RAVV shedding, as both shed at levels greater than the 80th percentile (Oral = 4.18 $log_{10}TCID_{50}$ equivalents/mL; rectal = 2.64 $log_{10}TCID_{50}$ equivalents/mL, respectively) and together accounted for 69.4 and 89.2% of the total RAVV oral and rectal shedding, respectively. RAVV oral and rectal shedding was detected 12 and 10 times in bat 452121 and eight and six times in bat 452049, respectively. Infectious virus was isolated from four out of four (100%) oral swabs taken from bat 452121 and four out of five (80%) oral swabs taken from bat 452049.

No evidence of clinical disease

Consistent with previous MARV experimental studies in ERBs[4,46], no disease-related morbidity or mortality was observed in any of the ERBs and normal social and feeding behaviors were maintained. All bats maintained normal body weights and rectal temperatures, consistent with previous studies (Fig. 4-5).[4]

Discussion

This study provides the first measure of the shedding dynamics of experimental RAVV infection in ERBs, a natural reservoir host. Similar to MARV, RAVV reaches a viremic peak at approximately 5-6 DPI, with viral shedding peaking in oral secretions around 7 DPI and in fecal secretions around 6 DPI[4,45,46]. These findings suggest that RAVV, like MARV, is likely horizontally transmitted through direct and/or indirect contact with infected bodily fluids.[4,46] A recent study found that infectious MARV can persist on contaminated fruit spats for up to 6 h, providing an additional route of exposure to other animals, including other bat species or other susceptible animals hosts, such as non-human primates.[14]

A comparison between RAVV and MARV shedding dynamics can be drawn between the current study and that of Schuh et al.[46]. In Schuh et al.[46], 12 naïve ERBs were subcutaneously inoculated with an identical experimental dose (4 $\log_{10}TCID_{50}$) and route of MARV and underwent oral and rectal swab sampling over an identical timeline to the current RAVV study. While the infection timeline between MARV and RAVV is comparable, experimentally inoculated ERBs produce higher rectal RAVV shedding loads with a longer shedding duration compared to Schuh et al.[46], along with prolonged oral shedding and higher peak viremia (Fig. 4-2). This striking variation in rectal

shedding may elucidate why, in a recent surveillance study of rectal swab samples from ERBs in South Africa, only RAVV was detected out of 416 samples tested.[96]

It is currently unclear as to how these two orthomarburgviruses, RAVV and MARV, continue to circulate in free-ranging ERB populations yet remain genetically distinct. As mentioned earlier, the full genomic sequence of RAVV differs by up to 21% from MARV (Fig. 4-1), with the most notable variation (~22%) in the amino acid sequence of the RAVV glycoprotein (GP).[48,49] Investigation into generation of protective and cross-reactive monoclonal antibodies via exposure to engineered MARV GPs found that RAVV has 4 unique residues on the GP2 "wing", which is a 66 amino-acid N-terminal GP2 extension, when compared to other MARV variants.[623] Additionally, a recent study investigating the use of mRNA vaccines against MARV and RAVV, developed based on sequences of their respective GPs and glycan caps, found differences in antibody frequencies, antibody binding, neutralizing capacity and linear epitope recognition.[624] This suggests structural divergence between the GPs of distant orthomarburgviruses potentially affects stability, alterations, and/or the spatial location of domains.[624] These differences may contribute to the differences noted between RAVV and MARV shedding in this study.

Variations in viral GPs of other viruses can have significant implications for infection and pathogenicity.[625] For instance, a point mutation in the influenza C virus GP was found to increase receptor-binding efficiency.[626] Similarly, mutations within the hepatitis C virus E2 GP increased its affinity to its receptor and reduced the virus's sensitivity to neutralization.[627] An amino acid mutation in the GP of lymphocytic choriomeningitis virus (Clone 13 isolate) is thought to be responsible for the long-term

persistence of Clone 13 infections.[628] Additionally, six mutations generated in vitro at the interface of Ebola virus (EBOV) GP_1 and GP_2 resulted in confirmational changes rendered the virus independent of Cathepsin B, a protease required for EBOV cellular entry.[629] Substitutions in many conserved residues of the MARV GP led to significant defects in GP expression, incorporation into HIV virions, and the ability to mediate viral entry.[630] Furthermore, a naturally occurring polymorphism in the Sudan virus GP_1 decreased GP stability, therefore potentially affecting viral infectivity.[631] These findings underscore the critical role of glycoprotein variations in viral infectivity, stability, and immune evasion, highlighting their potential as targets for therapeutic intervention and possibly explaining the variation in fecal shedding dynamics observed thus far in ERBs experimentally infected with either RAVV or MARV.

Variation in infection and shedding loads and their impact on disease transmission dynamics have been well documented in both human[615,618,632] and veterinary literature[46,129,611,612,614,616,633,634] and linked to between- and within-host variations[619,621,633,635], immune suppression[632], and viral[632,636], bacterial[637-639], and/or parasitic coinfections[638]. The Pareto Principle (or 80/20 rule) originally applied to wealth inequality states that ~80% of an effect (i.e., RAVV virus shedding) is produced by ~20% of the population.[611,622] This principle has been previously applied to experimental ERB MARV infection dynamics[46], where the Lorenz curve and Gini coefficient are used to graphically represent and quantify the cumulative inequality in viral shedding to allow for identification of viral "supershedders"[611] within the experimental cohort. Super-spreaders, or supershedders, are individuals who infect or shed disproportionately more than most infected individuals and have been described in both natural infections[611,633,640]

and in experimental infections[46] in which the infectious exposure dose, time course, and inoculation route are standardized. In this study, we found that 25.0% of the bats were responsible for 83.5% of RAVV oral shedding and 16.7% of the bats were responsible for 89.2% of the RAVV rectal shedding. Two bats (452121 and 452049) were classified as supershedders[611] for both oral and rectal RAVV shedding, as both shed at levels greater than the 80th percentile and accounted for 69.4% and 89.2% of the total RAVV oral and rectal shedding, respectively. Both supershedder bats also had prolonged shedding durations: bat 452121 shed RAVV orally for 12 days and rectally for 10 days, while bat 452049 shed RAVV orally for 8 days and rectally for 6 days. MARV loads detected in rectal swabs in Schuh et al.[46] were excluded from cumulative shedding calculations, making a direct comparison between MARV and RAVV cumulative rectal shedding unavailable. This heterogeneity in RAVV shedding loads and durations may contribute to the fitness of RAVV in natural outbred ERB populations. Additionally, the marked statistical significance in RAVV rectal shedding compared to MARV rectal shedding introduces the possibility that rectal shedding is a more robust component of environmental maintenance and spread for RAVV than it is for MARV.

Another factor that cannot be discounted in the variation in viral shedding dynamics between the current study and previous ERB MARV experimental studies could be age. Ecological studies have observed a seasonal pulse in viral circulation within natural bat reservoir hosts, with a higher prevalence of active infection in juvenile bats (~6 months old)[3,378,641,642] and age-dependent variations in disease outcomes[643,644]. This may reflect a "perfect storm" of reservoir infective permissiveness in which the weaned juvenile bats are no longer protected by material antibodies, are susceptible to horizontal

transmission of infectious disease within the densely packed roosts and lack immunologic maturity to temper viral infection, and subsequent shedding. As such, the standard experimental model for most MARV ERB research has been to use animals that are 5-7 months old to mimic the biological parameters found in free-ranging ERBs. Here, the ERBs in the current study were 12-14 months old, introducing the possibility that age-related variation in infection dynamics could be a factor in the observed experimental differences in viral rectal shedding.

This study shows that experimental RAVV infection in ERBs, a natural reservoir host for *Orthomarburgvirus marburgense* viruses, follows a similar viral shedding timeline as past experimental MARV infections in ERBs, but with increased virus rectal shedding. Future work is needed to fully characterize the pathogenesis of experimental RAVV infection in ERBs, including evaluation of clinical, histochemical, and immunohistochemical findings and tissue viral loads at serial time points, with heightened focus on the small and large intestines. Future RAVV research could additionally include comparisons to Sosuga virus, a paramyxovirus for which the ERB serves as a putative natural reservoir, as Sosuga virus has been shown to replicate extensively in the small intestines.[17] This work provides an important baseline for hypothesis-driven research, allowing successful extrapolation of research findings in controlled laboratory settings to wild ERB populations and enabling experimental comparisons between MARV and RAVV infections.

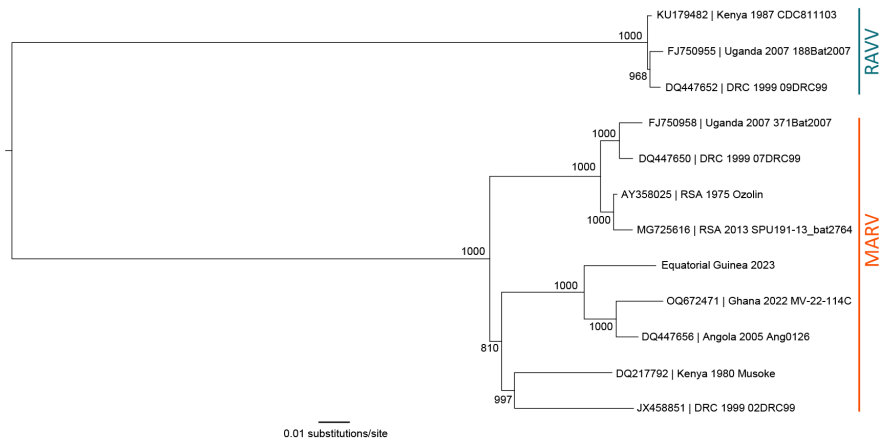

Figure 4-1: Midpoint-rooted, maximum-likelihood phylogeny of a subset of complete Marburg virus and Ravn virus genomes. Complete sequences from GenBank (accession numbers indicated) were aligned using Geneious Prime version 2024.0 (https://www.geneious.com/). The Equatorial Guinea 2023 sequence was acquired from https://virological.org/t/first-emergence-of-marburg-virus-in-equatorial-guinea-2023/924. ATGC Montpellier Bioinformatics Platform PhyML 3.0 (http://www.atgc-montpellier.fr/phyml/) was used to infer the maximum-likelihood tree after 1,000 bootstrap replicates. Node values indicate bootstrap support values. Scale bar indicates nucleotide substitutions per site. MARV, Marburg virus; RAVV, Ravn virus.

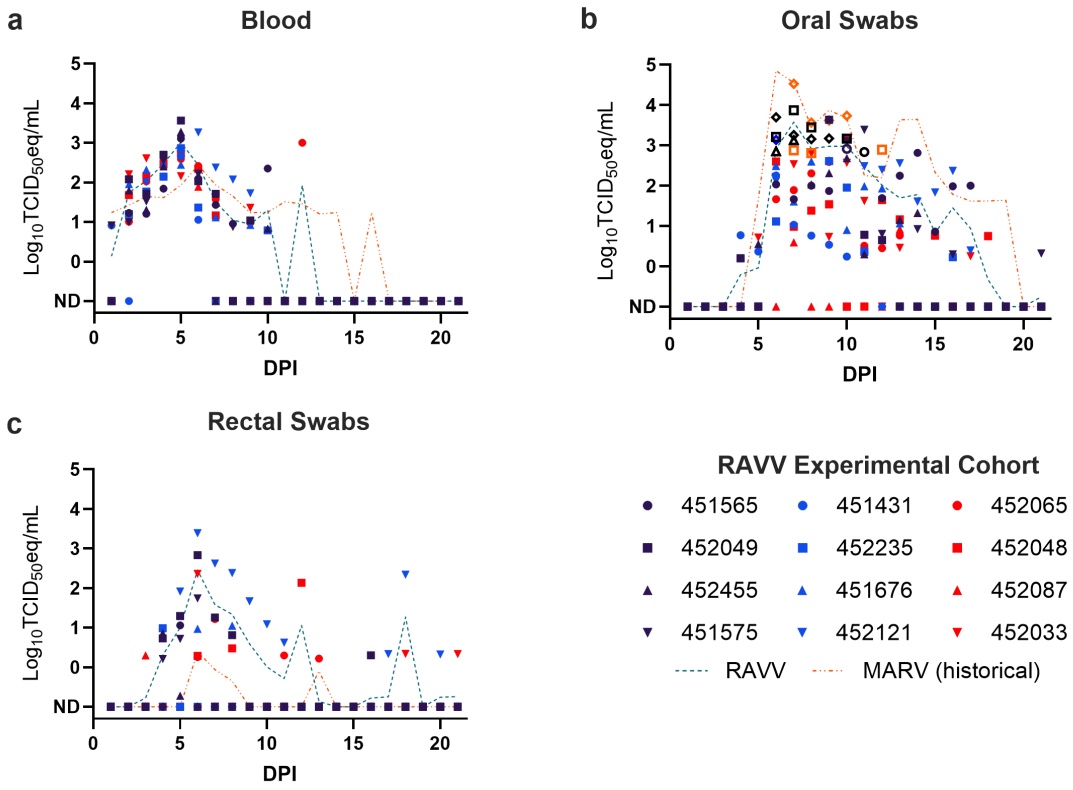

Figure 4-2: RAVV shedding dynamics in experimentally infected Egyptian rousette bats. RAVV loads (RT-qPCR-derived $log_{10}TCID_{50}$ equivalents/mL) in **a)** blood, **b)** oral swabs, and **c)** rectal swabs from experimentally infected Egyptian rousette bats. The teal dashed line represents the overall mean RAVV load in each sample. The orange dashed line represents the overall mean MARV load taken from historical MARV data [46]. Open symbols in **b** represent oral swabs from which infectious RAVV was isolated. ND: Not detected.

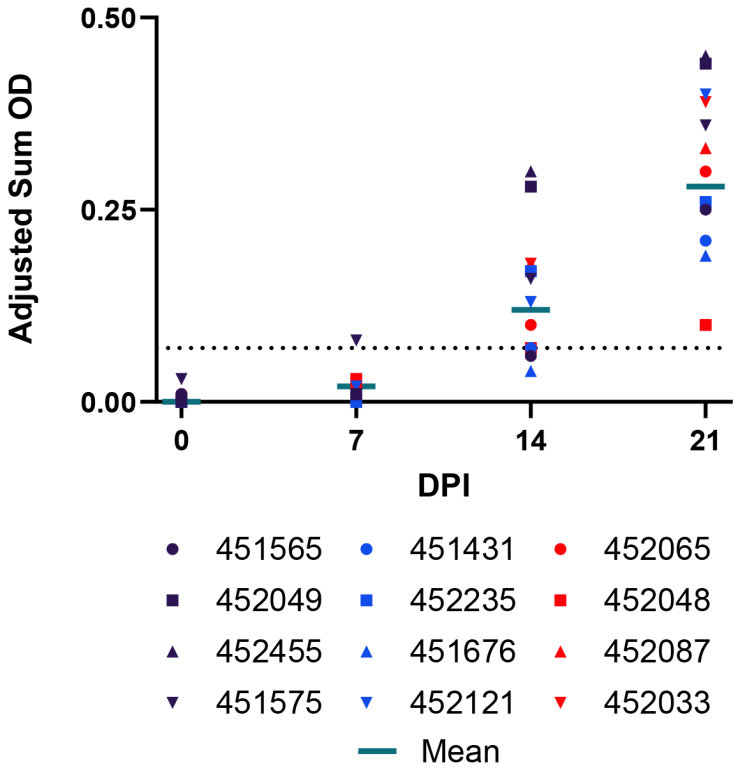

Figure 4-3: RAVV IgG antibody responses of experimentally infected Egyptian rousette bats. IgG antibodies were detected by ELISA with purified recombinant nucleoprotein of the Angola strain of MARV expressed in *Escherichia coli* from blood taken at 0, 7, 14, and 21 DPI. IgG antibody levels are expressed as adjusted sum OD values normalized between 0 and 1. The black dotted line represents the assay threshold (RAVV seropositive[3] 0.07).

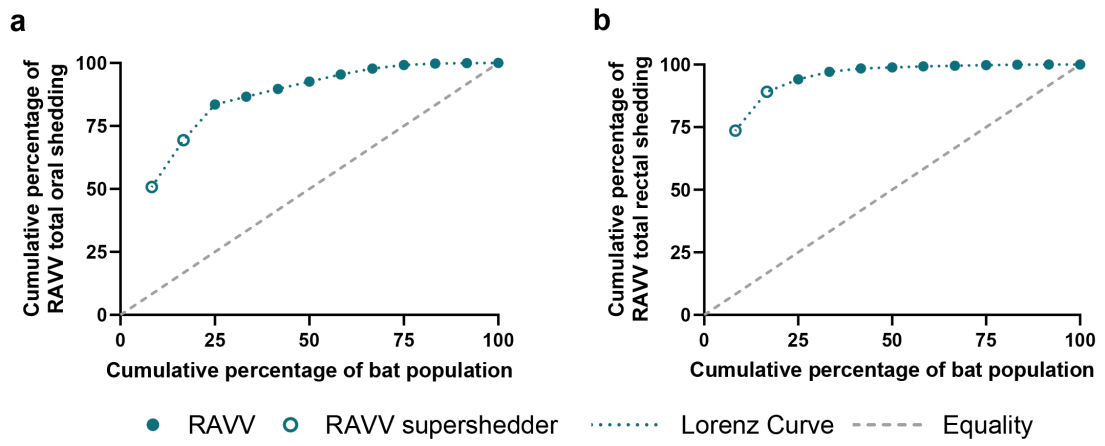

Figure 4-4: Cumulative RAVV shedding in experimentally infected Egyptian rousette bats. Lorenz curve of cumulative percentage of the inoculated bat population versus cumulative percentage of (a) oral and (b) rectal shedding ranked in descending order (i.e., the first circle on the circle represents bat 452121, which had the highest cumulative percentage of both rectal and oral shedding).

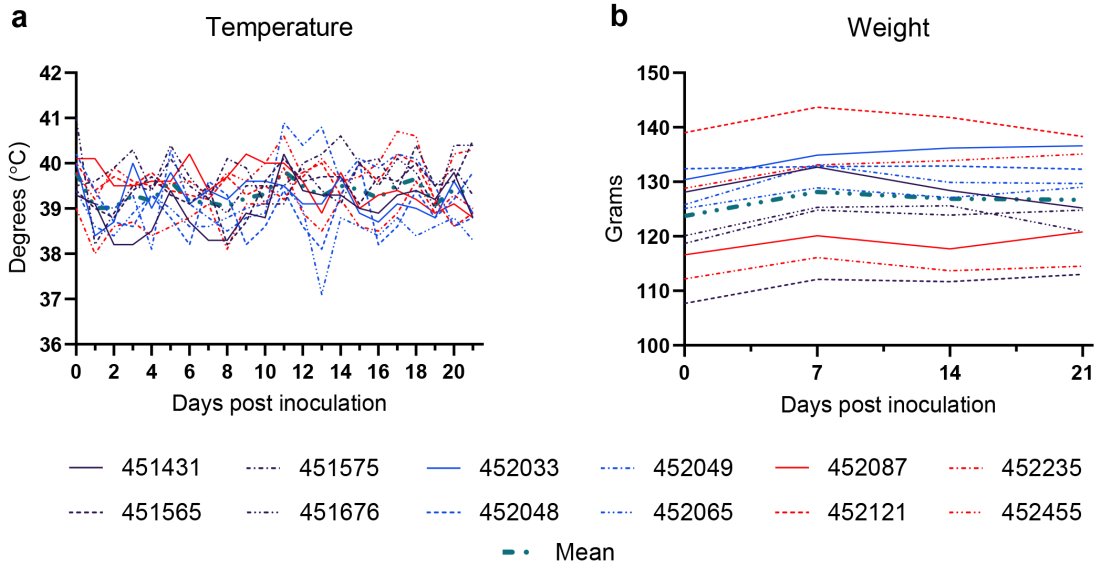

Figure 4-5: Clinical data. a) Temperatures (°C) acquired via rectal thermometer and b) weights (g) from experimentally infected Egyptian rousette bats.

CHAPTER 4B

EVALUATION OF LONG-TERM IMMUNITY FOLLOWING INOCULATION WITH HIGHLY DIVERSE ORTHOMARBURGVIRUS ISOLATES IN EGYPTIAN ROUSETTE BATS (ROUSETTUS AEGYPTIACUS)[6]

[6] Elbert JA, Schuh AJ, Amman BR, Guito JC, Graziano JC, Sealy TK, Howerth EW, Towner JS. Submitted to Journal of Virology, 5/12/2025. Pending revisions.

ABSTRACT

Viral coinfections and their impact on long-term immunity represent an understudied area in disease ecology and infectious disease research. Coinfections can influence the host's susceptibility to future infections, alter host and pathogen population dynamics, modify infection and shedding patterns, impose evolutionary pressures, and affect the risk of zoonotic spillover. Egyptian rousette bats (ERB; *Rousettus aegyptiacus*; common name: Egyptian rousettes) are a natural reservoir host for Marburg virus (MARV) and Ravn virus (RAVV), as well as a vertebrate reservoir for Kasokero virus (KASV) and a putative reservoir for Sosuga virus (SOSV). Viral coinfections have been documented in numerous free-ranging bat species as well as ERBs, raising questions about how these interactions influence immune responses, viral shedding, and pathogen maintenance within the natural host population. This is particularly critical given the genetic diversity among co-circulating viral species, e.g. MARV and RAVV, and the potential implications for the development of protective immunity and subsequent viral inoculation outcomes. In this study, ERBs previously infected with MARV alone or KASV+MARV were inoculated approximately 8 months later with homotypic (MARV) or heterotypic (RAVV) orthomarburgvirus isolates. The results demonstrated no viral replication or shedding post-inoculation, and all bats displayed strong secondary immune responses consistent with sterilizing immunity. These findings suggest that both MARV monoinfection and KASV+MARV coinfection confer robust protection against reinfection, regardless of the viral isolate. This research enhances our understanding of immune responses during viral coinfections in bats and their potential role in mitigating zoonotic pathogen spillover.

KEYWORDS: Egyptian rousette bat, Marburg virus, Ravn virus, Kasokero virus, virology, coinfection, immunology

INTRODUCTION

Understanding the effects of viral coinfections on long-term immunity is a minimally explored area in disease ecology and infectious disease research, and it is a topic of heightened importance in reservoir hosts that harbor zoonotic pathogens with significant public health impacts. Coinfections - instances where a host is either infected simultaneously or in close succession with two or more pathogens - can alter the host's susceptibility to future infections, affect both host and pathogen populations, create evolutionary pressures, and influence the risk of zoonotic spillover.[52,645-648] Gaining more insight into the consequences of pathogen coinfections is crucial for understanding the drivers of zoonotic pathogen transmission and for developing strategies to prevent future outbreaks.[314,649]

With over 1,400 recognized species, bats (Order Chiroptera) constitute approximately 20% of all mammalian species, second only to rodents in terms of diversity.[2] They are known to host an incredible diversity of viruses, with sequences of over 22,000 isolates from more than 200 viruses across 32 viral families associated with bats through serology, molecular detection, or virus isolation as of May 2024.[286] A significant portion of bat viral diversity remain uncharacterized, with discovery efforts often prioritizing viral families with known zoonotic potential such as *Coronaviridae*, *Filoviridae,* and *Paramyxoviridae*.[35,52,286,650] The Egyptian rousette bat (ERB; *Rousettus aegyptiacus*) is a natural reservoir host for Marburg virus and Ravn virus (MARV;

RAVV; family *Filoviridae*; genus *Orthomarburgvirus*)[3,48,50], as well as a vertebrate reservoir for Kasokero virus (KASV; family *Orthonairoviridae*, genus *Orthonairovirus*)[8] and a presumed reservoir for Sosuga virus (SOSV; family *Paramyxoviridae*, genus *Pararubulavirus*).[6,7,116,282]

MARV and RAVV, collectively called orthomarburgvirus and are the only two known virus members of the species *Orthomarburgvirus marburgense,* are causative agents of Marburg virus disease (MVD), a severe viral hemorrhagic fever that typically emerges in sub-Saharan Africa and is characterized by human-to-human transmission and high case fatalities.[196] MARV was first identified in 1967 following laboratory outbreaks in Marburg and Frankfurt, Germany and Belgrade (former Yugoslavia) linked to exposure to African green monkeys imported from Uganda.[210] To date, 18 known orthomarburgvirus outbreaks have occurred, most recently in Tanzania in January 2025.[40] Many MARV outbreaks have been epidemiologically linked to exposure to ERBs through gold mining activities or other human encroachment into ERB habitats, including tourism.[211-215,217-219] RAVV was first identified in 1987 following a fatal case in a tourist visiting Kitum Cave, Mount Elgon National Park, Kenya.[211] Designated as a distinct virus within the species in 1996, RAVV has since been identified in two subsequent outbreaks, the latest in Uganda in 2007.[48,211,212]

Experimental studies have provided insight into the natural history and pathogenesis of orthomarburgvirus infection in its reservoir host.[4,45-47,50,243,244] MARV-inoculated ERBs have limited and subclinical disease characterized by viremia, broad viral tissue dissemination, viral shedding in saliva, feces, and urine, and mild hepatitis characterized by multifocal aggregates of mononuclear cells and mild hepatocellular

necrosis with an increase in alanine aminotransferase (ALT).[4,45,50,98,243,244] MARV IgG antibodies peak by 28 days post-infection (DPI) and usually fall below the threshold of seropositivity by 3 months post-infection (MPI).[4,46,243,244] Horizontal transmission of infectious disease between experimentally inoculated and naïve, co-housed ERBs has been documented in a laboratory setting[46], as well as robust short-term[243] and long-term[47] immunity to reinfection upon experimental homotypic MARV inoculation 48 DPI and two years after initial infection, respectively. Vertical transmission has not been observed in MARV PCR-positive dams carrying newborn pups.[48]

Ecological and experimental studies have shown the ERB to be a natural vertebrate reservoir for KASV, a human-pathogenic virus maintained in an enzootic transmission cycle with ERBs and *Ornithodoros (Reticulinasus) faini* ticks.[8,16,19,140,571] Experimental KASV-infected bats develop mild to moderate, acute viral hepatitis, which first presents at 3 DPI and is cleared by 20 DPI, with viral shedding primarily detected in blood, but also in oral swabs, rectal swabs, and urine.[16,18,19] Viral replication occurs in the liver, spleen, lymph nodes, and tongue, with KASV RNA cleared from the spleen and liver by 6 DPI.[18]

The prevalence of coinfections in free-ranging bat populations is poorly understood, typically noted incidentally rather than through systematic study [52]. A recent retrospective analysis of ERB tissues from bats living in Kitaka Mine, Uganda and in Sierra Leone showed that 2.47% of juveniles infected with MARV were also infected with SOSV, with one bat coinfected with MARV, SOSV, and Yogue virus (family *Orthonairoviridae*, genus *Orthonairovirus*).[274] Worldwide surveillance efforts have documented widespread viral coinfections in bats, with up to 42% of sampled bats in

China coinfected with at least two viruses spanning 12 viral families[55], and similar findings reported globally involving diverse viral combinations including coronaviruses, astroviruses, paramyxoviruses, and others.[53,54,56-60,62-76] These studies underscore the remarkable virological diversity in bats and their role as reservoirs for multiple, often concurrent, viral infections, highlighting the need for comprehensive surveillance to better understand the prevalence, complexity and ecological significance of coinfections, both within individual animals and larger ecosystems.

A recent experimental study found that viral coinfection in ERBs can modulate viral shedding dynamics and subsequent antibody development, suggesting alterations to long-term immunity.[282] ERBs experimentally infected with SOSV+MARV had significant reduction in the duration of MARV shedding, whereas ERBs coinfected with KASV+MARV had significantly increased peak magnitude and duration of MARV viremia and oral shedding, resulting in significantly higher cumulative MARV shedding in KASV+MARV coinfected bats.[282] Prior to this study, experimental studies on coinfections in bats were limited to investigations into interactions between coronaviruses and non-viral pathogens. A 60-fold increase in coronavirus RNA was observed in the intestines of *Myotis lucifugus* bats coinfected with *Pseudogymnoascus destructans*, the fungal pathogen that causes white nose syndrome.[283] Considering the frequent occurrence of viral coinfections in free-ranging populations and the high contact rates in densely populated roosts that result in viral re-exposure, the effect of viral coinfections on subsequent viral inoculation needs to be better understood.

Despite being within the same viral species, the full genomic sequence of RAVV differs by up to 21% from MARV and the amino acid sequence of the RAVV

glycoprotein (GP) differs by ~22% from MARV GP[48,49], and as such may generate antigenically distinct pathogen-associated molecular patterns (PAMPs). Therefore, the more sensitive and specific actions of effector T cells and class-switched, affinity-matured antibodies that would provide protective immunity for homotypic inoculation may not be able to block infection of a heterotypic isolate, and viral replication and shedding may be seen. The extent to which heterotypic inoculation will allow viral replication and shedding in a previously monoinfected or coinfected ERB is currently unknown.

In this study, we assess whether inoculation with a homotypic or heterotypic orthomarburgvirus isolate (MARV or RAVV, respectively) influences viral reinfection, replication, and shedding in either previously MARV-monoinfected or KASV+MARV coinfected ERBs. Additionally, we assess whether coinfection with KASV+MARV confers long-term protective immunity against reinfection, replication, and shedding by challenging ERBs that had been experimentally infected ~8 months prior during a previous coinfection study.[282] Data for RAVV-monoinfected bats was taken from a recent characterization of RAVV viral shedding dynamics in experimentally infected ERBs[289] and was included as a control for baseline Ravn virus viral shedding dynamics. Following inoculation, MARV and RAVV detection in the blood and viral shedding from the oral and rectal mucosa is monitored for 10 days and MARV IgG antibody responses are monitored for 21 days. Here, we show that no bats previously infected in any group have evidence of MARV or RAVV replication or shedding regardless of prior infection history. Further, all bats developed virus-specific secondary immune responses, demonstrating that infection with MARV induces sterilizing immunity (defined herein as

absence of detectable viremia and viral shedding for 10 consecutive days post-inoculation) against orthomarburgvirus reinfection with a genetically distinct virus, even when the initial MARV infection was initiated in the context of KASV coinfection.

MATERIALS AND METHODS

Virus

Four $\log_{10}$ 50% tissue culture infective dose ($TCID_{50}$) of a MARV isolate (200704852 Uganda bat, termed MARV371; second passage on Vero E6 cells), obtained from a naturally infected ERB (371bat) and a RAVV isolate (200704669 Uganda bat; second passage on Vero E6 cells), obtained from a naturally infected ERB (188bat), both collected during a 2007 orthomarburgvirus outbreak ecological investigation at Kitaka Mine in southwestern Uganda, were prepared in 0.25 mL of sterile Dulbecco's modified Eagle's medium (DMEM).[48]

Bats

All experimental procedures were conducted with approval from the Centers for Disease Control and Prevention (CDC, Atlanta, Georgia, USA) Institutional Animal Care and Use Committee, and in strict accordance with the Guide for the Care and Use of Laboratory Animals (Committee for the Update of the Guide for the Care and use of Laboratory Animals 2011). The CDC is an Association for Assessment and Accreditation of Laboratory Animal Care International fully accredited research facility. No human patient-derived clinical materials were used in these studies.

Procedures conducted with infectious orthomarburgvirus or with infected bats were performed at the CDC under biosafety level 4 (BSL-4) laboratory conditions in accordance with Select Agent regulations (Animal and Plant Health Inspection Service

and Centers for Disease Control and Prevention 2014). All investigators and animal handlers followed strict BSL-4 safety and infection control practices.[610] 36 adult ERBs (12-14 months of age) were used in this study. All ERBs were captive-born bats and were managed as previously described.[4,289]

Experimental Design/Bat Groups

24 ERBs were previously utilized in an experimental infection study at CDC investigating viral shedding dynamics upon coinfection of ERBs bats with KASV+MARV.[282] In that study, ERBs were infected with 4 $\log_{10}TCID_{50}$ of KASV (-6 DPI) and/or MARV (0 DPI), underwent non-destructive sampling, and were maintained for 8 months in BSL-4 laboratory conditions prior to the onset of the experimental study described herein. 12 ERBs were undergoing a concurrent experimental study characterizing viral shedding dynamics of Ravn virus and will be highlighted here as Group 5, a control group for baseline Ravn virus viral shedding dynamics in primed ERBs.[289] Experimental groups are outlined in Table 4-1.

The experimental design is outlined in Table 4-2. ERBs from a previous coinfection study[282] (Groups 1-4) and naïve ERBs (Group 5)[289] were acclimated in the BSL-4 laboratory for 7 days before the beginning of the study (acclimation study phase). Baseline blood samples, body weights, and temperatures were taken prior to inoculation. At 0 days post inoculation (DPI), bats in Groups 1 - 2 were inoculated subcutaneously under isoflurane anesthesia with the above-described MARV inoculum in the caudal abdominal region. Bats in Groups 3 - 5 were inoculated subcutaneously under isoflurane anesthesia with the above-described RAVV inoculum in the caudal abdominal region. As

data from historical MARV control ERBs from previous studies was available, control ERBs were not utilized in this study.

Specimen Collection

Specimen collection has previously been described in detail[4,45,46]. Blood (whole, nonheparinized; 10 μL and 21 μL for RT-qPCR and serology, respectively) was taken on -1 DPI, daily from 1-10 DPI and then on 14 DPI and 21 DPI from the cephalic wing vein using a sterile lancet (C&A Scientific, Manassas, VA, USA). Blood was tested for the presence of orthomarburgvirus RNA by RT-qPCR through 10 DPI and orthomarburgvirus IgG antibody responses were monitored weekly through 21 DPI. The oral mucosa was sampled daily through 10 DPI by swabbing simultaneously with two polyester-tipped applicators the inside of the bat's mouth (Fisher Scientific, Grand Island, NY, USA). After sampling, one oral swab was immediately placed in either a deep-well plate with 500 μL of MagMAX lysis buffer solution (Life Technologies, Grand Island, New York, USA) for nucleic acid extraction and RT-qPCR analysis and one oral swab was placed in sterile viral transport medium for attempted virus isolation of any orthomarburgvirus RNA positive swabs. A temperature probe covered with a plastic sheath (MABIS Healthcare, Waukegan, Illinois, USA) was used to measure the rectal temperature of each bat through 10 DPI. The plastic sheath was then cut and place into a deep-well plate with 500 μL of MagMAX lysis buffer solution (Life Technologies) for nucleic acid extraction and RT-qPCR analysis.

Euthanasia

At 22 DPI, all bats were euthanized under anesthesia via an overdose of isoflurane followed by cardiac exsanguination. Cardiac blood was collected and retained.

Nucleic Acid Extraction

Nucleic acid was extracted from blood, oral swab, and rectal probe covers using the MagMAX Pathogen RNA/DNA Kit (Thermo Fisher Scientific, Waltham, MA, USA) on the KingFisher Apex 96 Deep-well Head Magnetic Particle Processor (Thermo Fisher Scientific, Waltham, MA, USA).

RT-qPCR

RT-qPCR procedures have previously been described in detail.[4,46] Reverse-transcribed orthomarburgviruses and ERB beta-2-microglobulin (B2M) RNA were detected on the CFX Opus 96 Real-Time PCR System (Bio-Rad, Hercules, CA, USA) using the Luna Probe One-Step RT-qPCR 4x Mix with UDG (New England Biolabs Inc, Ipswich, MA, USA), with amplification primer and reporter probes targeting the orthomarburgvirus viral protein 40 (VP40) gene (forward primer: GGACCACTGCTGGCCATATC, reverse primer: GAGAACATITCGGCAGGAAG, probe 1: 56-*FAM*-ATC CTA AAC-*ZEN*-AGG CTT GTC TTC TCT GGG ACT T-*3IABkFQ*, probe 2: 56-*FAM*-ATC CTG AAT-*ZEN*-AAG CTC GTC TTC TCT GGG ACT T-*3IABkFQ*) and the ERB B2M gene (forward primer: CAGCAAGGACTGGTCTTTCTAT, reverse primer: CCTCCATGATGCTGGTTAGTT, probe: *FAM*-TTC ACA CGG-*ZEN*-CAG CTG TAC TCA TCC-*IABkFQ*), respectively. This assay was designed to detect a conserved sequence of VP40 present in all known species of orthomarburgvirus, including Ravn virus.[49] Relative MARV and RAVV $TCID_{50}$eq/mL (blood, oral, and fecal specimens) were interpolated from standard curves generated from serial dilutions of the titrated 371bat MARV isolate and 188bat RAVV isolate spiked into appropriate biological specimens.

Serology

As previously described[4,46,47], ELISA plates were coated with 50 ng per well of purified recombinant Marburg Angola nucleoprotein (NP) or Reston NP expressed in *Escherichia coli* (GenScript, Piscataway, NJ, USA) diluted in PBS containing 1% thimerosal. The plates were incubated overnight at 4 °C and then washed with PBS containing 0.1% Tween-20 (PBS-T). A 1:100 dilution of gamma-irradiated bat whole blood in masterplate diluent (PBS containing 5% skim milk powder, 0.5% tween-20 and 1% thimerosal) was then added to the first well and fourfold serial dilutions in serum diluent (PBS containing 5% skim milk and 0.1% tween-20) were performed through 1:6400. After incubating for 1 hour at 37 °C, the plates were washed with PBS-T and bound antibody was detected using a 1:11000 dilution of anti-goat bat IgG (Bethyl Laboratories, Montgomery, TX, USA) in serum diluent. Following incubation with the secondary antibody for 1 hour at 37 °C, the plates were washed twice with PBS-T and the 2-Component ABTS Peroxidase System (KPL, Gaithersburg, MD, USA) was added. The substrate was allowed to incubate for 30 minutes at 37 °C before reading the plates on a microplate spectrophotometer at 410 nm. The adjusted sum OD values were calculated by subtracting the ODs at each fourfold dilution wells coated with Reston NP from their corresponding wells coated with Marburg Angola NP and then linearly transforming the values using the min-max normalization method. The threshold for seropositivity was set at 0.07 after in-house assay optimization. The cut-off value for assay seropositivity was determined by calculating the mean adjusted sum OD value plus 3─5 standard deviations (SDs) of 38 MARV naïve ERBs.

Results

No evidence of orthomarburgvirus replication or shedding

Consistent with previous studies that describe short- and long-term protective immunity against MARV infection, replication, and shedding in previously monoinfected ERBs[47,243,244], none of the either MARV-monoinfected or MARV+KASV bats (groups 1-4) developed detectable viremias or shed viral RNA when inoculated with either MARV or RAVV throughout the 10-day specimen collection period. Sample collection was originally scheduled to extend through the end of the study, however since all samples were universally negative for 10 consecutive days (1-10 DPI), daily sampling was ceased to avoid unnecessary stress on the animals. Due to the uniform negativity of the samples, tissues were not collected at necropsy for evaluation of MARV RNA viral loads. Data for RAVV monoinfected bats (Group 5) was taken from a recent characterization of RAVV viral shedding dynamics in experimentally infected ERBs[289] and was included as a control for baseline Ravn virus viral shedding dynamics in primed ERBs. As described previously[289], viremia was present in all Group 5 bats, peaking on 5 DPI and cleared by 13 DPI and positive oral and rectal swabs samples through 21 DPI.

Rapid immune response upon inoculation

During the previous coinfection study, all bats (12/12 KASV+MARV and 12/12 MARV monoinfected ERBs) seroconverted to MARV by the study end (21 DPI).[282] By the initiation of this study at ~8 MPI, 21/24 (87.5%) of the previously infected ERBs maintained MARV IgG antibody levels above the threshold of seropositivity. Upon viral inoculation, all groups developed a robust MARV IgG antibody response by Day 7 which was maintained through study end (21 DPI) (Fig. 4-6). There were no statistically

significant differences in MARV IgG antibody levels between the 4 inoculation groups ($F_{3,12}$ =0.02291; P=0.9950).

No evidence of clinical disease

As in previous studies[4,46,243,244], MARV- and RAVV- inoculated bats did not have any disease-related morbidity or mortality and normal social and feeding behaviors were maintained. One female bat (450979) was euthanized on 14 DPI due to declining health (multifocal alopecia, dehydration) and weight loss. Gross and histopathologic evaluation of the animal was consistent with superficial dermal trauma, mild adrenal cortical hyperplasia, atrophy of brown fat and the gastrointestinal system was largely devoid of digesta, with no evidence of an infectious or inflammatory process or neoplastic disease. Significant hepatocellular glycogenosis was present, however this is a common incidental finding in frugivorous bats.[18,437] Taken together, the post-mortem findings are suggestive of social "bullying" and deprivation of access to food and water by group conspecifics. Female bats cooperatively monopolizing and defending food resources from other females has previously been described.[651] Apart from this bat, all other bats had normal body weights and rectal temperatures, consistent with previous studies (Fig. 4-7).[4,16] As such, additionally histopathology was thus deemed not necessary for any other bats.

Discussion

This study demonstrates that ERBs experimentally inoculated with homotypic MARV or heterotypic RAVV isolates mounted robust, fully protective secondary immune responses 236 days post-primary infection. This protective response occurred regardless of whether the ERBs were initially monoinfected with MARV or coinfected with KASV+MARV. The immune response was characterized by the absence of

orthomarburgvirus replication in the blood, no viral shedding from the oral or rectal mucosa, and a rapid, robust orthomarburgvirus-specific IgG antibody response by 7 DPI across all groups. These findings align with previous studies investigating both short-term (48 DPI)[243] and long-term (17-24 MPI)[47] immune responses in MARV-monoinfected ERBs following homotypic inoculation.

Coinfection within a host involves complex interactions between pathogens, including competition for resources, modulation of immunological pathways or the production of chemical compounds.[652] Coinfecting viruses can lead to variety of outcomes, such as viral interference, synergy, or noninterference.[652-654] For instance, murine coinfection with ectromelia virus (ECTV) and lymphocytic choriomeningitis virus (LCMV) demonstrated that LCMV-induced type I interferons attenuated ECTV-induced disease while simultaneously weakening the immune response to LCMV, highlighting the complex, bi-directional effects of viral coinfections on immunity and disease.[655] Similarly, cattle coinfected with two foot-and-mouth disease virus (FMDV) isolates showed variable outcomes, ranging from transient protection to severe disease, depending on the timing of exposure.[656] Viral recombination in these superinfected animals suggests that persistently infected hosts may contribute to the emergence of new FMDV isolates.[656]

Mathematical models using susceptible (S), exposed (E), infectious (I), and recovered (R) compartments (SEIR models) have been employed to estimate orthomarburgvirus transmission patterns in ERB populations.[279] Using this model, a closed population of 40,000 ERBs with a biannual birth pulse and 21-day latent period predicted an active MARV infection prevalence of less than 2.0%, closely matching the

2.5% observed in previous ecological studies[3] and is corroborated by serological data from MARV experimental studies in managed care ERBs.[4,46,243,244] While the SEIR framework is useful for modeling filovirus ecology, additional ecological and biological factors likely shape reservoir host and infection trajectories, e.g. metapopulation dynamics, the duration of protective immunity, natural immune stressors, and the role of coinfection in shaping susceptibility patterns and immune responses.[98,280] Whether coinfection in ERBs alters the duration of immunity or hastens the return to susceptibility remains unknown but carries significant implications for viral persistence and transmission in free-ranging host populations.

In the previous experimental coinfection study from which our Group 1-4 bats were derived, ERBs coinfected with KASV+MARV had significantly increased peak magnitude and duration of MARV viremia and oral shedding, as well as having significantly higher cumulative MARV shedding loads.[282] This implies a positive, or synergistic, interaction in which KASV infection facilitates or potentiates MARV infection. KASV infection did not appear to hinder the development of a robust MARV-specific immune response, as all MARV-inoculated ERBs had sterilizing immunity identical to previously monoinfected ERBs.[47,243] Interestingly, in the previous experimental coinfection study, only 10/12 of the ERBs coinfected with SOSV+MARV seroconverted to MARV by the end of the study (18 DPI) and the cohort had significantly lower anti-MARV nucleoprotein IgG responses compared to the MARV-monoinfected group.[282] These findings raise the possibility that, unlike KASV+MARV coinfection, SOSV+MARV coinfection in ERBs might confer susceptibility to MARV reinfection, supported by the 2.5% annual prevalence of active MARV infection in adult ERBs.[3] The

possibility of increased susceptibility to MARV reinfection in adulthood is likely not limited to SOSV+MARV coinfection, as populations of ERBs are known to harbor multiple paramyxoviruses.[527] Future experimental studies are needed to investigate long-term immune outcomes in ERBs coinfected with various viruses, including SOSV, as this study specifically examined KASV+MARV coinfection. Such studies should include investigating the impact of inoculation order and variation of inoculation intervals on MARV replication and shedding. Variation in inoculation time intervals has been shown to have wide-ranging effects on susceptibility in the context of viral infections[654,657] and in subsequent immune responses.[658] As such, further work is needed to elucidate these topics in the context of the ERB as a host of diverse and taxonomically varied microorganisms.[282]

Compared to the results reported in this current study, previous investigations of long-term antibody dynamics in ERBs have yielded conflicting data. One study observed that virus-specific IgG levels in MARV-monoinfected ERBs declined rapidly after the initial infection peak, falling below the threshold of seropositivity by 3 months after infection, though a robust secondary immune response was observed upon homotypic inoculation 24 months later.[46] In contrast, another study found that 67% of bats experimentally infected with MARV retained detectable antibodies around 4 MPI, while 84% of naturally exposed bats captured in the wild showed MARV antibodies at least 11 months later.[382] While some MARV-naturally infected ERBs became viremic upon heterotypic inoculation, widespread tissue dissemination was not observed.[382] Future research is needed to better understand the duration of protective immunity, especially in

the context of previous coinfections that may affect differential immunity depending on the specific coinfecting agent, e.g., KASV+SOSV.

Overall, we have demonstrated that both prior MARV-monoinfection and KASV+MARV coinfection in ERBs confer a consistent and robust secondary immune response that prevents reinfection upon viral inoculation with homotypic or heterotypic orthomarburgvirus isolates, MARV or genetically diverse RAVV, respectively. These findings broaden our understanding of the factors that influence this bat species susceptibility to and maintenance of natural infections in free-ranging populations. Furthermore, these results offer new insights into immune dynamics in nature where viral coinfections are common and contribute to our understanding of how such interactions might impact the transmission of zoonotic pathogens from bats to susceptible hosts, including humans.

Table 4-1: Experimental Study ERB Groups. Tabular breakdown of the experimental groups.

Group	# ERB (n=36)	Sex Male (M) Female (F)	Prime Inoculation: March 2023	Challenge Inoculation: October 2023	Prime Inoculation: October 2023	Group Purpose
1	6	4 M, 2 F	MARV	MARV		Characterization of long-term immunity upon homotypic inoculation
2	6	4 M, 2 F	KASV + MARV	MARV		Assess role of viral coinfection on long term immunity upon homotypic inoculation
3	6	3 M, 3 F	MARV	RAVV		Characterization of long-term immunity upon heterotypic orthomarburgvirus inoculation
4	6	3 M, 3 F	KASV + MARV	RAVV		Assess role of viral coinfection on long term immunity upon heterotypic orthomarburgvirus inoculation
5	12	6 M, 6 F	-	-	RAVV	Establish baseline RAVV viral shedding dynamics

Table 4-2: Tabular breakdown of the experimental design. DPI: Days post inoculation. X: Procedure not performed.

DPI	Group 1	Group 2	Group 3	Group 4	DPI	Group 5
-236 (KASV Infection: 3/2/2023, MARV infection: 3/8/2023)[282]	Prime MARV inoculation	Prime KASV + MARV inoculation	Prime MARV inoculation	Prime KASV + MARV inoculation	**-236[289]**	X
-7	BSL-4 Acclimation				**-7**	BSL-4 Acclimation
-1	Pre-bleeds Body weights				**-1**	Pre-bleeds Body weights
0 (10/24/2023)	MARV inoculation	MARV inoculation	RAVV inoculation	RAVV inoculation	**0 (10/24/2023)**	Prime RAVV inoculation
1-10	Weekly body weights Daily temperatures Daily collection of blood, oral swabs, and rectal swabs				**1-21**	Weekly body weights Daily temperatures Daily collection of blood, oral swabs, and rectal swabs
11-21	Weekly body weights Weekly blood collection					
22	Euthanasia				**22**	Euthanasia

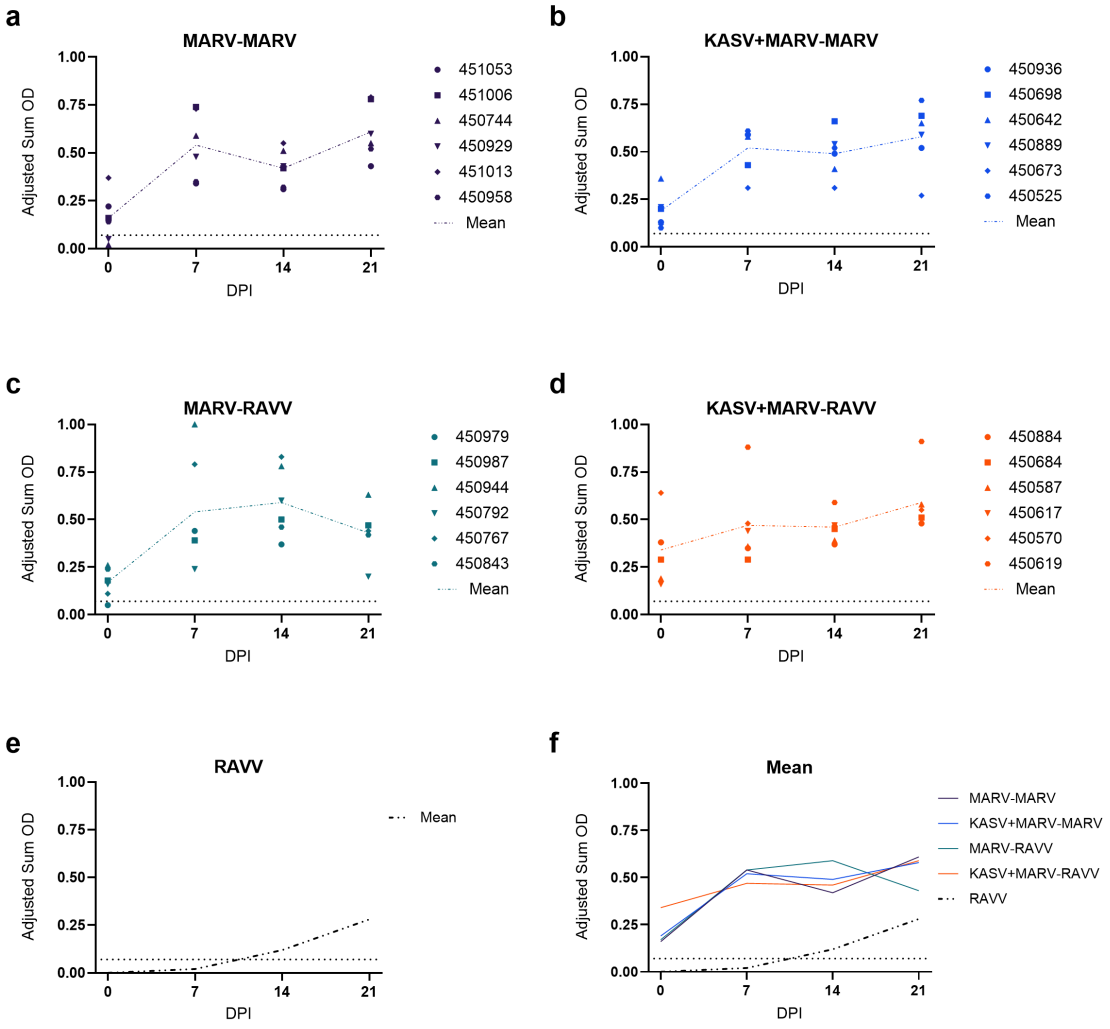

Figure 4-6: MARV IgG antibody responses of Egyptian rousette bats according to group. Orthomarburgvirus IgG antibody responses of experimentally inoculated bats, as detected by ELISA with purified recombinant nucleoprotein of the Angola isolate of MARV expressed in *Escherichia coli*. Data for RAVV monoinfected bats (e) was taken from a recent characterization of RAVV viral shedding dynamics in experimentally infected ERBs[289] and was included as a control for baseline Ravn virus shedding dynamics in primed ERBs. Means across all groups are compared in (f). The black dotted line represents the cutoff value of the assay (MARV seropositive ≥ 0.5). DPI = Days post inoculation.

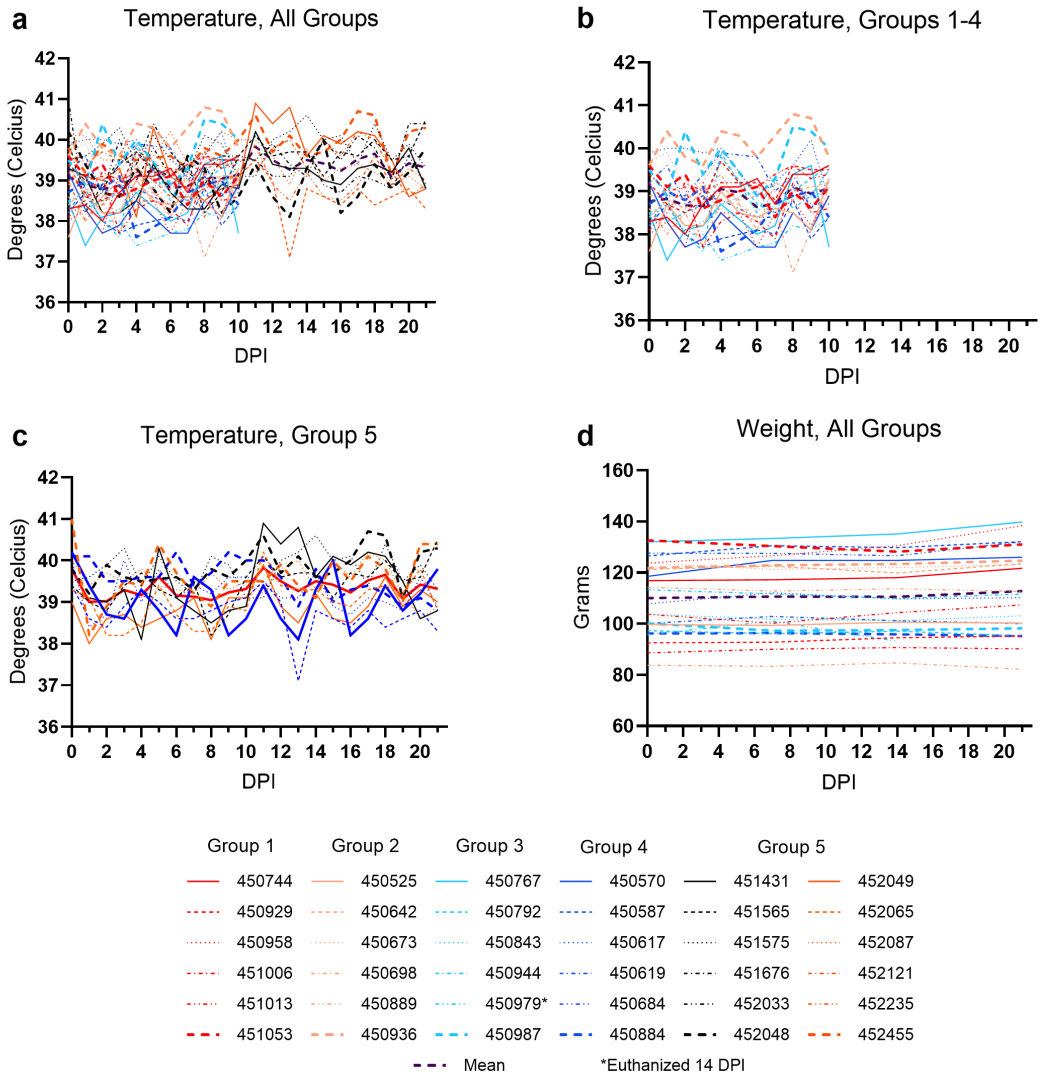

Figure 4-7: Clinical data. Temperatures (degrees Celsius) acquired via rectal thermometer in a) all bats b) Groups 1-4 c) Group 5 and d) weights (grams) from experimentally infected ERBs. The purple dashed lines in a-d represent the overall mean value of each parameter. Bat 450979 was euthanized 14 DPI due to weight loss and declining health. DPI = Days post inoculation.

CHAPTER 5

CONCLUSIONS

This dissertation provides a comprehensive and multifaceted investigation into the anatomy, immunobiology, pathology, and viral infection dynamics of the Egyptian rousette bat, the only confirmed natural reservoir for orthomarburgviruses MARV and RAVV. Through a combination of literature synthesis, histologic atlas development, experimental infection studies, and field-based pathologic assessments, this body of work fills several longstanding knowledge gaps in our understanding of ERB biology.

This dissertation is structured around three principal goals: 1) to characterize the lymphoid system and immune architecture of ERBs; 2) to evaluate histologic findings in free-ranging bats; and 3) to assess the virological and immunological consequences of infection and coinfection with genetically diverse orthomarburgviruses. Each chapter addresses a critical aspect of ERB pathobiology relevant to their role as reservoir hosts and provides novel insights with implications for both ERB health and zoonotic disease emergence.

Key Findings and Implications

Chapters 2 and 3B lay the anatomical and immunological groundwork by establishing a detailed atlas of ERB lymphoid tissues and a comprehensive reference of normal histology. This identification of structurally conserved yet functionally specialized lymphoid tissues, such as extensive GALT, periarterial macrophage sheaths,

and compartmentalized immune cell populations, provides the necessary framework to interpret immune responses in subsequent chapters. This foundational work also facilitates histologic interpretation in studies of viral infection, vaccine evaluation, and experimental pathology.

Chapter 3B offers the first systematic characterization of spontaneous gross and histologic changes in free-ranging ERBs, revealing widespread yet subclinical pathology. Most notably, perivascular inflammatory aggregates were frequent and multi-organ in distribution, suggesting chronic immune activation possibly driven by persistent pathogen exposure or environmental stressors. These findings underscore the importance of moving beyond single-pathogen surveillance of zoonotic viruses toward a more holistic understanding of reservoir host health, including how subclinical pathology might influence viral shedding, transmission potential, or host fitness.

Chapter 3C extends this perspective through comparative analysis of hepatic iron accumulation in free-ranging vs. managed care ERBs. Iron overload, a major cause of mortality in managed care ERBs, was not associated with morbidity in wild populations despite frequent hemosiderosis. Interestingly, MARV-infected bats had lower hepatic iron scores, potentially reflecting virus-induced hepcidin upregulation. This finding raises the provocative hypothesis that orthomarburgvirus infection may modulate host iron homeostasis in ways that benefit both host and virus, highlighting an underexplored axis of virus-host interaction with evolutionary and ecological implications.

Chapters 4A and 4B characterize infection and immunity in controlled experimental contexts. Chapter 4A shows that RAVV, despite significant genomic divergence from MARV, follows similar infection kinetics but is shed at higher loads and

for longer durations, especially rectally. These findings not only establish the shedding profile of RAVV but also suggest that differences in the glycoprotein, where the majority of the genomic and amino acid variation is found between MARV and RAVV, may influence viral transmission. Additionally, the identification of "supershedder" bats adds complexity to reservoir competence, with implications for outbreak risk modeling and targeted surveillance.

Chapter 4B demonstrates that prior MARV or MARV+KASV infection induces robust sterilizing immunity upon homotypic and heterotypic orthomarburgvirus inoculation. This cross-protection occurred even in the absence of strong neutralizing antibody responses, suggesting that ERBs rely on alternative immune mechanisms to achieve effective viral control. These findings support the notion that ERBs are uniquely adapted to control orthomarburgvirus infection without pathological consequences, and that coinfection does not universally compromise immunity.

Limitations

Several limitations should be acknowledged. First, many of the histologic samples were collected over a decade prior to analysis and subjected to prolonged fixation, potentially introducing artifacts, tissue contaminants, or antigen degradation. Second, while histologic and immunohistochemical data were informative, molecular diagnostics and transcriptomic analyses were limited or absent in several chapters due to nucleic acid degradation or sample contamination. Third, the use of juvenile bats in both field and experimental cohorts, while reflective of known epidemiological trends, limits the ability to generalize across life stages. Seasonal, geographic, and sex-based differences could not be robustly assessed. Finally, sample sizes, which large for wildlife studies, may still

underrepresent the natural variability of this species across its broad, fragmented host range.

Future Directions

This dissertation opens several avenues for future work:

1. **Molecular profiling of inflammation and immunity:** High-resolution techniques such as single-cell RNA sequencing, spatial transcriptomics, and multiplex immunohistochemistry or in situ hybridization should be applied to ERB tissues to elucidate cell-specific activation states and immune microenvironments, especially in lymphoid, hepatic, and mucosal tissues.
2. **Mechanistic investigation of iron metabolism:** Further research is needed to determine how MARV infection modulates hepcidin, ferroportin, and iron storage, and whether this influences viral persistence, pathogenesis, or host survival.
3. **Coinfection ecology and long-term immunity:** Broader studies of ERBs experimentally infected with diverse virus combinations (e.g., MARV+SOSV, MARV+paramyxoviruses) are needed to clarify how coinfection affects immune memory, reinfection risk, and cross-protective potential.
4. **Pathogen-vector-host interactions:** Systematic identification and experimental testing of ERB ectoparasites for vector competence will improve understanding of pathogen maintenance cycles and potential spillover routes.
5. **Digital and 3D pathology tools:** Integrating histologic atlases into interactive, digitized platforms will enhance accessibility, standardization, and training in ERB pathology.

6. **Comparative studies across bat species:** Extending this framework to other chiropteran taxa will help identify whether observed traits are species-specific, pan-chiropteran, or examples or convergent evolution toward viral disease tolerance.

Summary

This dissertation contributes a significant and novel body of work toward understanding the Egyptian rousette bat's immune system, pathology, and interactions with high-consequence zoonotic pathogens. By combining anatomical, ecological, experimental, and immunologic approaches, it highlights the extraordinary adaptability of ERBs as viral reservoirs and reveal how complex host-pathogen relationships may be shaped by immune architecture, coinfection, tissue-specific pathology, and evolutionary pressures. These findings are directly relevant to understanding filovirus ecology and spillover risk, but they also offer broader insights into mammalian immunology, viral disease tolerance, and the foundations of reservoir competence. In a time of increasing recognition of the global impact of emerging infectious diseases, this work underscores the critical importance of studying reservoir hosts not only as vectors, but as biological systems in the own right.

REFERENCES

1 Buckles, E. L. in *Fowler's Zoo and Wild Animal Medicine* Vol. 8 (eds RE Miller & ME Fowler) 281-290 (Elsevier Saunders, 2015).

2 Zenodo. *Bats of the World: A Taxonomic and Geographic Database. Species list and Change Logs (Version 1.7) [Data set]*, <https://zenodo.org/records/14796586> (2025).

3 Amman, B. R. *et al.* Seasonal pulses of Marburg virus circulation in juvenile *Rousettus aegyptiacus* bats coincide with periods of increased risk of human infection. *PLoS Pathog* **8**, 10: e1002877 (2012). https://doi.org/https://doi.org/10.1371/journal.ppat.1002877

4 Amman, B. R. *et al.* Oral shedding of Marburg virus in experimentally infected Egyptian fruit bats (*Rousettus aegyptiacus*). *J Wildl Dis* **51**, 1: 113-124 (2015).

5 Towner, J. S. *et al.* Marburg virus infection detected in a common African bat. *PLoS One* **2**, 8: e764 (2007). https://doi.org/10.1371/journal.pone.0000764

6 Amman, B. R. *et al.* A recently discovered pathogenic paramyxovirus, Sosuga virus, is present in *Rousettus aegyptiacus* fruit bats at multiple locations in Uganda. *J Wildl Dis* **51**, 3: 774-779 (2015).

7 Amman, B. R. *et al.* Experimental infection of Egyptian rousette bats (*Rousettus aegyptiacus*) with Sosuga virus demonstrates potential transmission routes for a bat-borne human pathogenic paramyxovirus. *PLoS Negl Trop Dis* **14**, 3: e0008092 (2020).

8 Kalunda, M. *et al.* Kasokero virus: a new human pathogen from bats (*Rousettus aegyptiacus*) in Uganda. *Am J Trop Med Hyg* **35**, 2: 387-392 (1986).

9 Kwiecinski, G. G. & Griffiths, T. A. *Rousettus egyptiacus*. *Mammal Spec* **611**: 1-9 (1999).

10 Monadjem, A., Taylor, P. J., Cotterill, F. P. D. W. & Schoeman, M. C. *Bats of Southern and Central Africa: A Biogeographic and Taxonomic Synthesis, 2nd Ed*. (Wits University Press, 2020).

11 Halley, A. C. *et al.* Coevolution of motor cortex and behavioral specializations associated with flight and echolocation in bats. *Curr Biol* **32**, 13: 2935-2941. e2933 (2022).

12 Genzel, D., Yovel, Y. & Yartsev, M. M. Neuroethology of bat navigation. *Current Biology* **28**: R997-R1004 (2018).

13 Rose, M. C., Styr, B., Schmid, T. A., Elie, J. E. & Yartsev, M. M. Cortical representation of group social communication in bats. *Science* **374**, 6566: eaba9584 (2021). https://doi.org/10.1126/science.aba9584

14 Amman, B. R., Schuh, A. J., Albariño, C. G. & Towner, J. S. Marburg virus persistence on fruit as a plausible route of bat to primate filovirus transmission. *Viruses* **13**, 12: 2394 (2021).

15 Larson, P. A. *et al.* Genomic features of humoral immunity support tolerance model in Egyptian rousette bats. *Cell Rep* **35**, 7: 109140 (2021). https://doi.org/10.1016/j.celrep.2021.109140

16 Schuh, A. J. *et al.* Natural reservoir *Rousettus aegyptiacus* bat host model of orthonairovirus infection identifies potential zoonotic spillover mechanisms. *Sci Rep* **12**, 1: 20936 (2022).

17 Kirejczyk, S. G. *et al.* Histopathologic and immunohistochemical evaluation of induced lesions, tissue tropism and host responses following experimental infection of Egyptian rousette bats (*Rousettus aegyptiacus*) with the zoonotic paramyxovirus, Sosuga virus. *Viruses* **14**, 6: 1278 (2022).
18 Kirejczyk, S. G. *et al.* Pathogenesis of Kasokero virus in experimentally infected Egyptian rousette bats (*Rousettus aegyptiacus*). *Vet Pathol* **60**, 3: 324-335 (2023).
19 Schuh, A. J. *et al.* Tick salivary gland components dampen Kasokero virus infection and shedding in its vertebrate reservoir, the Egyptian rousette bat *(Rousettus aegyptiacus)*. *Parasit Vectors* **16**, 1: 249 (2023). https://doi.org/10.1186/s13071-023-05853-7
20 Guito, J. C. *et al.* Peripheral immune responses to filoviruses in a reservoir versus spillover hosts reveal transcriptional correlates of disease. *Front Immunol* **14**, (2024). https://doi.org/10.3389/fimmu.2023.1306501
21 Lison, F. *et al.* Bat ecology and conservation in semi-arid and arid landscapes: A global systematic review. *Mammal Review* **50**: 52-67 (2020).
22 Fenton, M. B., Grinnell, A. D., Popper, A. N. & Fay, R. R. *Bat bioacoustics*. (Springer, 2016).
23 Corcoran, A. J. & Moss, C. F. Sensing in a noisy world: lessons from auditory specialists, echolocating bats. *J Exp Biol* **220**, 24: 4554-4566 (2017).
24 Tsagkogeorga, G., Parker, J., Stupka, E., Cotton, J. A. & Rossiter, S. J. Phylogenomic analyses elucidate the evolutionary relationships of bats. *Current Biology* **23**: 2262-2267 (2013).
25 Shen, Y.-Y. *et al.* Adaptive evolution of energy metabolism genes and the origin of flight in bats. *Proc Natl Acad Sci USA* **107**, 19: 8666-8671 (2010).
26 Schountz, T. Immunology of bats and their viruses: challenges and opportunities. *Viruses* **6**: 4880-4901 (2014).
27 Morales, A. E. *et al.* Bat genomes illuminate adaptations to viral tolerance and disease resistance. *Nature*: 1-10 (2025).
28 Liu, H., Wang, S. & Liu, T. Vortices and forces in biological flight: Insects, birds, and bats. *Annual Review of Fluid Mechanics* **56**: 147-170 (2024).
29 Swartz, S. M. & Middleton, K. M. Biomechanics of the bat limb skeleton: scaling, material properties and mechanics. *Cells Tissues Organs* **187**: 59-84 (2007).
30 Dimkić, I. *et al.* The microbiome of bat guano: for what is this knowledge important? *Appl Microbiol Biotechnol* **105**, 4: 1407-1419 (2021).
31 Geva-Sagiv, M., Las, L., Yovel, Y. & Ulanovsky, N. Spatial cognition in bats and rats: from sensory acquisition to multiscale maps and navigation. *Nat Rev Neurosci* **16**, 2: 94-108 (2015).
32 Harding, C. D., Yovel, Y., Peirson, S. N., Hackett, T. D. & Vyazovskiy, V. V. Re-examining extreme sleep duration in bats: implications for sleep phylogeny, ecology, and function. *Sleep* **45**: zsac064 (2022).
33 Eby, P. *et al.* Pathogen spillover driven by rapid changes in bat ecology. *Nature* **613**, 7943: 340-344 (2023).
34 Kreuder Johnson, C. *et al.* Spillover and pandemic properties of zoonotic viruses with high host plasticity. *Sci Rep* **5**, 1: 14830 (2015).
35 Wang, L.-F. & Anderson, D. E. Viruses in bats and potential spillover to animals and humans. *Current opinion in virology* **34**: 79-89 (2019).

36 Zhou, H. *et al.* Identification of novel bat coronaviruses sheds light on the evolutionary origins of SARS-CoV-2 and related viruses. *Cell* **184**: 4380-4391. e4314 (2021).
37 Zhou, P. *et al.* A pneumonia outbreak associated with a new coronavirus of probable bat origin. *nature* **579**: 270-273 (2020).
38 Lau, S. K. P. *et al.* Possible Bat Origin of Severe Acute Respiratory Syndrome Coronavirus 2. *Emerg Infect Dis* **26**, 7: 1542-1547 (2020). https://doi.org/10.3201/eid2607.200092
39 *World Health Organization. (2025). "WHO COVID-19 Dashboard". https://data.who.int/dashboards/covid19/deaths*, <https://data.who.int/dashboards/covid19/deaths> (Retrieved February 19, 2025.).
40 Caelers, D. Push to curb Tanzania's Marburg outbreak. *Nature Africa* (2025). <https://www.nature.com/articles/d44148-025-00029-0>.
41 *Centers for Disease Control and Prevention. (2025). Health Alert Network: "Ebola Outbreak Caused by Sudan virus in Uganda". https://www.cdc.gov/han/2025/han00521.html. Retrieved February 19, 2025.*
42 Dharmadhikari, A. S. *et al.* Natural infection of guinea pigs exposed to patients with highly drug-resistant tuberculosis. *Tuberculosis (Edinb)* **91**, 4: 329-338 (2011).
43 Converse, P. J. *et al.* The impact of mouse passaging of *Mycobacterium tuberculosis* strains prior to virulence testing in the mouse and guinea pig aerosol models. *PLoS One* **5**, 4: e10289 (2010).
44 David, J. M., Dick Jr, E. J. & Hubbard, G. B. Spontaneous pathology of the common marmoset (*Callithrix jacchus*) and tamarins (*Saguinus oedipus*, *Saguinus mystax*). *J Med Primatol* **38**, 5: 347-359 (2009).
45 Jones, M. E. *et al.* Experimental inoculation of Egyptian rousette bats (*Rousettus aegyptiacus*) with viruses of the Ebolavirus and Marburgvirus genera. *Viruses* **7**, 7: 3420-3442 (2015).
46 Schuh, A. J. *et al.* Modelling filovirus maintenance in nature by experimental transmission of Marburg virus between Egyptian rousette bats. *Nat Commun* **8**, 1: 14446 (2017).
47 Schuh, A. J. *et al.* Egyptian rousette bats maintain long-term protective immunity against Marburg virus infection despite diminished antibody levels. *Sci Rep* **7**, 1: 8763 (2017).
48 Towner, J. S. *et al.* Isolation of genetically diverse Marburg viruses from Egyptian fruit bats. *PLoS Pathog* **5**, 7: e1000536 (2009). https://doi.org/10.1371/journal.ppat.1000536
49 Towner, J. S. *et al.* Marburgvirus genomics and association with a large hemorrhagic fever outbreak in Angola. *J Virol* **80**, 13: 6497-6516 (2006).
50 Jones, M. E. *et al.* Clinical, histopathologic, and immunohistochemical characterization of experimental Marburg virus infection in a natural reservoir host, the Egyptian rousette bat (*Rousettus aegyptiacus*). *Viruses* **11**, 3: 214 (2019).
51 Towner, J. S. *et al.* Isolation of genetically diverse Marburg viruses from Egyptian fruit bats. *PLoS pathogens* **5**: e1000536 (2009).
52 Jones, B. D., Kaufman, E. J. & Peel, A. J. Viral Co-Infection in Bats: A Systematic Review. *Viruses* **15**, 9: 1860 (2023).

53 Orłowska, A. *et al.* First detection of bat astroviruses (BtAstVs) among bats in Poland: The genetic BtAstVs diversity reveals multiple co-infection of bats with different strains. *Viruses* **13**, 2: 158 (2021).
54 Chu, D., Peiris, J., Chen, H., Guan, Y. & Poon, L. Genomic characterizations of bat coronaviruses (1A, 1B and HKU8) and evidence for co-infections in *Miniopterus* bats. *J Gen Virol* **89**, 5: 1282-1287 (2008).
55 Wang, J. *et al.* Individual bat virome analysis reveals co-infection and spillover among bats and virus zoonotic potential. *Nat Commun* **14**: 4079 (2023).
56 Si, H.-R. *et al.* Individual virome analysis reveals the general co-infection of mammal-associated viruses with SARS-related coronaviruses in bats. *Virologica Sinica*, (2024).
57 Hoarau, A. O. *et al.* Investigation of astrovirus, coronavirus and paramyxovirus co-infections in bats in the western Indian Ocean. *Virol J* **18**: 1-8 (2021).
58 Ge, X.-Y. *et al.* Coexistence of multiple coronaviruses in several bat colonies in an abandoned mineshaft. *Virologica Sinica* **31**: 31-40 (2016).
59 Zhu, F. *et al.* Presence of recombinant Bat coronavirus GCCDC1 in Cambodian bats. *Viruses* **14**, 2: 176 (2022).
60 Mortlock, M., Dietrich, M., Weyer, J., Pawęska, J. T. & Markotter, W. Co-circulation and excretion dynamics of diverse rubula-and related viruses in Egyptian rousette bats from South Africa. *Viruses* **11**, 1: 37 (2019).
61 Baker, K. *et al.* Co-circulation of diverse paramyxoviruses in an urban African fruit bat population. *J Gen Virol* **93**, 4: 850-856 (2012).
62 Kohl, C. *et al.* Hervey virus: Study on co-circulation with Henipaviruses in Pteropid bats within their distribution range from Australia to Africa. *PLoS One* **13**, 2: e0191933 (2018).
63 Latinne, A. *et al.* One Health Surveillance Highlights Circulation of Viruses with Zoonotic Potential in Bats, Pigs, and Humans in Viet Nam. *Viruses* **15**: 790 (2023).
64 Suu-Ire, R. *et al.* Surveillance for potentially zoonotic viruses in rodent and bat populations and behavioral risk in an agricultural settlement in Ghana. *One Health Outlook* **4**, 1: 6 (2022).
65 Thompson, N. *et al.* Seroepidemiology of selected alphaviruses and flaviviruses in bats in Trinidad. *Zoonoses and public health* **62**: 53-60 (2015).
66 Mühldorfer, K. *et al.* Diseases and causes of death in European bats: dynamics in disease susceptibility and infection rates. *PLoS One* **6**, 12: e29773 (2011).
67 Wada, Y. *et al.* Detection of novel gammaherpesviruses from fruit bats in Indonesia. *Journal of medical microbiology* **67**: 415-422 (2018).
68 Kamau, J. *et al.* A novel coronavirus and a broad range of viruses in Kenyan cave bats. *Viruses* **14**: 2820 (2022).
69 Liang, J. *et al.* Detection of diverse viruses in alimentary specimens of bats in Macau. *Virol Sin* **32**, 3: 226-234 (2017).
70 Lazov, C. M., Belsham, G. J., Bøtner, A. & Rasmussen, T. B. Full-genome sequences of alphacoronaviruses and astroviruses from myotis and pipistrelle bats in Denmark. *Viruses* **13**, 6: 1073 (2021).

71 Chidoti, V. *et al.* Longitudinal survey of Astrovirus infection in different bat species in Zimbabwe: Evidence of high genetic Astrovirus diversity. *Peer Community J* **3**: e106 (2023).
72 Kemenesi, G. *et al.* Molecular survey of RNA viruses in Hungarian bats: discovering novel astroviruses, coronaviruses, and caliciviruses. *Vector Borne Zoonotic Dis* **14**, 12: 846-855 (2014). https://doi.org/10.1089/vbz.2014.1637
73 Seltmann, A. *et al.* Seasonal fluctuations of astrovirus, but not coronavirus shedding in bats inhabiting human-modified tropical forests. *Ecohealth* **14**, 2: 272-284 (2017).
74 Rizzo, F. *et al.* Coronavirus and paramyxovirus in bats from Northwest Italy. *BMC veterinary research* **13**: 1-11 (2017).
75 Lane, J. K. *et al.* Coronavirus and paramyxovirus shedding by bats in a cave and buildings in Ethiopia. *Ecohealth* **19**, 2: 216-232 (2022).
76 Lee, S.-Y., Chung, C.-U., Park, J. S. & Oem, J.-K. Novel viruses detected in bats in the Republic of Korea. *Scientific Reports* **10**: 20296 (2020).
77 Simmons, N. & Conway, T. in *Bat Ecology* (eds Thomas H Kunz & M Brock Fenton) 493-535 (The University of Chicago Press, 2003).
78 Vasenkov, D., Desmet, J.-F., Popov, I. & Sidorchuk, N. Bats can migrate farther than it was previously known: a new longest migration record by Nathusius' pipistrelle Pipistrellus nathusii (Chiroptera: Vespertilionidae). *Mammalia* **86**: 524-526 (2022).
79 Banerjee, A., Kulcsar, K., Misra, V., Frieman, M. & Mossman, K. Bats and coronaviruses. *Viruses* **11**, 1: 41 (2019).
80 Balkema, A., Bokelmann, M. & Balkema-Buschmann, A. Coronaviruses in Bats. *Berl Münch Tierärztl Wochenschr* **134**: 1-16 (2021).
81 Wellenberg, G. *et al.* Presence of European bat lyssavirus RNAs in apparently healthy *Rousettus aegyptiacus* bats. *Arch Virol* **147**, 2: 349-361 (2002). https://doi.org/10.1007/s705-002-8324-3
82 Vora, N. M. *et al.* Bat and lyssavirus exposure among humans in area that celebrates bat festival, Nigeria, 2010 and 2013. *Emerg Infect Dis* **26**, 7: 1399 (2020).
83 Constantine, D. G. & Blehert, D. S. *Bat Rabies and Other Lyssavirus Infections*. Vol. 1329 (US Geological Survey, 2009).
84 Mortlock, M. *et al.* Novel Paramyxoviruses in Bats from Sub-Saharan Africa, 2007-2012. *Emerg Infect Dis* **21**, 10: 1840-1843 (2015). https://doi.org/10.3201/eid2110.140368
85 Drexler, J. F. *et al.* Bats host major mammalian paramyxoviruses. *Nat Commun* **3**, 1: 796 (2012).
86 Schountz, T. Virology and immunology of bats. *Bat evolution, ecology, and conservation*: 393-412 (2013).
87 Moratelli, R. & Calisher, C. H. Bats and zoonotic viruses: can we confidently link bats with emerging deadly viruses? *Memórias do Instituto Oswaldo Cruz* **110**, 1: 1-22 (2015). https://doi.org/10.1590/0074-02760150048
88 Calisher, C. H., Childs, J. E., Field, H. E., Holmes, K. V. & Schountz, T. Bats: important reservoir hosts of emerging viruses. *Clin Microbiol Rev* **19**, 3: 531-545 (2006).

89 Holland, R. A. & Waters, D. A. Echolocation signals and pinnae movement in the fruitbat *Rousettus aegyptiacus*. *Acta Chiropt* **7**, 1: 83-90 (2005).
90 Holland, R. A., Waters, D. A. & Rayner, J. M. Echolocation signal structure in the Megachiropteran bat *Rousettus aegyptiacus* Geoffroy 1810. *J Exp Biol* **207**, 25: 4361-4369 (2004).
91 Waters, D. A. & Vollrath, C. Echolocation performance and call structure in the megachiropteran fruit-bat *Rousettus aegyptiacus*. *Acta Chiropt* **5**, 2: 209-219 (2003).
92 Yovel, Y., Geva-Sagiv, M. & Ulanovsky, N. Click-based echolocation in bats: not so primitive after all. *J Comp Physiol A* **197**: 515-530 (2011).
93 Amman, B. R. *et al.* Marburgvirus resurgence in Kitaka Mine bat population after extermination attempts, Uganda. *Emerg Infect Dis* **20**, 10: 1761 (2014).
94 Swanepoel, R. *et al.* Studies of reservoir hosts for Marburg virus. *Emerg Infect Dis* **13**, 12: 1847-1851 (2007). https://doi.org/10.3201/eid1312.071115
95 Pawęska, J. T. *et al.* Marburg virus infection in Egyptian rousette bats, South Africa, 2013–2014. *Emerg Infect Dis* **24**, 6: 1134 (2018).
96 Pawęska, J. T. *et al.* Shedding of Marburg virus in naturally infected Egyptian rousette bats, South Africa, 2017. *Emerg Infect Dis* **26**, 12: 3051 (2020).
97 Guito, J. C. *et al.* Asymptomatic infection of Marburg virus reservoir bats is explained by a strategy of immunoprotective disease tolerance. *Curr Biol* **31**, 2: 257-270.e255 (2021).
98 Guito, J. C. *et al.* Coordinated inflammatory responses dictate Marburg virus control by reservoir bats. *Nat Commun* **15**, 1: 1826 (2024).
99 Pavlovich, S. S. *et al.* The Egyptian rousette genome reveals unexpected features of bat antiviral immunity. *Cell* **173**: 1098-1110. e1018 (2018).
100 Prescott, J. *et al.* Rousette bat dendritic cells overcome Marburg virus-mediated antiviral responses by upregulation of interferon-related genes while downregulating proinflammatory disease mediators. *mSphere* **4**, 6: e00728-00719 (2019).
101 Arnold, C. E. *et al.* Transcriptomics Reveal Antiviral Gene Induction in the Egyptian Rousette Bat Is Antagonized In Vitro by Marburg Virus Infection. *Viruses* **10**, 11: 607 (2018). https://doi.org/10.3390/v10110607
102 Pavlovich, S. S. *et al.* Egyptian rousette IFN-ω subtypes elicit distinct antiviral effects and transcriptional responses in conspecific cells. *Front Immunol* **11**: 435 (2020).
103 Alvarez-Munoz, S., Upegui-Porras, N., Gomez, A. P. & Ramirez-Nieto, G. Key factors that enable the pandemic potential of RNA viruses and inter-species transmission: a systematic review. *Viruses* **13**, 4: 537 (2021).
104 Garcia-Blanco, M. A., Ooi, E. E. & Sessions, O. M. RNA viruses, pandemics and anticipatory preparedness. *Viruses* **14**: 2176 (2022).
105 Maganga, G. D. *et al.* Is Marburg virus enzootic in Gabon? *J Infect Dis* **204**, Suppl 3: S800-S803 (2011).
106 Pourrut, X. *et al.* Large serological survey showing cocirculation of Ebola and Marburg viruses in Gabonese bat populations, and a high seroprevalence of both viruses in *Rousettus aegyptiacus*. *BMC Infect Dis* **9**: 159 (2009). https://doi.org/10.1186/1471-2334-9-159

107 Kuzmin, I. V. *et al.* Marburg virus in fruit bat, Kenya. *Emerg Infect Dis* **16**, 2: 352 (2010).
108 Kajihara, M. *et al.* Marburgvirus in Egyptian fruit bats, Zambia. *Emerg Infect Dis* **25**, 8: 1577 (2019).
109 Tong, S. *et al.* Detection of novel SARS-like and other coronaviruses in bats from Kenya. *Emerg Infect Dis* **15**, 3: 482 (2009).
110 Li, B. *et al.* Discovery of bat coronaviruses through surveillance and probe capture-based next-generation sequencing. *Msphere* **5**: e00807-00819 (2020).
111 Anthony, S. J. *et al.* Global patterns in coronavirus diversity. *Virus Evol* **3**, 1: vex012 (2017).
112 Lacroix, A. *et al.* Wide diversity of coronaviruses in frugivorous and insectivorous bat species: a pilot study in Guinea, West Africa. *Viruses* **12**: 855 (2020).
113 Kading, R. C. & Schountz, T. Flavivirus infections of bats: potential role in Zika virus ecology. *The American journal of tropical medicine and hygiene* **95**: 993 (2016).
114 Fagre, A. C. *et al.* Subgenomic flavivirus RNA (sfRNA) associated with Asian lineage Zika virus identified in three species of Ugandan bats (family Pteropodidae). *Sci Rep* **11**, 1: 8370 (2021).
115 Kandeil, A. *et al.* Isolation and characterization of a distinct influenza A virus from Egyptian bats. *J Virol* **93**, 2: 10.1128/jvi. 01059-01018 (2019).
116 Amman, B. R. *et al.* Sosuga Virus Detected in Egyptian Rousette Bats (*Rousettus aegyptiacus*) in Sierra Leone. *Viruses* **16**, 4: 648 (2024).
117 Van der Poel, W. *et al.* Characterisation of a recently isolated lyssavirus in frugivorous zoo bats. *Archives of Virology* **145**: 1919-1931 (2000).
118 Jansen van Vuren, P. *et al.* A novel adenovirus isolated from the Egyptian fruit bat in South Africa is closely related to recent isolates from China. *Sci Rep* **8**, 1: 9584 (2018).
119 Pozo, F. *et al.* Identification of novel betaherpesviruses in Iberian bats reveals parallel evolution. *PLoS One* **11**, 12: e0169153 (2016).
120 Jánoska, M. *et al.* Novel adenoviruses and herpesviruses detected in bats. *The Veterinary Journal* **189**: 118-121 (2011).
121 Harima, H. *et al.* Surveillance, Isolation, and Genetic Characterization of Bat Herpesviruses in Zambia. *Viruses* **15**: 1369 (2023).
122 David, D. *et al.* A novel poxvirus isolated from an Egyptian fruit bat in Israel. *Vet Med Sci* **6**, 3: 587-590 (2020).
123 David, D. *et al.* Israeli *Rousettus aegyptiacus* Pox Virus (IsrRAPXV) Infection in Juvenile Egyptian Fruit Bat (*Rousettus aegyptiacus*): Clinical Findings and Molecular Detection. *Viruses* **13**, 3: 407 (2021).
124 Paran, Y. *et al.* Human Infection With IsrRAPXV: A Novel Zoonotic Bat-Derived Poxvirus. *J Infect Dis* **231**, 2: 495-500 (2025). https://doi.org/10.1093/infdis/jiae427
125 Held, J. *et al.* Bats are rare reservoirs of Staphylococcus aureus complex in Gabon. *Infection, Genetics and Evolution* **47**: 118-120 (2017).

126 Di Cataldo, S., Kamani, J., Cevidanes, A., Msheliza, E. G. & Millán, J. Hemotropic mycoplasmas in bats captured near human settlements in Nigeria. *Comp Immunol Microbiol Infect Dis* **70**: 101448 (2020).
127 Dietrich, M. *et al.* Biogeography of *Leptospira* in wild animal communities inhabiting the insular ecosystem of the western Indian Ocean islands and neighboring Africa. *Emerg Microbes Infect* **7**, 1: 1-12 (2018).
128 Qiu, Y. *et al.* Human borreliosis caused by a new world relapsing fever borrelia–like organism in the old world. *Clinical Infectious Diseases* **69**: 107-112 (2019).
129 Nowak, K. *et al.* Highly diverse and antimicrobial susceptible *Escherichia coli* display a naïve bacterial population in fruit bats from the Republic of Congo. *PLoS One* **12**, 7: e0178146 (2017).
130 Kosoy, M. *et al.* Bartonella spp. in bats, Kenya. *Emerg Infect Dis* **16**, 12: 1875 (2010).
131 Stuckey, M. J. *et al.* Bartonella, bats and bugs: a review. *Comparative Immunology, Microbiology and Infectious Diseases* **55**: 20-29 (2017).
132 Qiu, Y. *et al.* Isolation of Candidatus Bartonella rousetti and other bat-associated Bartonellae from bats and their flies in Zambia. *Pathogens* **9**: 469 (2020).
133 Dietrich, M. *et al.* Diversity of *Bartonella* and *Rickettsia* spp. in bats and their blood-feeding ectoparasites from South Africa and Swaziland. *PLoS One* **11**, 3: e0152077 (2016).
134 Weinberg, M., Nissan, Y. & Yovel, Y. in *Chiroptera. Handbook of the Mammals of Europe* (ed D Russo) 763-788 (Springer, Cham, 2023).
135 Benda, P. *et al.* Bats (Mammalia: Chiroptera) of the Eastern Mediterranean and Middle East. Part 13. Review of distribution and ectoparasites of bats in Lebanon. *Acta Soc Zool Bohem* **80**: 207-316 (2016).
136 Benda, P. *et al.* Bats (Mammalia: Chiroptera) of the Eastern Mediterranean and Middle East. Part 8. Bats of Jordan: fauna, ecology, echolocation, ectoparasites. *Acta Soc Zool Bohem* **74**: 185-353 (2010).
137 Špitalská, E., Ševčík, M., Peresh, Y.-Y. & Benda, P. Bartonella in bat flies from the Egyptian fruit bat in the Middle East. *Parasitology Research* **123**: 144 (2024).
138 Benda, P. *et al.* Bats (Mammalia: Chiroptera) of the Eastern Mediterranean and Middle East. Part 10. Bat fauna of Iran. *Acta Soc Zool Bohem* **76**: 163-582 (2012).
139 Szentiványi, T. *et al.* Vector-borne protozoan and bacterial pathogen occurrence and diversity in ectoparasites of the Egyptian Rousette bat. *Medical and Veterinary Entomology* **37**: 189-194 (2023).
140 Schuh, A. J. *et al.* Human-Pathogenic Kasokero Virus in Field-Collected Ticks. *Emerg Infect Dis* **26**, 12: 2944-2950 (2020). https://doi.org/10.3201/eid2612.202411
141 Schuh, A. J. *et al.* No evidence for the involvement of the argasid tick *Ornithodoros faini* in the enzootic maintenance of marburgvirus within Egyptian rousette bats *Rousettus aegyptiacus*. *Parasit Vectors* **9**: 128 (2016). https://doi.org/10.1186/s13071-016-1390-z
142 Fayed, H., Shazly, M. & El-Monem, S. Life cycle of Eimeria rousetti sp. nov. (Alveolata: Apicomplexa: Eimeriidae) infecting the frugivorous bat, *Rousettus aegyptiacus* Geoffroy, 1810 (Mammalia: Chiroptera: Pteropodidae) in Egypt. *J Am Sci* **7**, 12: 292-305 (2011).

143 Abd El Maleck, B. S., Abed, G. H., Maze, N. & Khalifa, R. Morphological and Ultrastructural of a New Species from Cephaline Gregarinidae Infected Fruit Egyptian Bat (*Rousettus aegyptiacus*) and its Vector. *J Bacteriol Parasitol* **6**, 5: 1 (2015).
144 Atama, N. *et al.* Survey of *Hepatocystis* parasites of fruit bats in the Amurum forest reserve, Nigeria, identifies first host record for *Rousettus aegyptiacus*. *Parasitology* **146**, 12: 1550-1554 (2019).
145 de Faveaux, M. A. Les Parasites des Chiroptères-Rôle épidémiologique chez les Animaux et l'Homme au Katanga. *Ann Parasitol Hum Comp* **40**, 1: 21-38 (1965).
146 Adam, J.-P. Transmission d'hemosporidies par des anophèles cavernicoles dans les grottes du Congo (Brazzaville). *Bull World Health Organ* **32**, 4: 598-602 (1965).
147 Witsenburg, F. *The role of bat flies (Nycteribiidae) in the ecology and evolution of the blood parasite Polychromophilus (Apicomplexa: Haemosporida)*, Université de Lausanne, Faculté de biologie et médecine, (2014).
148 Stevens, J., Teixeira, M., Bingle, L. & Gibson, W. The taxonomic position and evolutionary relationships of Trypanosoma rangeli. *International Journal for Parasitology* **29**: 749-757 (1999).
149 Clément, L. *et al.* Out of Africa: the origins of the protozoan blood parasites of the *Trypanosoma cruzi* clade found in bats from Africa. *Mol Phylogenet Evol* **145**: 106705 (2020).
150 Abed, G., Khalifa, R., A Mazen, N. & Abd—Elmaleck, B. Light and electron microscopic studies on the microfilariae of *Diptalonema vitae* Derpkagorskaya, 1923 (Nematoda: Filariidae) parasitizing the blood of fruit bats *Rousettus aegyptiacus* aegyptiacus at Assiut locality. *Assiut Veterinary Medical Journal* **51**, 105: 1-5 (2005).
151 Rønsholt, L. *et al.* Clinically silent rabies infection in (zoo) bats. *The Veterinary Record* **142**: 519-520 (1998).
152 Rector, A. *et al.* Genetic characterization of the first chiropteran papillomavirus, isolated from a basosquamous carcinoma in an Egyptian fruit bat: the *Rousettus aegyptiacus* papillomavirus type 1. *Vet Microbiol* **117**, 2-4: 267-275 (2006).
153 McKnight, C. A. *et al.* Papillomavirus-associated basosquamous carcinoma in an Egyptian fruit bat (*Rousettus aegyptiacus*). *J Zoo Wildl Med* **37**, 2: 193-196 (2006).
154 Modesto, M. *et al.* Characterization of Bifidobacterium species in feaces of the Egyptian fruit bat: Description of B. vespertilionis sp. nov. and B. rousetti sp. nov. *Systematic and Applied Microbiology* **42**: 126017 (2019).
155 Han, J. E. *et al.* Isolation of a zoonotic pathogen Kluyvera ascorbata from Egyptian fruit-bat *Rousettus aegyptiacus*. *J Vet Med Sci* **72**, 1: 85-87 (2010).
156 Hughes, K., Constantino-Casas, F., Haverson, V. A. & Philp, S. J. Pathology in Practice. *Journal of the American Veterinary Medical Association* **253**, 7: 865-868 (2018).
157 Nakamura, S. *et al.* Outbreak of yersiniosis in Egyptian rousette bats (*Rousettus aegyptiacus*) caused by *Yersinia pseudotuberculosis* serotype 4b. *J Comp Pathol* **148**, 4: 410-413 (2013).

158 Childs-Sanford, S. E. *et al. Yersinia pseudotuberculosis* in a closed colony of Egyptian fruit bats (*Rousettus aegyptiacus)*. *J Zoo Wildl Med* **40**, 1: 8-14 (2009).
159 Akbar, H. *et al.* Characterizing *Pneumocystis* in the lungs of bats: understanding *Pneumocystis* evolution and the spread of *Pneumocystis* organisms in mammal populations. *Appl Environ Microbiol* **78**, 22: 8122-8136 (2012).
160 Childs-Sanford, S., Garner, M., Raymond, J., Didier, E. & Kollias, G. Disseminated microsporidiosis due to Encephalitozoon hellem in an Egyptian fruit bat (*Rousettus aegyptiacus*). *J Comp Pathol* **134**, 4: 370-373 (2006).
161 Leone, A. M. *et al.* A retrospective study of the lesions associated with iron storage disease in captive Egyptian fruit bats (*Rousettus aegyptiacus*). *J Zoo Wildl Med* **47**, 1: 45-55 (2016).
162 Cushing, A. C., Ossiboff, R., Buckles, E. & Abou-Madi, N. Metastatic pancreatic carcinoma and bronchioloalveolar adenomas in an Egyptian fruit bat (*Rousettus aegyptiacus*). *J Zoo Wildl Med* **44**, 3: 794-798 (2013).
163 Bradford, C., Jennings, R. & Ramos-Vara, J. Gastrointestinal leiomyosarcoma in an Egyptian fruit bat (*Rousettus aegyptiacus*). *J Vet Diagn Invest* **22**, 3: 462-465 (2010).
164 Olds, J. E. & Derscheid, R. J. Extraskeletal osteosarcoma in an Egyptian fruit bat (*Rousettus aegyptiacus*). *Vet Rec Case Rep* **6**, 2: e000579 (2018).
165 Olds, J. E. *et al.* Retrospective evaluation of cases of neoplasia in a captive population of Egyptian fruit bats (*Rousettus aegyptiacus*). *J Zoo Wildl Med* **46**: 325-332 (2015).
166 McLelland, D. J., Dutton, C. J. & Barker, I. K. Sarcomatoid carcinoma in the lung of an Egyptian fruit bat (*Rousettus aegyptiacus*). *J Vet Diagn Invest* **21**, 1: 160-163 (2009).
167 Kawaguchi, N. *et al.* Hepatocellular carcinoma with lung metastasis showing hemochromatosis in an Egyptian fruit bat (*Rousettus aegyptiacus*). *J Vet Med Sci* **86**, 1: 49-53 (2024).
168 Siegal-Willott, J., Heard, D., Sliess, N., Naydan, D. & Roberts, J. Microchip-associated leiomyosarcoma in an Egyptian fruit bat (*Rousettus aegyptiacus)*. *J Zoo Wildl Med* **38**, 2: 352-356 (2007).
169 Kirejczyk, S. G. *et al.* A retrospective study of pathology in bats submitted to an exotic and zoo animal diagnostic service in Georgia, USA (2008–2019). *J Comp Pathol* **185**: 96-107 (2021).
170 Duncan, M. *et al.* Multicentric hyperostosis consistent with fluorosis in captive fruit bats (*Pteropus giganteus, P. poliocephalus,* and *Rousettus aegyptiacus*). *J Zoo Wildl Med* **27**, 3: 325-338 (1996).
171 Fountain, K. I., Stevens, K. B., Lloyd, D. H. & Loeffler, A. Skin disease in captive bats: results of an online survey of zoos and rehabilitators in Europe, North America and Australasia. *Vet Dermatol* **28**, 2: 219-e252 (2017).
172 Pastor, A. R., Stasiak, I., Nielsen, A. M. & Smith, D. A. Hepatic to pulmonary embolism of absorbable gelatin hemostatic sponge in two egyptian fruit bats (*Rousettus aegyptiacus*). *J Zoo Wildl Med* **53**, 3: 628-631 (2022).
173 Van Der Westhuyzen, J. Haematology and iron status of the Egyptian fruit bat, *Rousettus aegyptiacus*. *Comp Biochem Physiol A Comp Physiol* **90**, 1: 117-120 (1988).

174 Stasiak, I. M. *et al.* Iron storage disease (hemochromatosis) and hepcidin response to iron load in two species of pteropodid fruit bats relative to the common vampire bat. *J Comp Physiol B* **188**, 4: 683-694 (2018). https://doi.org/10.1007/s00360-018-1155-4
175 Farina, L. L. *et al.* Iron storage disease in captive Egyptian fruit bats (*Rousettus aegyptiacus*): Relationship of blood iron parameters to hepatic iron concentrations and hepatic histopathology. *J Zoo Wildl Med* **36**, 2: 212-221 (2005).
176 Clauss, M. & Paglia, D. E. Iron storage disorders in captive wild mammals: the comparative evidence. *J Zoo Wildl Med* **43**, 3: S6-18 (2012). https://doi.org/doi: 10.1638/2011-0152.1.
177 Theelen, M. J. P., Beukers, M., Grinwis, G. C. M. & Sloet van Oldruitenborgh-Oosterbaan, M. M. Chronic iron overload causing haemochromatosis and hepatopathy in 21 horses and one donkey. *Equine Vet J* **51**, 3: 304-309 (2019). https://doi.org/10.1111/evj.13029
178 Nojiri, K., Kondo, H., Nagamune, M., Yamashita, T. & Shibuya, H. First case of hemochromatosis in a sugar glider (Petaurus breviceps). *Journal of Veterinary Medical Science* **85**, 2: 194-198 (2023). https://doi.org/10.1292/jvms.22-0361
179 Smith, K. M. *et al.* Hematologic iron analyte values as an indicator of hepatic hemosiderosis in Callitrichidae. *Am J Primatol* **70**: 629-633 (2008). https://doi.org/10.1002/ajp.20538
180 Lamoureux, L. M., Coda, K. A. & Halliday, L. C. Hemochromatosis in Two Female Olive Baboons (Papio anubis). *Comparative Medicine* **71**: 99-105 (2021). https://doi.org/10.30802/AALAS-CM-20-000070
181 Cudd, S. K., Garner, M. M., Cartoceti, A. N. & LaDouceur, E. E. Hepatic lesions associated with iron accumulation in captive kori bustards (*Ardeotis kori*). *Vet Pathol* **59**, 1: 164-168 (2022).
182 Olias, P. *et al.* Iron overload syndrome in the black rhinoceros (*Diceros bicornis*): microscopical lesions and comparison with other rhinoceros species. *J Comp Pathol* **147**, 4: 542-549 (2012).
183 O'Connor, M. R. & Garner, M. M. Iron Storage Disease in African Grey Parrots (*Psittacus Erithacus*) Exposed to a Carnivorous Diet. *J Zoo Wildl Med* **49**, 1: 172-177 (2018). https://doi.org/10.1638/2016-0266R1.1
184 Sheppard, C. & Dierenfeld, E. Iron storage disease in birds: speculation on etiology and implications for captive husbandry. *Journal of Avian Medicine and Surgery* **16**: 192-197 (2002).
185 Bonar, C. J., Trupkiewicz, J. G., Toddes, B. & Lewandowski, A. H. Iron storage disease in tapirs. *J Zoo Wildl Med* **37**, 1: 49-52 (2006).
186 Arenales, A. *et al.* Pathologic Findings in 36 Sloths from Brazil. *J Zoo Wildl Med* **51**, 3: 672-677 (2020). https://doi.org/10.1638/2020-0002
187 Glenn, K. M., Campbell, J. L., Rotstein, D. & Williams, C. V. Retrospective evaluation of the incidence and severity of hemosiderosis in a large captive lemur population. *Am J Primatol* **68**, 4: 369-381 (2006). https://doi.org/10.1002/ajp.20231
188 Phillips, B. E., Venn-Watson, S., Archer, L. L., Nollens, H. H. & Wellehan Jr, J. F. Preliminary Investigation of Bottlenose Dolphins (Tursiops truncatus) for hfe Gene–related Hemochromatosis. *J Wildl Dis* **50**, 4: 891-895 (2014).

189 Olynyk, J. K. & Ramm, G. A. Hemochromatosis. *N Engl J Med* **387**, 23: 2159-2170 (2022).
190 Turshudzhyan, A., Wu, D. C. & Wu, G. Y. Primary Non-HFE Hemochromatosis: A Review. *J Clin Transl Hepatol* **11**, 4: 925-931 (2023).
191 Stasiak, I. M. *et al.* Characterization of the hepcidin gene in eight species of bats. *Res Vet Sci* **96**, 1: 111-117 (2014). https://doi.org/10.1016/j.rvsc.2013.10.013
192 Milward, E. A. *et al.* Noncitrus fruits as novel dietary environmental modifiers of iron stores in people with or without HFE gene mutations. *Mayo Clin Proc* **83**, 5: 543-549 (2008). https://doi.org/10.4065/83.5.543
193 Paganoni, R., Lechel, A. & Vujic Spasic, M. Iron at the interface of hepatocellular carcinoma. *Int J Mol Sci* **22**, 8: 4097 (2021).
194 Snow, R. *et al.* Concurrent iron overload and neoplasia in Leschenault's rousettes (*Rousettus leschenaultii)*: A case series. *J Zoo Wildl Med* **55**, 1: 235-247 (2024).
195 Drakesmith, H. & Prentice, A. Viral infection and iron metabolism. *Nat Rev Microbiol* **6**, 7: 541-552 (2008).
196 Brauburger, K., Hume, A. J., Mühlberger, E. & Olejnik, J. Forty-five years of Marburg virus research. *Viruses* **4**, 10: 1878-1927 (2012). https://doi.org/10.3390/v4101878
197 Bharat, T. A. *et al.* Cryo-electron tomography of Marburg virus particles and their morphogenesis within infected cells. *PLoS Biol* **9**, 11: e1001196 (2011). https://doi.org/10.1371/journal.pbio.1001196
198 Olejnik, J., Mühlberger, E. & Hume, A. J. Recent advances in marburgvirus research. *F1000Research* **8**, (2019).
199 Hume, A. J. & Mühlberger, E. Distinct genome replication and transcription strategies within the growing filovirus family. *Journal of molecular biology* **431**: 4290-4320 (2019).
200 Feldmann, H., Volchkov, V., Volchkova, V. & Klenk, H.-D. *The glycoproteins of Marburg and Ebola virus and their potential roles in pathogenesis*. (Springer, 1999).
201 Sanchez, A., Geisbert, T. & Feldmann, H. *Filoviridae: Marburg and Ebola Viruses. In: Fields Virology (6th Ed).* (Philadelphia, PA, USA: Lippincott Williams and Wilkins, 2013).
202 Gordon, T. B., Hayward, J. A., Marsh, G. A., Baker, M. L. & Tachedjian, G. Host and viral proteins modulating ebola and marburg virus egress. *Viruses* **11**: 25 (2019).
203 Olejnik, J., Ryabchikova, E., Corley, R. B. & Mühlberger, E. Intracellular events and cell fate in filovirus infection. *Viruses* **3**, 8: 1501-1531 (2011). https://doi.org/10.3390/v3081501
204 Ahmad, I. *et al.* An overview of the role of Niemann-pick C1 (NPC1) in viral infections and inhibition of viral infections through NPC1 inhibitor. *Cell Commun Signal* **21**, 1: 352 (2023).
205 Liu, N., Girvin, M. E., Brenowitz, M. & Lai, J. R. Conformational and lipid bilayer-perturbing properties of Marburg virus GP2 segments containing the fusion loop and membrane-proximal external region/transmembrane domain. *Heliyon* **5**, 12: e03018 (2019).

206 Miller, E. H. & Chandran, K. Filovirus entry into cells - new insights. *Curr Opin Virol* **2**, 2: 206-214 (2012). https://doi.org/10.1016/j.coviro.2012.02.015
207 Mittler, E., Kolesnikova, L., Hartlieb, B., Davey, R. & Becker, S. The cytoplasmic domain of Marburg virus GP modulates early steps of viral infection. *J Virol* **85**: 8188-8196 (2011). https://doi.org/10.1128/JVI.00453-11
208 Koehler, A., Pfeiffer, S., Kolesnikova, L. & Becker, S. Analysis of the multifunctionality of Marburg virus VP40. *J Gen Virol* **99**: 1614-1620 (2018). https://doi.org/10.1099/jgv.0.001169
209 Kolesnikova, L., Mittler, E., Schudt, G., Shams-Eldin, H. & Becker, S. Phosphorylation of Marburg virus matrix protein VP40 triggers assembly of nucleocapsids with the viral envelope at the plasma membrane. *Cell Microbiol* **14**: 182-197 (2012). https://doi.org/10.1111/j.1462-5822.2011.01709.x
210 Siegert, R., Shu, H., Slenczka, H., Peters, D. & Müller, G. The aetiology of an unknown human infection transmitted by monkeys (preliminary communication). *Ger Med Mon* **13**, 1: 1-2 (1968).
211 Johnson, E. *et al.* Characterization of a new Marburg virus isolated from a 1987 fatal case in Kenya. *Arch Virol Suppl* **11**: 101-114 (1996). https://doi.org/10.1007/978-3-7091-7482-1_10
212 Bausch, D. G. *et al.* Marburg hemorrhagic fever associated with multiple genetic lineages of virus. *N Engl J Med* **355**: 909-919 (2006).
213 Pigott, D. M. *et al.* Mapping the zoonotic niche of Marburg virus disease in Africa. *Trans R Soc Trop Med Hyg* **109**, 6: 366-378 (2015). https://doi.org/10.1093/trstmh/trv024
214 Conrad, J. *et al.* Epidemiologic investigation of Marburg virus disease, Southern Africa, 1975. *Am J Trop Med Hyg* **27**, 6: 1210-1215 (1978). https://doi.org/doi: 10.4269/ajtmh.1978.27.1210
215 Smith, D. *et al.* Marburg-virus disease in Kenya. *The Lancet* **319**: 816-820 (1982).
216 Nikiforov, V. *et al.* A case of a laboratory infection with Marburg fever. *Zhurnal Mikrobiologii, Epidemiologii I Immunobiologii*: 104-106 (1994).
217 Adjemian, J. *et al.* Outbreak of Marburg hemorrhagic fever among miners in Kamwenge and Ibanda Districts, Uganda, 2007. *J Infect Dis* **204**, Suppl 3: S796-S799 (2011).
218 CDC. Imported case of Marburg hemorrhagic fever – Colorado, 2008. *MMWR Morb Mortal Wkly Rep* **58**, 49: 1377-1381 (Centers for Disease Control and Prevention. 2009).
219 Timen, A. *et al.* Response to imported case of Marburg hemorrhagic fever, the Netherlands. *Emerg Infect Dis* **15**, 8: 1171 (2009).
220 Albariño, C. *et al.* Genomic analysis of filoviruses associated with four viral hemorrhagic fever outbreaks in Uganda and the Democratic Republic of the Congo in 2012. *Virology* **442**, 2: 97-100 (2013).
221 *Centers for Disease Control and Prevention. (2025). History of Marburg Outbreaks. https://www.cdc.gov/marburg/outbreaks/index.html#cdc_listing_res3-history-of-marburg-1967-2023. Retrieved February 21, 2025.*
222 Nyakarahuka, L. *et al.* Marburg virus disease outbreak in Kween District Uganda, 2017: Epidemiological and laboratory findings. *PLoS Negl Trop Dis* **13**, 3: e0007257 (2019).

223 Koundouno, F. R. *et al.* Detection of Marburg virus disease in Guinea. *N Engl J Med* **386**: 2528-2530 (2022).
224 Sah, R. *et al.* Marburg Virus and Monkeypox Virus: The Concurrent Outbreaks in Ghana and the lesson learned from the Marburg Virus Containment. *J Pure Appl Microbiol* **16**: 3179-3184 (2022).
225 Wellington, J. *et al.* Marburg virus outbreak in Ghana: An impending crisis. *Ann Med Surg (Lond)* **81**: 104377 (2022).
226 Sibomana, O. & Kubwimana, E. First-ever Marburg virus disease outbreak in Equatorial Guinea and Tanzania: An imminent crisis in West and East Africa. *Immunity, Inflammation and Disease* **11**: e980 (2023).
227 Samarasekera, U. Marburg virus outbreak in Equatorial Guinea. *The Lancet Infectious Diseases* **23**: 534 (2023).
228 Deb, N. *et al.* Marburg Virus Disease in Tanzania: The most recent outbreak. *New Microbes New Infect* **53**: 101123 (2023).
229 Butera, Y. *et al.* Genomic and transmission dynamics of the 2024 Marburg virus outbreak in Rwanda. *Nat Med* **31**, 2: 422-426 (2024).
230 Grobusch, M. P. *et al.* Marburg virus disease outbreak in Rwanda, 2024. *Clinical Microbiology and Infection*, (2024).
231 Gashugi, Y., Byiringiro, L. B., Rukundo, J., Society, R. P. & Gashugi, Y. Marburg virus disease outbreak in Rwanda: Current Efforts and Call to Action to mitigate MRV in Rwanda. *Research Gate*, (2024). https://doi.org/10.13140/RG.2.2.15846.43843
232 *World Health Organization. (2025). Disease Outbreak News; Marburg virus disease in the United Republic of Tanzania. https://www.who.int/emergencies/disease-outbreak-news/item/2025-DON554. Retrieved February 21, 2025.*
233 Shifflett, K. & Marzi, A. Marburg virus pathogenesis - differences and similarities in humans and animal models. *Virol J* **16**, 1: 165 (2019). https://doi.org/10.1186/s12985-019-1272-z
234 Bosio, C. M. *et al.* Ebola and Marburg viruses replicate in monocyte-derived dendritic cells without inducing the production of cytokines and full maturation. *J Infect Dis* **188**, 11: 1630-1638 (2003).
235 Cooper, T. K. *et al.* New Insights Into Marburg Virus Disease Pathogenesis in the Rhesus Macaque Model. *J Infect Dis* **218**, 5: S423-S433 (2018). https://doi.org/10.1093/infdis/jiy367
236 Blair, P. W. *et al.* Virulence of Marburg virus Angola compared to Mt. Elgon (Musoke) in macaques: a pooled survival analysis. *Viruses* **10**, 11: 658 (2018).
237 Hartman, A. L., Towner, J. S. & Nichol, S. T. Ebola and Marburg hemorrhagic fever. *Clin Lab Med* **30**, 1: 161-177 (2010).
238 Edwards, M. R. *et al.* Differential regulation of interferon responses by Ebola and Marburg virus VP35 proteins. *Cell Rep* **14**, 7: 1632-1640 (2016).
239 Valmas, C. & Basler, C. F. Marburg virus VP40 antagonizes interferon signaling in a species-specific manner. *J Virol* **85**, 9: 4309-4317 (2011).
240 Valmas, C. *et al.* Marburg virus evades interferon responses by a mechanism distinct from ebola virus. *PLoS Pathog* **6**, 1: e1000721 (2010).

241 Bausch, D. G. *et al.* Risk factors for Marburg hemorrhagic fever, Democratic Republic of the Congo. *Emerg Infect Dis* **9**, 12: 1531 (2003).
242 Kuhn, J. H. *et al.* Filovirus RefSeq entries: evaluation and selection of filovirus type variants, type sequences, and names. *Viruses* **6**, 9: 3663-3682 (2014).
243 Pawęska, J. T. *et al.* Lack of Marburg virus transmission from experimentally infected to susceptible in-contact Egyptian fruit bats. *J Infect Dis* **212**, 2: S109-S118 (2015).
244 Pawęska, J. T. *et al.* Virological and serological findings in *Rousettus aegyptiacus* experimentally inoculated with vero cells-adapted hogan strain of Marburg virus. *PLoS One* **7**, 9: e45479 (2012).
245 Nakayama, E. & Saijo, M. Animal models for Ebola and Marburg virus infections. *Front Microbiol* **4**: 267 (2013). https://doi.org/10.3389/fmicb.2013.00267
246 Glaze, E. R., Roy, M. J., Dalrymple, L. W. & Lanning, L. L. A comparison of the pathogenesis of Marburg virus disease in humans and nonhuman Primates and evaluation of the suitability of these animal models for predicting clinical efficacy under the 'Animal Rule'. *Comp Med* **65**, 3: 241-259 (2015).
247 Cross, R. W. *et al.* Comparison of the pathogenesis of the Angola and Ravn strains of Marburg virus in the outbred guinea pig model. *J Infect Dis* **212**, 2: S258-S270 (2015).
248 Geisbert, T. W., Strong, J. E. & Feldmann, H. Considerations in the use of nonhuman primate models of Ebola virus and Marburg virus infection. *J Infect Dis* **212**, 2: S91-S97 (2015).
249 Warfield, K. L. *et al.* Development and characterization of a mouse model for Marburg hemorrhagic fever. *J Virol* **83**, 13: 6404-6415 (2009).
250 Krähling, V. *et al.* Establishment of fruit bat cells (*Rousettus aegyptiacus*) as a model system for the investigation of filoviral infection. *PLoS Negl Trop Dis* **4**, 8: e802 (2010).
251 Bradfute, S. B., Warfield, K. L. & Bray, M. Mouse models for filovirus infections. *Viruses* **4**: 1477-1508 (2012).
252 Gentles, A. D., Guth, S., Rozins, C. & Brook, C. E. A review of mechanistic models of viral dynamics in bat reservoirs for zoonotic disease. *Pathog Glob Health* **114**, 8: 407-425 (2020).
253 Reynolds, P. & Marzi, A. Ebola and Marburg virus vaccines. *Virus Genes* **53**, 4: 501-515 (2017).
254 Cross, R. W., Mire, C. E., Feldmann, H. & Geisbert, T. W. Post-exposure treatments for Ebola and Marburg virus infections. *Nat Rev Drug Discov* **17**, 6: 413-434 (2018).
255 Grant-Klein, R. J. *et al.* A multiagent filovirus DNA vaccine delivered by intramuscular electroporation completely protects mice from ebola and Marburg virus challenge. *Hum Vaccin Immunother* **8**, 11: 1703-1706 (2012). https://doi.org/10.4161/hv.21873
256 Wang, D. *et al.* Complex adenovirus-vectored vaccine protects guinea pigs from three strains of Marburg virus challenges. *Virology* **353**, 2: 324-332 (2006). https://doi.org/10.1016/j.virol.2006.05.033

257 Mire, C. E. *et al.* Therapeutic treatment of Marburg and Ravn virus infection in nonhuman primates with a human monoclonal antibody. *Sci Transl Med* **9**, 384: eaai8711 (2017).
258 Thi, E. P. *et al.* siRNA rescues nonhuman primates from advanced Marburg and Ravn virus disease. *J Clin Invest* **127**, 12: 4437-4448 (2017).
259 Wong, G. *et al.* Marburg and Ravn virus infections do not cause observable disease in ferrets. *J Infect Dis* **218**, 5: S471-S474 (2018).
260 Cross, R. W. *et al.* Marburg and Ravn viruses fail to cause disease in the domestic ferret (*Mustela putorius furo*). *J Infect Dis* **218**, 5: S448-S452 (2018).
261 Nicholas, V. V. *et al.* Distinct biological phenotypes of Marburg and Ravn virus infection in macaques. *J Infect Dis* **218**, 5: S458-S465 (2018).
262 Baker, M., Schountz, T. & Wang, L. F. Antiviral immune responses of bats: a review. *Zoonoses Public Health* **60**, 1: 104-116 (2013).
263 Peel, A. J. *et al.* Synchronous shedding of multiple bat paramyxoviruses coincides with peak periods of Hendra virus spillover. *Emerg Microbes Infect* **8**, 1: 1314-1323 (2019).
264 Mahalingam, S. *et al.* Hendra virus: an emerging paramyxovirus in Australia. *The Lancet Infectious Diseases* **12**, 10: 799-807 (2012).
265 Yadav, P. D. *et al.* Nipah Virus Sequences from Humans and Bats during Nipah Outbreak, Kerala, India, 2018. *Emerg Infect Dis* **25**, 5: 1003-1006 (2019). https://doi.org/10.3201/eid2505.181076
266 Sohayati, A. *et al.* Evidence for Nipah virus recrudescence and serological patterns of captive Pteropus vampyrus. *Epidemiol Infect* **139**, 10: 1570-1579 (2011).
267 Jayaprakash, A. D. *et al.* Marburg and Ebola virus infections elicit a complex, muted inflammatory state in bats. *Viruses* **15**, 2: 350 (2023).
268 Guyton, J. A. & Brook, C. E. African bats: Conservation in the time of Ebola. *Therya* **6**: 69-88 (2015).
269 Crits-Christoph, A. *et al.* Genetic evidence of susceptible wildlife in SARS-CoV-2 positive samples at the Huanan Wholesale Seafood Market, Wuhan: Analysis and interpretation of data released by the Chinese Center for Disease Control. *Zenodo*, (2023). https://doi.org/10.5281/zenodo.7754299
270 Olival, K. J. *et al.* Possibility for reverse zoonotic transmission of SARS-CoV-2 to free-ranging wildlife: A case study of bats. *PLoS Pathog* **16**, 9: e1008758 (2020).
271 Schlottau, K. *et al.* SARS-CoV-2 in fruit bats, ferrets, pigs, and chickens: an experimental transmission study. *Lancet Microbe* **1**, 5: e218-e225 (2020). https://doi.org/10.1016/s2666-5247(20)30089-6
272 Jebb, D. *et al.* Six reference-quality genomes reveal evolution of bat adaptations. *Nature* **583**, 7817: 578-584 (2020).
273 Fujii, H. *et al.* Functional analysis of *Rousettus aegyptiacus* "signal transducer and activator of transcription 1" (STAT1). *Dev Comp Immunol* **34**, 5: 598-602 (2010).
274 Amman, B. R. & Towner, J. S. Orthomarburgvirus, Paramyxovirus, and Orthonairovirus Co-Infections in Egyptian Rousette Bats, Uganda and Sierra Leone. *Emerg Infect Dis* **Submitted 2024**, (2025).

275 Fagre, A. C. *et al. Bartonella* infection in fruit bats and bat flies, Bangladesh. *Microb Ecol* **86**, 4: 2910-2922 (2023).
276 Han, H.-J. *et al.* Novel Bartonella species in insectivorous bats, northern China. *PLoS One* **12**, 1: e0167915 (2017).
277 Dietrich, M. *et al. Leptospira* and paramyxovirus infection dynamics in a bat maternity enlightens pathogen maintenance in wildlife. *Environ Microbiol* **17**, 11: 4280-4289 (2015).
278 Menozzi, B. D. *et al.* Rabies virus and Histoplasma suramericanum coinfection in a bat from southeastern Brazil. *Zoonoses and public health* **67**: 138-147 (2020).
279 Hayman, D. T. Biannual birth pulses allow filoviruses to persist in bat populations. *Proceedings of the Royal Society B: Biological Sciences* **282**: 20142591 (2015).
280 Plowright, R. K. *et al.* Transmission or within-host dynamics driving pulses of zoonotic viruses in reservoir–host populations. *PLoS Negl Trop Dis* **10**, 8: e0004796 (2016).
281 Murphy, K., Weaver, C., Berg, L., Barton, G. & Janeway, C. *Janeway's Immunobiology*. 10th edition edn, (W.W. Norton and Company, 2022).
282 Schuh, A. J. *et al.* Modelling natural coinfection in bat reservoir shows modulation of Marburg virus shedding and spillover potential. *PLoS Pathog* **21**, 3: e1012901 (2025).
283 Davy, C. M. *et al.* White-nose syndrome is associated with increased replication of a naturally persisting coronaviruses in bats. *Sci Rep* **8**, 1: 15508 (2018).
284 Teeling, E. C. *et al.* A molecular phylogeny for bats illuminates biogeography and the fossil record. *Science* **307**: 580-584 (2005). https://doi.org/10.1126/science.1105113
285 Almeida, F. C., Giannini, N. P., Simmons, N. B. & Helgen, K. M. Each flying fox on its own branch: a phylogenetic tree for Pteropus and related genera (Chiroptera: Pteropodidae). *Molecular Phylogenetics and Evolution* **77**: 83-95 (2014).
286 ZOVER. *The Database of Zoonotic and Vector-Borne Viruses. Live Data Statistics of Bat-Associated Viruses*, <http://www.mgc.ac.cn/cgi-bin/ZOVER/statistics.cgi?db=bat> (2024).
287 Anthony, S. J. *et al.* A strategy to estimate unknown viral diversity in mammals. *mBio* **4**, 5: e00598-00513 (2013).
288 Raut, C. G. *et al.* Isolation of a novel adenovirus from *Rousettus leschenaultii* bats from India. *Intervirology* **55**, 6: 488-490 (2012). https://doi.org/10.1159/000337026
289 Elbert, J. *et al.* Characterization of Ravn virus viral shedding dynamics in experimentally infected Egyptian rousette bats (*Rousettus aegyptiacus*). *J Virol* **e00045-25**, (2025). https://doi.org/10.1128/jvi.00045-25
290 Williamson, M. M., Hooper, P. T., Selleck, P. W., Westbury, H. A. & Slocombe, R. F. Experimental hendra virus infection in pregnant guinea-pigs and fruit Bats (*Pteropus poliocephalus*). *J Comp Pathol* **122**, 2-3: 201-207 (2000). https://doi.org/10.1053/jcpa.1999.0364

291 Middleton, D. J. *et al.* Experimental Nipah virus infection in pteropid bats (*Pteropus poliocephalus*). *J Comp Pathol* **136**, 4: 266-272 (2007). https://doi.org/10.1016/j.jcpa.2007.03.002
292 Field, H., McCall, B. & Barrett, J. Australian bat lyssavirus infection in a captive juvenile black flying fox. *Emerg Infect Dis* **5**, 3: 438-440 (1999). https://doi.org/10.3201/eid0503.990316
293 McColl, K. A. *et al.* Pathogenesis studies with Australian bat lyssavirus in grey-headed flying foxes (*Pteropus poliocephalus*). *Aust Vet J* **80**, 10: 636-641 (2002). https://doi.org/10.1111/j.1751-0813.2002.tb10973.x
294 Downs, W. G., Anderson, C. R., Spence, L., Aitken, T. H. & Greenhall, A. H. Tacaribe virus, a new agent isolated from *Artibeus* bats and mosquitoes in Trinidad, West Indies. *Am J Trop Med Hyg* **12**: 640-646 (1963). https://doi.org/10.4269/ajtmh.1963.12.640
295 Cogswell-Hawkinson, A. *et al.* Tacaribe virus causes fatal infection of an ostensible reservoir host, the Jamaican fruit bat. *J Virol* **86**, 10: 5791-5799 (2012). https://doi.org/10.1128/jvi.00201-12
296 Negredo, A. *et al.* Discovery of an ebolavirus-like filovirus in Europe. *PLoS Pathog* **7**, 10: e1002304 (2011). https://doi.org/10.1371/journal.ppat.1002304
297 Hoyt, J. R., Kilpatrick, A. M. & Langwig, K. E. Ecology and impacts of white-nose syndrome on bats. *Nat Rev Microbiol* **19**, 3: 196-210 (2021).
298 Evans, N. J., Bown, K., Timofte, D., Simpson, V. R. & Birtles, R. J. Fatal borreliosis in bat caused by relapsing fever spirochete, United Kingdom. *Emerg Infect Dis* **15**, 8: 1331 (2009).
299 Mühldorfer, K. Bats and bacterial pathogens: a review. *Zoonoses and public health* **60**: 93-103 (2013).
300 Weinberg, M. *et al.* Seasonal challenges of tropical bats in temperate zones. *Scientific Reports* **12**: 16869 (2022).
301 Brook, C. E. & Dobson, A. P. Bats as 'special' reservoirs for emerging zoonotic pathogens. *Trends Microbiol* **23**, 3: 172-180 (2015).
302 Makenov, M. T. *et al.* Marburg virus in Egyptian Rousettus bats in Guinea: Investigation of Marburg virus outbreak origin in 2021. *PLoS Negl Trop Dis* **17**, 4: e0011279 (2023).
303 Khannoon, E. R., Usui, K. & Tokita, M. Embryonic development of the Egyptian fruit bat *Rousettus aegyptiacus* (Mammalia: Chiroptera: Pteropodidae). *Acta Chiropt* **21**, 2: 309-319 (2019).
304 Baker, M. L. & Schountz, T. in *Advances in Comparative Immunology* (ed E Cooper) 839-862 (Springer International Publishing, 2018).
305 Schountz, T., Baker, M. L., Butler, J. & Munster, V. Immunological control of viral infections in bats and the emergence of viruses highly pathogenic to humans. *Front Immunol* **8**: 1098 (2017).
306 Butler, J., Wertz, N. & Baker, M. in *Comparative Immunoglobulin Genetics* (eds AK Kaushik & Y Pasman) 54-84 (Apple Academic Press, 2014).
307 Butler, J. E. *et al.* The two suborders of chiropterans have the canonical heavy-chain immunoglobulin (Ig) gene repertoire of eutherian mammals. *Dev Comp Immunol* **35**, 3: 273-284 (2011).

308 Baker, M. L. & Zhou, P. in *Bats and Viruses: A New Frontier of Emerging Infectious Diseases* (eds L-F Wang & C Cowled) 327-348 (John Wiley & Sons, 2015).
309 Becker, D. J. *et al.* Diverse hosts, diverse immune systems: evolutionary variation in bat immunology. *EcoEvoRxiv*, (2025). https://doi.org/10.32942/X2HD0D
310 Ahn, M. *et al.* Dampened NLRP3-mediated inflammation in bats and implications for a special viral reservoir host. *Nat Microbiol* **4**, 5: 789-799 (2019).
311 Zhang, G. *et al.* Comparative analysis of bat genomes provides insight into the evolution of flight and immunity. *Science* **339**, 6118: 456-460 (2013).
312 Haydon, D. T., Cleaveland, S., Taylor, L. H. & Laurenson, M. K. Identifying reservoirs of infection: a conceptual and practical challenge. *Emerg Infect Dis* **8**, 12: 1468-1473 (2002). https://doi.org/10.3201/eid0812.010317
313 Amman, B. R., Swanepoel, R., Nichol, S. T. & Towner, J. S. in *Marburg-and Ebolaviruses: From Ecosystems to Molecules Current Topics in Microbiology and Immunology* (eds Elke Mühlberger, Lisa L Hensley, & Jonathan S Towner) 23-61 (Springer International Publishing, 2017).
314 Plowright, R. K. *et al.* Pathways to zoonotic spillover. *Nat Rev Microbiol* **15**: 502-510 (2017).
315 Luis, A. D. *et al.* A comparison of bats and rodents as reservoirs of zoonotic viruses: are bats special? *Proc Biol Sci* **280**: 20122753 (2013).
316 Irving, A. T., Ahn, M., Goh, G., Anderson, D. E. & Wang, L.-F. Lessons from the host defences of bats, a unique viral reservoir. *Nature* **589**, 7842: 363-370 (2021).
317 Brook, C. E., Rozins, C., Guth, S. & Boots, M. Reservoir host immunology and life history shape virulence evolution in zoonotic viruses. *PLoS Biol* **21**, 9: e3002268 (2023). https://doi.org/10.1371/journal.pbio.3002268
318 Levinger, R. *et al.* Single-cell and Spatial Transcriptomics Illuminate Bat Immunity and Barrier Tissue Evolution. *Mol Biol Evol* **42**, 2 (2025). https://doi.org/10.1093/molbev/msaf017
319 Pei, G., Balkema-Buschmann, A. & Dorhoi, A. Disease tolerance as immune defense strategy in bats: One size fits all? *PLoS Pathog* **20**, 9: e1012471 (2024).
320 Hiller, M. *et al.* Reference-quality bat genomes illuminate adaptations to viral tolerance and disease resistance. (2023).
321 Mougari, S., Gonzalez, C., Reynard, O. & Horvat, B. Fruit bats as natural reservoir of highly pathogenic henipaviruses: balance between antiviral defense and viral tolerance. *Current Opinion in Virology* **54**: 101228 (2022).
322 Hayman, D. T. Bat tolerance to viral infections. *Nat Microbiol* **4**, 5: 728-729 (2019).
323 Randolph, H. E. & Barreiro, L. B. Holy immune tolerance, Batman! *Immunity* **48**: 1074-1076 (2018).
324 McCarville, J. L. & Ayres, J. S. Disease tolerance: concept and mechanisms. *Curr Opin Immunol* **50**: 88-93 (2018). https://doi.org/10.1016/j.coi.2017.12.003
325 Mandl, J. N., Schneider, C., Schneider, D. S. & Baker, M. L. Going to Bat(s) for Studies of Disease Tolerance. *Front Immunol* **9**: 2112 (2018). https://doi.org/10.3389/fimmu.2018.02112
326 Abbas, A., Lichtman, A. & Pillai, S. in *Cellular and Molecular Immunology (Tenth Edition)* 63-102 (Elsevier, 2022).

327 Turvey, S. E. & Broide, D. H. Innate immunity. *J Allergy Clin Immunol* **125**, 2: S24-S32 (2010).
328 Yan, N. & Chen, Z. J. Intrinsic antiviral immunity. *Nat Immunol* **13**, 3: 214-222 (2012).
329 Iha, K. *et al.* Molecular cloning and expression analysis of bat toll-like receptors 3, 7 and 9. *Journal of Veterinary Medical Science* **72**: 217-220 (2010).
330 Zeng, J., Zhang, X., Huang, C., Tian, S. & Zhao, H. Dampened TLR2–mediated Inflammatory Signaling in Bats. *Mol Biol Evol* **42**, 1: msae253 (2025).
331 Lee, A. K. *et al.* De novo transcriptome reconstruction and annotation of the Egyptian rousette bat. *BMC Genomics* **16**, 1: 1-11 (2015).
332 Schneor, L. *et al.* Comparison of antiviral responses in two bat species reveals conserved and divergent innate immune pathways. *iScience* **26**, 8: 107435 (2023).
333 Hayward, J. A. *et al.* Unique evolution of antiviral tetherin in bats. *J Virol* **96**, 20: e01152-01122 (2022).
334 Gutierrez, E. G. & Ortega, J. Uncovering selection pressures on the IRF gene family in bats' immune system. *Immunogenetics* **77**: 10 (2025).
335 Omatsu, T. *et al.* Induction and sequencing of Rousette bat interferon α and β genes. *Veterinary immunology and immunopathology* **124**, 1-2: 169-176 (2008).
336 Bonjardim, C. A. Interferons (IFNs) are key cytokines in both innate and adaptive antiviral immune responses—and viruses counteract IFN action. *Microbes Infect* **7**, 3: 569-578 (2005).
337 Escudero-Pérez, B. & Muñoz-Fontela, C. Role of type I interferons on filovirus pathogenesis. *Vaccines* **7**, 1: 22 (2019).
338 Ivashkiv, L. B. & Donlin, L. T. Regulation of type I interferon responses. *Nat Rev Immunol* **14**, 1: 36-49 (2014). https://doi.org/10.1038/nri3581
339 McNab, F., Mayer-Barber, K., Sher, A., Wack, A. & O'Garra, A. Type I interferons in infectious disease. *Nat Rev Immunol* **15**, 2: 87-103 (2015). https://doi.org/10.1038/nri3787
340 Schroder, K., Hertzog, P. J., Ravasi, T. & Hume, D. A. Interferon-gamma: an overview of signals, mechanisms and functions. *J Leukoc Biol* **75**, 2: 163-189 (2004). https://doi.org/10.1189/jlb.0603252
341 Schoenborn, J. R. & Wilson, C. B. Regulation of interferon-gamma during innate and adaptive immune responses. *Adv Immunol* **96**: 41-101 (2007). https://doi.org/10.1016/s0065-2776(07)96002-2
342 Donnelly, R. P. & Prokunina-Olsson, L. The Interferon-Lambda Family Celebrates 20 Years of Scientific Discovery. *J Interferon Cytokine Res* **43**, 9: 359-362 (2023). https://doi.org/10.1089/jir.2023.0122
343 Lazear, H. M., Schoggins, J. W. & Diamond, M. S. Shared and Distinct Functions of Type I and Type III Interferons. *Immunity* **50**, 4: 907-923 (2019). https://doi.org/10.1016/j.immuni.2019.03.025
344 Li, Y., Dong, B., Wei, Z., Silverman, R. H. & Weiss, S. R. Activation of RNase L in Egyptian Rousette bat-derived RoNi/7 cells is dependent primarily on OAS3 and independent of MAVS signaling. *MBio* **10**: 10.1128/mbio. 02414-02419 (2019).
345 Gyurkovska, V. & Ivanovska, N. Distinct roles of TNF-related apoptosis-inducing ligand (TRAIL) in viral and bacterial infections: from pathogenesis to pathogen

clearance. *Inflamm Res* **65**, 6: 427-437 (2016). https://doi.org/10.1007/s00011-016-0934-1
346 Kuzmin, I. V. *et al.* Innate immune responses of bat and human cells to filoviruses: commonalities and distinctions. *J Virol* **91**, 8: 10.1128/jvi. 02471-02416 (2017).
347 Kellner, M. J. *et al.* Bat organoids reveal antiviral responses at epithelial surfaces. *Nat Immunol*, (2025). https://doi.org/10.1038/s41590-025-02155-1
348 Zhou, P. *et al.* Contraction of the type I IFN locus and unusual constitutive expression of IFN-alpha in bats. *Proc Natl Acad Sci USA* **113**, 10: 2696-2701 (2016). https://doi.org/10.1073/pnas.1518240113
349 Zhou, P. *et al.* IRF7 in the Australian black flying fox, *Pteropus alecto*: evidence for a unique expression pattern and functional conservation. *PLoS One* **9**, 8: e103875 (2014). https://doi.org/10.1371/journal.pone.0103875
350 Bondet, V. *et al.* Constitutive IFNα protein production in bats. *Front Immunol* **12**: 735866 (2021).
351 Tisoncik-Go, J. & Gale, M., Jr. Enhanced antiviral innate immunity supports the bat reservoir of Marburg virus. *Nat Immunol*, (2025). https://doi.org/10.1038/s41590-025-02170-2
352 Banchereau, J. & Steinman, R. M. Dendritic cells and the control of immunity. *Nature* **392**, 6673: 245-252 (1998). https://doi.org/10.1038/32588
353 Pulendran, B., Tang, H. & Manicassamy, S. Programming dendritic cells to induce T(H)2 and tolerogenic responses. *Nat Immunol* **11**, 8: 647-655 (2010). https://doi.org/10.1038/ni.1894
354 Swiecki, M. & Colonna, M. The multifaceted biology of plasmacytoid dendritic cells. *Nat Rev Immunol* **15**, 8: 471-485 (2015). https://doi.org/10.1038/nri3865
355 Long, E. O., Kim, H. S., Liu, D., Peterson, M. E. & Rajagopalan, S. Controlling natural killer cell responses: integration of signals for activation and inhibition. *Annu Rev Immunol* **31**: 227-258 (2013). https://doi.org/10.1146/annurev-immunol-020711-075005
356 Björkström, N. K., Strunz, B. & Ljunggren, H.-G. Natural killer cells in antiviral immunity. *Nat Rev Immunol* **22**, 2: 112-123 (2022).
357 Abel, A. M., Yang, C., Thakar, M. S. & Malarkannan, S. Natural Killer Cells: Development, Maturation, and Clinical Utilization. *Front Immunol* **9**: 1869 (2018).
358 Cooper, M. A. *et al.* Interleukin-1beta costimulates interferon-gamma production by human natural killer cells. *Eur J Immunol* **31**, 3: 792-801 (2001). https://doi.org/10.1002/1521-4141(200103)31:3<792::aid-immu792>3.0.co;2-u
359 Vivier, E. *et al.* Innate or adaptive immunity? The example of natural killer cells. *Science* **331**, 6013: 44-49 (2011). https://doi.org/10.1126/science.1198687
360 Friedrichs, V. *et al.* Landscape and age dynamics of immune cells in the Egyptian rousette bat. *Cell Rep* **40**, 10: 111305 (2022). https://doi.org/10.1016/j.celrep.2022.111305
361 Abbas, A., Lichtman, A. & Pillai, S. in *Cellular and Molecular Immunology (Tenth Edition)* 123-150 (Elsevier, 2022).
362 Abbas, A., Lichtman, A. & Pillai, S. in *Cellular and Molecular Immunology (Tenth Edition)* 1-11 (Elsevier, 2022).

363 Zhu, J. & Paul, W. E. CD4 T cells: fates, functions, and faults. *Blood* **112**, 5: 1557-1569 (2008). https://doi.org/10.1182/blood-2008-05-078154
364 Curtsinger, J. M. & Mescher, M. F. Inflammatory cytokines as a third signal for T cell activation. *Curr Opin Immunol* **22**, 3: 333-340 (2010). https://doi.org/10.1016/j.coi.2010.02.013
365 Smith-Garvin, J. E., Koretzky, G. A. & Jordan, M. S. T cell activation. *Annu Rev Immunol* **27**: 591-619 (2009). https://doi.org/10.1146/annurev.immunol.021908.132706
366 Roffler, A. A. *et al.* Bat humoral immunity and its role in viral pathogenesis, transmission, and zoonosis. *Front Immunol* **15**: 1269760 (2024).
367 Chakravarty, A. & Sarkar, S. Immunofluorescence analysis of immunoglobulin bearing lymphocytes in the Indian fruit bat: *Pteropus giganteus*. *Lymphology* **27**, 2: 97-104 (1994).
368 Ma, L. *et al.* Landscape of IGH germline genes of Chiroptera and the pattern of *Rhinolophus affinis* bat IGH CDR3 repertoire. *Microbiol Spectr* **12**, 4: e0376223 (2024). https://doi.org/10.1128/spectrum.03762-23
369 Chakraborty, A. K. & Chakravarty, A. K. Antibody-mediated immune response in the bat, *Pteropus giganteus*. *Dev Comp Immunol* **8**, 2: 415-423 (1984). https://doi.org/10.1016/0145-305x(84)90048-x
370 Papenfuss, A. T. *et al.* The immune gene repertoire of an important viral reservoir, the Australian black flying fox. *BMC genomics* **13**: 1-17 (2012).
371 Wynne, J. W. *et al.* Purification and characterisation of immunoglobulins from the Australian black flying fox (*Pteropus alecto*) using anti-fab affinity chromatography reveals the low abundance of IgA. *PLoS One* **8**, 1: e52930 (2013). https://doi.org/10.1371/journal.pone.0052930
372 Wellehan, J. F., Jr. *et al.* Detection of specific antibody responses to vaccination in variable flying foxes (*Pteropus hypomelanus*). *Comp Immunol Microbiol Infect Dis* **32**, 5: 379-394 (2009). https://doi.org/10.1016/j.cimid.2007.11.002
373 Baker, M. L., Tachedjian, M. & Wang, L. F. Immunoglobulin heavy chain diversity in Pteropid bats: evidence for a diverse and highly specific antigen binding repertoire. *Immunogenetics* **62**, 3: 173-184 (2010). https://doi.org/10.1007/s00251-010-0425-4
374 Toshkova, N. *et al.* Temperature sensitivity of bat antibodies links metabolic state of bats with antigen-recognition diversity. *Nat Commun* **15**, 1: 5878 (2024). https://doi.org/10.1038/s41467-024-50316-x
375 Schuh, A. J. *et al.* Antibody-mediated virus neutralization is not a universal mechanism of Marburg, Ebola, or Sosuga virus clearance in Egyptian rousette bats. *J Infect Dis* **219**, 11: 1716-1721 (2019).
376 Ilinykh, P. A. *et al.* Non-neutralizing antibodies from a Marburg infection survivor mediate protection by Fc-effector functions and by enhancing efficacy of other antibodies. *Cell Host Microbe* **27**, 6: 976-991 (2020).
377 Epstein, J. H. *et al.* Duration of Maternal Antibodies against Canine Distemper Virus and Hendra Virus in Pteropid Bats. *PLoS One* **8**, 6: e67584 (2013). https://doi.org/10.1371/journal.pone.0067584
378 Peel, A. J. *et al.* Support for viral persistence in bats from age-specific serology and models of maternal immunity. *Sci Rep* **8**, 1: 3859 (2018).

379 Baker, K. S. *et al.* Viral antibody dynamics in a chiropteran host. *J Anim Ecol* **83**, 2: 415-428 (2014). https://doi.org/10.1111/1365-2656.12153
380 Geldenhuys, M. *et al.* Viral maintenance and excretion dynamics of coronaviruses within an Egyptian rousette fruit bat maternal colony: considerations for spillover. *Sci Rep* **13**, 1: 15829 (2023).
381 Omatsu, T. *et al.* Molecular cloning and sequencing of the cDNA encoding the bat CD4. *Vet Immunol Immunopathol* **111**, 3-4: 309-313 (2006). https://doi.org/10.1016/j.vetimm.2005.12.002
382 Storm, N., Jansen Van Vuren, P., Markotter, W. & Pawęska, J. T. Antibody responses to Marburg virus in Egyptian rousette bats and their role in protection against infection. *Viruses* **10**: 73 (2018).
383 Peters, C. *et al.* Vaccination of Egyptian fruit bats (*Rousettus aegyptiacus)* with monovalent inactivated rabies vaccine. *J Zoo Wildl Med* **35**, 1: 55-59 (2004). https://doi.org/10.1638/03-027
384 Drexler, J. F. *et al.* Amplification of emerging viruses in a bat colony. *Emerg Infect Dis* **17**, 3: 449-456 (2011). https://doi.org/10.3201/eid1703.100526
385 Pawęska, J. T. *et al.* Experimental Inoculation of Egyptian Fruit Bats (*Rousettus aegyptiacus*) with Ebola Virus. *Viruses* **8**, 2 (2016). https://doi.org/10.3390/v8020029
386 Biesold, S. E. *et al.* Type I interferon reaction to viral infection in interferon-competent, immortalized cell lines from the African fruit bat *Eidolon helvum*. *PLoS One* **6**, 11: e28131 (2011). https://doi.org/10.1371/journal.pone.0028131
387 Brook, C. E. *et al.* Accelerated viral dynamics in bat cell lines, with implications for zoonotic emergence. *Elife* **9**: e48401 (2020).
388 Elbadawy, M. *et al.* Establishment of a bat lung organoid culture model for studying bat-derived infectious diseases. *Sci Rep* **15**, 1: 4035 (2025).
389 Liu, X. *et al.* Analogous comparison unravels heightened antiviral defense and boosted viral infection upon immunosuppression in bat organoids. *Signal Transduct Target Ther* **7**, 1: 392 (2022).
390 Hashimi, M. *et al.* Antiviral response mechanisms in a Jamaican Fruit Bat intestinal organoid model of SARS-CoV-2 infection. (2022).
391 Zhou, J. *et al.* Infection of bat and human intestinal organoids by SARS-CoV-2. *Nature Medicine* **26**: 1077-1083 (2020).
392 Berman, T. S., Weinberg, M., Moreno, K. R., Czirják, G. Á. & Yovel, Y. In sickness and in health: the dynamics of the fruit bat gut microbiota under a bacterial antigen challenge and its association with the immune response. *Front Immunol* **14**: 1152107 (2023).
393 Zhou, P. *et al.* Unlocking bat immunology: establishment of *Pteropus alecto* bone marrow-derived dendritic cells and macrophages. *Sci Rep* **6**, 1: 38597 (2016).
394 Sarkar, S. K. & Chakravarty, A. K. Analysis of immunocompetent cells in the bat, *Pteropus giganteus*: isolation and scanning electron microscopic characterization. *Dev Comp Immunol* **15**, 4: 423-430 (1991).
395 Abbas, A., Lichtman, A. & Pillai, S. in *Cellular and Molecular Immunology (Tenth Edition)* 13-41 (Elsevier, 2022).
396 Attia, W. Y., El-Desouki, N., Madkour, G. A., Sayed, A. & El-Refaiy, A. A study on some lymphoid organs of two common species of bats from Egypt, *Rousettus*

aegypticus and *Taphozous nudiventris*. *Egypt J Exp Biol (Zool)* **3**: 151-161 (2007).
397 Travlos, G. S. Normal structure, function, and histology of the bone marrow. *Toxicol Pathol* **34**, 5: 548-565 (2006).
398 Travlos, G. S. Histopathology of bone marrow. *Toxicol Pathol* **34**, 5: 566-598 (2006).
399 Pearse, G. in *Immunopathology in Toxicology and Drug Development: Volume 2, Organ Systems* (ed GA Parker) 1-35 (Springer International Publishing, 2017).
400 Pearse, G. Normal structure, function and histology of the thymus. *Toxicol Pathol* **34**, 5: 504-514 (2006).
401 Pearse, G. Histopathology of the thymus. *Toxicol Pathol* **34**, 5: 515-547 (2006).
402 Elmore, S. A. & Bouknight, S. A. in *Immunopathology in Toxicology and Drug Development. Volume 2, Organ Systems* (ed GA Parker) 59-80 (Springer International Publishing, 2017).
403 Willard-Mack, C. L. Normal structure, function, and histology of lymph nodes. *Toxicol Pathol* **34**, 5: 409-424 (2006).
404 Abel-Galil, D. Y., Tawfik, A.-R. & Saad, A.-H. Anatomical and comparative distribution of lymph nodes in some Egyptian chiroptera. *Scholar.cu.edu.eg*, (2012).
405 Haley, P. J. From bats to pangolins: new insights into species differences in the structure and function of the immune system. *Innate Immun* **28**, 3-4: 107-121 (2022).
406 Elmore, S. A. Histopathology of the lymph nodes. *Toxicol Pathol* **34**, 5: 425-454 (2006).
407 Cesta, M. F. Normal structure, function, and histology of the spleen. *Toxicol Pathol* **34**, 5: 455-465 (2006).
408 Papenfuss, T. L. & Cesta, M. F. in *Immunopathology in Toxicology and Drug Development: Volume 2, Organ Systems* (ed GA Parker) 37-57 (Springer International Publishing, 2017).
409 Mebius, R. E. & Kraal, G. Structure and function of the spleen. *Nat Rev Immunol* **5**, 8: 606-616 (2005). https://doi.org/10.1038/nri1669
410 Hanadhita, D. *et al.* The spleen morphophysiology of fruit bats. *Anat Histol Embryol* **48**, 4: 315-324 (2019).
411 Baranga, J. Splenic weights and their possible relationship to adrenocortical function in a wild population of *Rousettus aegyptiacus* E. Geoffroy. *Afr J Ecol* **16**, 1: 49-58 (1978).
412 Hanadhita, D. *et al.* Extracellular matrix composition of different spleen compartments of fruit bats. *Anat Histol Embryol* **49**, 2: 281-289 (2020). https://doi.org/10.1111/ahe.12526
413 Sørby, R., Wien, T. N., Husby, G., Espenes, A. & Landsverk, T. Filter function and immune complex trapping in splenic ellipsoids. *J Comp Pathol* **132**, 4: 313-321 (2005). https://doi.org/10.1016/j.jcpa.2004.11.003
414 Kreukniet, M. B. *et al.* The B cell compartment of two chicken lines divergently selected for antibody production: differences in structure and function. *Vet Immunol Immunopathol* **51**, 1-2: 157-171 (1996). https://doi.org/10.1016/0165-2427(95)05505-3

415 Suttie, A. W. Histopathology of the spleen. *Toxicol Pathol* **34**, 5: 466-503 (2006).
416 Cesta, M. F. Normal structure, function, and histology of mucosa-associated lymphoid tissue. *Toxicol Pathol* **34**, 5: 599-608 (2006).
417 Kuper, C. F., Wijnands, M. V. & Zander, S. A. in *Immunopathology in Toxicology and Drug Development: Volume 2, Organ Systems* (ed GA Parker) 81-121 (Springer International Publishing, 2017).
418 Ciminski, K. *et al.* Bat influenza viruses transmit among bats but are poorly adapted to non-bat species. *Nat Microbiol* **4**, 12: 2298-2309 (2019). https://doi.org/10.1038/s41564-019-0556-9
419 Kuper, C. F. Histopathology of mucosa-associated lymphoid tissue. *Toxicol Pathol* **34**, 5: 609-615 (2006).
420 Schuh, J. C. Mucosa-associated lymphoid tissue and tertiary lymphoid structures of the eye and ear in laboratory animals. *Toxicol Pathol* **49**, 3: 472-482 (2021).
421 Hughes, C. E., Benson, R. A., Bedaj, M. & Maffia, P. Antigen-Presenting Cells and Antigen Presentation in Tertiary Lymphoid Organs. *Front Immunol* **7**: 481 (2016). https://doi.org/10.3389/fimmu.2016.00481
422 Willard-Mack, C. L. *et al.* Nonproliferative and Proliferative Lesions of the Rat and Mouse Hematolymphoid System. *Toxicol Pathol* **47**, 6: 665-783 (2019). https://doi.org/10.1177/0192623319867053
423 Restucci, B. *et al.* Histopathological and microbiological findings in buffalo chronic mastitis: evidence of tertiary lymphoid structures. *J Vet Sci* **20**, 3: e28 (2019). https://doi.org/10.4142/jvs.2019.20.e28
424 Pezzolato, M. *et al.* Development of tertiary lymphoid structures in the kidneys of pigs with chronic leptospiral nephritis. *Vet Immunol Immunopathol* **145**, 1-2: 546-550 (2012). https://doi.org/10.1016/j.vetimm.2011.12.011
425 Rugh, K. M., Ashton, L. V., Schaffer, P. A. & Olver, C. S. Lymphoid Aggregates in Canine Cutaneous and Subcutaneous Sarcomas: Immunohistochemical and Gene Expression Evidence for Tertiary Lymphoid Structures. *Vet Comp Oncol* **23**, 1: 10-19 (2025). https://doi.org/10.1111/vco.13020
426 Ramos-Vara, J. A. in *Drug Safety Evaluation: Methods and Protocols, Second Edition* Vol. 1641 *Methods in Molecular Biology* (ed Jean-Charles Gautier) 115-128 (Humana, 2017).
427 Turmelle, A. S., Ellison, J. A., Mendonça, M. T. & McCracken, G. F. Histological assessment of cellular immune response to the phytohemagglutinin skin test in Brazilian free-tailed bats (*Tadarida brasiliensis*). *J Comp Physiol B* **180**: 1155-1164 (2010).
428 Hansen, D. *et al.* Morphological and quantitative analysis of leukocytes in free-living Australian black flying foxes (Pteropus alecto). *PLoS One* **17**, 5: e0268549 (2022).
429 Rissmann, M. *et al.* Baseline of Physiological Body Temperature and Hematological Parameters in Captive *Rousettus aegyptiacus* and *Eidolon helvum* Fruit Bats. *Front Physiol* **13**: 910157 (2022). https://doi.org/10.3389/fphys.2022.910157
430 Cavaleros, M., Buffenstein, R., Ross, F. P. & Pettifor, J. M. Vitamin D metabolism in a frugivorous nocturnal mammal, the Egyptian fruit bat (*Rousettus*

aegyptiacus). *Gen Comp Endocrinol* **133**, 1: 109-117 (2003). https://doi.org/10.1016/s0016-6480(03)00150-3

431 van der Westhuizen, J. The Diurnal Cycle of Some Energy Substrates in the Fruit Bat *Rousettus aegyptiacus*. *S Afr J Sci* **74**, 3: 99-101 (1978).

432 Moretti, P. *et al.* Haematological, serum biochemical and electrophoretic data on healthy captive Egyptian fruit bats (*Rousettus aegyptiacus*). *Lab Anim* **55**, 2: 158-169 (2021).

433 Korine, C., Zinder, O. & Arad, Z. Diurnal and seasonal changes in blood composition of the free-living Egyptian fruit bat (*Rousettus aegyptiacus*). *J Comp Physiol B* **169**: 280-286 (1999).

434 Arad, Z. & Korine, C. Effect of water restriction on energy and water balance and osmoregulation of the fruit bat *Rousettus aegyptiacus*. *J Comp Physiol B* **163**: 401-405 (1993).

435 Noll, U. G. Body temperature, oxygen consumption, noradrenaline response and cardiovascular adaptations in the flying fox, *Rousettus aegyptiacus*. *Comp Biochem Physiol A Physiol* **63**, 1: 79-88 (1979).

436 Eldeify, A., Ali, A. O., Fawaz, M. M. & Mohamed, A. E. A. Effect of sex and age on some Morphometric, Hematological and Biochemical Parameters in Egyptian Fruit Bat (*Rousettus aegyptiacus*). *SVU - Int J Vet Sci* **6**, 4: 93-111 (2023).

437 Farina, L. L. & Lankton, J. S. in *Chiroptera. In: Pathology of Wildlife and Zoo Animals* 607-633 (Elsevier, 2018).

438 Maseko, B. C., Bourne, J. A. & Manger, P. R. Distribution and morphology of cholinergic, putative catecholaminergic and serotonergic neurons in the brain of the Egyptian Rousette flying fox, *Rousettus aegyptiacus*. *J Chem Neuroanat* **34**, 3-4: 108-127 (2007).

439 Jacobsen, B. *et al.* Organization of projections from the entorhinal cortex to the hippocampal formation of the Egyptian fruit bat *Rousettus aegyptiacus*. *Hippocampus* **33**, 8: 889-905 (2023).

440 Czaplewski, N., Morgan, G. & Mcleod, S. in *Evolution of Tertiary Mammals of North America* (eds CM Janis, GF Gunnell, & MD Uhen) 174-197 (Cambridge University Press, 2008).

441 Mutere, F. A. The breeding biology of the fruit bat *Rousettus aegyptiacus* E. Geoffroy living at o degrees 22'S. *Acta Trop* **25**, 2: 97-108 (1968).

442 Bergmans, W. Taxonomy and biogeography of African fruit bats (Mammalia, Megachiroptera). 4. The genus *Rousettus* Gray, 1821. *Beaufortia* **44**, 4: 79-126 (1994).

443 Mainoya, J. & Howell, K. Histology of the neck 'glandular' skin patch in *Eidolon helvum*, *Rousettus aegyptiacus* and *R. angolensis* (Chiroptera: Pteropodidae). *Afr J Ecol* **17**, 3: 159-164 (1979).

444 Desroche, K., Fenton, M. B. & Lancaster, W. C. Echolocation and the thoracic skeletons of bats: a comparative morphological study. *Acta Chiropt* **9**, 2: 483-494 (2007).

445 Norberg, U. M. Functional osteology and myology of the wing of the dog-faced bat *Rousettus aegyptiacus* (E. Geoffroy)(Mammalia, Chiroptera). *Z Morphol Tiere* **73**: 1-44 (1972).

446 Panyutina, A. A., Korzun, L. P. & Kuznetsov, A. N. in *Flight of Mammals: From Terrestrial Limbs to Wings* 115-203 (Springer International Publishing, 2015).
447 Norberg, U. M. Bat wing structures important for aerodynamics and rigidity (Mammalia, Chiroptera). *Z Morphol Tiere* **73**: 45-61 (1972).
448 Kissane, R. W., Griffiths, A. & Sharp, A. C. Functional anatomy of the wing muscles of the Egyptian fruit bat (*Rousettus aegyptiacus*) using dissection and diceCT. *J Anat*, (2024). https://doi.org/0.1111/joa.14145
449 Luziga, C., Miyata, H., Nagahisa, H., Oji, T. & Wada, N. Muscle fibre distribution in forelimb, hindlimb and trunk muscles in three bat species: The little Japanese horseshoe, greater horseshoe and Egyptian fruit. *Anat Histol Embryol* **50**, 4: 685-693 (2021). https://doi.org/10.1111/ahe.12670
450 Pietschmann, M., Bartels, H. & Fons, R. Capillary supply of heart and skeletal muscle of small bats and non-flying mammals. *Respir Physiol* **50**: 267-282 (1982). https://doi.org/10.1016/0034-5687(82)90023-8
451 Elangovan, V., Raghuram, H., Satya Priya, E. Y. & Marimuthu, G. Wing morphology and flight performance in *Rousettus leschenaulti*. *J Mammal* **85**, 4: 806-812 (2004).
452 Greville, L. J., Ceballos-Vasquez, A., Valdizón-Rodríguez, R., Caldwell, J. R. & Faure, P. A. Wound healing in wing membranes of the Egyptian fruit bat (*Rousettus aegyptiacus*) and big brown bat (*Eptesicus fuscus*). *J Mammal* **99**, 4: 974-982 (2018).
453 Sterbing, S. & Moss, C. Comparative analysis of the distribution and morphology of tactile hairs on the wing membrane of four bat species. *Journal of Mammalogy* **99**: 124-130 (2018).
454 Pennycuick, C. J. Gliding flight of the dog-faced bat Rousettus aegyptiacus observed in a wind tunnel. *J Exp Biol* **55**, 3: 833-845 (1971).
455 Schutt Jr, W. A. & Simmons, N. B. Morphology and homology of the chiropteran calcar, with comments on the phylogenetic relationships of Archaeopteropus. *Journal of Mammalian Evolution* **5**, 1: 1-32 (1998).
456 Eilam-Altstadter, R., Las, L., Witter, M. & Ulanovsky, N. *Stereotaxic brain atlas of the Egyptian fruit bat*. (Academic Press, 2021).
457 Bhatnagar, K. P., Wible, J. & Karim, K. Development of the vomeronasal organ in *Rousettus leschenaulti* (Megachiroptera, Pteropodidae). *J Anat* **188**, Pt 1: 129 (1996).
458 Cooper, J. G. & Bhatnagar, K. P. Comparative anatomy of the vomeronasal organ complex in bats. *J Anat* **122**, Pt 3: 571 (1976).
459 Frahm, H. D. & Bhatnagar, K. P. Comparative morphology of the accessory olfactory bulb in bats. *J Anat* **130**, Pt 2: 349-365 (1980).
460 Meisami, E. & Bhatnagar, K. P. Structure and diversity in mammalian accessory olfactory bulb. *Microsc Res Tech* **43**, 6: 476-499 (1998).
461 Herculano-Houzel, S. *et al.* Microchiropterans have a diminutive cerebral cortex, not an enlarged cerebellum, compared to megachiropterans and other mammals. *J Comp Neurol* **528**, 17: 2978-2993 (2020). https://doi.org/10.1002/cne.24985
462 Green, R., van Tonder, S. V., Oettle, G. J., Cole, G. & Metz, J. Neurological changes in fruit bats deficient in vitamin B12. *Nature* **254**, 5496: 148-150 (1975).

463 van der Westhuyzen, J. & Cantrill, R. Lipid composition and sphingolipid fatty acids of myelin in fruit bat brain. *Neurochem Int* **5**, 4: 365-368 (1983).
464 Van der Westhuyzen, J. Lipid composition of the spinal cord in the fruit bat *Rousettus aegyptiacus*. *Comp Biochem Physiol B* **75**, 3: 441-444 (1983).
465 Bojarski, C. & Bernard, R. Comparison of the morphology of the megachiropteran and microchiropteran eye. *Afr Zool* **23**, 3: 155-160 (1988).
466 Aboelnour, A., Noreldin, A. E., Massoud, D. & Abumandour, M. M. Retinal characterization in the eyes of two bats endemic in the Egyptian fauna, the Egyptian fruit bat (*Rousettus aegyptiacus*) and insectivorous bat (*Pipistrellus kuhlii*), using the light microscope and transmission electron microscope. *Microsc Res Tech* **83**, 11: 1391-1400 (2020).
467 Brudenall, D., Schwab, I., Lloyd III, W., Giorgi, P. & Graydon, M. Optimized architecture for nutrition in the avascular retina of Megachiroptera. *Anat Histol Embryol* **36**, 5: 382-388 (2007).
468 El-Mansi, A. A., Al-Kahtani, M., Al-Sayyad, K., Ahmed, E. & Gad, A. Visual adaptability and retinal characterization of the Egyptian fruit bat (*Rousettus aegyptiacus*, Pteropodidae): New insights into photoreceptors spatial distribution and melanosomal activity. *Micron* **137**: 102897 (2020).
469 Thiele, A., Vogelsang, M. & Hoffmann, K. P. Pattern of retinotectal projection in the megachiropteran bat *Rousettus aegyptiacus*. *J Comp Pathol* **314**, 4: 671-683 (1991).
470 Gholami, S. & Ghasemi, F. The Study of Retinal Structure in Frugivorous Bat (*Rousettus Aegyptiacus*) by Light and Electron Microscope. *Egypt J Histol* **44**, 4: 941-949 (2021).
471 Simelane, T. *Visual ecology and topographic distribution of photoreceptor density in the retina of the Egytian rousette bat, Rousettus aegyptiacus*, University of Johannesburg (South Africa), (2024).
472 Pettigrew, J. D., Maseko, B. C. & Manger, P. R. Primate-like retinotectal decussation in an echolocating megabat, *Rousettus aegyptiacus*. *Neuroscience* **153**, 1: 226-231 (2008). https://doi.org/10.1016/j.neuroscience.2008.02.019
473 Schwab, I. & Pettigrew, J. A choroidal sleight of hand. *Br J Ophthalmol* **89**, 11: 1398 (2005).
474 Soliman, S. & Taha, A. Dried eye lens weight as an indicator of age in *Rousettus aegyptiacus*: Comparison with some other tools of age determination in bats (Chiroptera: Pteropodidae). *Lynx, n. s.* **54**, 1: 147–153 (2023).
475 Rehorek, S. J., Smith, T. D. & Bhatnagar, K. P. The orbitofacial glands of bats: An investigation of the potential correlation of gland structure with social organization. *Anat Rec (Hoboken)* **293**, 8: 1433-1448 (2010).
476 Danilovich, S. *et al.* Bats regulate biosonar based on the availability of visual information. *Curr Biol* **25**, 23: R1124-1125 (2015). https://doi.org/10.1016/j.cub.2015.11.003
477 Eitan, O. *et al.* Functional daylight echolocation in highly visual bats. *Curr Biol* **32**, 7: R309-R310 (2022).
478 Friauf, E. & Herbert, H. Topographic organization of facial motoneurons to individual pinna muscles in rat (*Rattus rattus*) and bat (*Rousettus aegyptiacus*). *J Comp Neurol* **240**, 2: 161-170 (1985). https://doi.org/10.1002/cne.902400206

479 Tandler, B., Gresik, E. W., Nagato, T. & Phillips, C. J. Secretion by striated ducts of mammalian major salivary glands: review from an ultrastructural, functional, and evolutionary perspective. *The Anatomical Record: An Official Publication of the American Association of Anatomists* **264**: 121-145 (2001).
480 Massoud, D. & Abumandour, M. M. Anatomical features of the tongue of two chiropterans endemic in the Egyptian fauna; the Egyptian fruit bat (*Rousettus aegyptiacus*) and insectivorous bat (*Pipistrellus kuhlii*). *Acta Histochem* **122**, 2: 151503 (2020).
481 El-Mansi, A. A., Al-Kahtani, M. & Abumandour, M. M. Comparative phenotypic and structural adaptations of tongue and gastrointestinal tract in two bats having different feeding habits captured from Saudi Arabia: Egyptian fruit bat (*Rousettus aegyptiacus*) and Egyptian tomb bat (*Taphozous perforatus*). *Zoologischer Anzeiger* **281**: 24-38 (2019).
482 Tandler, B., Phillips, C. J., Nagato, T. & Toyoshima, K. Ultrastructural diversity in chiropteran salivary glands. *Ultrastructure of the Extraparietal Glands of the Digestive Tract*: 31-52 (1990).
483 Kandyel, R. *et al.* Structural and functional adaptation of the lingual papillae of the Egyptian fruit bat (*Rousettus aegyptiacus*): Specific adaptive feeding strategies. *Folia Morphol (Warsz)* **81**, 2: 400-411 (2022).
484 Ghassemi, F. & Jahromi, H. K. Histological study of tongue in *Rousettus aegyptiacus* in the southwest of Iran (Jahrom). *IMPACT: IJRANSS* **1**, 6: 41-49 (2013).
485 Attaallah, A., Fouda, Y., El-Beltagy, A. E.-F. B. & Saleh, A. M. Comparative studies on the tongue of the Egyptian fruit bat (*Rousettus aegyptiacus*) and the common quail (*Coturnix coturnix*). *Egypt J Basic Appl Sci* **10**, 1: 476-492 (2023).
486 Trzcielińska-Lorych, J., Jackowiak, H., Skieresz-Szewczyk, K. & Godynicki, S. Morphology and morphometry of lingual papillae in adult and newborn Egyptian fruit bats (*Rousettus aegyptiacus*). *Anat Histol Embryol* **38**, 5: 370-376 (2009).
487 Jackowiak, H., Trzcielinska-Lorych, J. & Godynicki, S. The microstructure of lingual papillae in the Egyptian fruit bat (*Rousettus aegyptiacus*) as observed by light microscopy and scanning electron microscopy. *Arch Histol Cytol* **72**, 1: 13-21 (2009).
488 Ben-Hamo, M., Muñoz-Garcia, A. & Pinshow, B. in *Comparative physiology of fasting, starvation, and food limitation* 257-275 (Springer, 2012).
489 Michelmore, A., Keegan, D. & Kramer, B. Immunocytochemical identification of endocrine cells in the pancreas of the fruit bat, *Rousettus aegyptiacus*. *Gen Comp Endocrinol* **110**, 3: 319-325 (1998).
490 Abumandour, M. & Pérez, W. Morphological and Scanning Electron Microscopy Studies of the Stomach of the Egyptian Fruit Bat (*Rousettus aegyptiacus*). *Int J Morphol* **35**, 1: 242-250 (2017).
491 El-Desouki, N. I., Madkour, G., Sayed, A., Attia, W. Y. & El-Refaiy, A. I. Histological, cytological and histochemical studies on the stomach of two common species of Egyptian bats, *Rousettus aegyptiacus* and *Taphozous nudiventris*. *Egypt J Exp Biol (Zool)* **152**: 137-152 (2006).
492 Keegan, D. & Modinger, R. Microvilli of the intestinal mucosal cells of *Rousettus aegyptiacus*. *Afr Zool* **14**, 4: 220-223 (1979).

493 Selim, A. & El Nahas, E. Comparative histological studies on the intestinal wall between the prenatal, the postnatal and the adult of the two species of Egyptian bats. Frugivorous *Rousettus aegyptiacus* and insectivorous *Taphozous nudiventris*. *J Basic Appl Zool* **70**: 25-32 (2015).
494 Keegan, D. Aspects of the assimilation of sugars by *Rousettus aegyptiacus*. *Comparative Biochemistry and Physiology* **58A**: 349-352 (1977).
495 Keegan, D. Aspects of the absorption of fructose in *Rousettus aegyptiacus*. *S Afr J Med Sci* **40**: 49-55 (1975).
496 Tracy, C. R. *et al.* Absorption of sugars in the Egyptian fruit bat (*Rousettus aegyptiacus*): a paradox explained. *J Exp Biol* **210**, Pt 10: 1726-1734 (2007). https://doi.org/10.1242/jeb.02766
497 Keegan, D., Levine, L. & Balgobind, N. Absorption of calcium in the small intestine of the bat, *Rousettus aegyptiacus*. *S Afr J Sci* **76**, 7: 328 (1980).
498 Rahma, A. *et al.* Radiographic anatomy of the heart of fruit bats. *Anat Histol Embryol* **50**, 3: 604-613 (2021).
499 Alijani, B. & Ghassemi, F. Anatomy and histology of the heart in Egyptian fruit bat (*Rossetus aegyptiacus*). *J Entomol Zool Stud* **4**, 5: 50-56 (2016).
500 Kamali, Y. & Ghasemi, F. Morphology of the Great Cardiac Vessels in Egyptian Fruit Bat *(Rousettus aegyptiacus)*. *Anat Sci* **18**, 2: 79-84 (2021).
501 Maina, J. & King, A. Correlations between structure and function in the design of the bat lung: a morphometric study. *J Exp Biol* **111**, 1: 43-61 (1984).
502 Maina, J., King, A. & King, D. A morphometric analysis of the lung of a species of bat. *Respir Physiol* **50**, 1: 1-11 (1982).
503 Maina, J. N., Thomas, S. P. & Hyde, D. M. A morphometric study of the lungs of different sized bats: correlations between structure and function of the chiropteran lung. *Philos Trans R Soc Lond B Biol Sci* **333**, 1266: 31-50 (1991).
504 Numata, T. Histology and innervation of lung in bat. *Arch Histol Jpn* **9**, 4: 491-506 (1956).
505 Meyerholz, D. K., Suarez, C. J., Dintzis, S. M. & Frevert, C. W. in *Comparative Anatomy and Histology: A Mouse, Rat, and Human Atlas* (eds Piper M. Treuting, Suzanne M. Dintzis, & Kathleen S. Montine) 147-162 (Elsevier Science & Technology, 2018).
506 Selim, A., Elnahass, E. & Ebrahim, S. Histological and Ultra Structure Observations of the Adrenal Gland of Fruit Eating Bat (*Rousettus aegyptiacus*). *Am J Biomed Sci & Res* **5**, (2019). https://doi.org/10.34297/AJBSR.2019.05.000961
507 Baranga, J. The incidence of accessory adrenocortical bodies in *Rousettus aegyptiacus* E. Geoffroy (Megachiroptera: Mammalia). *Mammalia* **48**, 2: 267-273 (1984).
508 Baranga, J. The adrenal weight changes of a tropical fruit bat, *Rousettus aegyptiacus* E. Geoffroy. *Zeitschrift für Säugetierkunde* **45**: 321-336 (1980).
509 Gopal, P. K. Morphological adaptations in the kidney and urine concentrating ability in relation to dietary habit in the three species of bats. *WJZ* **8**, 2: 198-205 (2013).

510 Eshar, D., Lapid, R., Weinberg, M., King, R. & Pohlman, L. M. Refractometric urine specific gravity of free-living Egyptian fruit bats (*Rousettus aegyptiacus*). *J Zoo Wildl Med* **48**, 3: 878-881 (2017). https://doi.org/10.1638/2016-0214.1
511 El-Nahass, E. E.-S., Ebrahim, S. & Selim, A. Comparative Histological and Ultrastructural Studies of the Thyroid Gland in Postnatal and Adult Female Egyptian Frugivorous Bat (*Rousettus aegyptiacus*). *Egypt J Histol* **46**, 2: 575-587 (2023).
512 Kwiecinski, G. G., Wimsatt, W. A. & Krook, L. Morphology of thyroid C-cells and parathyroid glands in summer-active little brown bats, *Myotis lucifugus lucifugus*, with particular reference to pregnancy and lactation. *Am J Anat* **178**, 4: 421-427 (1987).
513 Nunez, E. A., Whalen, J. P. & Krook, L. An ultrastructural study of the natural secretory cycle of the parathyroid gland of the bat. *Am J Anat* **134**, 4: 459-479 (1972).
514 Barclay, R. M. *et al.* Thermoregulation by captive and free-ranging Egyptian rousette bats (*Rousettus aegyptiacus*) in South Africa. *J Mammal* **98**, 2: 572-578 (2017).
515 Madkour, G., Hammouda, E. & Ibrahim, I. Histomorphology of the male genitalia of two common Egyptian bats. *Ann Zool* **20**: 1-24 (1983).
516 Fard, E. A. & Ghassemi, F. Histological and morophometrical study of male reproductive tract in *Rousettus aegyptiacus (*Mammalia: Megachiroptera) in Iran. *J Entomol Zool Stud* **5**, 1: 229-234 (2017).
517 Madkour, G. Structure of the penis in the fruit bat *Rousettus aegyptiacus* (Megachiroptera). *J Mammal* **57**, 4: 769-771 (1976).
518 Zhang, X. *et al.* Wild fulvous fruit bats (*Rousettus leschenaulti*) exhibit human-like menstrual cycle. *Biol Reprod* **77**, 2: 358-364 (2007). https://doi.org/10.1095/biolreprod.106.058958
519 Pow, C. & Martin, L. The ovarian–uterine vasculature in relation to unilateral endometrial growth in flying foxes (genus Pteropus, suborder Megachiroptera, order Chiroptera). *J Reprod Fertil* **101**, 2: 247-255 (1994). https://doi.org/10.1530/jrf.0.1010247
520 Bernard, R. An ovarian rete arteriosum may facilitate reproductive asymmetry in the Egyptian fruit bat (*Rousettus aegyptiacus*). *S Afr J Sci* **84**, 10: 856-857 (1988).
521 Hood, C. S. Comparative morphology and evolution of the female reproductive tract in macroglossine bats (Mammalia, Chiroptera). *J Morphol* **199**, 2: 207-221 (1989).
522 Wimsatt, W. A. Reproductive asymmetry and unilateral pregnancy in Chiroptera. *Reproduction* **56**: 345-357 (1979).
523 Rasweiler, J. J. t. Early embryonic development and implantation in bats. *J Reprod Fertil* **56**, 1: 403-416 (1979). https://doi.org/10.1530/jrf.0.0560403
524 Carter, A. M. & Enders, A. C. Comparative aspects of trophoblast development and placentation. *Reprod Biol Endocrinol* **2**: 46 (2004).
525 Carter, A. M. Genomics, the diversification of mammals, and the evolution of placentation. *Dev Biol* **516**: 167-182 (2024). https://doi.org/10.1016/j.ydbio.2024.08.011

526 Montgomery, C. A. & Alison, R. H. Nonneoplastic lesions of the ovary in Fischer 344 rats and B6C3F1 mice. *Environ Health Perspect* **73**: 53-75 (1987). https://doi.org/10.1289/ehp.877353
527 Mortlock, M. *et al.* Seasonal shedding patterns of diverse henipavirus-related paramyxoviruses in Egyptian rousette bats. *Sci Rep* **11**, 1: 24262 (2021).
528 Pawęska, J. T., Storm, N., Jansen van Vuren, P., Markotter, W. & Kemp, A. Attempted Transmission of Marburg Virus by Bat-Associated Fleas Thaumapsylla breviceps breviceps (Ischnopsyllidae: Thaumapsyllinae) to the Egyptian Rousette Bat (Rousettus aegyptiacus). *Viruses* **16**, (2024). https://doi.org/10.3390/v16081197
529 Lowenstine, L. J. & Stasiak, I. M. in *Fowler's Zoo and Wild Animal Medicine, Volume 8* 674-681 (Elsevier, 2015).
530 Lavin, S. R., Chen, Z. & Abrams, S. A. Effect of tannic acid on iron absorption in straw-colored fruit bats (Eidolon helvum). *Zoo Biol* **29**: 335-343 (2010). https://doi.org/10.1002/zoo.20258
531 Abalaka, S. E. *et al.* Histopathological and health risk assessment of heavy metals in the straw-colored fruit bat, *Eidolon helvum*, in Nigeria. *Environ Monit Assess* **195**, 3: 411 (2023).
532 Elbert, J. A. *et al.* Histopathologic comparison of hepatic iron overload in managed care and free-ranging Egyptian rousette bats (*Rousettus aegyptiacus*). *Vet Pathol* **Submitted June 2024; Accepted pending minor revisions.**, (2025).
533 Crawshaw, G., Oyarzun, S., Valdes, E. & Rose, K. Hemochromatosis (iron storage disease) in fruit bats. *Proc Am Zoo Aquat Assoc Nutr Advis Group* **17**: 136-147 (1995).
534 Toshkova, N., Zlatkov, B., Fakirova, A., Zhelyazkova, V. & Simov, N. First record of Psorergatoides Fain, 1959 (Acari, Cheyletoidea, Psorergatidae) for the Balkan Peninsula with description of the cutaneous lesions on the wing membrane of its hosts Myotismyotis (Borkhausen, 1797) and Myotisblythii (Tomes, 1857)(Chiroptera, Vespertilionidae). *Biodiversity Data Journal* **10**, (2022).
535 Cierocka, K., Izdebska, J. N., Rolbiecki, L. & Ciechanowski, M. The occurrence of skin mites from the Demodecidae and Psorergatidae (Acariformes: Prostigmata) families in bats, with a description of a new species and new records. *Animals (Basel)* **12**, 7: 875 (2022).
536 Nelson, L. J., Seeman, O. D. & Shinwari, M. W. Psorergatoides cf. kerivoulae (Acari: Psorergatidae) induces cutaneous lesions on the wings of Myotis macropus (Chiroptera: Vespertilionidae). *Systematic and Applied Acarology* **22**: 446-448 (2017).
537 Baker, A. S. *Psorergatoides nyctali* (Prostigmata: Psorergatidae), a new mite species parasitizing the bat *Nyctalus noctula* (Mammalia: Chiroptera) in the British Isles. *Syst Appl Acarol* **10**, 1: 67-74 (2005).
538 Fain, A. Les Acariens psoriques parasites des Chauves-souris VII.–Nouvelles observations sur le genre *Nycteridocoptes* Oudemans 1898. *Acarologia* **1**, 3: 335-353 (1959).
539 Klompen, J. Phylogenetic relationships in the mite family Sarcoptidae (Acari: Astigmata). (1992).

540 Beck, S. *et al.* Pathobiological investigation of naturally infected canine rabies cases from Sri Lanka. *BMC Vet Res* **13**, 1: 99 (2017).

541 De Nardo, T. F. *et al.* Contribution of astrocytes and macrophage migration inhibitory factor to immune-mediated canine encephalitis caused by the distemper virus. *Vet Immunol Immunopathol* **221**: 110010 (2020).

542 Slaviero, M. *et al.* Pathological findings and patterns of feline infectious peritonitis in the respiratory tract of cats. *J Comp Pathol* **210**: 15-24 (2024).

543 Moncayo, A. *et al.* West Nile virus and epizootic hemorrhagic disease virus co-infection in a novel host at the Nashville Zoo. *The American Journal of Tropical Medicine and Hygiene* **108**: 705 (2023).

544 Bagatella, S., Tavares-Gomes, L. & Oevermann, A. *Listeria monocytogenes* at the interface between ruminants and humans: A comparative pathology and pathogenesis review. *Vet Pathol* **59**, 2: 186-210 (2022).

545 Walker, D. H., Ismail, N., Olano, J. P., Valbuena, G. & McBride, J. in *Rickettsial diseases* 27-38 (CRC Press, 2007).

546 Wheatley, M. A. *et al.* Eosinophilic pericardial effusion and pericarditis in a cat. *Journal of Feline Medicine and Surgery Open Reports* **9**: 20551169231213498 (2023).

547 Ruppert, S., Lee, J. K. & Marsh, A. E. Equine Protozoal Myeloencephalitis associated with Neospora caninum in a USA captive bred zebra (Equus zebra). *Veterinary Parasitology: Regional Studies and Reports* **26**: 100620 (2021).

548 Oliveira, M. D., Flores, M. M., Mazzanti, A., Fighera, R. A. & Kommers, G. D. Neurocryptococcosis in dogs and cats: Anatomopathological and fungal morphological aspects in a case series. *Pesquisa Veterinária Brasileira* **44**: e07447 (2024).

549 Elbert, J. A., Yau, W. & Rissi, D. R. Neuroinflammatory diseases of the central nervous system of dogs: a retrospective study of 207 cases (2008–2019). *The Canadian Veterinary Journal* **63**: 178 (2022).

550 Al-Khafaf, A., Ismail, H. K. & Alsaidya, A. Histopathological effects of experimental exposure to lead on nervous system in albino female rats. *Iraqi J Vet Sci* **35**, 1: 45-48 (2021).

551 Ilha, M. R., Hawkins, I. K. & Jones, A. L. Case report: Systemic granulomatous disease with vasculitis in a bull due to hairy vetch (Vicia villosa) toxicosis. *The Bovine Practitioner* **27**: 60-66 (2023).

552 Hu, Y., Chi, L., Kuebler, W. M. & Goldenberg, N. M. Perivascular inflammation in pulmonary arterial hypertension. *Cells* **9**: 2338 (2020).

553 Shi, H. *et al.* Perivascular adipose tissue in autoimmune rheumatic diseases. *Pharmacological research* **182**: 106354 (2022).

554 Gazzinelli-Guimarães, P. H. *et al.* Concomitant helminth infection downmodulates the Vaccinia virus-specific immune response and potentiates virus-associated pathology. *International journal for parasitology* **47**: 1-10 (2017).

555 Cox, F. Concomitant infections, parasites and immune responses. *Parasitology* **122**, Suppl: S23-S38 (2001).

556 Estrada-Peña, A., Venzal, J. M., Kocan, K. M. & Sonenshine, D. E. Overview: ticks as vectors of pathogens that cause disease in humans and animals. (2008).

557 Fischer, K. & Walton, S. Parasitic mites of medical and veterinary importance–is there a common research agenda? *Int J Parasitol* **44**, 12: 955-967 (2014).
558 Cooper, L. N. *et al.* Bats as instructive animal models for studying longevity and aging. *Ann N Y Acad Sci* **1541**, 1: 10-23 (2024).
559 Ricci, M., Peona, V. & Taccioli, C. Involvement of non-LTR retrotransposons in mammal cancer incidence and ageing. *bioRxiv*: 2021.2009. 2027.461867 (2021).
560 Foley, N. M. *et al.* Growing old, yet staying young: The role of telomeres in bats' exceptional longevity. *Sci Adv* **4**, 2: eaao0926 (2018).
561 Scheben, A. *et al.* Long-read sequencing reveals rapid evolution of immunity-and cancer-related genes in bats. *Genome biology and evolution* **15**: evad148 (2023).
562 Wylie, T. N., Wylie, K. M., Herter, B. N. & Storch, G. A. Enhanced virome sequencing using targeted sequence capture. *Genome Res* **25**, 12: 1910-1920 (2015).
563 Rougeron, V. *et al.* Characterization and phylogenetic analysis of new bat astroviruses detected in Gabon, Central Africa. *Acta Virol* **60**, 4: 386-392 (2016). https://doi.org/10.4149/av_2016_04_386
564 Waruhiu, C. *et al.* Molecular detection of viruses in Kenyan bats and discovery of novel astroviruses, caliciviruses and rotaviruses. *Virol Sin* **32**, 2: 101-114 (2017).
565 Amman, B. R. *et al.* Isolation of Angola-like Marburg virus from Egyptian rousette bats from West Africa. *Nat Commun* **11**, 1: 510 (2020).
566 Simpson, D., Williams, M., O'sullivan, J., Cunningham, J. & Mutere, F. Studies on arboviruses and bats (Chiroptera) in East Africa: II.—Isolation and haemagglutination-inhibition studies on bats collected in Kenya and throughout Uganda. *Annals of Tropical Medicine & Parasitology* **62**, 4: 432-440 (1968).
567 Akov, Y. & Goldwasser, R. Prevalence of antibodies to arbovirus in various animals in Israel. *Bull World Health Organ* **34**, 6: 901-909 (1966).
568 Quan, P.-L. *et al.* Bats are a major natural reservoir for hepaciviruses and pegiviruses. *Proc Natl Acad Sci USA* **110**, 20: 8194-8199 (2013).
569 Simpson, D. & O'Sullivan, J. Studies on arboviruses and bats (Chiroptera) in East Africa: I.—Experimental infection of bats and virus transmission attempts in Aedes (Stegomyia) aegypti (Linnaeus). *Ann Trop Med Parasitol* **62**, 4: 422-431 (1968).
570 Kalunda M, M. L., Mukuye A, Lule M, Sekyalo E, Wright J, Casals J. Kasokero virus: a new human pathogen from bats (Rousettus aegyptiacus) in Uganda. *The American journal of tropical medicine and hygiene.* **35**: 387-392 (1986 Mar 1).
571 Walker, P. J. *et al.* Genomic characterization of Yogue, Kasokero, Issyk-Kul, Keterah, Gossas, and Thiafora viruses: nairoviruses naturally infecting bats, shrews, and ticks. *The American journal of tropical medicine and hygiene* **93**: 1041 (2015).
572 Müller, M. A. *et al.* Evidence for widespread infection of African bats with Crimean-Congo hemorrhagic fever-like viruses. *Scientific Reports* **6**: 26637 (2016).
573 Harima, H. *et al.* Detection of novel orthoreovirus genomes in shrew (Crocidura hirta) and fruit bat (*Rousettus aegyptiacus*). *J Vet Med Sci* **82**, 2: 162-167 (2020).
574 Harima, H. *et al.* Attenuated infection by a Pteropine orthoreovirus isolated from an Egyptian fruit bat in Zambia. *PLoS Negl Trop Dis* **15**, 9: e0009768 (2021).

575 Amponsah-Mensah, K. *Ecology of Fruit Bats in Ghana, with Special Focus on Epomophorus Gambianus, and the Role of Fruit Bats in Zoonotic Disease Transmission*, University of Ghana Digital Collections, http://ugspace.ug.edu.gh/, (2017).
576 Kading, R. C. *et al.* Neutralizing antibodies against flaviviruses, Babanki virus, and Rift Valley fever virus in Ugandan bats. *Infect Ecol Epidemiol* **8**, 1: 1439215 (2018).
577 Picard-Meyer, E. *et al.* Genetic analysis of European bat lyssavirus type 1 isolates from France. *Veterinary record* **154**: 589-595 (2004).
578 Kuzmin, I. V. *et al.* Lagos bat virus in Kenya. *Journal of Clinical Microbiology* **46**: 1451-1461 (2008).
579 Kuzmin, I. V. *et al.* Commerson's leaf-nosed bat (Hipposideros commersoni) is the likely reservoir of Shimoni bat virus. *Vector-Borne and Zoonotic Diseases* **11**: 1465-1470 (2011).
580 Sasaki, M. *et al.* Identification of group A rotaviruses from Zambian fruit bats provides evidence for long-distance dispersal events in Africa. *Infection, genetics and evolution* **63**: 104-109 (2018).
581 Fagre, A. C. *et al.* Discovery and characterization of Bukakata orbivirus (Reoviridae: Orbivirus), a novel virus from a Ugandan bat. *Viruses* **11**, 3: 209 (2019).
582 Fagre, A. C. & Kading, R. C. Can bats serve as reservoirs for arboviruses? *Viruses* **11**, 3: 215 (2019).
583 Dietrich, M., Kearney, T., Seamark, E. C., Pawęska, J. T. & Markotter, W. Synchronized shift of oral, faecal and urinary microbiotas in bats and natural infection dynamics during seasonal reproduction. *R Soc Open Sci* **5**, 5: 180041 (2018). https://doi.org/10.1098/rsos.180041
584 Carr, M. *et al.* Discovery of African bat polyomaviruses and infrequent recombination in the large T antigen in the Polyomaviridae. *J Gen Virol* **98**, 4: 726-738 (2017).
585 Tao, Y. *et al.* Discovery of diverse polyomaviruses in bats and the evolutionary history of the Polyomaviridae. *J Gen Virol* **94**, 4: 738 (2013).
586 Bai, Y. *et al.* Human exposure to novel *Bartonella* species from contact with fruit bats. *Emerg Infect Dis* **24**, 12: 2317 (2018).
587 Tocidlowski, M. E. in *Annual Conference of the American Association of Zoo Veterinarians.* (ed CK Baer) 141-142.
588 Reinhardt, K., Naylor, R. A. & Siva-Jothy, M. T. Temperature and humidity differences between roosts of the fruit bat, *Rousettus aegyptiacus* (Geoffroy, 1810), and the refugia of its ectoparasite, *Afrocimex constrictus*. *Acta Chiropt* **10**, 1: 173-176 (2008).
589 Braack, L. Arthropod inhabitants of a tropical cave 'island' environment provisioned by bats. *Biol Conserv* **48**, 2: 77-84 (1989).
590 Nartey, N. Common parasites of fruit-eating bats in southern Ghana. *Accra (Ghana): University of Ghana*: 1-144 (2015).
591 Jansen van Vuren, P. *et al.* Isolation of a novel fusogenic orthoreovirus from *Eucampsipoda africana* bat flies in South Africa. *Viruses* **8**, 3: 65 (2016).

592 Obame-Nkoghe, J. *et al.* Bat flies (Diptera: Nycteribiidae and Streblidae) infesting cave-dwelling bats in Gabon: diversity, dynamics and potential role in Polychromophilus melanipherus transmission. *Parasites & vectors* **9**: 1-12 (2016).
593 Peirce, M. Parasites of Chiroptera in Zambia. *J Wildl Dis* **20**, 2: 153-154 (1984).
594 Malek-Hosseini, M. J., Sadeghi, S., Bakhshi, Y. & Dashan, M. Ectoparasites (Insecta and Acari) associated with bats in south and south-western caves of Iran. *Ambient Science* **3**: 22-28 (2016).
595 Çetin, H., Coşkun, G. & Dick, C. W. Ectoparasitic Bat Flies (*Eucampsipoda hyrtlii*) Detected on the Egyptian Fruit Bat (*Rousettus aegyptiacus*) in Antalya, Turkey. *Turkiye Parazitol Derg* **44**, 2: 115-117 (2020).
596 Maa, T. Review of the Streblidae (Diptera) parasitic on megachiropteran bats. *Pacific Insects Monograph* **28**: 213-243 (1971).
597 Hafez, S., Ebaid, N., Tharwat, M. & Abdel-Megeed, A. Bat mites of Egypt (Acari: Spinturnicidae). (1994).
598 Estrada-Peña, A., Ballesta, R. J. & Ibañez, C. Three new species of spinturnicid mites (Acari: Mesostigmata) from bats in Africa. *int J Acarol* **18**, 4: 307-313 (1992).
599 Negm, M. W. & Fakeer, M. M. Rediscovery of *Meristaspis lateralis* (Kolenati) (Acari: Mesostigmata: Spinturnicidae) parasitizing the Egyptian fruit bat, *Rousettus aegyptiacus* (Geoffroy) (Mammalia: Chiroptera), with a key to mites of bats in Egypt. *J Egypt Soc Parasitol* **44**, 1: 25-32 (2014). https://doi.org/10.12816/0006443
600 Sylla, M., Cornet, J. & Marchand, B. Description of *Alectorobius* (*Reticulinasus*) *camicasi* sp. nov.(Acari: Ixodoidea: Argasidae), a parasite of fruit bats *Rousettus aegyptiacus occidentalis* in Senegal. *Acarologia* **38**, 3: 239-254 (1997).
601 Sándor, A. D., Mihalca, A. D., Domşa, C., Péter, Á. & Hornok, S. Argasid ticks of palearctic bats: distribution, host selection, and zoonotic importance. *Frontiers in Veterinary Science* **8**: 684737 (2021).
602 American Veterinary Medical Association. 2020. AVMA Guidelines for the Euthanasia of Animals: 2020 Edition. https://www.avma.org/sites/default/files/2020-02/Guidelines-on-Euthanasia-2020.pdf. Accessed March 17, 2025.
603 National *et al. Guide for the Care and Use of Laboratory Animals. 8th Ed*. (National Academies Press (US), 2011).
604 Bassioni, G., Korin, A. & Salama, A. E.-D. Stainless steel as a source of potential hazard due to metal leaching into beverages. *Int J Electrochem Sci* **10**, 5: 3792-3802 (2015).
605 Zhou, S., Evans, B., Schöneich, C. & Singh, S. K. Biotherapeutic formulation factors affecting metal leachables from stainless steel studied by design of experiments. *AAPS PharmSciTech* **13**: 284-294 (2012).
606 United, States, Environmental, Protection & Agency. *Secondary Drinking Water Standards: Guidance for Nuisance Chemicals*, <https://www.epa.gov/sdwa/secondary-drinking-water-standards-guidance-nuisance-chemicals> (Accessed October 17, 2023.).
607 DeKalb *et al.* <https://www.dekalbcountyga.gov/watershed-management/drinking-water-quality-report> (Accessed September 16, 2024.).

608 Venkatesan, P. Marburg virus outbreak in Tanzania. *Lancet Microbe*, (2025). https://doi.org/10.1016/j.lanmic.2025.101121. Epub ahead of print. PMID: 40081397.
609 Carroll, S. A. *et al.* Molecular evolution of viruses of the family Filoviridae based on 97 whole-genome sequences. *J Virol* **87**, 5: 2608-2616 (2013).
610 Meechan, P. J. & Potts, J. *Biosafety in Microbiological and Biomedical Laboratories, 6th Ed.*, (Centers for Disease Control and Prevention, National Institutes of Health, 2020).
611 Jankowski, M. D., Williams, C. J., Fair, J. M. & Owen, J. C. Birds shed RNA-viruses according to the Pareto principle. *PloS One* **8**, 8: e72611 (2013).
612 Courcoul, A. *et al.* Modelling the effect of heterogeneity of shedding on the within herd *Coxiella burnetii* spread and identification of key parameters by sensitivity analysis. *J Theor Biol* **284**, 1: 130-141 (2011).
613 Fleming-Davies, A. E., Dukic, V., Andreasen, V. & Dwyer, G. Effects of host heterogeneity on pathogen diversity and evolution. *Ecol Lett* **18**, 11: 1252-1261 (2015).
614 Lambert, S. *et al.* High shedding potential and significant individual heterogeneity in naturally-infected Alpine ibex (*Capra ibex*) with *Brucella melitensis*. *Front Microbiol* **9**: 1065 (2018).
615 Lau, L. L. *et al.* Heterogeneity in viral shedding among individuals with medically attended influenza A virus infection. *J Infect Dis* **207**, 8: 1281-1285 (2013).
616 Matthews, L. *et al.* Heterogeneous shedding of *Escherichia coli* O157 in cattle and its implications for control. *Proc Natl Acad Sci USA* **103**, 3: 547-552 (2006).
617 Matthews, L. *et al.* Exploiting strain diversity to expose transmission heterogeneities and predict the impact of targeting supershedding. *Epidemics* **1**, 4: 221-229 (2009).
618 Milbrath, M., Spicknall, I., Zelner, J., Moe, C. & Eisenberg, J. Heterogeneity in norovirus shedding duration affects community risk. *Epidemiol Infect* **141**, 8: 1572-1584 (2013).
619 Siva-Jothy, J. A. & Vale, P. F. Dissecting genetic and sex-specific sources of host heterogeneity in pathogen shedding and spread. *PLoS Pathog* **17**, 1: e1009196 (2021).
620 VanderWaal, K. L. & Ezenwa, V. O. Heterogeneity in pathogen transmission. *Func Ecol* **30**, 10: 1606-1622 (2016).
621 White, L. A., Forester, J. D. & Craft, M. E. Covariation between the physiological and behavioral components of pathogen transmission: host heterogeneity determines epidemic outcomes. *Oikos* **127**, 4: 538-552 (2018).
622 Woolhouse, M. E. *et al.* Heterogeneities in the transmission of infectious agents: implications for the design of control programs. *Proc Natl Acad Sci USA* **94**, 1: 338-342 (1997).
623 Fusco, M. L. *et al.* Protective mAbs and cross-reactive mAbs raised by immunization with engineered Marburg virus GPs. *PLoS Pathog* **11**, 6: e1005016 (2015).

624 Bukreyev, A. *et al.* Divergent antibody recognition profiles are generated by protective mRNA vaccines against Marburg and Ravn viruses. *Res Sq [Preprint]*, (2024). https://doi.org/10.21203/rs.3.rs-4087897/v1
625 Yang, Z. Y. *et al.* Identification of the Ebola virus glycoprotein as the main viral determinant of vascular cell cytotoxicity and injury. *Nat Med* **6**, 8: 886-889 (2000).
626 Szepanski, S., Gross, H. J., Brossmer, R., Klenk, H. D. & Herrler, G. A single point mutation of the influenza C virus glycoprotein (HEF) changes the viral receptor-binding activity. *Virology* **188**, 1: 85-92 (1992).
627 Dhillon, S. *et al.* Mutations within a conserved region of the hepatitis C virus E2 glycoprotein that influence virus-receptor interactions and sensitivity to neutralizing antibodies. *J Virol* **84**, 11: 5494-5507 (2010).
628 Sullivan, B. M. *et al.* Point mutation in the glycoprotein of lymphocytic choriomeningitis virus is necessary for receptor binding, dendritic cell infection, and long-term persistence. *Proc Natl Acad Sci USA* **108**, 7: 2969-2974 (2011).
629 Wong, A. C., Sandesara, R. G., Mulherkar, N., Whelan, S. P. & Chandran, K. A forward genetic strategy reveals destabilizing mutations in the Ebolavirus glycoprotein that alter its protease dependence during cell entry. *J Virol* **84**, 1: 163-175 (2010).
630 Manicassamy, B. *et al.* Characterization of Marburg virus glycoprotein in viral entry. *Virology* **358**, 1: 79-88 (2007). https://doi.org/10.1016/j.virol.2006.06.041
631 Lennemann, N. J. *et al.* A naturally occurring polymorphism in the base of Sudan virus glycoprotein decreases glycoprotein stability in a species-dependent manner. *J Virol* **95**, 18: 10.1128/jvi. 01073-01021 (2021).
632 Witteck, A., Yerly, S. & Vernazza, P. Unusually high HIV infectiousness in an HIV-, HCV- and HSV-2-coinfected heterosexual man. *Swiss Med Wkly* **139**, 13-14: 207-209 (2009). https://doi.org/10.4414/smw.2009.12575
633 Chase-Topping, M., Gally, D., Low, C., Matthews, L. & Woolhouse, M. Super-shedding and the link between human infection and livestock carriage of *Escherichia coli* O157. *Nat Rev Microbiol* **6**, 12: 904-912 (2008).
634 Cobbold, R. N. *et al.* Rectoanal junction colonization of feedlot cattle by *Escherichia coli* O157: H7 and its association with supershedders and excretion dynamics. *Appl Environ Microbiol* **73**, 5: 1563-1568 (2007).
635 Barfield, M., Orive, M. E. & Holt, R. D. The role of pathogen shedding in linking within-and between-host pathogen dynamics. *Math Biosci* **270**, Pt B: 249-262 (2015).
636 Augenbraun, M. *et al.* Increased genital shedding of herpes simplex virus type 2 in HIV-seropositive women. *Ann Intern Med* **123**, 11: 845-847 (1995).
637 Cohen, M. S. *et al.* Reduction of concentration of HIV-1 in semen after treatment of urethritis: implications for prevention of sexual transmission of HIV-1. *Lancet* **349**, 9069: 1868-1873 (1997).
638 Lass, S. *et al.* Generating super-shedders: co-infection increases bacterial load and egg production of a gastrointestinal helminth. *J R Soc Interface* **10**, 80: 20120588 (2013).
639 Stein, R. A. & Bianchini, E. C. Bacterial–viral interactions: a factor that facilitates transmission heterogeneities. *FEMS Microbes* **3**: xtac018 (2022).

640 Lukicheva, N., Ebel, E. D., Williams, M. S. & Schlosser, W. D. Characterizing the concentration of pathogen occurrence across meat and poultry industries. *Microb Risk Anal* **4**: 29-35 (2016).
641 Wacharapluesadee, S. *et al.* Longitudinal study of age-specific pattern of coronavirus infection in Lyle's flying fox (*Pteropus lylei*) in Thailand. *Virol J* **15**: 1-10 (2018).
642 Rahman, S. A. *et al.* Risk factors for Nipah virus infection among pteropid bats, Peninsular Malaysia. *Emerg Infect Dis* **19**, 1: 51 (2013).
643 Brändel, S. D. *et al.* Astrovirus infections induce age-dependent dysbiosis in gut microbiomes of bats. *ISME J* **12**, 12: 2883-2893 (2018).
644 Mendenhall, I. H. *et al.* Influence of age and body condition on astrovirus infection of bats in Singapore: an evolutionary and epidemiological analysis. *One Health* **4**: 27-33 (2017).
645 Lian, S., Liu, J., Wu, Y., Xia, P. & Zhu, G. Bacterial and viral co-infection in the intestine: competition scenario and their effect on host immunity. *Int J Mol Sci* **23**: 2311 (2022).
646 Kaaijk, P. *et al.* Contribution of influenza viruses, other respiratory viruses and viral co-infections to influenza-like illness in older adults. *Viruses* **14**: 797 (2022).
647 Wang, J. *et al.* Individual bat viromes reveal the co-infection, spillover and emergence risk of potential zoonotic viruses. *bioRxiv*, (2022). https://doi.org/10.1101/2022.11.23.517609
648 Machado, P. R. *et al.* Viral co-infection and leprosy outcomes: a cohort study. *PLoS Negl Trop Dis* **9**, 8: e0003865 (2015).
649 Hayman, D. *et al.* Ecology of zoonotic infectious diseases in bats: current knowledge and future directions. *Zoonoses Public Health* **60**, 1: 2-21 (2013).
650 Ruiz-Aravena, M. *et al.* Ecology, evolution and spillover of coronaviruses from bats. *Nat Rev Microbiol* **20**: 299-314 (2022).
651 Carter, G. G. & Wilkinson, G. S. in *Bat evolution, ecology, and conservation* 225-242 (Springer, 2013).
652 Hoarau, A. O., Mavingui, P. & Lebarbenchon, C. Coinfections in wildlife: Focus on a neglected aspect of infectious disease epidemiology. *PLoS Pathog* **16**, 9: e1008790 (2020).
653 Du, Y., Wang, C. & Zhang, Y. Viral Coinfections. *Viruses* **14**, 12: 2645 (2022).
654 Kumar, N., Sharma, S., Barua, S., Tripathi, B. N. & Rouse, B. T. Virological and immunological outcomes of coinfections. *Clinical Microbiology Reviews* **31**: 10.1128/cmr. 00111-00117 (2018).
655 McAfee, M. S., Huynh, T. P., Johnson, J. L., Jacobs, B. L. & Blattman, J. N. Interaction between unrelated viruses during in vivo co-infection to limit pathology and immunity. *Virology* **484**: 153-162 (2015).
656 Arzt, J. *et al.* Simultaneous and staggered foot-and-mouth disease virus coinfection of cattle. *J Virol* **95**, 24: 10.1128/jvi. 01650-01621 (2021).
657 Dunn, J. R. *et al.* The effect of the time interval between exposures on the susceptibility of chickens to superinfection with Marek's disease virus. *Avian Dis* **54**, 3: 1038-1049 (2010). https://doi.org/10.1637/9348-033010-Reg.1
658 Kenney, L. L. *et al.* Increased Immune Response Variability during Simultaneous Viral Coinfection Leads to Unpredictability in CD8 T Cell Immunity and

Pathogenesis. *J Virol* **89**, 21: 10786-10801 (2015).
https://doi.org/10.1128/jvi.01432-15